Universitat Politècnica de València
I.U.I. CMT – Clean Mobility & Thermofluids

UNIVERSITAT POLITÈCNICA DE VALÈNCIA

DOCTORAL THESIS

IMPACT OF DIFFERENT E-FUELS TYPES ON LIGHT-DUTY COMPRESSION IGNITION ENGINE PERFORMANCE, EMISSIONS AND CO_2 LIFE CYCLE ANALYSIS

Presented by:
María Gabriela Guzmán Mendoza

Directed by:
Prof. Dr. Antonio García Martínez
Dr. David Villalta

in fulfillment of the requirements for the degree of
Doctor of Philosophy

Valencia, December 2023

Doctoral Thesis

IMPACT OF DIFFERENT E-FUELS TYPES ON LIGHT-DUTY COMPRESSION IGNITION ENGINE PERFORMANCE, EMISSIONS AND CO2 LIFE CYCLE ANALYSIS

Presented by:	María Gabriela Guzmán Mendoza
Directed by:	Prof. Dr. Antonio García Dr. David Villalta

Examining committee:

President:	Prof. Raúl Payri
Secretary:	Prof. Juan José Hernández
Examiner:	Prof. Martin Davy

Reviewing board:

Prof. José Rodríguez

Prof. Martin Davy

Dr. Silvana di Iorio

Valencia, December 2023

Abstract

Low carbon fuels (LCFs) are evaluated as a suitable replacement for current fossil heavy fuels for a compression ignition internal combustion engine (CI ICE) in terms of engine performance, pollutant emissions and environmental impact. The fuels are evaluated according to their feasibility to substitute current market fuels with the LCF alternatives. Through drop-in studies and fuel-specific optimized calibration, the low emission characteristics of the LCFs to achieve fewer polluting emissions without sacrificing the engine efficiency are exploited. The calibration is achieved by the realization of a design of experiments (DOE) from which models are obtained for each fuel, to be later optimized for low NOx-soot emissions. Finally, the impact of both the drop-in and optimized calibration are compared in a life cycle analysis (LCA) that considers the CO_2 footprint, as well as other impact categories such as terrestrial acidification, particulate matter formation, water consumption and ozone formation.

Overall, it was found that the tested LCFs can be suitable replacements for CI ICEs in both the drop-in and optimized calibrations (albeit with some hardware considerations), where engine performance similar to current diesel baselines can be reached with important reductions in pollutants like NOx and soot. And additionally, it was verified that the renewability proportion of the fuel is highly beneficial to the reduction of the environmental impact of the fuel, where completely renewable fuels (like the tested LCD100) could have CO_2 footprints by kilometer similar to those of electric vehicles in Europe, assuming that raw materials and energy for the fuel production come from renewable sources.

Resumen

Los combustibles bajos en carbono (LCF) se evalúan como un sustituto adecuado de los combustibles pesados fósiles actuales para un motor de combustión interna de encendido por compresión (CI ICE) en términos de rendimiento del motor, emisiones contaminantes e impacto ambiental. Los combustibles se evalúan de acuerdo con su factibilidad para sustituir los combustibles actuales del mercado con las alternativas LCF. A través de estudios directos y calibración optimizada específica del combustible, se aprovechan las características de bajas emisiones de los LCF para lograr menos emisiones contaminantes sin sacrificar la eficiencia del motor. La calibración se logra mediante la realización de un diseño de experimentos (DOE) a partir del cual se obtienen modelos para cada combustible, para posteriormente optimizar para bajas emisiones de NOx-hollín. Por último, se compara el impacto tanto de la calibración drop-in como de la calibración optimizada en un análisis de ciclo de vida (LCA) que tiene en cuenta la huella de CO2, así como otras categorías de impacto como la acidificación terrestre, la formación de partículas, el consumo de agua y la formación de ozono.

En general, se encontró que los LCF probados pueden ser reemplazos adecuados para los CI ICE tanto en las calibraciones directas como en las optimizadas (aunque con algunas consideraciones de hardware), donde se puede alcanzar un rendimiento del motor similar a las líneas de base diésel actuales con importantes reducciones de contaminantes como NOx y hollín. Y adicionalmente, se comprobó que la proporción de renovabilidad del combustible es altamente beneficiosa para la reducción del impacto ambiental del combustible, donde los combustibles completamente renovables (como el LCD100 probado) podrían tener huellas de CO2 por kilómetro similares a las de los vehículos eléctricos en Europa, asumiendo que las materias primas y la energía para la producción de combustible provienen de fuentes renovables.

Resum

Els combustibles baixos en carboni (LCF) s'avaluen com un reemplaçament adequat dels combustibles pesats fòssils actuals per a un motor de combustió interna d'encesa per compressió (CI ICE) en termes de rendiment del motor, emissions contaminants i impacte ambiental. Els combustibles s'avaluen segons la seva viabilitat per substituir els combustibles actuals del mercat per les alternatives LCF. Mitjançant estudis d'abandonament i calibratge optimitzat específic del combustible, s'exploten les característiques de baixes emissions dels LCF per aconseguir emissions menys contaminants sense sacrificar l'eficiència del motor. El calibratge s'aconsegueix mitjançant la realització d'un disseny d'experiments (DOE) a partir del qual s'obtenen models per a cada combustible, per posteriorment optimitzar per a baixes emissions de NOx-sutge. Finalment, es compara l'impacte tant de la caiguda com del calibratge optimitzat en una anàlisi de cicle de vida (LCA) que considera la petjada de CO2, així com altres categories d'impacte com l'acidificació terrestre, la formació de partícules en suspensió, el consum d'aigua i la formació d'ozó.

En general, es va trobar que els LCF provats poden ser reemplaçaments adequats per als CI ICE tant en les calibracions d'entrada com optimitzades (encara que amb algunes consideracions de maquinari), on es pot assolir un rendiment del motor similar a les línies de base dièsel actuals amb reduccions importants de contaminants com el NOx i el sutge. I addicionalment, es va comprovar que la proporció de renovable del combustible és altament beneficiosa per a la reducció de l'impacte ambiental del combustible, on els combustibles completament renovables (com el provat LCD100) podrien tenir petjades de CO2 per quilòmetre similars a les dels vehicles elèctrics a Europa, assumint que les matèries primeres i l'energia per a la producció de combustible provenen de fonts renovables.

To my younger self
To David
To my parents and brother
To Cayena (the dog)

Acknowledgements

There are several reasons to get to this point. Although there can be an overlap between the reasons, everyone that reaches this step has **one** that is specific to themselves. My case is not different. I surely am glad for the motivation mine provided to complete this task. At times the work could be time consuming and feel lonesome, but it would be foolish to say this was a solo endeavor. Behind the results there is an army of people to whom to express gratitude:

The love of my life, David. Thanks for growing together and for making across the sea be our home. Thanks for understanding me even when I don't find the words to understand myself. Your sweetness, patience and wisdom gave me the strength to continue this journey. I hope I can bring as much happiness and warmth to your life as you bring to mine. We did it! And the best is yet to come.

My parents, Erika and Franzel, for their support and caring. Here's to seeing each other more often and enjoying our time together. To my brother, Daniel, for your easygoing self which contrasts my perpetual stress. I will always be there for you.

My official advisors Antonio García and David Villalta, and the unofficial advisor Javier Monsalve-Serrano. For the education on combustion, engines, research, and academia. Also, the professional and personal growth you helped me achieve. I will carry on the lessons you taught me through the years. The colleagues that have become friends and animate office work, Álvaro, Erasmo, Carlos, Diego and Imad; and the ones that raised the bar, "Rafa" and "Santi".

CMT-Motores Térmicos and the combustion department, for the opportunity of joining this research group and developing this investigation. To the secretary, in particular Amparo Cutillas, for being more aware than anybody about what and when documentation was needed at every stage of the process. To "Dani", Hector and all the amazing technicians for being pivotal in the development of this work. Thanks for making testing so entertaining.

Aramco Overseas Company, GM and PUNCH Torino for funding and providing the resources for the work in this thesis. Thanks to Patrick Gaillard, Alberto Vassallo, Francesco Pesce and Russell Durrett for the collaboration and interesting discussions about the project; and to Alberto and Francesco for welcoming me in Torino during my internship.

This doctoral thesis has been partially supported by the Conselleria d'Innovació, Universitats, Ciència i Societat Digital de la Generalitat Valenciana through the predoctoral contract (ACIF/2021/200).

Contents

List of Figures

List of Tables

List of equations

Chapter 3 – Tools and methodology

Chapter 6 – Life Cycle Analysis of Low Carbon Fuels for Light-Duty Combustion Engine Vehicles

Nomenclature

Acronyms

AFR	Air-to-Fuel Ratio
AP	Acidification Potential
ATS	Aftertreatment System
BMEP	Brake Mean Effective Pressure
BSEC	Brake Specific Energy Consumption
BSFC	Brake Specific Fuel Consumption
BSFCeq	Equivalent Brake Specific Fuel Consumption
BTE	Brake Thermal Efficiency
BTL	Biomass-to-Liquid
CA50	Combustion Phasing/Crank Angle at which 50 % of the heat from combustion has been released
CC	Catalytic Converter
CCS	Carbon Capture and Storage
CCU	Carbon Capture and Utilization
CDPF	Catalyzed Diesel Particulate Filter
CED	Cumulative Energy Demand
CFCs	Chlorofluorocarbons
CFPP	Cold Filter Plugging Point
CH4	Methane
CI	Compression Ignition
CN	Cetane Number
CNR	Combined Normalized Response
CO	Carbon Monoxide
CO2	Carbon Dioxide
COME	Castor Oil Methyl Ester
CP	Cloud Point
CR	Compression Ratio
DAC	Direct Air Capture
DI	Direct Injection
DICI	Direct Injection Compression Ignition
DMF	Dimethyl Furan
DNPE	Di-n-pentyl Ether
DOC	Diesel Oxidation Catalyst

DOE	Design of Experiments
DPF	Diesel Particulate Filter
ECU	Engine Control Unit
EEPS	Engine Exhaust Particle Sizer
EF	Environmental Footprint
EGR	Exhaust Gas Recirculation
EGT	Exhaust Gas Temperature
EOC	End of Combustion
EOL	End of Life
EP	Euthrophication Potential
ET	Energizing Time
EV	Electric Vehicle
EVO	Exhaust Valve Opening
FAME	Fatty Acid Methyl Ester
FFA	Free Fatty Acid
FID	Flame Ionization Detector
FIS	Fuel Injection System
FSN	Filter Smoke Number
FT	Fischer-Tropsch
FTIR	Fourier-transform infrared spectroscopy
FU	Functional Unit
GBE	Gross Brake Efficiency
GHG	Greenhouse Gas
GM	General Motors
GREET	Greenhouse Gases, Regulated Emissions and Energy Use in Technologies
GTL	Gas-to-Liquid
GWP	Global Warming Potential
HC	Hydrocarbons
HCLD	Heated Chemiluminescence Detector
HHV	Higher Heating Value
HOFP	Human Ozone Formation Potential
HPA	Heteropoly Acids
HRL	Total Heat Released
HRR	Heat Release Rates
HTP	Human Toxicity Potential
HVO	Hydrotreated Vegetable Oil
ICE	Internal Combustion Engine

ICEV	Internal Combustion Engine Vehicle
IDID	Internal Diesel Injector Deposits
IDT	Ignition Delay Time
IMEP	Indicated Mean Effective Pressure
IP	Injection Pressure
IQR	Interquartile Range
ISCC	International Sustainability and Carbon Certification
ISFC	Indicated Specific Fuel Consumption
ITE	Indicated Thermal Efficiency
IVC	Inlet Valve Closing
LCA	Life Cycle Assessment
LCF	Low Carbon Fuel
LCI	Life Cycle Inventory
LCIA	Life Cycle Impact Assessment
LHV	Lower Heating Value
LNT	Lean-Nox Trap
LO	Lemon Oil
LTHR	Low Temperature Heat Release
MFB	Mass Fraction Burned
MPD	Magneto-Pneumatic Detector
N2O	Nitrous Oxide
NDIR	Non-Dispersive InfraRed
NG	Natural Gas
NMVOC	Non-Methane Volatile Organic Compound
NO	Nitrogen Monoxide
NO2	Nitrogen Dioxide
NOx	Nitrogen Oxides
NP	Nanoparticles
NR	Normalized Response
NVH	Noise Vibration and Harshness
ODP	Ozone Depletion Potential
OEF	Organization Environmental Footprint
OESI	Oxygen Extended Sooting Index
OMEx	Oxymethylene Dimethyl Ethers
PAHs	Polycyclic Aromatic Hydrocarbons
PCS	Post-combustion Capture System
PEF	Product Environmental Footprint

PKME	Pistacia Khinjuk Methyl Ester
PM	Particulate Matter
PMFP	Particle Matter Formation Potential
PODEs	Polyoxymethylene Ethers
POME	Palm Oil Methyl Ester
PRR	Pressure Rise Rates
PSO-NS	Particle Swarm Optimization-Novelty Search
PSZ	Partially Stabilized Zirconia
PTG	Power-to-Gas
PTL	Power-to-Liquid
PY	Pyrogallol
RDE	Real Driving Emissions
RME	Rapeseed Methyl Ester
RSB	Roundtable of Sustainable Biofuels
RSM	Response Surface Methodology
SCR	Selective Catalytic Reducer
SI	Spark Ignition
SO2	Sulfur Dioxide
SOC	Start of Combustion/State of Charge
SOI	Start of Injection
SR	Standardized Response
SX	Specific Emissions
TDC	Top Dead Center
THC	Total Hydrocarbon
TTW	Tank-to-Wheel
TWC	Three-way Catalyst
VGT	Variable Geometry Turbine
WCP	Water Consumption Potential
WLTC	Worldwide harmonized Light vehicles Test Cycle
WPO	Waste Plastic Oil
WSD	Wear Scar Diameter
WTT	Well-to-Tank
WTT CI	Well-to-Tank Carbon Intensity
WTW	Well-to-Wheel

Chapter 1
Introduction

Contents

1 The imperative for transitioning to sustainable transportation: low carbon fuels as a solution for reducing transport sector emissions

In a rapidly evolving world, marked by technological innovations and shifting paradigms, one of the most pressing challenges humanity faces is mitigating the catastrophic effects of climate change [1]. At the forefront of this lies the urgent need to reduce carbon emissions. The consequences of inaction are dire [2]. Rising global temperatures, extreme weather events, sea-level rise, and disruptions to ecosystems are just some of the myriad challenges we face due to unabated carbon emissions [3, 4, 5].

Over the past two decades, the transport and energy sectors have consistently stood out as major contributors to greenhouse gas (GHG) emissions, as illustrated in Figure 1. This trend holds true not only in Europe but on a global scale [6]. And, within the transport sector, automobiles accounted for a 45.1% of the sector's emissions in 2018 [7].

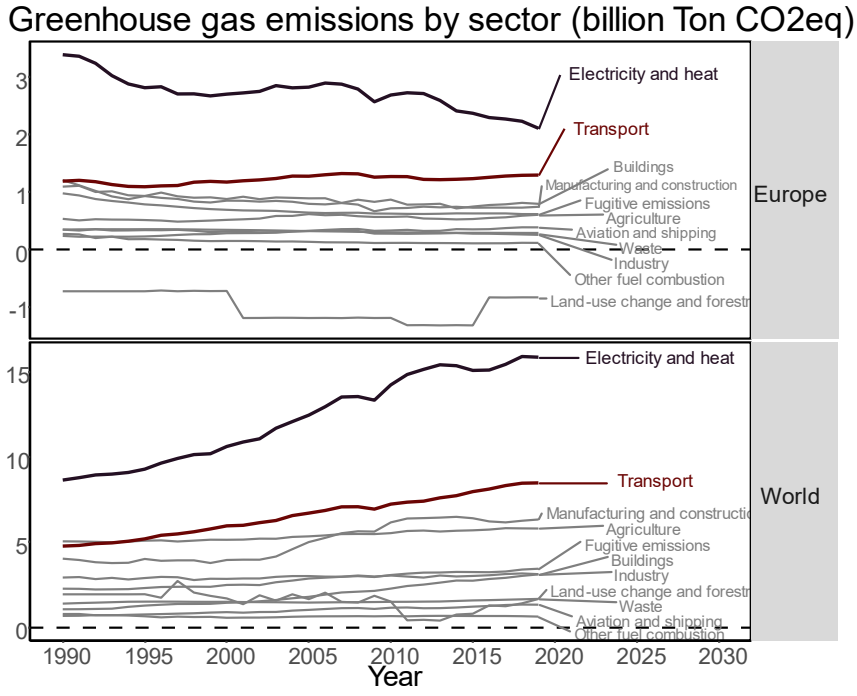

Figure 1. GHG emissions by sector for Europe and the World (data up to 2019 from [6])

Internal combustion engine vehicles (ICEVs), powered predominantly by fossil fuels, have played a pivotal role in shaping the modern world. However, this convenience has come at a steep cost - a steady increase in GHG emissions, primarily carbon dioxide (CO_2), which is one of the principal drivers of global warming and climate change [2]. As the transportation sector continues to be a major contributor to CO_2 emissions, the imperative to transition towards cleaner, more sustainable alternatives becomes increasingly evident.

The pursuit of environmentally friendly and sustainable transportation has taken on heightened urgency. With the global community deeply committed to mitigating climate change and curbing GHG emissions, the automotive industry finds itself at the forefront of a transformative shift. In response to this environmental challenge, the concept of Low Carbon Fuels (LCFs) has emerged as a strategic tool to directly address the high GHG emissions associated with the transport sector.

LCFs have the potential to alleviate the adverse environmental consequences associated with conventional fossil fuel combustion. They achieve this by significantly reducing the CO_2 footprint during their production, and in some cases, even achieving net-zero or carbon-negative production [8]. Embracing LCFs could offer a pathway to curbing GHG emissions, enhancing air quality, and decreasing our reliance on fossil resources. Moreover, the adoption of these fuels allows for the re-utilization of existing engine technologies, mitigating the need to produce more vehicles using further resources.

By providing an insightful exploration of LCFs and signaling compatibilities and incompatibilities with other GHG reducing alternatives this thesis seeks to present the reader with a comprehensive view of the LCFs as an energy vector for ICEVs and the transportation sector.

2 Alternatives for addressing carbon emissions in the transportation sector

In the quest to combat carbon emissions within the transportation sector, several alternative strategies stand out as promising avenues. LCFs, like biofuels and synthetic fuels, offer a means to reduce emissions without requiring an immediate overhaul of existing ICEVs. Electric vehicles (EVs), when powered by electricity from renewable sources, present a zero-emission solution that is gaining momentum, although challenges related to battery production and infrastructure remain [9]. Hybrid vehicles present a balance between both the powertrains of EVs and ICEVs, having some of the benefits and drawbacks of both [10, 11, 12].

EVs represent a promising pathway to significantly reduce carbon emissions in the transportation sector. Unlike ICEVs, EVs produce zero tailpipe emissions and can be charged using electricity generated from renewable sources, effectively decoupling their operation from fossil fuels. As battery technology continues to improve, the range and affordability of EVs are becoming increasingly competitive with conventional vehicles [13, 14, 15, 16]. Moreover, governments and industries worldwide are investing heavily in EV infrastructure and incentives to accelerate their adoption [17]. However, challenges remain, including addressing the environmental impact of battery production and disposal [18, 19], as well as the need for a robust and extensive charging infrastructure to support widespread EV use [20]. Additionally, in regions where electricity generation relies heavily on fossil fuels, the overall GHG reduction potential of EVs may be limited. Therefore, the transition to electric vehicles should be accompanied by a shift towards cleaner and renewable sources of electricity to maximize their environmental advantages.

There is an ongoing debate between personal use passenger vehicles (independently of whether they are EVs, hybrid or ICEVs) and public transportation as emission-reduction strategies [21]. Personal vehicles offer individuals flexibility, convenience, and a sense of autonomy in travel choices. Advocates argue that promoting more fuel-efficient and electrified personal vehicles can lead to emissions reductions while preserving individual mobility. On the other hand, proponents of "only" public transportation emphasize its potential to reduce traffic congestion and emissions by encouraging shared mobility and decreasing the overall number of vehicles on the road. They argue that investments in public transportation infrastructure, coupled with policies that promote its use, can lead to significant emissions reductions and other social benefits.

The debate hinges on factors such as urban planning, population density, and the availability of public transportation options. It is important to recognize that a one-size-fits-all approach may not be suitable, and regional elements must be considered when determining the most effective strategy to reduce carbon emissions in the transportation sector. Regardless, even public transport alternatives, like buses, benefit from the development of personal transport and alternative forms of propelling powertrains as the technological advancement can be transversally used in mass transit options [22]. In this sense, changing user behavior can help encourage the use of public transportation or less impacting alternatives and selecting vehicles, energy sources, fuels and driving patterns that reduce emissions.

LCFs encompass a range of options designed to reduce the carbon footprint of ICEVs. These fuels typically emit less (or none) GHG during their production

compared to conventional gasoline or diesel. Examples include biofuels like ethanol and biodiesel, as well as synthetic fuels produced through renewable energy sources such as hydrogen and synthetic natural gas. The adoption of LCFs is appealing because it allows existing ICEVs to operate with reduced emissions, and hybrid vehicles also receive the benefits of lower carbon emissions fuels.

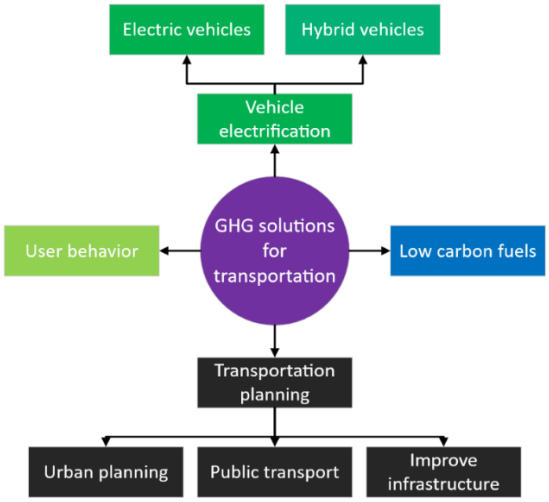

Figure 2. Different alternatives to solving the GHG dilemma in the transport sector.

LCFs offer a promising solution to capitalize on localized production in rich renewable energy sources and otherwise infertile regions [23]. These fuels, often derived from biomass or captured CO_2, can be efficiently manufactured in areas where renewable energy generation is abundant, such as wind and solar farms. By coupling the intermittent nature of renewable energy with fuel production, excess electricity can be harnessed during periods of peak generation and stored in the form of LCFs, acting as valuable energy storage means. Furthermore, situating these production facilities in regions devoid of competing food industries ensures that land and resources are dedicated solely to fuel production, preventing potential conflicts between food and energy production.

The environmental impacts of ICEVs, EVs and hybrids vary widely depending on the energy source selected to move the vehicle, and the materials required for their manufacturing. It is generally accepted that the environmental impact of EVs is lower than ICEVs fueled with fossil fuels. Nonetheless, when comparing EVs (with varying energy sources) and ICEVs fueled with LCFs, the environmental impact of

both types of vehicles becomes closer [24, 25, 26, 27]. This will be extensively discussed in Chapter 6 of this thesis, where a life cycle assessment of different types of passenger vehicles will be done with LCFs of different renewable proportions.

Addressing carbon emissions in the transportation sector requires a multifaceted approach that considers various alternatives, including LCFs and electric vehicles. Because of the wide impact of the transportation sector in day-to-day human activities, there is a need for a nuanced approach that takes into account individual preferences, urban planning, and local infrastructure to develop effective strategies for reducing carbon emissions in this critical sector. This work will primarily focus on LCFs and their use in light-duty vehicles and delve into the critical advantages and drawbacks essential for considering their widespread adoption, providing insights to inform their integration into the transportation sector.

3 Challenges and concerns related to tailpipe emissions from internal combustion engine vehicles using low carbon fuels

While LCFs offer promising pathways for reducing the carbon footprint of transportation, the challenge of tailpipe emissions remains a critical concern. Internal combustion engines (ICEs), even when powered by LCFs, can still emit harmful pollutants such as nitrogen oxides (NOx) and soot, which have adverse effects on air quality and public health.

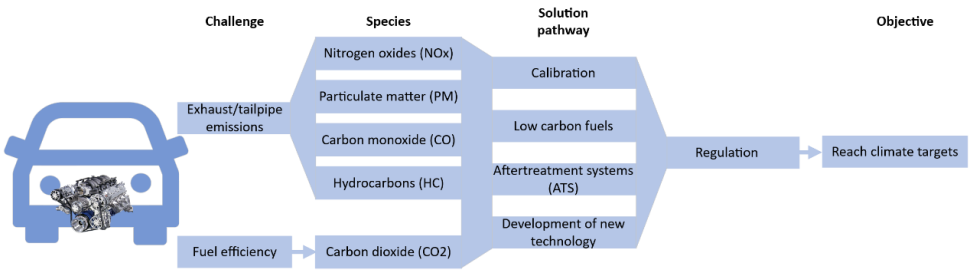

Figure 3. Main challenges on the emissions of ICEVs.

LCF production on its own does not completely resolve the emissions challenge associated with ICEVs. While LCFs may lower the carbon intensity of the fuel during the production phase, emissions from the tailpipe of the vehicle during the usage phase remain prevalent. Therefore, the adoption of LCFs alone – without strategies to also mitigate tailpipe emissions – is not sufficient to achieve the desired reduction in GHG emissions and other harmful pollutants from the transportation

sector. The complexity of addressing tailpipe emissions necessitates ongoing research and development efforts.

Vehicle researchers are dedicated to devising innovative strategies to reduce tailpipe emissions effectively. This includes optimizing combustion processes, implementing advanced exhaust aftertreatment technologies, and developing cleaner engine designs. It is crucial to ensure that the environmental benefits gained from using LCFs are not negated by increased tailpipe emissions of pollutants or GHGs like nitrous oxide (N_2O) due to altered combustion characteristics. Additionally, while LCFs can be used in conventional ICE vehicles, they can also be integrated into hybrid powertrains, taking advantage of electric machines to optimize the operation of both the ICE and the vehicle's battery and motor operate.

The aim of this thesis is to experimentally investigate the potential of various LCFs when used in conventional light-duty internal combustion engines. This research intends to comprehensively assess the impact of LCF blends on engine combustion, performance, and pollutant emissions, and assess the calibration parameters that best suit the LCFs while also considering their life cycle environmental impact in comparison to conventional fuels. Similarly, the hardware limitations and tradeoffs of some LCFs when used in current engine technologies. Finally, this study seeks to contribute valuable insights into the potential benefits and challenges associated with the adoption of LCFs in light-duty vehicles, with implications for sustainable transportation.

4 Document content and structure

This thesis emphasizes the technical and environmental considerations of the ICEV paradigm shift. In the next chapters the relationship between LCFs and ICEs will be explored through a literature review, experimental techniques, and statistical modelling, finalizing in a lifecycle assessment to evaluate the possible impact of the adoption of the selected LCFs into current passenger vehicle technology.

This thesis is structured in 7 chapters, which are outlined as follows:

- Chapter 2: This chapter conducts a comprehensive evaluation of low carbon fuels for internal combustion vehicles, considering their state of the art, applications, benefits, and disadvantages. The chapter explores various fuel options, such as biofuels and synthetic fuels, highlighting their environmental benefits over fossil fuels, their effect on engine performance and emissions as well as the engine hardware challenges that might be present with their use. The benefits of low carbon fuels, including reduced

greenhouse gas emissions, air pollution mitigation, are discussed, while acknowledging some of the challenges related to feedstock availability, production costs, and infrastructure.

- Chapter 3: This chapter describes the techniques, equipment, and procedures used in the experimental work, modeling, and optimization of the LCFs operation in a light-duty internal combustion engine. The chapter will inform the reader of how the research was conducted and how the results were obtained.
- Chapter 4: In this chapter, the drop-in potential of the selected low-carbon fuels will be identified. The fuels are evaluated in terms of whether it is possible or not to achieve drop-in operation, and the characteristics of the combustion, emissions and the engine settings that result from this type of operation.
- Chapter 5: In this chapter the focus is the modelling and optimization of a light-duty ICE using low carbon fuels. The calibration settings of the engine are adapted to best fit the properties of the fuels and reduce NOx emissions. In addition, the effects of the LCFs on engine performance and emissions are analyzed. Through this work, insights into the potential benefits and challenges associated with the use of LCFs in ICEs and strategies for optimizing their performance are provided.
- Chapter 6: This chapter presents a life cycle assessment (LCA) of LCFs used in a light-duty ICEVs with a focus on GHG emissions and their potential reduction with the use of non-fossil fuels. The study consideres the entire life cycle of the fuels, including their production, transportation, and combustion emissions.
- Chapter 7: This chapter provides a summary of the study's findings, highlighting its key contributions and the most important conclusions drawn from the research. Additionally, it suggests areas for improvement and proposes future research directions related to this topic.

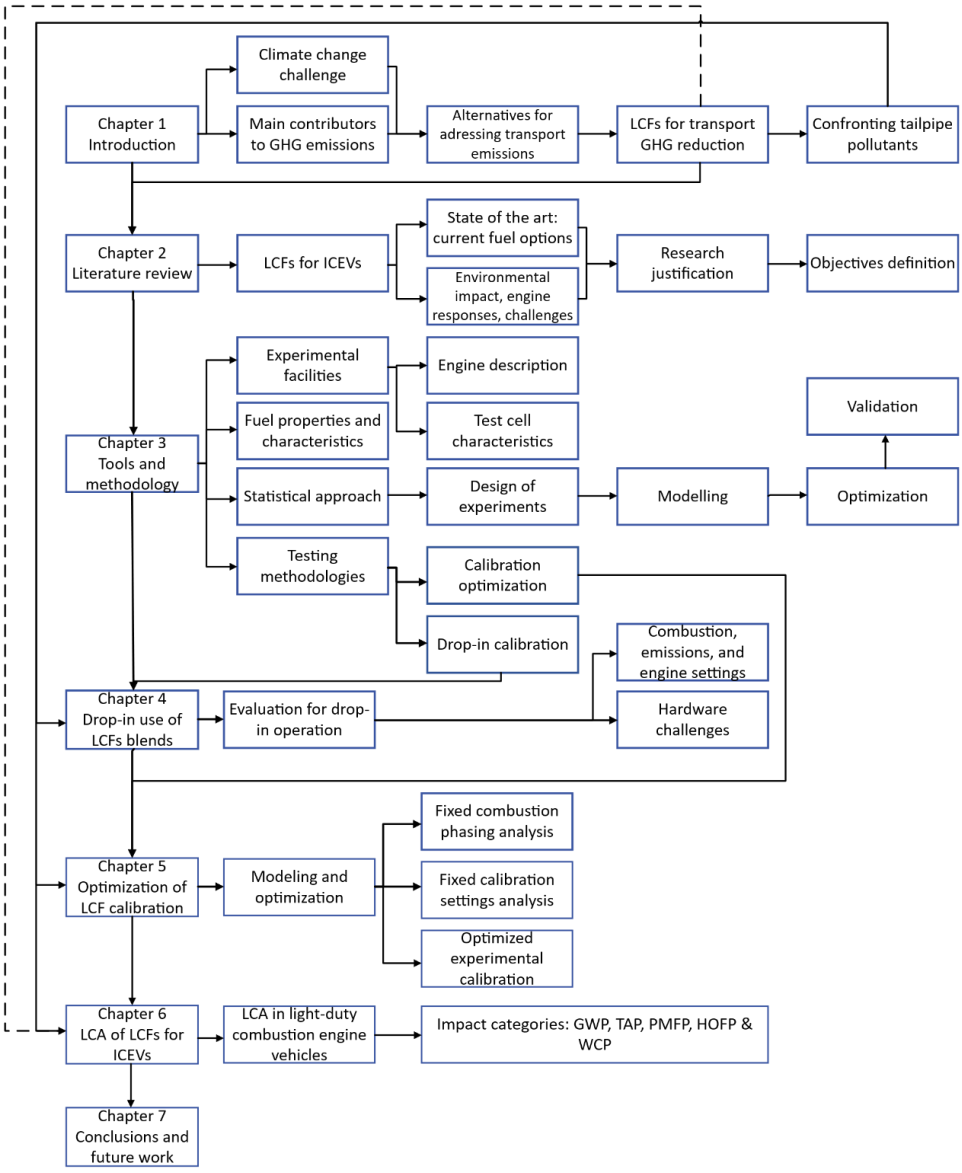

Figure 4. Graphical representation of the argument line followed in the investigation.

5 References

[1] W. Steffen, J. Rockström, K. Richardson, T. M. Lenton, C. Folke, D. Liverman, C. P. Summerhayes, A. D. Barnosky, S. E. Cornell, M. Crucifix, J. F. Donges, I. Fetzer, S. J. Lade, M. Scheffer, R. Winkelmann y H. J. Schellnhuber, «Trajectories of the Earth System in the Anthropocene,» *Proceedings of the National Academy of Sciences*, vol. 115, nº 33, pp. 8252-8259, 2018.

[2] N. Wunderling, R. Winkelmann, J. Rockström y e. al., «Global warming overshoots increase risks of climate tipping cascades in a network model,» *Nature Climate Change*, vol. 13, pp. 75-82, 2023.

[3] V. Masson-Delmotte, P. Zhai, H.-O. Pörtner, D. Roberts, J. Skea, P. Shukla, A. Pirani, W. Moufouma-Okia, C. Péan, R. Pidcock, S. Connors, J. Matthews, Y. Chen, X. Zhou, M. Gomis, E. Lonnoy, T. Maycock, M. Tignor y T. Waterfield, «Global Warming of 1.5°C. An IPCC Special Report on the impacts,» IPCC, 2018.

[4] UN General Assembly, *United Nations Framework Convention on Climate Change : resolution / adopted by the General Assembly*, UN General Assembly, 1994.

[5] J. Lelieveld, J. Evans, D. Giannadaki y A. Pozzer, «The contribution of outdoor air pollution sources to premature mortality on a global scale,» *Nature*, vol. 525, pp. 367-371, 2015.

[6] H. Ritchie, M. Roser and P. Rosado, "CO_2 and Greenhouse Gas Emissions," OurWorldInData.org, 2020. [Online]. Available: https://ourworldindata.org/co2-and-greenhouse-gas-emissions. [Accessed April 2023].

[7] H. Ritchie, "Cars, planes, trains: where do CO2 emissions from transport come from?," Our World in Data, 06 October 2020. [Online]. Available: https://ourworldindata.org/co2-emissions-from-transport. [Accessed 11 April 2023].

[8] H. Ishaq y C. Crawford, «CO2-based alternative fuel production to support development of CO2 capture, utilization and storage,» *Fuel*, vol. 331, nº Part 2, p. 125684, 2023.

[9] B. Sen, N. C. Onat, M. Kucukvar y O. Tatari, «Material footprint of electric vehicles: A multiregional life cycle assessment,» *Journal of Cleaner Production*, vol. 209, pp. 1033-1043, 2019.

[10] G. Puig-Samper Naranjo, D. Bolonio, M. F. Ortega y M.-J. García-Martínez, «Comparative life cycle assessment of conventional, electric and hybrid passenger vehicles in Spain,» *Journal of Cleaner Production*, p. 125883, 2021.

[11] E. Karaaslan, Y. Zhao y O. Tatari, «Comparative life cycle assessment of sport utility vehicles with different fuel options,» *Int J Life Cycle Assess*, vol. 23, p. 333–347, 2018.

[12] L. La Picirelli de Souza, E. E. Silva Lora, J. C. Escobar Palacio, M. H. Rocha, M. L. Grillo Renó y O. J. Venturini, «Comparative environmental life cycle assessment of conventional vehicles with different fuel options, plug-in hybrid and electric vehicles for a sustainable transportation system in Brazil,» *Journal of Cleaner Production*, vol. 203, pp. 444-468, 2018.

[13] T. Gersdorf, P. Schaufuss, S. Schenk and P. Hertzke, "McKinsey Electric Vehicle Index: Europe cushions a global plunge in EV sales," July 2020. [Online]. Available: https://www.mckinsey.com/~/media/McKinsey/Industries/Automotive%20and%20Assembly/Our%20Insights/McKinsey%20Electric%20Vehicle%20Index%20Europe%20cushions%20a%20global%20plunge%20in%20EV%20sales/McKinsey-Electric-Vehicle-Index-Europe-cushions-a-global-plun. [Accessed 10 April 2021].

[14] Z. Liu, J. Song, J. Kubal, N. Susarla, K. W. Knehr, E. Islam, P. Nelson y S. Ahmed, «Comparing total cost of ownership of battery electric vehicles and internal combustion engine vehicles,» *Energy Policy*, vol. 158, p. 112564, 2021.

[15] Y. Zhou, R. Wen, H. Wang y H. Cai, «Optimal battery electric vehicles range: A study considering heterogeneous travel patterns, charging behaviors, and access to charging infrastructure,» *Energy*, vol. 197, p. 116945, 2020.

[16] Y. Zeng, D. Chalise, s. D. Lubner, S. Kaur y R. S. Prasher, «A review of thermal physics and management inside lithium-ion batteries for high energy density and fast charging,» *Energy Storage Materials,* vol. 41, pp. 264-288, 2021.

[17] European Comission, *Proposal for a REGULATION OF THE EUROPEAN PARLIAMENT AND OF THE COUNCIL amending Regulation (EU) 2019/631 as regards strengthening the CO2 emission performance standards for new passenger cars and new light commercial vehicles in line with the Union's inc,* Brussels: European Comission, 2021.

[18] C. Zhang, X. Zhao, R. Sacchi y F. You, «Trade-off between critical metal requirement and transportation decarbonization in automotive electrification,» *Nature Communications,* vol. 14, p. 1616, 2023.

[19] R. B. Kaunda, «Potential environmental impacts of lithium mining,» *Journal of Energy & Natural Resources Law,* vol. 38, nº 3, pp. 237-244, 2020.

[20] A. M. Haidar, K. Muttaqi y D. Sutanto, «Technical challenges for electric power industries due to grid-integrated electric vehicles in low voltage distributions: A review,» *Energy Conversion and Management,* vol. 86, pp. 689-700, 2014.

[21] N. Ortar y M. Ryghaug, «Should All Cars Be Electric by 2025? The Electric Car Debate in Europe,» *Sustainability,* vol. 11, nº 7, p. 1868, 2019.

[22] F. Alanazi, «Electric Vehicles: Benefits, Challenges, and Potential Solutions for Widespread Adaptation,» *Applied Sciences,* vol. 13, nº 10, p. 6016, 2023.

[23] B. Mohamed, B. Ali, B. Ahmed, B. Ahmed, L. Salah y D. Rachid, «Study of hydrogen production by solar energy as tool of storing and utilization renewable energy for the desert areas,» *International Journal of Hydrogen Energy,* vol. 41, nº 45, pp. 20788-20806, 2016.

[24] D. Candelaresi, A. Valente, D. Iribarren, J. Dufour y G. Spazzafumo, «Comparative life cycle assessment of hydrogen-fuelled passenger cars,» *International Journal of Hydrogen Energy,* vol. 46, pp. 35961-35973, 2021.

[25] O. Winjobi, J. C. Kelly y Q. Dai, *Life-cycle analysis, by global region, of automotive lithium-ion nickel manganese cobalt batteries of varying nickel content,* 2022.

[26] M. Q. Wang, *GREET 1.5 - transportation fuel-cycle model - Vol. 1 : methodology, development, use, and results. Office of Scientific and Technical Information (OSTI),* 1999.

[27] D. A. Notter, M. Gauch, R. Widmer, P. Wäger, A. Stamp, R. Zah y H.-J. Althaus, «Contribution of Li-Ion Batteries to the Environmental Impact of Electric Vehicles,» *Environmental Science & Technology,* vol. 44, nº 17, pp. 6550-6556, 2010.

Chapter 2
A Comprehensive Review of Low Carbon Fuels for Diesel Engines

Contents

1 Introduction

Low carbon fuels (LCFs) offer the potential to significantly reduce carbon footprints compared to conventional fossil fuels, making them an appealing option for mitigating emissions without the need for immediate changes to existing internal combustion engine vehicles (ICEVs) or distribution infrastructure. Fundamentally, an LCF is a type of fuel that generates fewer greenhouse gas (GHG) emissions, particularly carbon dioxide (CO_2), when produced compared to conventional fossil fuels like gasoline or diesel (even neutral or negative carbon emissions [1, 2]). These fuels are often produced from renewable resources or incorporate advanced technologies to reduce their carbon footprint, making them a more environmentally friendly option for powering vehicles, industries, or other energy needs.

In recent decades, internal combustion engines (ICEs) have remained the dominant force in land transportation [3]. Significant progress has been made in enhancing their efficiency, reducing emissions, and implementing advanced combustion techniques. These advancements have led to a sharp decline in criteria emissions, largely due to regulations like the Euro 6 normative in Europe [4, 5], which have rendered engines cleaner and more efficient [6, 7]. Key developments in this area encompass improved fuel injection systems, enhanced aftertreatment systems, advanced combustion strategies, and downsizing methods, among others. However, these strategies primarily focus on improving vehicle hardware and do not directly tackle a crucial issue of our time: the energy source.

While electric vehicles (EVs) are a viable alternative with zero engine-out emissions, projections suggest that ICEs will still constitute over 70% of vehicles on the road by 2040 [8, 9]. Hybrid electric vehicles, while offering some improvement in fuel consumption, introduce additional complexity to the vehicle [10]. Therefore, mitigating CO_2 emissions and reducing exhaust pollutants from ICEs could have a substantial impact, potentially affecting nearly 25% of total GHG emissions in Europe [11].

Addressing carbon emissions in the transportation sector requires a multifaceted approach that considers LCFs, strategies for reducing tailpipe emissions of ICEVs, EVs, and urban planning strategies that can solve the challenge of transporting people and goods from one place to another with the least negative environmental and social impact. Continuing research on LCFs ensures that their GHG mitigation can surpass the conceptual paradigm and be applicable in the transition towards renewable energy and away from fossil resources. In addition, researching the application of LCFs beyond just GHG effects can potentially limit other harmful pollutants which can lead to improved air quality and public health. Similarly, LCFs

can address sectors that are difficult to electrify due to their energy density and operational requirements like aviation, heavy industry, and long-haul freight transport.

This chapter will explore LCFs, how they burn in the engine, their pollutants, and their environmental impact. By doing so, the emissions reduction potential of LCFs will be highlighted while simultaneously identifying the critical areas where further improvements and research are warranted.

2 Types of low carbon fuels for compression ignition engines

In the realm of energy resources, the classification of fuels helps to understand the diversity and utility of these energy sources. Figure 1 provides a structured overview of fuel classifications along four distinct dimensions: state of matter, feedstock origin, composition, and final use. By categorizing fuels based on their physical state—gaseous, liquid, or solid—their differing properties and storage requirements are acknowledged. Distinguishing fuels by their feedstock origin—whether fossil, renewable, or synthetic—underscores the environmental implications of their utilization. The consideration of composition reveals the elemental makeup of fuels, elucidating distinctions between hydrocarbon-based and non-hydrocarbon fuels. Lastly, categorizing fuels by their intended use, such as transportation, industrial, residential, or power generation, underscores the practical applications that guide fuel selection.

Due to the importance of the origin of the raw material and the production pathway for the definition of a fuel as an LCF, as well as the interest in addressing emissions from the road transportation sector, the focus of this section is the classification of the fuels according to their feedstock. This in turn introduces the importance of the life cycle assessment (LCA) as a method for evaluating the environmental impacts of a fuel throughout its entire life cycle. Still, the discussion on different fuels regarding their compositions and the explanations on how these properties affect the combustion of ICEs will be detailed.

LCFs encompass a range of options. These fuels can be categorized into various types, each with their unique production methods and sources. Biofuels are produced from plant materials and vegetable oils. Meanwhile, synthetic fuels, like power-to-liquid (PTL) and power-to-gas (PTG), offer flexibility and potential for emissions reduction by converting electricity into synthetic hydrocarbons or hydrogen. There can also be an overlap between synthetic and biofuels as feedstocks of biological origin go through chemical and industrial processes to be synthetized into new fuel

products. Nonetheless, in this chapter a binary classification is adopted for simplicity.

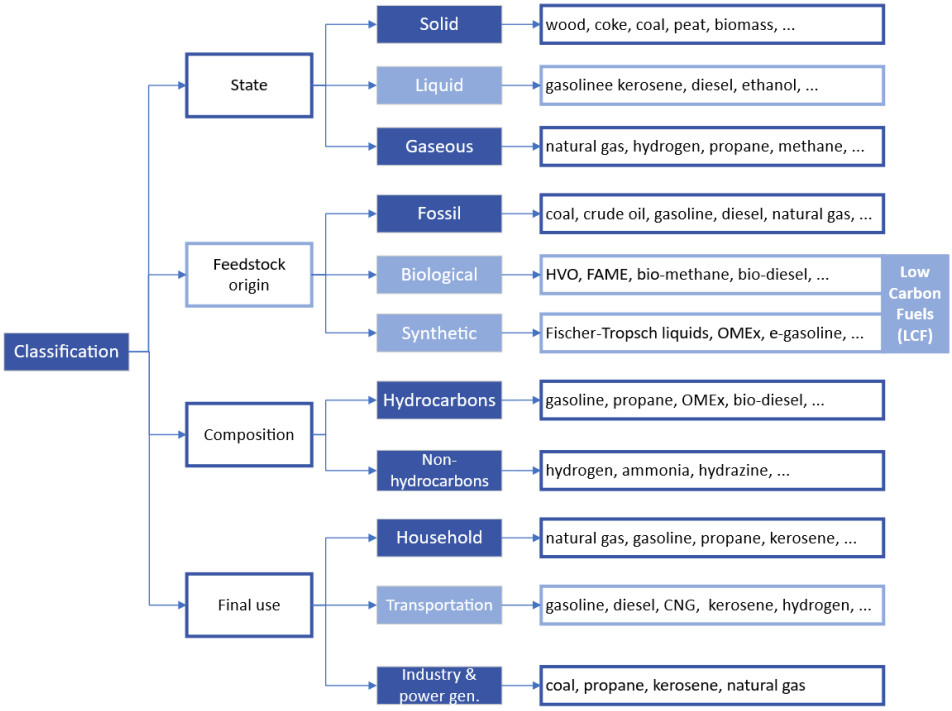

Figure 1. Classification of fuels by different criteria

2.1 Biofuels: from the first generation to the state-of-the-art

Biofuel is a type of renewable energy vector derived from organic materials, primarily plants and microorganisms. Biofuels are generally classified by their generation, for which four are usually listed. First-generation biofuels were derived from sugars, starches and oils [12]. These first-generation fuels were criticized for having low yields, competing with food crops and causing environmental harm [13].

Second-generation biofuels utilized specific plants (dedicated feedstocks) to directly extract oil from their roots, reducing the fuel-food competition. In this generation, higher fuel yields were also achieved [14]. The biofuels can be produced through biochemical or thermochemical routes [15]. In the biochemical route, enzymes and microorganisms convert cellulose and hemicellulose to sugars, which are then fermented to produce biofuels. In the thermochemical route, pyrolysis or gasification technologies convert biomass into a synthesis gas that can be further converted into

various biofuels. Besides the advancement of this generation, significant technical challenges persisted for 2nd-generation biofuel production.

Third-generation biofuels are primarily derived from microalgae cultivated in various water sources, such as shallow lagoons, raceway ponds, or closed ponds year-round (unless limited by the sun). Microalgae have a high lipid content, which can be converted into biofuels [16, 17]. Unlike the first two generations, they do not rely on food or dedicated crops. These fuels provided a high yield potential and suitability for growth in various environments. In this generation, one of the difficulties was scaling up algae cultivation and lipid extraction [13].

Fourth-generation biofuels involve the metabolic engineering of microorganisms, such as bacteria or cyanobacteria, to produce biofuels directly from CO_2 or other feedstocks [18]. These biofuels are produced by modifying the metabolic pathways of microorganisms to enhance biofuel production. Metabolic engineering allows for the efficient production of biofuels with minimal environmental impact, requiring fewer resources like water and land [12].

In addition to the advances in the production of fuels, new regulation has been proposed to guarantee that the fuels do not further harm the environment nor the food supplies. To comply with EU biofuel sustainability criteria, new facilities must adopt voluntary verification schemes to ensure that biofuel production doesn't harm biodiversity or soil organic carbon while maintaining substantial GHG reductions compared to fossil fuels [19]. For this purpose, several verification schemes, such as ISCC (International Sustainability and Carbon Certification) and RSB (Roundtable of Sustainable Biofuels) can help monitor feedstock traceability, mass balances, and GHG emissions [20].

The following subsections will delve into the specific characteristics and properties of three distinct fuels that form a crucial part of the composition examined LCFs in this thesis. These fuels, namely Hydrotreated Vegetable Oil (HVO), Fatty Acid Methyl Ester (FAME), and Rapeseed Methyl Ester (RME), have garnered significant attention in recent years due to their renewable attributes.

2.1.1 Fatty Acid Methyl Ester and Rapeseed Methyl Ester

FAME and RME are both biodiesel fuels that have gained significant attention in recent years as environmentally friendly alternatives to traditional fossil fuels. FAME is derived from renewable resources such as vegetable oils, animal fats, or recycled cooking oils and extraction from algae. The production process involves a transesterification reaction (exchange of one ester group in a molecule with another

alcohol or ester group), where triglycerides present in these feedstocks are converted into fatty acid methyl esters using methanol or ethanol. RME, on the other hand, is a specific type of oxygenated biodiesel primarily derived from rapeseed oil, hence the name "Rapeseed Methyl Ester." Rapeseed oil is a popular feedstock for biodiesel production due to its favorable fatty acid composition, making it a suitable source for the transesterification process. RME is known for its good cold flow properties and can be used in colder climates without significant performance concerns.

Vyas et al. [21] discuss literature on transesterification reactions using homogeneous, heterogeneous, and enzyme catalysts, along with techniques like ultrasound, microwave, and supercritical alcohol, as well as algae-based biodiesel. The work goes on to discuss various transesterification methods, including homogeneous alkali-catalyzed, homogeneous acid-catalyzed, and heterogeneous acid and base-catalyzed transesterification. It highlights the advantages and limitations of these processes, emphasizing the importance of feedstock purity and free fatty acid (FFA) content, which should be below 0.5% by weight to prevent saponification [22].

Enzymatic transesterification using lipase was examined by [23], emphasizing its advantages in terms of product separation, wastewater treatment, glycerol recovery and no side reactions. The challenges of enzyme cost and water content are discussed. Supercritical and subcritical alcohol transesterification methods are presented, highlighting their rapid reaction rates and single-phase reactions. The work of [21] also explores the use of microwave irradiation for transesterification, noting its efficiency in reducing reaction times and energy consumption.

The production of FAME (and thus also RME) through transesterification is a crucial process for biodiesel production. To make this process more efficient and environmentally friendly, researchers are exploring various catalysts. Nisar et al. [24] indicated in 2021 that currently, both homogeneous and heterogeneous catalysts are used in the transesterification process. Homogeneous catalysts, which are soluble in the reaction media, have been widely employed, particularly alkaline ones, due to their high reaction rates. However, they are less effective when dealing with feedstocks containing high levels of FFA, as they can lead to saponification. On the other hand, heterogeneous catalysts, such as heteropoly acids (HPAs), polyoxometalate compounds, carbonaceous materials, and vanadium phosphate, are gaining attention for their ability to handle high-FFA feedstocks and for their environmental benefits. Enzymatic catalysts, like lipases, are also explored, offering advantages such as renewable residues and thermostability.

A 2020 report by Prussi et al. [25] analyzes various pathways for biodiesel production in Europe. Biodiesel in Europe is primarily made from rapeseed as RME, with some usage of sunflower, soybeans, palm oil, tallow, and waste cooking oils as feedstocks. Methanol is commonly used for transesterification in FAME production (Figure 2) but ethanol can also replace methanol in some cases.

In a publication that discusses the production and use of alternative fuels in the context of decarbonizing road transportation in the EU and the United States from the perspective of the GREET and JEC v5 studies, Cai et al. [26] examine various fuel categories, as well as electricity. The analysis centers on key feedstock types and conversion technologies relevant to commercialization. Among the fuels, the authors discuss the production of FAME from sources like soybean oil, canola oil, used cooking oil, and animal fats. In the United States, soybean serves as a primary source for FAME production. Different allocation methods for co-products during the FAME production process result in variations in emissions estimates between the two methods discussed. Canola oil and inedible tallow are also examined as FAME feedstocks. The paper highlights the differences in emissions estimates for various fuels and feedstocks, such as soybean FAME and canola FAME. Regardless of the feedstock and the perspective used for the analysis, FAME was estimated to have carbon neutrality in terms of biogenic carbon and biodiesel is shown to have a carbon offset potential in its well-to-tank (WTT).

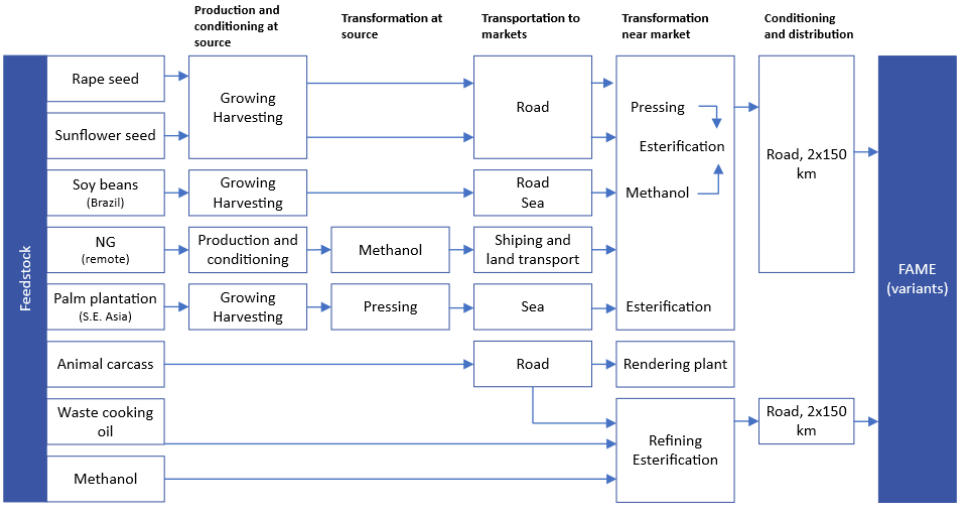

Figure 2. FAME production pathways (adapted from [25])

A comparison between biofuels and conventional fuel made by Tucki et al. [27] found that FAME fuel had higher direct emissions of CO_2 compared to conventional diesel but had a more favorable overall emission balance when considering the entire life cycle. The study used various assessment methods to evaluate the impact of fuels on human health, ecosystems, climate change, and resources, finding that different fuels had varying impacts, with FAME fuel having a beneficial effect on climate change due to carbon dioxide absorption during plant growth.

2.1.1.1 Use of FAME and RME in ICEs

Using optical engine diagnostics in engine, Cheng et al. [28] assessed the combustion of RME (a representative of FAME) finding that RME exhibited the shortest ignition delay time (IDT) with fast luminous intensity increase during ignition and premixed combustion. Additionally, HVO and RME showed faster flame expansion during combustion, leading to shorter combustion durations.

The use of FAME as a substitute for fossil diesel can have varying benefits in terms of fuel consumption. Substitutions of up to 35% of RME in diesel resulted in a maximum reduction of 6% in fuel consumption, while with a 10% replacement with RME resulted in a best case scenario of 9% reduction as reported in the work of Labeckas and Slavinskas [29]; nonetheless, when the authors tested neat RME an increase of nearly 9% in fuel consumption was observed. In their work, at lower speeds, blends of 5% to 35% RME had similar brake specific fuel consumption (BSFC) to diesel due to their higher oxygen content, which promoted more complete combustion. However, at higher speeds, only 5% and 10% RME maintained lower BSFC, indicating reduced oxygen's impact. The authors speculated that the blend's structure, physical properties, injection timing, and combustion processes played a role, especially at high speeds.

Tsolakis et al. [30], Novakovic et al. [31], Kroyan et al. [32] and Al Ezzi et al. [33] also tested RME in CI engines of different sizes. Their results show a consisted increase in fuel consumption of up to 17-20% compared to diesel when using neat RME, while blends of 10 and 20% RME show increases in fuel consumption close to 6%. The difference in the fuel consumption is agreed by the authors to be related to lower lower heating value (LHV) of the RME fuel in comparison to diesel. Although most studies reported an increase in fuel consumption when using the biofuel, the authors observed that under high engine load conditions, the difference in BSFC between RME and diesel was lower compared to low engine load conditions, where incomplete fuel combustion inside the cylinder contributed to increased BSFC.

The NOx-soot tradeoff of FAME across different studies can be seen in Figure 3. In many of the reviewed studies the use of FAME at different proportions can reduce soot emissions when compared to diesel. In [30, 33] the authors argue that the higher oxygen content in the biodiesel, such as RME, contributes to improved fuel oxidation even in locally rich fuel combustion zones, leading to reduced smoke emissions, effect which is notable at the center line of the fuel jet, where increased oxygen concentration and reduced fuel residence time enhance soot reduction as soot precursor species tend to react with molecular oxygen or oxygen-containing radicals (e.g., OH, O) and produce CO rather than aromatics and soot. Additionally, the reduction of the aromatics content in the fuel is cited as a cause for the soot emissions reduction.

The NOx compared to diesel has a wider range of possible outcomes, where NOx emissions can either be increased or decreased using FAME. According to [33], RME combustion leads to higher NOx emissions compared to diesel at low engine load, while the opposite is true at high engine load. The faster combustion and higher heat release of RME contribute to increased NOx formation.

In [29] the authors distinguish between nitrogen monoxide (NO) and nitrogen dioxide (NO_2), and their results show that NO emissions increase gradually with load, with FAME biofuel blends showing mixed results compared to Diesel fuel, depending on the oxygen content. Notably, the 5% blend consistently exhibited lower NO emissions. Furthermore, the study highlights that biofuels tend to exhibit lower NO_2 emissions, possibly due to their oxygenated nature, which encourages NO_2 conversion back to NO. Neat RME, without aromatic compounds, shows lower NOx emissions compared to other blends, although its NOx emissions remain slightly higher than Diesel fuel, primarily due to the effect of fuel oxygen.

For the CO and HC emissions (Figure 4), the FAME fuel results remain relatively close to diesel values. Tongroon et al. [34] observed CO emissions experienced a reduction when a FAME blend was utilized, and a similar decrease was observed in total hydrocarbon emissions (THC). This phenomenon is primarily attributed to the influence of the air/fuel ratio. When the air/fuel ratio shifts from stoichiometric to lean mixtures, combustion tends to produce lower CO because the fuel is oxidized in the presence of sufficient oxygen. The FAME blend, characterized by a high oxygen content, results in a leaner mixture compared to diesel fuel, leading to lower CO emissions. Furthermore, the high oxygen content promotes more complete combustion, ultimately resulting in reduced levels of THC.

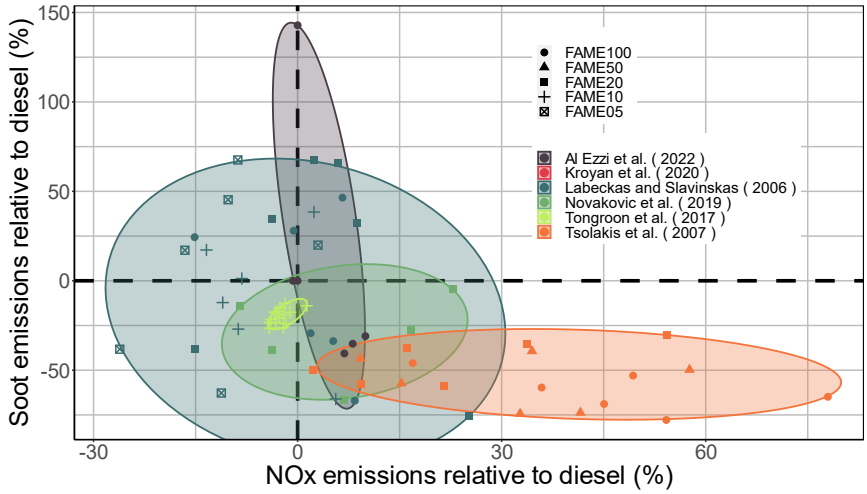

Figure 3. NOx-soot tradeoff compared to diesel across different studies with FAME (data from [33, 32, 29, 31, 34, 30])

A similar comparison of emissions was done in a review by Unglert et al. [35] reaching similar conclusions to this work, NOx rises an average of 13% because the use of biodiesel has led to higher combustion temperatures for the different works the authors reviewed. Meanwhile, on average, HC emissions show a reduction of 36%, while carbon monoxide emissions exhibit a 25% decrease, and there is a 31% decline in particulate mass emissions.

FAME and by extension RME can also have effects on the engine beyond just emissions. The formation of particulate matter (PM) can have a large impact on engine durability. Diagnostics reported by Cieślikowski [36] reveal issues such as injector dysfunction contributing to PM formation, emphasizing the importance of timely service interventions. Fuel properties like high viscosity, low volatility, and the presence of biocomponents in FAME are identified as factors facilitating PM formation, leading to engine failure states. The analysis extends to various engine components, including turbochargers and exhaust gas recirculation (EGR) valves. Furthermore, the paper discusses the formation of internal diesel injector deposits (IDID), emphasizing the role of FAME additives in their formation and the need for preventive maintenance through diagnostics.

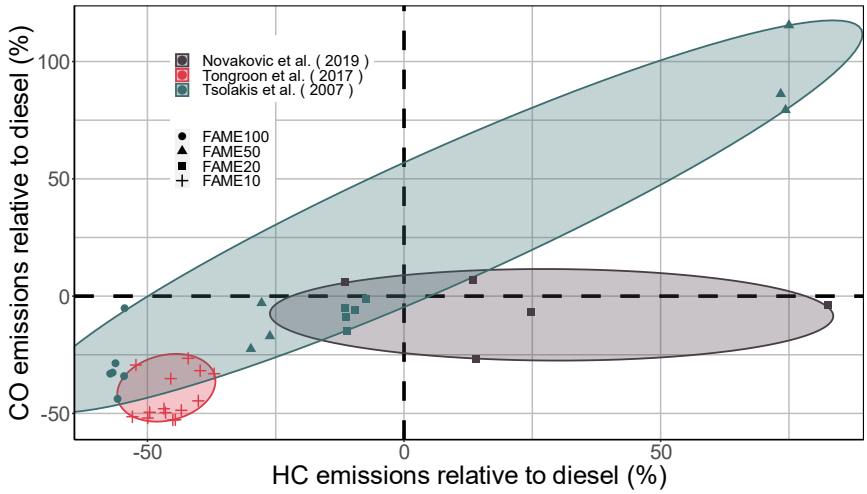

Figure 4. HC-CO tradeoff compared to diesel across different studies with FAME (data from [31, 34, 30])

One specific challenge posed by FAME, according to Unglert et al. [35], lies in the accumulation of fuel in the oil without evaporation, resulting in a continuous dilution of the engine lubricant. Three primary factors contribute to this problem. First, ester oils, like FAME, exhibit significant creep capabilities compared to hydrocarbons of equivalent viscosity, leading to increased unburned FAME entering the engine oil. Second, modern diesel engines equipped with diesel particulate filters (DPF) often employ post-injection systems to regenerate the filter by increasing the exhaust temperate, which introduces additional fuel into the engine oil due to higher partially burned fuel at the exhaust. Lastly, the higher boiling temperature of FAME compared to diesel fuel causes a substantial portion of FAME to remain in the lubricant, resulting in permanent dilution. At elevated engine oil temperatures, biodiesel remains in the oil while fossil diesel evaporates. This oil dilution can reach up to 20% FAME by the end of conventional oil change intervals, posing a risk of viscosity reduction and wear. Additionally, the dilution of engine oil additives, such as ZDDP, by biodiesel can hinder their effectiveness. These issues are less pronounced with vegetable oil fuel due to differences in viscosity.

2.1.2 Hydrotreated vegetable oil

HVO, also known as renewable diesel, is a non-oxygenated fuel produced through the hydrogenation process of vegetable oils or animal fats via a catalytic process [37]. The fuel is considered a third-generation fuel, whose quality is independent of the feedstock [38]. It shares several similarities with traditional diesel, like a high

cetane number due to its high paraffin content. Additionally, HVO boasts better cold-weather performance, better stability during storage, slower aging and reduced emissions of NOx and deposit formation. The slower aging and lower deposit formation help improve the compatibility with ICE components, especially the injection system. HVO also meets European diesel standards (EN 590) except for density, but up to 30% can be blended into diesel without issue [39]. Additionally, HVO's production is not affected by the FFA percentage allowing in part to sustain higher yields [40].

In a 2011 study, Arvidsson et al. [41] presented an LCAof HVO biofuel covering the entire life cycle, including vegetable oil production from sources like rape, oil palm, or Jatropha, oil transport, HVO production, and HVO combustion in heavy-duty trucks. The study found that HVO produced from palm oil, when combined with biogas production from palm oil mill effluent, has the lowest environmental impact among the feedstocks studied. More importantly, they found that HVO has a significantly lower global warming potential (GWP) compared to conventional diesel for all feedstocks (rape oil, oil palm and Jatropha), with GWP similar to results for rape methyl ester reported in literature [42]. In their study they also found soil emissions, primarily nitrous oxide (N_2O), are the largest contributors to most environmental impact categories for HVO, regardless of the feedstock.

The emissions from two Euro 6b diesel passenger cars using different blends of HVO, fossil diesel, and commercial diesel B7 under various temperature conditions was done by [38]. Tests were conducted in a laboratory and on-road in Italy. The HVO blends included Neat HVO (100% HVO), 30% HVO, and 7% HVO. Overall, the use of different HVO blends and diesel did not significantly affect vehicle emissions. However, HVO-100 resulted in about 4% lower CO_2 emissions compared to other fuels. On-road tests showed similar NOx emissions for all HVO blends, suggesting that SCR systems may perform differently in laboratory and real driving conditions. HVO-100 also had significantly lower CO_2 emissions compared to other HVO blends both on-road and in the laboratory.

In the JEC Well-to-Tank report [25], HVO is considered either alone or mixed with petroleum products. The report highlights different production pathways, indicating that its production results in high-quality diesel fuel but requires additional energy for the hydrotreating process (see Figure 5). Comparing HVO pathways with FAME pathways shows that overall energy consumption is similar for both HVO and FAME production methods.

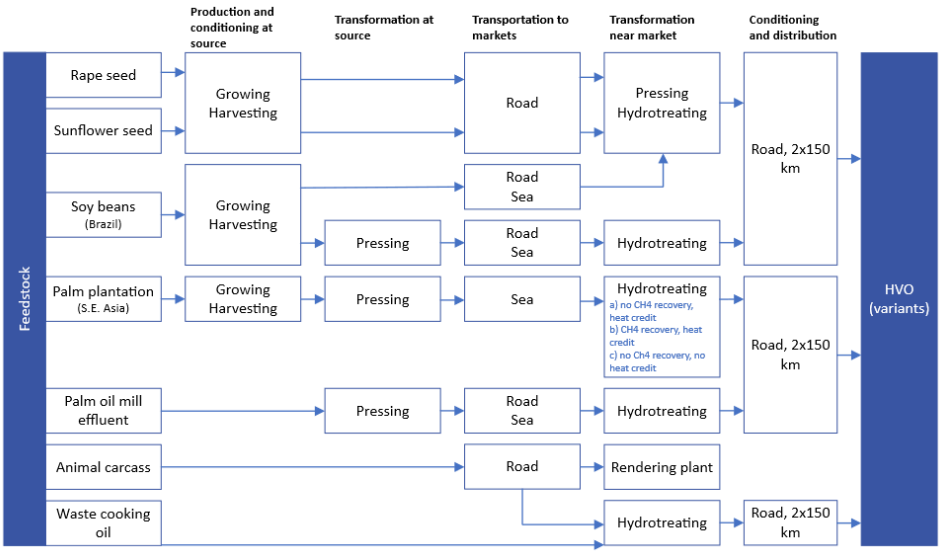

Figure 5. HVO production pathways (adapted from [25])

The choice of feedstock used in HVO production is a key factor in determining its sustainability. European HVO production plants currently source feedstocks from various parts of the world, including palm oil and PFAD from Southeast Asia, but also from wastes, residues, used cooking oil, and vegetable oils. HVO produced from residual feedstocks significantly reduces GHG emissions, meeting EU sustainability criteria [20].

Rodríguez-Fernández et al. [43] investigated the property changes of the addition of biofuels to diesel from 0% biofuel content to 100% biofuel content. For the HVO fuel they found that the density of HVO blends is lower than that of diesel, while a blend of FAMEs and FAGEs increases the density. HVO has a higher LHV in mass units compared to diesel, but in volume units, it's lower due to the paraffinic nature of the fuel. Cold flow properties, such as cloud point (CP) and cold filter plugging point (CFPP), are important for preventing startability issues in cold weather and HVO is improved over diesel. Water content in fuel is a crucial property to control and to prevent corrosion, microbial growth, and decreased fuel lubricity. European Standards EN 590 and EN 15940 limit water content to under 200 mg/kg. HVO has low water content, meeting the respective quality standards.

2.1.2.1 Use of HVO in ICEs

The production of HVO, as discussed, has a considerably lower environmental impact than diesel in most categories. And even though HVO is considered almost an equivalent to diesel, in the fact that it can be substituted without modifications to the engine, its differences modify the combustion process of compression ignition (CI) engines and thus it changes the efficiency, performance, and emissions of the engine. The combustion behavior of HVO differs significantly from other fuels, primarily due to its unique composition. HVO contains long straight carbon-chain compounds, which set it apart from conventional fuels like diesel. This distinctive composition allows HVO to initiate combustion much earlier in the engine's combustion cycle [44]. The long and straight carbon chains in HVO are more readily reactive, making it easier for them to ignite and contribute to the combustion process.

In terms of fuel consumption, the higher than diesel's LHV of HVO generally improve the fuel consumption of the engine when compared to diesel. On average across different engine operating conditions, Bortel et al. [45] obtained a reduction of around 3% in fuel consumption when using a 30% blend of HVO with diesel, and a reduction of nearly 5% when using 100% HVO. Similarly, Preuß et al. [46] found an average reduction of 2.8% in a heavy duty engine using HVO, while in a light-duty engine they found a reduction of 2.5%. Meanwhile, in the work of Mancarella and Marello [47] the reduction was on average 3.3% at 1250 rpm @ 2 bar, and 2.2% at 2000 rpm @ 9 bar of brake mean effective pressure (BMEP).

Figure 6 shows the NOx-soot tradeoff of HVO relative to diesel across different studies with HVO. In the studies the NOx and soot emissions of HVO relative to diesel can be seen to achieve reductions of up to 20% in NOx [47] and more than 75% in soot [48], with a significant portion of the tested operating conditions below their respective diesel reference. However, the figure also shows scenarios where although NOx emissions are lower than diesel the soot emission are up to 62% higher (with a difference of 0.026 g/kWh [47]), or when soot emissions are lower than diesel, NOx emissions are up to 32.9% higher (0.4 g/kWh [46]). The study of Bortel et al. [45] also tests a 30% HVO – 70% diesel blend, which indicates a good reduction of NOx with respect to diesel when adding a proportion of the biofuel, while at the same time reducing the FSN with exceptions.

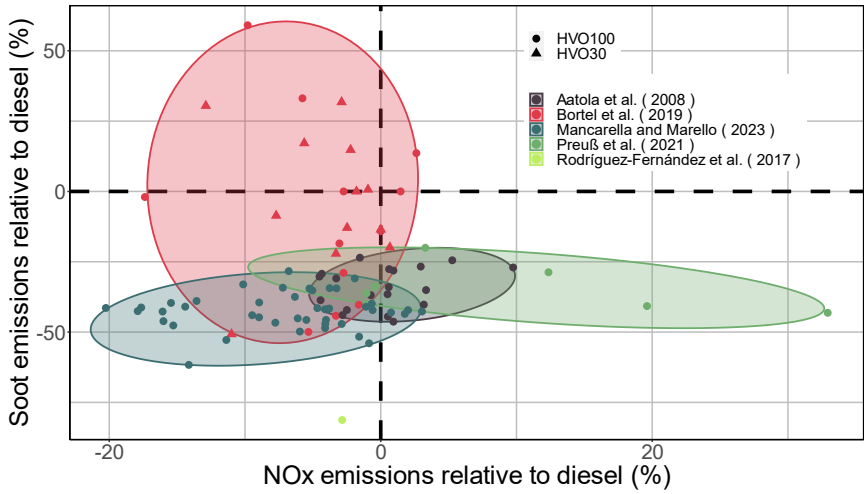

Figure 6. NOx-soot tradeoff compared to diesel across different studies with HVO (data from [37, 45, 47, 46, 48])

In Figure 7 we can see the experimental results from the previously discussed studies [45, 47], where it can be seen that HVO is able to both reduce the CO and HC emissions with respect to diesel. One explanation provided is that because HVO has a lower distillation range the fuel evaporation and mixing with air is improved, while its higher cetane number (CN) ensures heightened reactivity during combustion at lower temperatures and lighter loads.

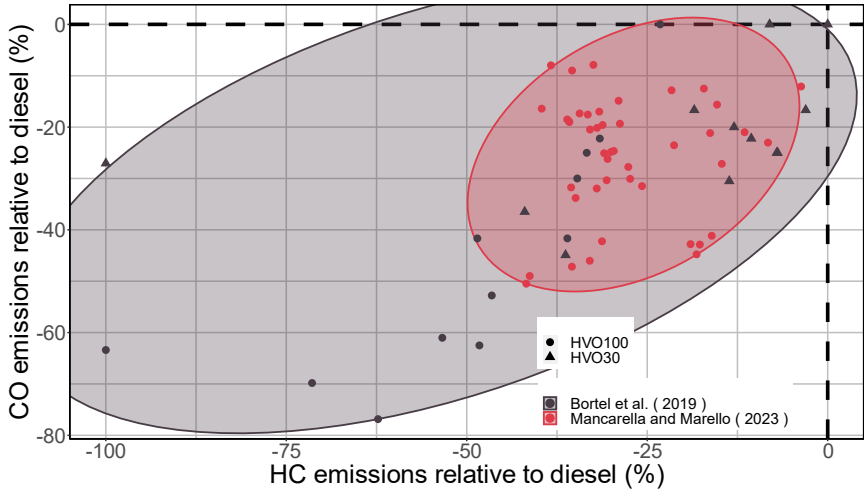

Figure 7. HC-CO tradeoff compared to diesel across different studies with HVO (data from [45, 47])

The review by Unglert et al. [35] agrees with this review as HVO leads to a noticeable reduction in emissions of HC, CO, and PM compared to diesel fuel, and this decrease is directly proportional to the HVO content in the fuel. In contrast, NOx exhibits a non-uniform pattern.

2.2 Synthetic fuels: recycling existing carbon

Synthetic fuels, also known as synfuels, are liquid or gaseous fuels that are produced through chemical processes using feedstocks such as CO_2, water, and renewable energy sources like electricity or solar power. These fuels are designed to mimic the properties and energy content of conventional fossil fuels like gasoline, diesel, or natural gas. Common examples of synthetic fuels include hydrogen, synthetic gasoline, synthetic diesel, and synthetic natural gas. The production of synthetic fuels typically involves the conversion of renewable resources into energy carriers using various technologies, such as electrolysis for hydrogen production or Fischer-Tropsch synthesis for liquid hydrocarbons. Synthetic fuels are considered an important part of efforts to decarbonize the transportation and energy sectors, as they can be produced using renewable energy sources and can potentially reduce GHG emissions when used in place of traditional fossil fuels. They also have the advantage of compatibility with existing infrastructure and vehicles, making them a transitional solution toward a more sustainable energy future.

Carbon capture and storage (CCS) and carbon capture and utilization (CCU) are critical components in the quest to reduce emissions from synthetic fuel production. CCS involves capturing carbon dioxide emissions and storing them safely, while CCU as the name indicates refers to the use of the carbon. Various CCS and CCU technologies, including post-combustion capture and oxy-fuel combustion, contribute to emissions reduction. CCU processes involve using the captured CO_2 as a feedstock in combination with hydrogen to produce synthetic hydrocarbon fuels like synthetic gasoline or synthetic natural gas. This method not only reduces greenhouse gas emissions by preventing CO_2 release but also contributes to the production of cleaner, carbon-neutral, or even carbon-negative fuels [2].

Prussi et al. [25] comment for CCS processes that the energy required for CO_2 capture is often intertwined with the overall plant operations. In the production of transportation fuel through the gasification of coal and biomass followed by Fischer-Tropsch (FT) synthesis, CO_2 separation is necessary due to the need for low CO_2 content in the FT reactors (see Figure 8). The primary difference between plants with and without CCS lies in the energy-intensive process of compressing CO_2 for transport and injection into CO_2 repositories. The difference in coal input with and without CCS is minimal, likely due to differences in the overall process layout.

However, plants with CCS exhibit increased electricity requirements for CO_2 compression. In addition, processes involving FT synthesis for hydrogen and electricity production increase natural gas and coal requirements with CCS.

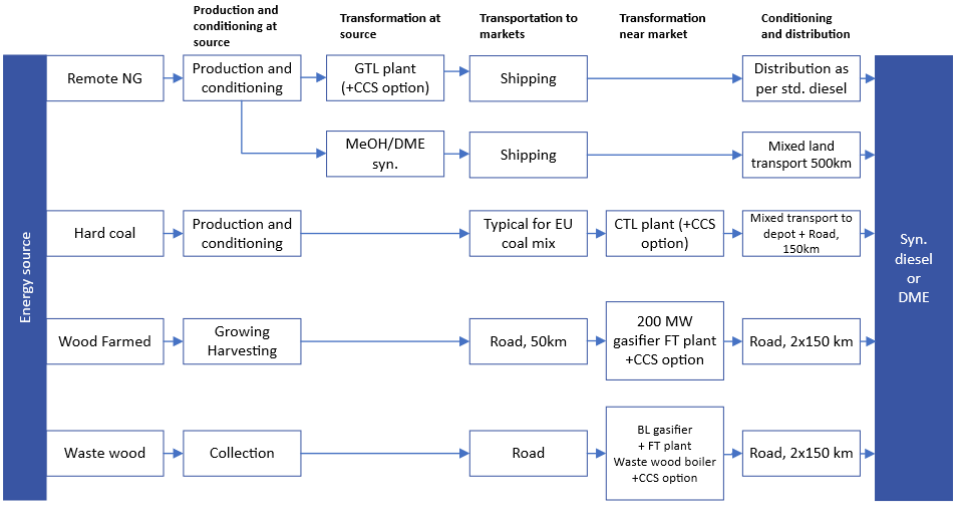

Figure 8. Synthetic diesel production pathways (adapted from [25])

Diesel-like synthetic fuels possess characteristics that make them an attractive alternative to conventional diesel fuels. Factors such as cetane number and energy density are vital considerations. Additionally, these fuels can be produced from a variety of feedstocks, including biomass-to-liquid (BTL) processes convert organic materials such as agricultural waste, forestry residues, and algae into synthetic diesel; and gas-to-liquid (GTL) processes convert natural gas into synthetic diesel.

2.2.1 Fischer-Tropsch Diesel

Early experiments with coal liquefaction and the FT process laid the groundwork for their application. FT synthesis is a chemical process used to produce synthetic liquid hydrocarbon fuels, such as diesel and gasoline, from carbon-containing feedstocks like coal, natural gas, or biomass. This process was originally developed in 1952 by chemists Franz Fischer and Hans Tropsch [49] and has since been refined and commercialized for various applications, including fuel production.

The FT synthesis process involves several key steps [49]. In the first step, the carbon-containing feedstock is gasified to produce a mixture of CO and hydrogen; this can be achieved through processes like steam gasification of coal or partial oxidation of natural gas. The raw syngas produced in the gasification step contains impurities and

must be cleaned to remove contaminants like sulphur and particulates, as these can interfere with the FT synthesis catalysts. The cleaned syngas is then fed into a reactor where it comes into contact with a catalyst, typically consisting of metal nanoparticles, often cobalt or iron. The catalyst facilitates a series of chemical reactions that convert the syngas into long-chain hydrocarbons [50]. These hydrocarbons can range from methane to high-molecular-weight waxes. The resulting hydrocarbon mixture may need further processing to obtain the desired range of liquid hydrocarbon fuels [51]. This can involve hydrocracking to break down heavy waxes into lighter fractions, followed by distillation to separate and isolate the specific fuels like diesel or gasoline. The final synthetic fuels may undergo refining processes to meet the required specifications for use in engines and vehicles. This can include removing impurities, adjusting the cetane number for diesel, or ensuring the correct octane rating for gasoline.

Regarding its lifecycle, the FT process does not rely on pre-existing hydrocarbons, however it has temperature and pressure requirements, and can release GHG in the process [52]. The GHG emissions from the fuel production process can be reduced if, for example, hydrogen production for the fuel is done in a more efficient manner.

One of the environmentally friendly pathways for FT fuel production could be the biomass-to-fuel pathway. Utilizing unfermentable biomass from bioethanol industries, one study [53] explores the feasibility of integrating FT synthesis using syngas derived from gasified dry distillers' grain. Environmental considerations are addressed, with the integration of the process being deemed environmentally benign. Individual impact categories highlight the role of catalyst components and suggest the need for alternative formulations to reduce environmental impact and human toxicity potential.

FT fuels can also take advantage of direct air capture (DAC). DAC is a technology designed to remove CO_2 from the atmosphere, either chemically or physically. A study by Liu et al. [54] conducts an LCA of the GHG emissions associated with DAC paired with FT synthesis to produce synthetic transportation fuel, specifically diesel. The study finds that the carbon intensity is highly sensitive to the emissions factor of the electricity used in the process, with a factor of less than 139 grams of CO_2 equivalent per kilowatt-hour required for the system to provide a climate benefit over conventional diesel fuel. When low-carbon electricity sources are used, this pathway can deliver transport fuels with a lower CI than conventional diesel and various biofuels.

FT diesel is composed of n-alkanes molecules [55] and has similar characteristics to conventional diesel, facilitating its direct use in ICES while it has low sulphur

content and aromatic content [56], preventing noxious pollutants. FT fuels maintains a high CN and a high LHV [57]. For taking good advantage of the production of synthetic fuels like FT diesel, it is important to locate fuel synthesis facilities in regions with very low grid emissions or co-locating them with new renewable electricity infrastructure to prevent high carbon intensities.

2.2.1.1 Use of FT-diesel in ICEs

Numerous researchers have extensively investigated the combustion and performance characteristics of FT diesel fuels in diesel engines. Yuan et al. [58] emphasized that FT diesel's high CN led to a decrease in ignition delay and premixed combustion phase time compared to conventional diesel. Cai et al. [57] observed lower heat release rates (HRR) and pressure rise rates (PRR) with FT and diesel blends due to the differences in properties of the synthetic fuel compared to the fossil fuel. Additionally, some studies [59, 60] reported benefits like shorter premixed combustion periods, reduced peak combustion pressure, increased thermal efficiency, and decreased PM and NOx emissions when using FT diesel or its blends. The studies on the effect of the properties of FT diesel on injection rate carried by Pastor et al. [61] evidenced that a shorter energizing time (ET), and thus a smaller injected mass was required for FT diesel compared to conventional diesel.

Yuan et al. [58] found that at high loads both GTL and conventional diesel exhibited typical diesel combustion patterns, with diffusive combustion following rapid premixed combustion as intake oxygen decreased. At medium load, diffusive combustion shortened further with decreasing oxygen, displaying characteristics of premixed combustion for both fuels. Throughout load conditions, GTL had a smaller peak heat release but a longer diffusion combustion due to its shorter ignition delay and less efficient premixing. At medium load and 12% intake oxygen, diesel had almost no premixing, while GTL initiated ignition during injection. At high load, both fuels had extended combustion durations and delayed CA50 as oxygen decreased, attributed to increased premixing period. GTL had lower cooling losses at 21% and 14% intake oxygen concentrations at high load, resulting in improved indicated thermal efficiency. At medium load, GTL exhibited reduced cooling loss at 21% intake oxygen, leading to improved thermal efficiency. However, at 14% and 12% intake oxygen concentrations, differences in cooling loss and thermal efficiency between the two fuels were not significant, possibly due to their distillation characteristics under fully premixed combustion conditions.

Testing GTL diesel derived from the FT synthesis, Bassiony et al. [62] observed that neat GTL and blended at 50%v/v with diesel slightly reduced the engine's maximum power compared to diesel fuel across most engine speeds (3.2% for the neat synthetic

fuel and 1.2% for the 50% blend). Both GTL and the 50% blend fuels exhibit lower BSFC and higher thermal efficiency compared to diesel due to their higher cetane numbers, resulting in shorter ignition delays, reduced heat losses, and improved combustion efficiency. Additionally, using GTL and the 50% blend fuels results in a decrease in both maximum in-cylinder pressure and the maximum rate of pressure rise. Ye et al. [63] found an average 6% reduction in fuel consumption, similar to Cai et al. [64] and Zhang et al. [60].

Figure 9 shows the NOx-soot trade-off of FT diesel compared to conventional diesel across different studies [62, 57, 63, 58, 60]. In the figure, besides some exceptions, the FT diesel improves both the NOx and the soot emissions. The reduction of soot is generally explained by the better ignitability of the fuel and more homogeneous fuel-air mixture. In blends of FT and conventional diesel [57] the reduction of soot emissions is attributed to the dilution effect of FT diesel, which reduces the number of aromatic hydrocarbons that are known to impact soot aggregation. Additionally, the presence of n-alkanes and iso-alkanes in FT diesel reduces soot precursors, meanwhile better break-up and atomization properties also contribute to decreased soot aggregation.

NOx emissions, on the other hand, are reported to be correlated with the effects observed in the combustion of the fuel. The FT starts its ignition earlier than diesel, there is a smaller fraction of fuel burned during the premixed phase , which as a consequence the in-cylinder temperature is reduced, reducing with that the NOx emissions.

The benefits of FT diesel on emissions reduction extend to the CO and HC emissions. With reports of 7-78% reduction in HC and 2-68% reduction in CO [63, 60]. Zhong et al. [65] state HC emissions arise from regions of the combustion process where the fuel-air mixture is overly dilute, preventing proper flame propagation, causing incomplete combustion, and forming quench zones from fuel spray impingement; the low density and volatility of FT diesel fuel facilitate good mixing with air in the cylinder, reducing the impact of changes in the actual air-fuel ratio.

A correlation between the HC and PM is explored by Yehliu et al. [66]. FT fuel has a higher particle concentration (number of particles per volume) in all engine modes compared to biodiesel and diesel, however FT diesel does not have higher soot emissions than diesel by mass. The authors explain this apparent contradiction by the CN which affects combustion and produces more – but smaller – carbon-containing particles during the combustion process which during the PM measurements by mass has a lower quantity for FT, while they are increased for diesel. Since the measurement includes adsorbed unburned or partially burned HC,

the mass is higher for diesel. In terms of CO emissions both the work of [66] and [67], as well as other studies, report lower CO emissions which are in part related to the smaller ignition delay providing ample time for the CO to be fully oxidized.

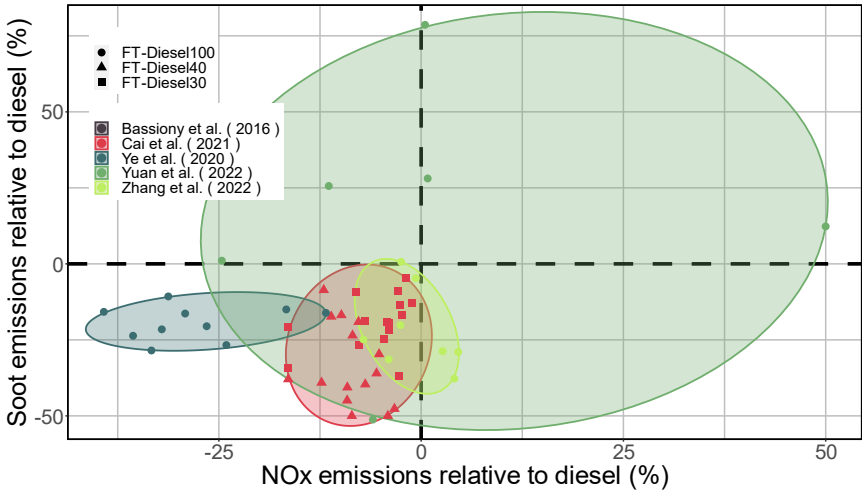

Figure 9. NOx-soot tradeoff compared to diesel across different studies with FT-Diesel (data from [62, 57, 63, 58, 60])

2.2.2 OMEx

Oxymethylene dimethyl ethers (OMEx) – also known as polyoxymethylene ethers (PODEs) –are a type of synthetic diesel alternative fuels. The general structure of the fuels is CH_3-O-$(CH_2$-O$)_n$-CH_3, where the *n* is the polymerization degree. The fuels have a large oxygenation by weight with values above 40% for n values equal or larger than 1 [68], while they have CNs that are comparable to diesel and biodiesel [69], thus being favourable for the autoignition of the fuel. The fuel lacks C-C bonds, which in addition to their large oxygen proportion propitiates low soot emissions [70], by inhibiting the formation of polycyclic aromatic hydrocarbons (PAHs). Regardless of the OMEx, the polymerization degree does not seem to have a large effect in the reduction of soot emissions [71]. The offset of having high oxygen proportions in the fuels is, however, a low gravimetric energy density of nearly half that of diesel or gasoline.

OMEx are a promising alternative to fossil-based, with the potential to reduce global warming impacts by up to 20% [72]. Deutz et al. [73] found that OME1 has the potential to serve as an almost carbon-neutral blending component for diesel fuel. Replacing 24% m/m of diesel with OME1 could reduce the global warming impact by 22%, and the emissions of NOx and soot by 43% and 75%, respectively. These

significant environmental benefits are achieved by integrating renewable energy in the production of OME1, specifically by using wind power to produce hydrogen through water electrolysis. Similarly, a well-to-wheel (WTW) LCA of OME3–5 produced via the PTL [74] showed that in scenarios with a high share of renewable electricity, WTW GHG emissions for OME3–5 fuel is advantageous compared to fossil diesel. For the best case, WTW GHG emissions can be reduced by 86%, corresponding to 29 gCO_2eq/km of OME3–5-fuel compared to 209 gCO_2eq/km of diesel fuel.

The use of OMEx, nonetheless can have an adverse effect on other impact categories under human health and ecosystems quality and have a higher cumulative energy demand (CED) during its lifecycle than diesel. In [73] it is reported that the CED for OME1 is nearly double that of diesel, which if the energy source is not renewable can have negative environmental impacts upstream of the fuel production. While [74] presents that for other environmental impact categories, acidification, eutrophication, respiratory effects, photochemical ozone creation and resource depletion significantly exceed the fossil fuel reference. A high share of these impacts can be assigned to electricity production, either through direct electricity consumption in the PtL system or during upstream production of hardware components.

2.2.2.1 Use of OMEx in ICEs

Due to the large oxygen proportion in the OMEx molecule, this fuel is considered a great alternative to address soot emissions in ICEs. Nonetheless, as the oxygen proportion increases the LHV of the fuel is reduced. Because of this low LHV (nearly 45% lower than diesel) gravimetric fuel consumption reported with OMEx fuels are extremely high. In a study by [75] it was observed that using proportions of 15% and 25% of OMEx the effect on BSFC is an increase of 1-3.2% at low and medium loads, while at high loads the percentage of substitution of OMEx favours a decrease up to 5.5% in BSFC when using proportions of EGR above 10%.

The authors [75] justify these effects by explaining that at low loads as EGR increases, diesel has the advantage due to longer ignition delays which lead to a higher proportion of premixed combustion, maintaining high combustion efficiencies due to sufficient fresh air supply. The smaller ignition delay of OMEx is corroborated by Pastor et al. [61], it was observed through natural luminosity analysis that OMEx injection exhibits an earlier combustion than a similar energy diesel injection done at an earlier time. Additionally, according to [75], the larger mass needed of OMEx to reach the same injected energy, combined with larger fuel density, results in greater spray momentum which can lead to increased fuel

penetration, causing more air-fuel mixture to diffuse and burn closer to the cylinder liner than with diesel, resulting in increased heat transfer loss. However, at high loads, the difference in efficiency between diesel and the OMEx blends becomes smaller due to higher combustion efficiency and a faster combustion rate in the late combustion phase. This suggests that the advantage of OMEx high oxygen content and volatility is better utilized in improving combustion efficiency, especially at high load conditions with significant EGR.

Regardless of the slight benefits observed at high loads with blends of lower proportion of diesel and OMEx due to the improve in the combustion ascribable to the oxygen present in the molecules, when using neat OMEx as a fuel for ICEs there is a penalty in fuel consumption due to its low LHV. On a study on stoichiometric OMEx combustion in a single cylinder engine, García et al. [76] reported an increase of 14% to 39% in equivalent fuel consumption (fuel consumption normalized by multypliing LHV_{OMEx}/LHV_{diesel}, see Chapter 3 for further information on the metric) when comparing the stoichiometric combustion of OMEx with the baseline calibrated lean diesel combustion. In fact, when assuming a direct comparison of the fuel consumption OMEx has an increase of up to 207% with respect to diesel. Results are improved as the air-to-fuel ratio (AFR) becomes leaner; however, this only leads to the expected relation of fuel consumption of around 2 times that of diesel.

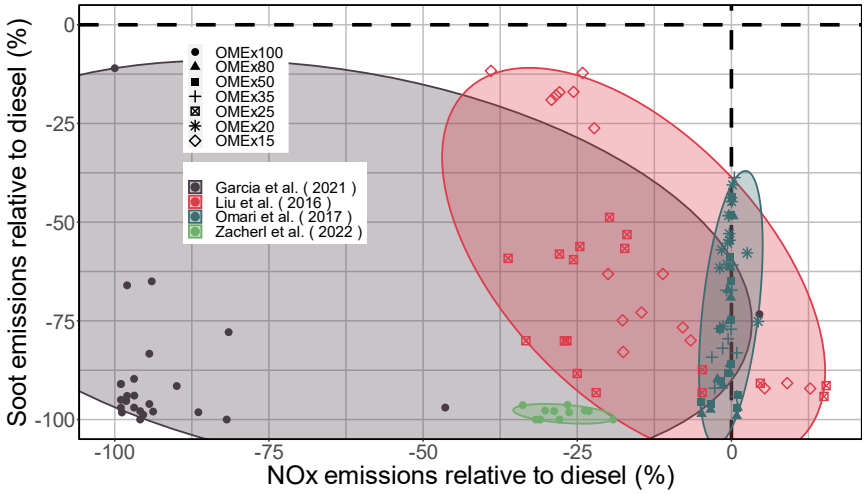

Figure 10. NOx-soot tradeoff compared to diesel across different studies with OMEx (data from [76, 75, 77, 78])

The real advantage of OMEx as a fuel for ICEs is its mentioned capacity to reduce soot emissions to virtually undetectable values, which also allow to adopt NOx

reduction strategies without increasing soot levels. This is observed in Figure 10 which recalls the comparisons with conventional diesel of the NOx-soot trade-off for different OMEx proportions.

Garcia et al. [76] show the biggest reductions in both NOx and soot due to the stoichiometric combustion of neat OMEx. The NOx reduction of nearly 100% percent is explained by the reductions of the maximum peak temperature during the combustion, thus limiting the formation of thermal NOx. Additionally, the combustion in the study is achieved with large EGR quantities that slow the reactivity of the mixture while at the same time act as a heat sink. In turn, the soot emissions are the result of the molecular composition of the OMEx, which offer the advantages previously stated in the section, although the authors caution that due to the nature of the equipment used soot emissions with oxygenated fuels might be underreported.

At 15% and 25% OMEx blends [75] and 20% OMEx blends [77] some operating conditions have higher NOx emissions than diesel. However, for the most part the emissions from these studies remain below the diesel threshold from 5% to almost 40%. The reductions in NOx emissions are again fundamentally explained by the reduced HRR and premixed combustion.

In the work of Zacherl et al. [78] OMEx exhibits lower volatile organic compounds (VOC) and CO emissions compared to diesel, mainly due to its oxygen content and improved mixture formation. Regarding the combustion proper, both VOC and CO emissions increase with late center of combustion (combustion phasing) because combustion occurring late in the expansion phase leads to lower combustion temperatures, inhibiting the complete oxidation of intermediates and resulting in increased incomplete combustion products. Lower turbulence in the combustion chamber and impaired jet decay due to low backpressure and low temperatures also contribute to this effect.

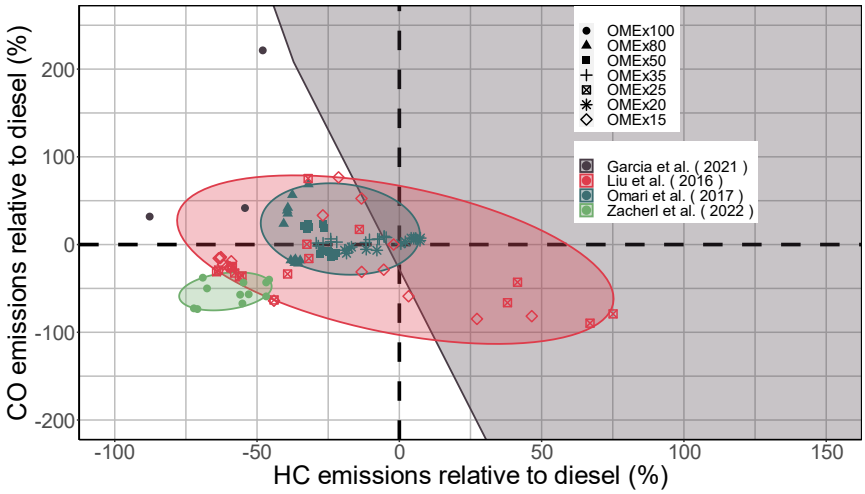

Figure 11. HC-CO tradeoff compared to diesel across different studies with OMEx (data from [76, 75, 77, 78])

Other works have a less clear outcome of CO and HC emissions of OMEx with respect to diesel. OMEx blends up to 80% and neat OMEx can have higher CO and HC emissions than diesel. Liu et al. [75] found that at lower loads the CO emissions are similar to diesel as diesel has sufficient oxygen to be fully oxidized into CO_2, but at higher loads OMEX can present an advantage. Omari et al. [77] saw that at the same NOx level, increasing the OMEx proportion with respect to diesel can reduce both CO and HC emissions at higher loads, while at lower loads the inclusion of additional percentages of OMEx increases the CO emissions. Authors argue that when the engine is running at very low loads, the fuel's low CN becomes more important, causing more premixed combustion to occur, which in turn leads to higher levels of CO emissions.

The most drastic increase of both CO and HC is found in the work of Garcia et al. [76] who reported a maximum increase of HC emissions of 68 times the emissions of diesel and 602 times for CO emissions. It is worth re-stating that during this work the combustion was stoichiometric with high levels of EGR and thus the fuel did not have sufficient oxygen to complete the combustion (even with the 47.1%m/m of oxygen in the fuel molecule). Additionally, the combustion temperature reduced the reactivity of these species. However, once the authors tested leaner mixtures, with abundant oxygen, they were able to achieve engine out emissions without aftertreatment that were below the requirements of Euro VI for the type-class vehicle.

The mechanism for the OME3 pyrolysis and soot inception was investigated by Xing et al. [79] via the analysis of the conversion of three main species: CH_2O, $CH_3O\cdot$, and $\cdot CH_3$. Soot formation is reduced with the OME_3 as the CH_2O molecule is converted into CO by continuous dehydrogenation revealing that carbon atoms converted to CO did not contribute to soot precursor formation. Additionally, oxidizing groups, mainly ·OH, were primarily generated from $CH_3O\cdot$ radicals, which reacted with small gaseous soot precursors to form stable oxides, thus inhibiting soot formation.

Besides its benefits in GHG emissions reductions from its production and their capability to reduce both NOx and soot emissions from the engine combustion, the compatibility of the OMEx fuels with conventional components of the vehicles must be addressed. The CN of the OMEx molecule increases as the molecule is longer; however, if the OMEx molecule is too long ($n > 5$) the pumping performance of the fuel can be negatively affected as the viscosity of the fuel increases with molecule size [80]. Similarly, the larger OMEx molecule can lead to larger diameter of the droplets during atomization, which causes poorer mixtures and could detriment the combustion efficiency and the emissions.

A study by Kass et al. [81] investigated the compatibility of PODEs with a variety of elastomers using a combination of exposure studies and Hansen solubility analysis. The results showed that overall, PODEs have poor compatibility with elastomers, with the exception of fluorosilicone. At the 33% blend level, all elastomers except fluorosilicone exhibited volume swell greater than 30%. The general trend across the elastomers was either a consistent increase in volume swell with PODE concentration, or a maximum in volume swell at an intermediate blend fraction.

For OMEx to be used pure or at high blend rates with diesel without issues some modifications can be required for conventional compression ignition engines. The injection system has been reported to need modification at high ratios of OMEx with $n < 2$ (higher than 30%) due to the high vapor pressure and low boiling point of the fuel which can cause issues like vapor lock or cold-start problems [82, 73]. Increasing the value of n ($3 \leq n \leq 5$), OMEx has lower vapor pressure and higher boiling point [83]; thus, reducing the magnitude of these issues. Pastor et al. [61] reported that OMEx injector behaviour also changes when compared to diesel, taking more time for the injector to close once the ET has finished, likely due to its higher density and lower viscosity.

3 Low carbon fuel blends: achieving specific fuel characteristics

When used in ICEs in their pure form, LCFs can offer significant environmental benefits due to their lower carbon intensity and possible cleaner combustion. However, blending LCFs, either with conventional fuels like diesel or with other LCFs, can enhance their advantages or mitigate certain drawbacks. For instance, blending oxygenated fuels like OMEx, which often have a lower LHV, with diesel can increase the oxygen percentage in the diesel fuel, resulting in more complete combustion and reduced emissions while the low LHV of OMEx is somewhat compensated by the higher energy density of diesel. Blends with alcohol, such as ethanol or methanol, can further reduce carbon emissions and improve octane ratings for spark ignition (SI) engines, enhancing engine efficiency. Additionally, incorporating cetane improvers can enhance ignition quality in CI engines, while additives can combat corrosion issues, ensuring the longevity of engine components. These blending strategies highlight the versatility and potential of LCFs to address various challenges.

Fuel blends represent a compelling strategy for addressing the demands of CI engines. Exploration of various fuel blend combinations has led in some cases to optimize engine performance while minimizing environmental impacts. This approach offers a potential means of reducing emissions but also enables the attainment of desirable fuel properties crucial for engine operation and efficiency.

In this section, the benefits of LCF blends in the context of CI engines are explored through a comprehensive review of the current literature, including how the mixing of fuels contributes to the realization of key fuel properties that are essential for engine combustion and overall performance.

3.1 Multi-fuel blends

A multifuel blend refers to a mixture of various fuels that can be used simultaneously to power the engine. These blends typically consist of diesel fuel and one or more alternative fuels, such as biodiesel or alcohol. The purpose of creating multifuel blends is to enhance engine performance, reduce emissions, and improve overall fuel efficiency while offering flexibility in fuel choices.

The idea behind blending fuels is improving the quality of the final product according to desirable properties. As such some of the more useful characteristics of a fuel are partially transferred to the final blend when combined with other fuels with different characteristics; the resulting fuel blend would have properties with values

averaging different components of the blend. For example, in the work of Preuß et al. [46] they tested so called OME blends (OME blend 1, OME blend 2 and OME blend 3), which are composed by varying proportions of pure OME3-5, HVO, RME and 2-Ethylhexanol. Observing the properties of the pure fuels in Table 1 shows the high oxygen proportion of the OMEx fuel and of the RME, as well as the high LHV of the HVO fuel and its high CN. Then observing the final properties of the OME blend 1, OME blend 2 and OME blend 3 in Table 2 it can be seen that the OME blend 1, which has the highest proportion of HVO in turn has the highest LHV. Meanwhile the OME blend 3, which has the highest proportion of OMEx ends up having the highest oxygen proportion of the final fuel.

The fuels presented in Table 2, are the result of the combinations of the properties of the pure fuels shown in Table 1. In the fossil diesel-biodiesel-alcohol blends in the work of Yesilyurt et al. [84], similar to OMEx, the alcohols provide oxygenation to the fuel. The vastly different compositions of the fuels in this study were mixed by splash-blending method and the authors report that no separation was observed during the application tests. Nonetheless, it has been reported [85] that phase separation can occur in high-concentration ethanol-diesel blends due to the high water content of ethanol.

Methanol and ethanol are biofuels that can reduce particulate emissions and GHGs. Methanol is high-octane but toxic, with varying emissions trends. Ethanol, derived from biomass, is widely used and has lower production costs (21 to 46 USD per GJ) and lower GHG emissions (4 to 32 kg CO_2eq per GJ) compared to methanol [85]. Ethanol can be blended with diesel without engine modifications, and it is commonly used in gasoline engines due to its high octane number and high combustion speed, which can improve thermal efficiency and reduce emissions. In turn, ethanol has a low CN, which can be problematic for diesel engines; however, cetane improvers can be added to the blend to overcome this issue.

Like alcohols, the properties of biodiesel are also transferred to the final fuel when blended. According to the study by Millo et al. [86], RME B30 exhibits higher viscosity and altered spray characteristics compared to diesel, while HVO B30 closely matches diesel properties. The study also discusses the energy content differences and the potential for engine performance recovery with biofuel blends.

In a previous review on the use of LCFs in blends, Singh et al. [87] mention that vegetable oils have high viscosity and LHVs compared to diesel fuels due to their molecular structure; however, the presence of oxygen in vegetable oils lowers their heating value. The authors also state that biodiesel from various sources, such as jatropha oil, linseed oil, neem oil, and fish oil, shows different effects on engine

performance and emissions for which researchers have explored the optimal blending ratios for improved performance and emissions. Meanwhile, higher alcohols like n-butanol offer advantages in terms of heating value and miscibility with diesel, making them viable as fuel additives.

The use of LCFs blends can also help keep the cost of the final fuel down. Due to relying on recently developed technologies, like DAC, the cost of synthetic LCFs can be higher than their fossil fuel counterparts; for example, OMEx and FT fuels produced with CCS can cost 26.5£/GJ and 23.4 £/GJ [88], values which are high compared to fossil diesel. Because of that, blends that contain less expensive LCFs or even fractions of the still cheaper fossil fuels can partially provide the environmental benefits of the LCF (proportional to the fraction of renewable energy) while getting the fuel blend to a more attractive price point.

Although there is a general appraisal for using fuel blends, there are still some limits for the proportions of the fuels that can be used. For example, regarding OMEx blends one caveat, according to Preuß et al. [46], is that the fuel is difficult to be blended at room temperature with HVO. Seraç et al. [89] speak about a blend proportion limit imposed not by miscibility of the liquids but regulation, in this case for the limit of biodiesel that a fuel can contain. Similarly, the use of alcohols and even OMEx can be limited by the reduction they can cause on the lubricity of the fuel, the viscosity, or even the vapor pressure changes which can cause trouble in the fuel injection system (as was commented on section 2.2.2.1).

3.1.1.1 Engine performance on low carbon fuel blends

The combined properties of LCF blends can have diverse effects on the engine performance and emissions. In previous sections binary blends of neat LCFs and conventional diesel have been discussed highlighting both the benefits and the challenges for these fuels. This section will focus on the engine responses of fuel blends with more than two components as well as binary blends of two LCFs.

Preuß et al. [46] analyzed the performance and emissions of three oxygenated fuels blends (OME blends from Table 2) in comparison to diesel and HVO fuels using heavy-duty and light-duty CI engines. The OME blends had variable oxygen content, and adjustments were made to injection duration to maintain consistent engine load. In heavy-duty engines, the indicated specific fuel consumption (ISFC) increased significantly with higher OME content in the blends compared to diesel, ranging from 6.4% to 20.5%. Light-duty engines also saw ISFC increases of 2.3% to 24.8% for OME blends. Efficiency trends were consistent for both engines, with OME Blends 2 and 3 outperforming diesel and HVO, while OME Blend 1 showed similar

efficiency. Faster combustion led to lower exhaust gas temperatures, reduced soot emissions, and slightly increased NOx emissions for the OME blends. The study also observed an increase in nucleation mode particles with higher OME content. The results also suggest that OME3-5 blends, along with HVO, RME, and octanol, can be used as drop-in fuels for CI engines without hardware modifications, but further research on material compatibility is needed.

The work of Millo et al. [86] evaluates the effects of using blended renewable diesel fuels (RME B30 and HVO B30) in a Euro 5 small displacement passenger car diesel engine. The study investigates various aspects, starting with the hydraulic behavior of the common rail injection system and the analysis of fuel spray characteristics for RME B30 and HVO B30 compared to standard diesel fuel finding that when tested at different rail pressure levels (400 bar, 800 bar, and 1200 bar), RME B30 consistently had a lower mean injected volume compared to diesel fuel while HVO B30 had injected volumes more similar to diesel. The study also found that RME B30 resulted in a somewhat retarded injection process and a lower peak needle lift, leading to a lower injected volume compared to diesel. Conversely, HVO B30 had an injection process start similar to diesel and achieved higher instantaneous flow rates, resulting in larger injected volumes. The impact of these biofuel blends on BSFC and exhaust emissions is assessed under seven different part load operating conditions resembling the New European Driving Cycle and full load. In terms of emissions, both biofuel blends show potential reductions in smoke and particulate matter emissions, with RME B30 offering additional benefits due to increased oxygen availability.

Yesilyurt et al. [84] tested quaternary blends consisting of diesel, safflower oil biodiesel, neat safflower oil, and various alcohols. The authors conducted experiments at five engine loads while maintaining a fixed engine speed of 3000 rpm, examining parameters such as BSFC, brake specific energy consumption (BSEC), brake thermal efficiency (BTE), exhaust gas temperature (EGT), and various emissions, including CO, CO_2, HC, NOx, and smoke opacity, as well as in-cylinder pressure, HRR, and ignition delay period. The study found that the inclusion of LCFs such as vegetable oil, biodiesel, and alcohols led to increased BSFC values; B20O1E10 had the highest BSFC. Pentanol addition resulted in lower BSFC compared to other alcohol types, attributed to its higher heating value. Conventional diesel fuel had higher BTE values than the B20 blend due to its higher LHV, while ethanol-blended fuels had lower BTE values due to their lower LHV. B20O10Pt10 had the best BTE values of LCF blends due to its higher heating value and complete combustion process. Alcohol reduced EGT due to their cooling effect and higher oxygen content, which improved combustion rates. Oxygenated components in

biodiesel and alcohols reduce CO emissions, with pentanol showing the most significant reduction; biodiesel and alcohol additives reduce HC emissions. Ethanol and pentanol exhibit greater effectiveness in decreasing HC emissions compared to other alcohols.

Similarly, Sathish et al. [90] tested blends of diesel, biofuel and ethanol, which are described in Table 2. D80B20 (80% diesel + 20% biofuel of Azadirachta indica oil) exhibited the highest BTE, followed by D60B20E20 (60% diesel + 20% biofuel of Azadirachta indica oil + 20% ethanol) and B80E20 (80% diesel + 20% ethanol). Smoke intensity increased with load, with D80E20 having the lowest at full load, followed by B80E20, pure diesel and biodiesel having the highest smoke intensity. HC emissions increased with load, with diesel having the highest and the biodiesel the lowest at full load. NOx emissions increased with load for all blends, with neat biodiesel having the highest. The study also analyzed peak pressure, which was lower for diesel and higher for the other blends, with B80E20 having the highest peak pressure. These variations were attributed to properties like CN, volatility, and viscosity of the fuels, as well as ethanol content.

Researchers Gómez et al. [91] studied the impact of different fuels mixed with gasoline and how these blends affect soot production in Diesel engines. The researchers use a parameter called the Oxygen Extended Sooting Index (OESI) to measure the tendency of these fuels to produce smoke. The results show that when gasoline is added to Diesel, the soot production decreases. This is because gasoline reduces the aromatic content and unsaturation in the fuel, making it less likely to produce soot. On the other hand, when LCFs like biodiesel, GTL and Farnesane fuels are mixed with gasoline, the tendency to produce soot increases due to its higher aromatic content and unsaturation. The study also suggests that even a small amount of Farnesane or GTL in a blend with Diesel and Gasoline can reduce soot production in certain engine types.

The research presented in this section underscores the intricate interplay of different fuel blends and their diverse impacts on engine performance and emissions. From binary blends of LCFs with conventional diesel to complex quaternary mixtures, the studies highlight the potential advantages and challenges associated with these alternative fuel formulations.

Table 1. Chemical and physical properties of different pure fuels

Fuel	%C (m/m)	%H (m/m)	%O (m/m)	Density (kg/m3)	Kin. Visc. (mm^2/s)	CN (-)	LHV (MJ/kg)	Ref
Diesel	86.20-87.05	12.95-13.80	0	818-866	2.55-4.19	49-55	42.45-44.8	[46, 57, 62, 75, 84, 92, 93, 90, 94]
RME			10.8	880	4.4	52	38	[46]
HVO				779.9	2.6	75	44.1	[46]
OME3-5			43.1	1066.5	1.18	54	19.1	[46]
OMEx	47.4	10.5	42.1	859	0.36	24	23.4	[77]
OME2			45.2	960		63		[75]
OME3			47	1020		78		[75]
OME4			48.1	1070		90		[75]
OME5			48.9	1100		100		[75]
OME6			49.5	1130		104		[75]
FT-Diesel				760		70	47.3	[62]
Safflower oil biodiesel	76.88	11.65	11.46	883.3	4.986	55.7	39.25	[84]
Safflower oil	76.9	11.63	11.47	923	36.03		39.03	[84]
B100 (100% neem oil biofuel)				870	4.62	51	41	[84]
WPO (waste plastic oil)				824	3.76	60.0*	40.58	[92]
POME (palm oil methyl ester)				874	6.46	48.7*	36.79	[92]
COME (castor oil methyl ester)				909	18.61	39.4*	37.95	[92]
1-pentanol				815	2.89	20	34.65	[93]
2-Ethylhexanol			12.3	832	5.2	23.2	38.4	[46]
Ethanol	52.17	13.04	34.78	780.15-790	1.072-1.31	8-10	27.53-26.9	[84, 90]
Isopropanol	60	13.33	26.67	782.3	1.796	12	31.02	[84]
Isopentanol	68.18	13.64	18.18	813.2	2.984	20	37.03	[84]
n-butanol	64.87	13.51	21.62	807.6	2.288	17	35.08	[84]

Table 2. Chemical and physical properties of different fuel blends

Fuel	Diesel (%)	FAME (%)	HVO (%)	OMEx (%)	Other	%C (m/m)	%H (m/m)	%O (m/m)	Density (kg/m3)	Kin. Visc. (mm2/s)	CN (-)	LHV (MJ/kg)	Ref
OME blend 1		7	76	7	2-Ethylhexanol			6.4	808.9		68	40.75	[46]
OME blend 2		7	65	18	2-Ethylhexanol			12.8	840.4		66.6	37.4	[46]
OME blend 3		7	56	27	2-Ethylhexanol			17.8	866.2		65.1	34.84	[46]
RME B30	70		30			83.4	13.2	3.4	853	3.183	52.8	41.24	[86]
HVO B30	70		30			85.4	14.1		812.2	2.545	60.7	43.29	[86]
15HVO-fossil	85		15			86.2	13.8		830.7	3.578	60.6	43.34	[94]
30HVO-fossil	70		30			86	14		827.9	4.022	68.4	43.47	[94]
OMEx20	80			20		77.9	12.9	9.3	836		53	38.8	[77]
OMEx35	65			35		72	12.4	15.6	840		51	35.9	[77]
OMEx50	50			50		66.2	12	21.8	845		8	33	[77]
OMEx80	20			80		54.8	11.1	34.1	853		37	27.2	[77]
OMEx (44.8%OME3 + 28.24%OME4 + 17.09%OME5 + 9.87%OME6)				100		43.53	8.52	47.95	834.2		60.7	21.77	[75]
OMEx15	85			15		78.75	12.56	8.69	866.1		54	36.62	[75]
OMEx25	75			25		73.86	12	14.14	887.4		57.8	33.79	[75]
B20 (20% biodiesel + 80% diesel fuel)	80	20				85.02	12.69	2.29	842.66	3.036		42.75	[84]
B20O10 (20% biodiesel + 10% vegetable oil + 70% diesel fuel)	70	20	10			84	12.56	3.44	851.71	6.384		42.29	[84]
B20O10E10 (20% biodiesel + 10% vegetable oil + 60% diesel fuel + 10% ethanol)	60	20	10		ethanol	80.51	12.57	6.92	846.48	6.236		40.68	[84]
B20O10Pr10 (20% biodiesel + 10% vegetable oil + 60% diesel fuel + 10% isopropanol)	60	20	10		isopropanol	81.3	12.6	6.1	846.69	6.309		41.03	[84]
B20O10Bt10 (20% biodiesel + 10% vegetable oil + 60% diesel fuel + 10% n-butanol)	60	20	10		n-butanol	81.78	12.62	5.6	849.2	6.358		41.44	[84]
B20O10Pt10 (20% biodiesel + 10% vegetable oil + 60% diesel fuel + 10% isopentanol)	60	20	10		isopentanol	82.11	12.63	5.26	849.8	6.427		41.63	[84]
SOB5 (5% biodiesel)	95	5							826.2	2.607	56.9*	43.58	[89]
SOB20 (20% biodiesel)	80	20							830.3	2.792	58.7*	42.32	[89]
WPOP10 (90% WPO + 10% palm oil)		10			WPO				829	4.11	59.6*	39.18	[92]
WPOC10 (90% WPO + 10% castor oil)		10			WPO				844	4.29	54.5*	39.64	[92]
DP5 (5% pentanol)	95				1-pentanol				817	2.94	52.3	44.3	[93]
DP10 (10% pentanol)	90				1-pentanol				816	2.93	50.6	43.8	[93]
DP20 (20% pentanol)	80				1-pentanol				814	2.91	47.2	42.83	[93]
DP25 (25% pentanol)	75				1-pentanol				813	2.9	45.5	42.35	[93]
DP35 (35% pentanol)	65				1-pentanol				811	2.88	42.1	41.4	[93]
D80B20 (80% diesel + 20% biofuel)	80	20							840	4.21	49.4	43.4	[90]
D60B20E20 (60% diesel + 20% biofuel + 20% ethanol)	60	20			ethanol				830	3.65	43	39.98	[90]
B80E20 (80% diesel + 20% ethanol)	80				ethanol				850	3.15	46	38.4	[90]

3.2 Additives

Recent studies have examined the use of additives that promote cleaner combustion and reduce the formation of NOx and soot. These additives, when combined with LCFs or traditional fuels, can improve combustion, wear of the engine components, and mitigate the release of harmful pollutants into the atmosphere. By optimizing fuel formulations with such additives, researchers aim to achieve a balance between performance and emissions reduction.

For ethanol-diesel blends, non-ionic surfactants such as SPAN (hydrophobic) and TWEEN (hydrophilic) are commonly used to stabilize these blends and prevent phase separation. These surfactants when used for blending fuels, allow reducing corrosion and act as emulsifiers to improve the water tolerance of the blend [95]. Verger et al. [85] conducted diesel-ethanol miscibility tests at different proportions finding that in a 70%-30% diesel-ethanol blend phase separation occurred after two weeks, but the addition of a 3% blend of Span 80 and Span 85 surfactants helped stabilize the blend. In a 60%-40% diesel-ethanol blend phase separation occurred after 48 hours due to the higher ethanol content, yet stabilization was achieved by adding a 3% blend of Span 80 and Span 85 surfactants. In the 50%-50% blend separation occurred within 2 hours due to the 50% ethanol composition and stabilization was achieved with a 5% blend of Span 80 and Span 85 surfactants. Finally, the 40%-60% diesel-ethanol blend resulted in an oil-in-water emulsion with phase separation occurring after 24 hours with stabilization achieved by adding 4% of Span 85 surfactant. t's worth noting that blends with higher ethanol content tend to be more challenging to stabilize, and the choice of surfactants and their concentrations plays a crucial role in achieving stability.

Unglert et al. [35] discuss the significance of the chemical-physical behavior of modern fuels in addition to factors like sustainability, emission reduction potential, and production costs. It highlights the diverse range of biofuels available, showcasing differences in polarity, low-temperature performance, miscibility, stability, lubricity, and other properties. These variations, from highly polarized OME to non-polar paraffinic HVO in the middle distillate range, necessitate the maintenance of fuel properties required by standards like the "Worldwide Fuel Charter" to ensure drop-in compatibility across a wide range of applications. The authors highlight R33 (one of the fuels explored in this thesis) as an example of blending unpolarizable substances like HVO and polar biodiesel in mineral oil-based diesel fuel with additives to create a stable fuel that combines their positive properties.

The use of nanoparticles (NPs) in biodiesel production and their effects on the performance, combustion, and emission characteristics of diesel engines has been reviewed by Bidir et al. [96]. While pure biodiesel can be used in diesel engines, it has some drawbacks like lower energy density, a lower CN, and reduced LHV compared to conventional diesel fuel. Therefore, using biodiesel blends with biofuels could improve the biodiesel. The review mentions the use of various NPs like metals, metallic oxides, and metallic combinations as additives in biofuel production. These NPs can enhance fuel properties and performance. Magnetic NPs are also mentioned for large-scale biodiesel production due to their ease of separation and reuse. Nanotechnology is explored for enzyme immobilization, which can improve catalyst stability and reusability, ultimately reducing biofuel production costs. Additionally, the authors discuss the potential applications of nanotechnology in various areas of biofuel production, such as fermentation, pyrolysis, biochar, and gasification, to improve efficiency and reduce environmental impact. The use of NPs in diesel engines is also explored. Adding NPs to diesel-biodiesel fuel blends can enhance thermo-physical properties, leading to improved engine performance and reduced emissions. However, the specific effects depend on the type and concentration of NPs used.

In the context of performance Bidir et al. [96] reiterate that the addition of oxygenated fuels to diesel fuel has been found to increase the oxygen content of the blend while reducing its density and viscosity. However, higher ethanol percentages in diesel-biodiesel-ethanol blends can lead to a reduction in BTE and an increase in BSFC. To enhance BTE, various metallic and metallic oxide NPs such as Al2O3, CuO, TiO_2, GO, and graphene have been added to diesel or diesel blends with biodiesel and ethanol in direct injection CI (DICI) diesel engines. These NPs have been shown to increase BTE by up to 25%, primarily due to their catalytic effect and improved combustion compared to blends without NPs. Concerning combustion, the addition of NPs has led to a shortened ignition delay. The addition of ethanol in diesel-biodiesel blends and various NPs, including Al_2O_3, CeO_2, TiO_2, GO, and graphene, has been found to enhance the HRR and in-cylinder pressure, contributing to improved combustion efficiency. In terms of emissions, the use of biofuel blends with NPs has generally led to reduced emissions of HC, CO, and smoke. Notably, the addition of specific NPs, such as CNTs and TiO_2, has led to a substantial decrease in NOx emissions, showing potential for emission control.

Preuß et al. [46] 200 ppm added Trigonox B, a lubricity agent, for blends with OMEx and 2-ethylhexanol. Methanol (and other short-chain alcohols) lubricity is extremely low, and the fuel can cause corrosion on metal components. Researchers that have used methanol as a fuel (like in previous work by the author [97], Shamun et al. [98]

and Aziz et al. [99]) use additive like Infineum R566 and VpCI®-706 to try to improve the lubricity and prevent the corrosion. As methanol is severely lacking in these two aspects the quantity of both additives should be used in relatively high quantities from 200 to 300 ppm (parts per million) by mass. Nonetheless, the additives can be introduced to methanol without altering emission levels or combustion characteristics within the cylinder, mitigating some of the corrosion issues.

In the review by Singh et al. [87] oxygenated additives like clove oil, eugenol, eugenyl acetate, and di-n-pentyl ether (DNPE) have been studied for their effects on combustion and emissions. The results revealed that when incorporating a 0.2% bio-additive into the fuel, it was possible to lower BSFC and decrease engine exhaust emissions. Additionally, the esterification process enhanced oxygen enrichment in eugenol, which contributed to achieving optimal fuel combustion.

Fuel properties, including viscosity, surface tension, and evaporation, along with structural properties, significantly influence spray formation in various fuel blends. Ul Haq et al.'s review [100] emphasizes alcohols as potential fuel additives, focusing on their fluid properties like viscosity and density, which impact spray quality, as well as their effects on ignition delay and soot emissions. For instance, ethanol can enhance spray quality but may lead to longer penetration lengths under certain conditions. Ether-based additives have shown potential in improving fuel spray quality and combustion efficiency in diesel engines, offering benefits such as increased cetane number, improved atomization, and reduced emissions, depending on the specific ether used and the blending ratio with diesel. Aliphatic compounds, often used as corrosion inhibitors and fuel additives, can increase ignition delay and reduce ignition quality, with common examples like n-heptane, n-octane, and iso-octane. A toluene and n-heptane mixture serves as a proposed surrogate for diesel blends, and aromatic compounds like toluene and dimethyl furan (DMF), despite their challenging preparation process, have potential as biofuel additives for diesel.

Karthickeyan et al. [101] conducted a comprehensive investigation into the engine characteristics of a single-cylinder Direct Injection (DI) diesel engine fueled with Lemon Oil (LO) biofuel, which was derived from lemon peels through steam distillation. The physio-chemical properties of LO were analyzed and compared with diesel based on ASTM biodiesel standards. To improve LO's properties, a cetane enhancer called Pyrogallol (PY) was added. Improved performance and combustion characteristics were observed with LO and PY blend, resulting in reduced CO, HC, and smoke emissions.

While promising advancements have been achieved through the incorporation of additives, challenges persist. Additionally, the integration of nanoparticles and oxygenated additives shows immense potential in improving combustion efficiency and reducing emissions, although the precise effects depend on various factors.

4 Optimizing the vehicle for low carbon fuels

Adapting a vehicle for use with low carbon fuels represents a crucial step in reducing our carbon footprint and mitigating the impacts of climate change. This transformation involves not only modifying the engine design but also optimizing the entire vehicle system. The engine must be tailored to efficiently combust LCFs, which may require adjustments to the fuel injection system, ignition timing, and compression ratios to ensure proper combustion and performance. Additionally, the aftertreatment system (ATS), which is responsible for reducing harmful emissions, must be recalibrated to effectively treat the exhaust gases generated from these alternative fuels. By aligning the vehicle, engine, and aftertreatment system with LCFs, we can significantly reduce greenhouse gas emissions, enhance fuel efficiency, and contribute to a more sustainable and environmentally responsible transportation sector.

4.1 Aftertreatment systems with low carbon fuels

The manufacturers' current approach to address emissions in engines involves enhancing thermal efficiency to reduce fuel consumption while keeping emissions within regulatory limits through an ATS. Typically, a conventional diesel engine ATS includes a diesel oxidation catalyst (DOC) for CO and HC emissions reduction, a selective catalytic reducer (SCR) for NOx emissions, and a DPF for soot emissions treatment. However, stricter emission regulations have led some manufacturers to adopt dual-SCR or even three-SCR configurations [102], increasing the complexity and cost of ATS, particularly due to the consumption of urea for NOx reduction.

The use of oxygenated fuels like OMEx in engines reduces exhaust temperatures [76], complicating the DOC's operation, which requires higher temperatures for efficient conversion. This temperature reduction may also lead to elevated CO and HC emissions. However, OMEx shows promise in NOx reduction due to reduced peak temperatures and extensive EGR use. At full load, where NOx emissions rise, it might be possible to eliminate SCR from ATS since emissions exceed limits only in rarely used conditions. Regarding UHC and CO emissions, high EGR rates and low in-cylinder temperatures result in significantly increased UHC levels but may still be manageable with a properly designed ATS. However, CO emissions are

problematic and cannot be effectively reduced with conventional ATS systems, making this concept less viable due to a 30% fuel consumption penalty.

Vallinayagam et al. [103] observed that a 50% blend of pine oil with a SCR and catalytic converter (CC) exhibited a 7.5% higher BTE compared to diesel fuel, while also reducing smoke, CO, HC, and NOx by 70.1%, 67.5%, 58.6%, and 15.2%, respectively, at full load conditions. Gren et al. [104] studied primary and secondary aerosol (from atmospheric processing) HVO and RME emissions from a heavy-duty diesel engine with and without exhaust ATS. The results indicate that replacing petroleum diesel with HVO and RME reduces primary PM emissions and secondary aerosol production. The DOC effectively reduces primary nucleation mode emissions and mitigates secondary particle production. Notably, the DOC combined with a DPF removes over 99% of particle number and equivalent black carbon emissions. Furthermore, the study delves into the role of lubricating oil in aerosol emissions and the effectiveness of the DOC in removing lubricant-derived particles, suggesting that while the DOC contributes to reducing secondary aerosol emissions, its effect is overshadowed by the altered HC emissions due to different fuel types. The results emphasize the potential of renewable diesel fuels, like HVO and RME, to reduce both primary and secondary PM emissions; however, it is also noted that findings may not account for all real-world operating conditions and atmospheric factors that can affect secondary aerosol formation.

Wu et al. [105] investigated the combustion and emission performance of GTL fuel in an IVECO EURO5 DI diesel engine equipped with a DOC and DPF. Results showed that increasing the GTL fuel fraction led to a significant reduction in particle emissions at both engine-out and DPF-out, in nucleation and accumulation modes due to its chemical composition that promotes more complete combustion. The DPF achieved over 99% filtration; however, at higher engine power settings, diesel fuel generated more accumulation mode particles that exceeded the DPF's filtration capacity.

Zhang et al. [106] examined the effectiveness of a DOC and a catalyzed diesel particulate filter (CDPF) ATS in reducing emissions from biodiesel blends. The introduction of the DOC + CDPF ATS significantly improved emission reductions. This system effectively reduced CO and THC emissions, with greater reductions observed at higher speeds and with higher biodiesel blending ratios. Furthermore, the ATS achieved reductions exceeding 99% for both PN and PM emissions, irrespective of fuel type or driving conditions. Karthickeyan et al. [101] also extended their investigation by applying a SCR and a CC as ATS to reduce NOx emissions. With post-treatment, LO and PY blends showed lower NOx emissions

than diesel and LO, making them advantageous in terms of performance, combustion, and emission characteristics.

Lean-NOx Trap (LNT) systems function as a storage-reduction catalyst with a two-step process involving the storage and subsequent reduction of NOx. These systems have been optimized for conventional diesel fuels, but the introduction of new biofuels could significantly affect their performance in terms of exhaust gas temperature, flow rate, and composition. Hernández et al. [107] provide preliminary findings on the interaction between advanced biofuels and LNT in a Euro 6 diesel vehicle under the Worldwide harmonized Light vehicles Test Cycle (WLTC). The choice of biofuel has a substantial impact on NOx emissions, with different biofuels exhibiting varying effects on LNT efficiency. For instance, MoBio® (20% v/v oBio®[1] + 80% v/v diesel fuel) leads to higher engine-out NOx levels, possibly due to its oxygen content, resulting in higher combustion temperatures. On the other hand, HVO, with its high CN reduces premixed combustion phases, resulting in lower NOx emissions. However, the study also highlights that the trends in LNT efficiency do not align with those in engine-out emissions, suggesting that MoBio® negatively affects LNT performance, potentially due to catalyst saturation and hydrocarbon buildup.

Diesel outperforms Pistacia khinjuk methyl ester (PKME) blends in terms of engine performance (due to its higher LHV and lower density); however, PKME blends exhibit lower exhaust emissions across all loads in a study by Karthickeyan et al. [108]. To mitigate emissions without compromising performance, a post-combustion capture system (PCS) is installed, which includes a SCR and CC. This system helps reduce emissions of CO, HC, and NOx. With PCS, the 20% biodiesel blend showed lower BSCO, BSHC, BSNO and smoke emissions than diesel.

While advanced ATS have been a standard approach, the adoption of oxygenated fuels, renewable diesel fuels like HVO and RME, and innovative fuel blends have shown great promise in reducing engine-out emissions. These alternative approaches not only offer significant reductions in CO, HC, NOx, and particulate matter but also challenge the need for over dimensioned and costly ATS configurations. As we continue to navigate the path toward more sustainable transportation, it becomes evident that a holistic approach, considering both fuel and aftertreatment innovations, holds the key to achieving cleaner and more cost-effective engine solutions for the future.

[1] oBio® is a biofuel combining FAME and glycerol formal esters (FAGE)

4.2 Re-designing the engine for low carbon fuels

Although using LCF as drop-in substitutes for fossil fuels has great advantages in terms of reducing the manufacturing of new parts (and in turn reducing GHG emissions and other impact factors associated to the fabrication of new products), the potential benefits of designing engine component for the improvement of the fuel efficiency and emissions of LCFS are important to be studied.

A study by Novella et al. [109] used a combination of particle swarm optimization-novelty search (PSO-NS) algorithm and CFD modeling to optimize the combustion system of an engine using OMEx as a fuel with the goal to improve efficiency and reduce NOx emissions. The optimization process resulted in a 2.2% increase in engine efficiency and a 35.7% reduction in NOx emissions. A parametric study was then performed to evaluate how each parameter affects efficiency and NOx emissions. The results showed that the number of holes, spray angle, and IVC pressure have little impact on efficiency, while the injection pressure and EGR rate have a significant impact. The EGR rate has the greatest impact on NOx emissions.

A few works [110, 111] study the impact of a novel wave-shaped piston bowl design on combustion characteristics and emissions in a heavy-duty Diesel engine. Various LCF blends, including n-butanol, n-octanol, 2-ethylhexanol, HVO, and RME, were tested alongside conventional diesel fuel. The different blends were formulated to match the cetane numbers of fossil diesel. The experiments were conducted on a single-cylinder Diesel engine equipped with different piston bowl designs (a standard ω-bowl and the 6-wave shape). The results indicated that the LCF blends generally produced lower soot emissions, but slightly higher NOx emissions compared to diesel. In addition, the wave-shaped piston had a positive effect on thermal efficiency and soot emissions, particularly for conventional diesel fuel. However, its benefits were less pronounced with oxygenated blends. The study also highlighted the influence of piston bowl geometry on combustion behavior and emissions, emphasizing the potential for optimizing engine performance based on the choice of piston design, fuel composition, and operating conditions.

Karthickeyan et al. [101] thermally coated the engine's combustion chamber components with Partially Stabilized Zirconia (PSZ), transforming it into a low heat rejection engine. In the PSZ-coated engine, the research demonstrated the potential of LCFs, such as LO and PY blends, in improving engine efficiency and reducing emissions when combined with advanced engine modifications and ATS.

For OMEx fuels several works have stated incompatibility with elastomers. Kass et al. [81] conclusion suggests that adjustments should be made to the rubber

components within the engine to withstand OME3-5 blends, or alternatively, a lower proportion of OME3-5 should be incorporated into the blend. Additionally, in work by Pastor et al. [112] with OMEx as a fuel a change of fuel pump was made, replacing a regular fuel pump by diaphragm pump that uses polymerizing tetrafluoroethylene, which is more appropriate for low-lubricant hydrocarbons. This last effort indicates that for OMEx to be effectively used in vehicles redesigning the fuel injection system might be a worth endeavor.

The methanol autoignition observations point out that both large and small CI engines must be adjusted due to methanol's low reactivity and high latent heat of vaporization. Previous research has tackled these challenges through various methods, such as employing glow plugs [113], using intake heaters, raising the compression ratio (CR) to values as high as 27:1 [98], and exploring concepts like spark-assisted ignition [114]. These approaches aim to enhance the available energy for autoignition, with a primary focus on increasing temperature, which is considered essential for effective methanol combustion in engine applications. Similarly, Svenson et al. [115] discovered that increasing the CR can improve combustion stability without the need for intake heating.

Re-designing ICEVs to accommodate LCFs presents a multifaceted challenge with promising rewards. Optimizing engine components specifically for LCFs can yield significant improvements in fuel efficiency and emissions reduction. Nevertheless, it is also important to address with these re-disigns issues like elastomer compatibility and fuel injection system redesign, as highlighted by prior research, to ensure the effective implementation of certain LCFs.

5 Challenges and barriers for low carbon fuels

Transitioning from fossil fuels to non-fossil or LCFs is often viewed as a key strategy in combating climate change and reducing the environmental impact of transportation and energy production. However, despite the many claimed benefits of these alternative fuels, there are several challenges and arguments against their widespread adoption.

One of the primary challenges is the cost associated with the production and distribution of non-fossil fuels. Technologies for producing fuels like hydrogen, biofuels, and synthetic fuels can be expensive to develop and deploy, particularly when compared to the existing infrastructure for extracting and refining fossil fuels [116]. This initial cost hurdle can deter investment and slow down the transition process. Additionally, the energy input required to produce some non-fossil fuels,

such as hydrogen, can be substantial, potentially limiting the overall carbon intensity reduction if the energy source is not renewable.

Another significant challenge is the infrastructure needed for non-fossil fuels. Transitioning from gasoline and diesel to alternative gaseous fuels (like hydrogen) could require significant changes in fueling stations, transportation networks, and vehicle technologies. This infrastructure investment can be a barrier to adoption, as it necessitates substantial upfront costs and planning. Furthermore, the availability and accessibility of non-fossil fuel infrastructure may vary significantly depending on geographic location, potentially leading to disparities in access and adoption rates. Liquid LCFs do not necessarily face these issues.

Arguments against non-fossil fuels also revolve around issues like energy density and scalability. Some critics argue that alternative fuels like hydrogen or biofuels have lower energy densities than conventional fossil fuels, which can result in reduced driving ranges for vehicles or less efficient energy storage solutions. Additionally, scaling up the production of non-fossil fuels to meet global energy demands may require vast amounts of land, water, and other resources, potentially causing unintended environmental consequences such as deforestation or water scarcity. This will be discussed more in detail in Chapter 6.

Greenwashing is another significant concern when it comes to the adoption of LCFs. Greenwashing refers to the deceptive practice of marketing products or services as environmentally friendly or sustainable when they are, in reality, doing little to address environmental issues. In the context of alternative fuels, greenwashing can take several forms. Companies may exaggerate, make false claims about the environmental benefits of their non-fossil fuels or not provide enough information about the sourcing, production, and life cycle emissions of their LCFs, misleading consumers and policymakers into thinking that they are making a more significant contribution to reducing carbon emissions than they actually are. Additionally, some companies may engage in token efforts to promote non-fossil fuels, such as producing a small quantity of biofuels while continuing to rely heavily on fossil fuels. To combat greenwashing in the transportation industry is important for researchers to continue investigating the benefits and challenges of these new types of fuel to evaluate their complete potential to address the GHG dilemma. This aims to ensure that claims about environmental benefits are accurate.

6 Motivation of the study

The conclusions drawn from the literature review highlight the pressing need to address carbon emissions within the transportation sector and the complexity of the solutions available. As the transportation sector continues to be a significant contributor to GHG emissions, it is imperative to explore and implement strategies that can effectively reduce its environmental impact.

One of the key motivations for this thesis is the evaluation of promising avenues for reducing carbon emissions in transportation, such as LCFs blends, including biofuels and synthetic fuels. These options offer varying degrees of environmental benefits and challenges, making it essential to analyze and compare their impacts comprehensively. The thesis seeks to delve into the details of LCFs properties, and their potential to reduce emissions in ICEVs. Additionally, this thesis aims to provide insights and data to inform the transition towards cleaner means of transportation debate by analyzing the environmental impact of different vehicle types using LCFs, considering factors like energy sources and manufacturing materials. The literature review indicates that there remains a particular research domain that necessitates further exploration to expand the application of this concept to real-world scenarios:

- While LCFs can reduce carbon emissions from ICEVs, the challenge of tailpipe emissions remains significant. The emissions of harmful pollutants from internal combustion engines, even when using LCFs, highlight the need for ongoing research and development efforts to mitigate these emissions effectively. This thesis contributes to this ongoing effort by investigating the effects of LCFs on performance and emissions in a light-duty ICE.

- The drop-in potential of different LCF emphasizes the critical role of assessing the feasibility of LCFs as direct replacements for conventional diesel fuels in ICEs. Understanding how these fuels perform in real-world engine settings is essential for their widespread adoption and for achieving emissions reductions in the transportation sector.

- The relationship between fuel properties, engine settings, and emissions provides valuable insights. For instance, fuels with lower LHV may require higher fuel mass demands to achieve the same engine load, but the reduction in energy density doesn't necessarily translate to an equivalent increase in fuel consumption due to increased combustion efficiency, this non-linear

effect underscores the complexity of optimizing engine performance with LCFs. The influence of factors such as oxygen content, turbocharger operation, and specific combustion characteristics on air mass, exhaust energy, and overall engine behavior necessitates further exploration.

- The importance of achieving similar or lower regulated emissions and fuel efficiency compared to diesel for any LCF to be considered a fossil fuel replacement candidate is a critical motivation. The analysis of BSFC and energy equivalent BSFC for different LCF blends seeks to explore the potential of these fuels to meet or exceed diesel performance in terms of fuel consumption and efficiency. Additionally, the variation in NOx and soot emissions among LCFs highlights the need for careful consideration of emissions control strategies when adopting LCFs. This underscores the importance of a comprehensive approach to emissions control and the need to tailor solutions to specific LCFs.

- The effects of LCFs on the durability of engine components highlights a crucial challenge that must be addressed for the successful integration of LCFs into existing vehicle fleets. The need for rigorous durability and wear testing, as well as potential improvements in fuel additives or hardware design, underscores the complexity of transitioning to alternative fuels.

- An in-depth analysis of the environmental impacts of LCFs across different vehicle segments and compared them to a diesel reference aims to assess not only the reduction in the carbon footprint of fuel usage and production but also other often overlooked environmental impacts that can have significant consequences for both human health and the environment. This study provides valuable insights into the environmental impacts of different fuels and emphasizes the need to consider a broader range of impact categories beyond just GWP when evaluating the sustainability of alternative fuels.

7 Objectives of the study

Considering the comprehensive literature review and the identified research gaps, the main objective of this study is to *evaluate the potential of various fuels within the LCFs category when applied to a conventional light-duty engine in terms of combustion, performance, reduction of pollutant emissions, and the impact of their life cycle* compared to conventional fuels in different passenger vehicle segments.

The specific objectives defined to achieve the general objective are as follows:

- Analyze the impact of various LCF blends on the performance and emissions of light-duty internal combustion engines while identifying the key factors influencing their effects on engine behavior.
- Assess the potential of LCFs as drop-in replacements for conventional diesel fuels in internal combustion engines and compare them in terms of regulated emissions and fuel efficiency.
- Analyze the relationships between variations in fuel properties, engine settings, and emissions, and analyze the complexities associated with optimizing engine performance using LCFs.
- Evaluate the most efficient emissions control strategies for LCF usage, particularly in varying NOx and soot emissions among different LCFs and assess the impact of these strategies on fuel consumption while comparing them to traditional diesel fuels.
- Examine the challenges related to the durability of common-rail injectors and fuel pumps when incorporating LCFs into existing vehicle fleets and propose potential enhancements in testing methods and hardware design to mitigate these challenges.
- Realize an LCA to evaluate the environmental impacts of LCFs across diverse vehicle segments and make comparisons with diesel fuel, considering not only their carbon footprint but also other frequently neglected environmental impact categories.

8 References

[1] U. K. Roy, T. Radu and J. L. Wagner, "Carbon-negative biomethane fuel production: Integrating anaerobic digestion with algae-assisted biogas purification and hydrothermal carbonisation of digestate," *Biomass and Bioenergy*, vol. 148, no. May, p. 106029, 2021.

[2] P. Wienchol, A. Szlęk and M. Ditaranto, "Waste-to-energy technology integrated with carbon capture – Challenges and opportunities," *Energy*, vol. 198, no. May, p. 117352, 2020.

[3] Kalghatgi, "Is it really the end of internal combustion engines and petroleum in transport?," *Applied Energy*, vol. 225, no. September, pp. 965-974, 2018.

[4] E. Bannon, "Road to Zero: the last EU emission standard," *Transport & Environment*, pp. 1-19, 2020.

[5] International Council on Clean Transportation, " EU: Heavy-duty: Emissions," TransportPolicy.net, [Online]. Available: https://www.transportpolicy.net/standard/eu-heavy-duty-emissions/. [Accessed 20 July 2020].

[6] N. Duarte Souza Alvarenga Santos, V. Rückert Roso, A. C. Teixeira Malaquias, C. Baêta and J. Guilherme, "Internal combustion engines and biofuels: Examining why this robust combination should not be ignored for future sustainable transportation," *Renewable and Sustainable Energy Reviews*, vol. 148, no. September, p. 111292, 2021.

[7] A. EL-Seesy, M. Nour, H. Hassan, A. Elfasakhany, Z. He and M. Mujtaba, "Diesel-oxygenated fuels ternary blends with nano additives in compression ignition engine: A step towards cleaner combustion and green environment," *Case Studies in Thermal Engineering*, vol. 25, no. June, p. 100911, 2021.

[8] A. Arora, N. Niese, E. Dreyer, A. Waas and A. Xie, "Why Electric Cars Can't Come Fast Enough," BCG, 20 April 2021. [Online]. Available: https://www.bcg.com/publications/2021/why-evs-need-to-accelerate-their-market-penetration.

[9] IEA, "Global EV Outlook 2021," IEA, Paris, 2021.

[10] A. García, J. Monsalve-Serrano, D. Villalta and M. Guzmán-Mendoza, "Impact of low carbon fuels (LCF) on the fuel efficiency and NOx emissions of a light-duty series hybrid commercial delivery vehicle," *Fuel*, vol. 321, no. August, p. 124035, 2022.

[11] E. Commission, "A European Strategy for low-emission mobility," European Union, 2020. [Online]. Available: https://ec.europa.eu/clima/eu-action/transport-emissions_en. [Accessed 6 June 2020].

[12] Z. Mushtaq, R. Maqbool and K. Ahmad Bhat, "Chapter 13 - Genetic engineering and fifth-generation biofuels," in *Environmental Sustainability of Biofuels*, Elsevier, 2023, pp. 237-251.

[13] K. Dutta, A. Daverey and J.-G. Lin, "Evolution retrospective for alternative fuels: First to fourth generation," *Renewable Energy*, vol. 69, no. September, pp. 114-122, 2014.

[14] R. E. Sims, W. Mabee, J. N. Saddler and M. Taylor, "An overview of second generation biofuel technologies," *Bioresource Technology*, vol. Volume 101, no. 6, pp. 1570-1580, 2010.

[15] Y. Y. Tye, K. T. Lee, W. N. W. Abdullah and C. P. Leh, "Potential of Ceiba pentandra (L.) Gaertn. (kapok fiber) as a resource for second generation bioethanol: Effect of various simple pretreatment methods on sugar production," *Bioresource Technology*, vol. 116, no. July, pp. 536-539, 2012.

[16] J. Singh and S. Gu, "Commercialization potential of microalgae for biofuels production," *Renwable and Sustainable Energy Reviews*, vol. 14, no. 9, pp. 2596-2610, 2010.

[17] E. Suali and R. Sarbatly, "Conversion of microalgae to biofuel," *Renewable and Sustainable Energy Reviews*, vol. 16, no. 6, pp. 4316-4342, 2012.

[18] S. G. Hays and D. Ducat, "Engineering cyanobacteria as photosynthetic feedstock factories," *Photosynthesis Research*, vol. 123, pp. 285-295, 2015.

[19] European Commission, "Communication from the Commission on voluntary schemes and default values in the EU biofuels and bioliquids sustainability scheme (2010/C 160/01)," Official Journal of the European Union , 2010.

[20] S. Soam and K. Hillman, "Factors influencing the environmental sustainability and growth of hydrotreated vegetable oil (HVO) in Sweden," *Bioresource Technology Reports,* vol. 7, no. September, p. 100244, 2019.

[21] A. P. Vyas, J. L. Verma and N. Subrahmanyam, "A review on FAME production processes," *Fuel,* vol. 89, no. 1, pp. 1-9, 2010.

[22] B. Freedman, E. Pryde and T. Mounts, "Variables affecting the yields of fatty esters from transesterified vegetable oils," *Journal of the American Oil Chemists Society,* vol. 61, no. 10, pp. 1638-1643, 1984.

[23] K. R. Jegannathan, S. Abang, D. Poncelet, E. S. C. Chan and P. Ravindra, "Production of biodiesel using immobilized lipase – a critical review," *Critical Reviews in Biotechnology,* vol. 28, no. 4, pp. 253-264, 2008.

[24] S. Nasar, M. A. Hanif, U. Rashid, A. Hanif, M. N. Akhtar and C. Ngamcharussrivichai, "The production of fatty acid methyl esters (FAME) through transesterification is a crucial process for biodiesel production. To make this process more efficient and environmentally friendly, researchers are exploring various catalysts. Currently, both hom," *Catalysts,* vol. 11, no. 9, p. 1085, 2021.

[25] M. Prussi, M. Yugo, L. De Prada, M. Padella, R. Edwards and L. Lonza, "JEC Well-to-Tank report v5, EUR 30269 EN," Publications Office of the European Union, Luxembourg,, 2020.

[26] H. Cai, M. Prussi, L. Ou, M. Wang, M. Yugo, L. Lonza and N. Scarlat, "Decarbonization potential of on-road fuels and powertrains in the European Union and the United States: a well-to-wheels assessment," *Sustainable Energy Fuels,* vol. 6, pp. 4398-4417, 2022.

[27] K. Tucki, O. Orynycz, R. Mruk, A. Świć and K. Botwińska, "Modeling of Biofuel's Emissivity for Fuel Choice Management," *Sustainability,* vol. 11, no. 23, p. 6842, 2019.

[28] Q. Cheng, H. Tuomo, O. Kaario and L. Martti, "HVO, RME, and Diesel Fuel Combustion in an Optically Accessible Compression Ignition Engine," *Energy Fuels*, vol. 33, no. 3, pp. 2489-2501, 2019.

[29] G. Labeckas and S. Slavinskas, "The effect of rapeseed oil methyl ester on direct injection Diesel engine performance and exhaust emissions," *Energy Conversion and Management*, vol. 47, no. 13-14, pp. 1954-1967, 2006.

[30] A. Tsolakis, A. Megaritis, M. Wyszynski and K. Theinnoi, "Engine performance and emissions of a diesel engine operating on diesel-RME (rapeseed methyl ester) blends with EGR (exhaust gas recirculation)," *Energy*, vol. 32, no. 11, pp. 2072-2080, 2007.

[31] M. Novakovic, S. Shamun, V. B. Malmborg, K. I. Kling, J. Kling, U. B. Vogel, P. Tunestal, J. Pagels and M. Tuner, "Regulated Emissions and Detailed Particle Characterisation for Diesel and RME Biodiesel Fuel Combustion with Varying EGR in a Heavy-Duty Engine," *SAE Technical Paper*, pp. 2019-01-2291, 2019.

[32] Y. Kroyan, M. Wojcieszyk, O. Kaario, M. Larmi and K. Zenger, "Modeling the end-use performance of alternative fuels in light-duty vehicles," *Energy*, vol. 205, no. August, p. 117854, 2020.

[33] A. Al Ezzi, M. A. Fayad, A. M. Al Jubori, A. A. Jaber, L. A. Alsadawi, H. A. Dhahad, M. T. Chaichan and T. Yusaf, "Influence of fuel injection pressure and RME on combustion, NOx emissions and soot nanoparticles characteristics in common-rail HSDI diesel engine," *International Journal of Thermofluids*, vol. 15, no. August, p. 100173, 2022.

[34] M. Tongroon, A. Suebwong, M. Kananont, J. Aunchaisri and N. Chollacoop, "High quality jatropha biodiesel (H-FAME) and its application in a common rail diesel engine," *Renewable Energy*, vol. 113, no. December, pp. 660-668, 2017.

[35] M. Unglert, D. Bockey, C. Bofinger, B. Buchholz, G. Fisch, R. Luther, M. Müller, K. Schaper, J. Schmitt, O. Schröder, U. Schümann, H. Tschöke, E. Remmele, R. Wicht, M. Winkler and Krahl, "Action areas and the need for research in biofuels," *Fuel*, vol. 268, no. May, p. 117227, 2020.

[36] B. Cieślikowski, Process of Gradual Dysfunction of a Diesel Engine Caused by Formation of PM Deposits of FAME Origin, Springer Proceedings in Energy.

[37] H. Aatola, M. Larmi, T. Sarjovaara and S. Mikkonen, "Hydrotreated Vegetable Oil (HVO) as a Renewable Diesel Fuel," *SAE International Journal of Engines,* vol. 1, no. 1, pp. 1251-1262, 2009.

[38] R. Suarez-Bertoa, M. Kousoulidou, M. Clairotte, B. Giechaskiel, J. Nuottimäki, T. Sarjovaara and L. Lonza, "Impact of HVO blends on modern diesel passenger cars emissions during real world operation," *Fuel,* vol. 235, no. January, pp. 1427-1435, 2019.

[39] L. Rantanen, R. Linnaila, P. Aakko and T. Harju, "NExBTL - Biodiesel Fuel of the Second Generation," *SAE Technical Paper,* pp. 2005-01-3771, 2005.

[40] C. J. Hor, Y. H. Tan, N. M. Mubarak, I. S. Tan, M. L. Ibrahim, P. Yek, R. R. Karri and M. Khalid, "Techno-economic assessment of hydrotreated vegetable oil as a renewable fuel from waste sludge palm oil," *Environmental Research,* vol. 220, no. March, p. 115169, 2023.

[41] R. Arvidsson, S. Persson, M. Fröling and M. Svanström, "Life cycle assessment of hydrotreated vegetable oil from rape, oil palm and Jatropha," *Journal of Cleaner Production,* vol. 19, no. 2-3, pp. 129-137, 2011.

[42] R. Edwards, J.-F. Larive and J.-C. Beziat, "Well-to-Wheels Analysis of Future Automotive Fuels and Power Trains in the European Context - Report, Version 3c. EUR 24952 EN.," Publications Office of the European Union, Luxembourg, 2011.

[43] J. Rodríguez-Fenández, J. J. Hernández, A. Calle-Asensio, Á. Ramos and J. Barba, "Selection of Blends of Diesel Fuel and Advanced Biofuels Based on Their Physical and Thermochemical Properties," *Energies,* vol. 12, no. 11, p. 2034, 2019.

[44] Y. Li, H. Xu, R. Cracknell, R. Head and S. Shuai, "An experimental investigation into combustion characteristics of HVO compared with TME and ULSD at varied blend ratios," *Fuel,* vol. 255, no. November, p. 115757, 2019.

[45] I. Bortel, J. Vávra and M. Takáts, "Effect of HVO fuel mixtures on emissions and performance of a passenger car size diesel engin," *Renewable Energy,* vol. 140, no. September, pp. 680-691, 2019.

[46] J. Preuß, K. Munch and I. Denbratt, "Performance and emissions of renewable blends with OME3-5 and HVO in heavy duty and light duty compression ignition engines," *Fuel,* vol. 303, no. November, p. 121275, 2021.

[47] A. Mancarella and O. Marello, "Effect of Coolant Temperature on Performance and Emissions of a Compression Ignition Engine Running on Conventional Diesel and Hydrotreated Vegetable Oil (HVO)," *Energies,* vol. 16, no. 1, p. 144, 2023.

[48] J. Rodríguez-Fernández, M. Lapuerta and J. Sánchez-Valdepeñas, "Regeneration of diesel particulate filters: Effect of renewable fuels," *Renewable Energy,* vol. 104, no. April, pp. 30-39, 2017.

[49] S. Hänggi, P. Elbert, T. Bütler, U. Cabalzar, S. Teske, C. Bach and C. Onder, "A review of synthetic fuels for passenger vehicles," *Energy Reports,* vol. 5, no. November, pp. 555-569, 2019.

[50] H. Mahmoudi, M. Mahmoudi, O. Doustdar, H. Jahangiri, A. Tsolakis, S. Gu and M. LechWyszynski, "A review of Fischer Tropsch synthesis process, mechanism, surface chemistry and catalyst formulation," *Biofuels Engineering,* vol. 2, no. 1, pp. 11-31, 2017.

[51] A. Y. Krylova, "Products of the Fischer-Tropsch synthesis (A Review)," *Solid Fuel Chemistry,* vol. 48, pp. 22-35, 2014.

[52] J. C. Ruth and G. Stephanopoulos, "Synthetic fuels: what are they and where do they come from?," *Current Opinion in Biotechnology,* vol. 81, no. June, p. 102919, 2023.

[53] V. B. Borugadda, G. Kamath and A. K. Dalai, "Techno-economic and life-cycle assessment of integrated Fischer-Tropsch process in ethanol industry for bio-diesel and bio-gasoline production," *Energy,* vol. 195, no. March, p. 116985, 2020.

[54] C. M. Liu, N. K. Sandhu, S. T. McCoy and J. A. Bergerson, "A life cycle assessment of greenhouse gas emissions from direct air capture and Fischer–Tropsch fuel production," *Sustainable Energy & Fuels,* vol. 4, pp. 3129-3142, 2020.

[55] B. Hao, C. Song, G. Lv, B. Li, X. Liu, K. Wang and Y. Liu, "Evaluation of the reduction in carbonyl emissions from a diesel engine using Fischer–Tropsch fuel synthesized from coal," *Fuel,* vol. 133, no. October, pp. 115-122, 2014.

[56] A. Y. Khodakov, W. Chu and P. Fongarland, "Advances in the Development of Novel Cobalt Fischer−Tropsch Catalysts for Synthesis of Long-Chain Hydrocarbons and Clean Fuels," *Chemical Reviews,* vol. 107, no. 5, pp. 1692-1744, 2007.

[57] P. Cai, C. Zhang, Z. Jing, Y. Peng, J. Jing and H. Sun, "Effects of Fischer-Tropsch diesel blending in petrochemical diesel on combustion and emissions of a common-rail diesel engine," *Fuel,* vol. 305, no. December, p. 121587, 2021.

[58] H. Yuan, T. Tsukuda, Y. Yang, G. Shibata, Y. Kobashi and H. Ogawa, "Effects of Chemical Compositions and Cetane Number of Fischer–Tropsch Fuels on Diesel Engine Performance," *Energies,* vol. 15, no. 11, p. 4047, 2022.

[59] M. H. McMillian and M. Gautam, "Consideration for Fischer-Tropsch Derived Liquid Fuels as a Fuel Injection Emission Control Parameter," *SAE Technical Paper,* p. 982489, 1998.

[60] C. Zhang, Z. Jing, P. Cai, Y. Li, H. Sun, W. Huang, J. Jing, H. Wang and X. Yu, "Experimental investigation on combustion and emission characteristics of Fischer-Tropsch diesel/gasoline in a multi-cylinder heavy-duty diesel engine under different loads," *Fuel,* vol. 324, no. Part A, p. 124504, 2022.

[61] J. V. Pastor, A. García, C. Micó and F. Lewiski, "An optical investigation of Fischer-Tropsch diesel and Oxymethylene dimethyl ether impact on combustion process for CI engines," *Applied Energy,* vol. 260, no. February, p. 114238, 2020.

[62] M. Bassiony, A. Ibrahim and M. El-Kassaby, "An experimental study on the effect of using gas-to-liquid (GTL) fuel on diesel engine performance and emissions," *Alexandria Engineering Journal*, vol. 55, no. 3, pp. 2115-2124, 2016.

[63] L. Ye, Y. Shi, T. Liu, Q. Zheng, M. M. Ashfaq, C. Sun, A. Shi and M. Ajmal, "Study on emission and particulate matter characteristics from diesel engine fueled with n-pentanol/Fischer–Tropsch diesel," *Energy Sources, Part A: Recovery, Utilization, and Environmental Effects*, 2020.

[64] P. Cai, C. Zhang, Z. Jing, Y. Peng, J. Jing and H. Sun, "Effects of Fischer-Tropsch diesel blending in petrochemical diesel on combustion and emissions of a common-rail diesel engine," *Fuel*, vol. 305, no. December, p. 121587, 2021.

[65] W. Zhong, J. Yang, L. Ruina and L. Shuai, "Gas emissions and particulate matter of non-road diesel engine fueled with F-T diesel with EGR," *Energy Sources, Part A: Recovery, Utilization, and Environmental Effects*, vol. 41, no. 5, pp. 542-555, 2019.

[66] K. Yehliu, A. Boehman and O. Armas, "Emissions from different alternative diesel fuels operating with single and split fuel injection," *Fuel*, vol. 89, no. 2, pp. 423-437, 2010.

[67] O. Armas, K. Yehliu and A. L. Boehman, "Effect of alternative fuels on exhaust emissions during diesel engine operation with matched combustion phasing," *Fuel*, vol. 89, no. 2, pp. 438-456, 2010.

[68] Z. Wang, H. L. Liu, X. Ma, J. Wang, S. Shuai and R. D. Reitz, "Homogeneous charge compression ignition (HCCI) combustion of polyoxymethylene dimethyl ethers (PODE)," *Fuel*, vol. 183, no. November, pp. 206-213, 2016.

[69] J. Yanowitz, M. A. Ratcliff, R. L. McCormick, J. D. Taylor and M. J. Murphy, "Compendium of Experimental Cetane Numbers," 2014.

[70] W. Sun, W. Guoquing, L. Shuang, Z. Ruzheng, Y. Bin, Y. Jiuzhong, L. Yuyang, C. K. Westbrook and C. K. Law, "Speciation and the laminar burning velocities of poly(oxymethylene) dimethyl ether 3 (POMDME3) flames: An experimental and modeling study," *Proceeding of the Combustion Institute*, vol. 36, no. 1, pp. 1269-1278, 2017.

[71] Y. R. Tan, M. L. Botero, Y. Sheng, J. A. H. Dreyer, R. Xu, W. Yang and M. Kraft, "Sooting characteristics of polyoxymethylene dimethyl ether blends with diesel in a diffusion flame," *Fuel*, vol. 224, no. July, pp. 499-506, 2018.

[72] D. F. Rodríguez-Vallejo, A. Valente, G. Guillén-Gosálbez and B. Chachuat, "Economic and life-cycle assessment of OME3–5 as transport fuel: a comparison of production pathways," *Sustainable Energy Fuels*, vol. 5, pp. 2504-2516, 2021.

[73] S. Deutz, D. Bongartz, B. Heuser, A. Kätelhön, L. S. Langenhorst, A. Omari, M. Walters, J. Klankermayer, W. Leitner, A. Mitsos, S. Pischinger and A. Bardow, "Cleaner production of cleaner fuels: wind-to-wheel – environmental assessment of CO2-based oxymethylene ether as a drop-in fuel," *Energy & Environmental Science*, vol. 11, pp. 331-343, 2018.

[74] C. Hank, L. Lazar, F. Mantei, M. Ouda, R. J. White, T. Smolinka, A. Schaadt, C. Hebling and H.-M. Henning, "Comparative well-to-wheel life cycle assessment of OME3–5 synfuel production via the power-to-liquid pathway," *Sustainable Energy & Fuels*, vol. 3, pp. 3219-3233, 2019.

[75] J. Liu, H. Wang, Y. Li, Z. Zheng, Z. Xue, H. Shang and M. Yao, "Effects of diesel/PODE (polyoxymethylene dimethyl ethers) blends on combustion and emission characteristics in a heavy duty diesel engine," *Fuel*, vol. 177, no. August, pp. 206-216, 2016.

[76] A. García, J. Monsalve-Serrano, D. Villalta and Á. Fogué-Robles, "Evaluating OMEx combustion towards stoichiometric conditions in a compression ignition engine," *Fuel*, vol. 303, no. November, p. 121273, 2021.

[77] A. Omari, B. Heuser and S. Pischinger, "Potential of oxymethylenether-diesel blends for ultra-low emission engines," *Fuel*, vol. 209, no. December, pp. 232-237, 2017.

[78] F. Zacherl, C. Wopper, P. Schwanzer and H.-P. Rabl, "Potential of the Synthetic Fuel Oxymethylene Ether (OME) for the Usage in a Single-Cylinder Non-Road Diesel Engine: Thermodynamics and Emissions," *Energies*, vol. 15, no. 21, p. 7932, 2022.

[79] Z. Xing, M. Yu, C. Chen and X. Jiang, "A molecular investigation on the effects of OMEX addition on soot inception of diesel pyrolysis," *Fuel,* vol. 346, no. August, p. 128357, 2023.

[80] S. Schemme, R. C. Samsun, R. Peters and D. Stolten, "Power-to-fuel as a key to sustainable transport systems – An analysis of diesel fuels produced from CO2 and renewable electricity," *Fuel,* vol. 205, no. October, pp. 198-221, 2017.

[81] M. Kass, M. Wissink, C. Janke, R. Connatser and S. Curran, "Compatibility of Elastomers with Polyoxymethylene Dimethyl Ethers and Blends with Diesel," *SAE International Journal Advances and Current Practices In Mobility,* vol. 2, no. 4, pp. 1693-1973, 2020.

[82] J. Tian, Y. Cai, Y. Shi, Y. Cui and R. Fan, "Effect of Polyoxymethylene Dimethyl Ethers/Diesel Blends on Fuel Properties and Particulate Matter Oxidation Activity of A Light-Duty Diesel Engine," *International Journal of Automotive Technology,* vol. 20, pp. 277-288, 2019.

[83] M. Härt, K. Gaukel, D. Pélerin and G. Wachtmeister, "Oxymethylene Ether as Potentially CO2-neutral Fuel for Clean Diesel Engines Part 1: Engine Testing," *MTZ worldwide,* vol. 78, pp. 52-59, 2017.

[84] M. K. Yesilyurt, M. Aydin, Z. Yilbasi and M. Arslan, "Investigation on the structural effects of the addition of alcohols having various chain lengths into the vegetable oil-biodiesel-diesel fuel blends: An attempt for improving the performance, combustion, and exhaust emission characteristics of a compressi," *Fuel,* vol. 269, no. June, p. 117455, 2020.

[85] T. Verger, U. Azimov and O. Adeniyi, "Biomass-based fuel blends as an alternative for the future heavy-duty transport: A review," *Renewable and Sustainable Energy Reviews,* vol. 161, no. June, p. 112391, 2022.

[86] F. Millo, F. Mallamo, T. Vlachos, C. Ciaravino, L. Postrioti and G. Buitoni, "Experimental Investigation on the Effects on Performance and Emissions of an Automotive Euro 5 Diesel Engine Fuelled with B30 from RME and HVO," *SAE Technical Paper,* pp. 2013-01-1679, 2013.

[87] B. Singh Chauhan, R. Kripal Singh and H. M. Cho, "Practice of diesel fuel blends using alternative fuels: A review," *Renewable and Sustainable Energy Reviews*, vol. 59, no. June, pp. 1358-1368, 2016.

[88] O. Emenike, S. Michailos, K. J. Hughes, D. Ingham and M. Pourkashanian, "Techno-economic and environmental assessment of BECCS in fuel generation for FT-fuel, bioSNG and OMEx," *Sustainable Energy Fuels*, vol. 5, pp. 3382-3402, 2021.

[89] M. R. Seraç, S. Aydın, A. Yılmaz and S. Şevik, "Evaluation of comparative combustion, performance, and emission of soybean-based alternative biodiesel fuel blends in a CI engine," *Renewable Energy*, vol. 148, no. April, pp. 1065-1073, 2020.

[90] T. Sathish, V. Mohanavel, M. Arunkumar, K. Rajan, M. E. Soudagar, M. Mujtaba, S. H. Salmen, S. A. Obaid, H. Fayaz and S. Sivakumar, "Utilization of Azadirachta indica biodiesel, ethanol and diesel blends for diesel engine applications with engine emission profile," *Fuel*, vol. 319, no. July, p. 123798, 2022.

[91] A. Gómez, R. García-Contreras, J. Soriano and C. Mata, "Comparative study of the opacity tendency of alternative diesel fuels blended with gasoline," *Fuel*, vol. 264, no. March, p. 116860, 2020.

[92] C. Kaewbuddee, E. Sukjit, J. Srisertpol, S. Maithomklang, K. Wathakit, N. Klinkaew, P. Liplap and W. Arjharn, "Evaluation of Waste Plastic Oil-Biodiesel Blends as Alternative Fuels for Diesel Engines," *Energies*, vol. 13, no. 11, p. 2823, 2020.

[93] A. Atmanli and N. Yilmaz, "Comparative assessment of different diesel engines fueled with 1-pentanol and diesel blends," *Sustainable Energy*, vol. 40, no. 5, p. e13663, 2021.

[94] P. Napolitano, C. Beatrice, C. Guido, N. Del Giacomo, L. Pellegrini and P. Scorletti, "Hydrocracked Fossil Oil and Hydrotreated Vegetable Oil (HVO) Effects on Combustion and Emissions Performance of “Torque-Controlled” Diesel Engines," *SAE Technical Paper*, pp. 2015-24-2497, 2015.

[95] M. G. Kassem, A.-M. M. Ahmed, H. H. Abdel-Rahman and A. H. Moustafa, "Use of Span 80 and Tween 80 for blending gasoline and alcohol in spark ignition engines," *Energy Reports*, vol. 5, no. November, pp. 221-230, 2019.

[96] M. G. Bidir, N. Millerjothi, M. S. Adaramola and F. Y. Hagos, "The role of nanoparticles on biofuel production and as an additive in ternary blend fuelled diesel engine: A review," *Energy reports*, vol. 7, no. November, pp. 3614-3627, 2021.

[97] A. García, J. Monsalve-Serrano, C. Micó and M. Guzmán-Mendoza, "Parametric evaluation of neat methanol combustion in a light-duty compression ignition engine," *Fuel Processing Technology*, vol. 249, no. October, p. 107850, 2023.

[98] S. Shamun, C. Haşimoğlu, A. Murcak, Ö. Andersson, M. Tunér and P. Tunestål, "Experimental investigation of methanol compression ignition in a high compression ratio HD engine using a Box-Behnken design," *Fuel*, vol. 209, pp. 624-633, 2017.

[99] A. Aziz, L. Xu, A. Garcia and M. Tuner, "Influence of Injection Timing on Equivalence Ratio Stratification of Methanol and Isooctane in a Heavy-Duty Compression Ignition Engine," *SAE Technical Paper*, pp. 2020-01-2069, 2020.

[100] M. Ul Haq, A. T. Jafry, S. Ahmad, T. Ahmad Cheema, M. Q. Ansari and N. Abbas, "Recent Advances in Fuel Additives and Their Spray Characteristics for Diesel-Based Blends," *Energies*, vol. 15, no. 19, p. 7281, 2022.

[101] V. Karthickeyan, S. Thiyagarajan, V. Edwin Geo, B. Ashok, K. Nanthagopal, O. H. Chyuan and R. Vignesh, "Simultaneous reduction of NOx and smoke emissions with low viscous biofuel in low heat rejection engine using selective catalytic reduction technique," *Fuel*, vol. 255, no. November, p. 115854, 2019.

[102] J. Demuynck, C. Favre, D. Bosteels, F. Bunar, J. Spitta and A. Kuhrt, "Diesel Vehicle with Ultra-Low NOx Emissions on the Road," *SAE Technical Paper*, pp. 2019-24-0145, 2019.

[103] R. Vallinayagam, S. Vedharaj, W. Yang, C. Saravanan, P. Lee, K. Chua and S. Chou, "Emission reduction from a diesel engine fueled by pine oil biofuel

using SCR and catalytic converter," *Atmospheric Environment*, vol. 80, no. December, pp. 190-197, 2013.

[104] L. Gren, V. B. Malmborg, J. Falk, L. Markula, M. Novakovic, S. Shamun, A. C. Eriksson, T. B. Kristensen, B. Svenningsson, M. Tunér, P. Karjalainen and J. Pagels, "Effects of renewable fuel and exhaust aftertreatment on primary and secondary emissions from a modern heavy-duty diesel engine," *Journal of Aerosol Science*, vol. 156, no. August, p. 105781, 2021.

[105] Y. Wu, H. Li and G. Andrews, "Particle Emissions and Size Distribution across the DPF from a Modern Diesel Engine Using Pure and Blended GTL Fuels," *SAE Technical Paper*, pp. 2020-01-2059, 2020.

[106] Y. Zhang, D. Lou, P. Tan, Z. Hu and L. Fang, "Effects of waste-cooking-oil biodiesel blends on diesel vehicle emissions and their reducing characteristics with exhaust after-treatment system," *Journal of Cleaner Production*, vol. 381, no. Part 1, p. 135190, 2022.

[107] J. Hernández, J. Rodríguez-Fernández and A. Calle-Asensio, "When diesel NOx aftertreatment systems meet advanced biofuels," *Results in Engineering*, vol. 2, no. June, p. 100009, 2019.

[108] V. Karthickeyan, B. Ashok, K. Nanthagopal, S. Thiyagarajan and V. Edwin Geo, "Investigation of novel Pistacia khinjuk biodiesel in DI diesel engine with post combustion capture system," *Applied Thermal Engineering*, vol. 159, no. August, p. 113969, 2019.

[109] R. Novella, G. Bracho, J. Gomez-Soriano, C. S. Fernandes and T. Lucchini, "Combustion system optimization for the integration of e-fuels (Oxymethylene Ether) in compression ignition engines," *Fuel*, vol. 305, no. December, p. 121580, 2021.

[110] T. Zhang, J. Eismark, K. Munch and Denbratt, "Effects of a wave-shaped piston bowl geometry on the performance of heavy duty Diesel engines fueled with alcohols and biodiesel blends," *Renewable Energy*, vol. 148, no. April, pp. 512-522, 2020.

[111] J. Eismark, M. Christensen, M. Andersson, A. Karlsson and I. Denbratt, "Role of fuel properties and piston shape in influencing soot oxidation in

heavy-duty low swirl diesel engine combustion," *Fuel*, vol. 254, no. October, p. 115568, 2019.

[112] J. V. Pastor, J. M. Garcia-Oliver, C. Micó and F. J. Tejada, "Comparison of the Diffusive Flame Structure for Dodecane and OMEX Fuels for Conditions of Spray A of the ECN," *SAE Int. J. Adv. & Curr. Prac. in Mobility*, vol. 3, no. 1, pp. 402-411, 2021.

[113] C. Kroeger, "A Neat Methanol Direct Injection Combustion System for Heavy-Duty Applications," *SAE Technical Paper*, p. 861169, 1986.

[114] K. Hikino and T. Suzuki, "Development of Methanol Engine with Autoignition for Low Nox Emission and Better Fuel Economy," *SAE Technical Paper*, no. 891842, 1989.

[115] M. Svensson, M. Tuner and S. Verhelst, "Low Load Ignitability of Methanol in a Heavy-Duty Compression Ignition Engine," *SAE Technical Paper*, pp. 2022-01-1093, 2022.

[116] S. Sgouridis, Carbajales-Dale, Michael, D. Csala, M. Chiesa and U. Bardi, "Comparative net energy analysis of renewable electricity and carbon capture and storage," *Nature Energy*, vol. 4, pp. 456-465, 2019.

Chapter 3
Tools and Methodology

Contents

1 Introduction

This chapter delves into the comprehensive methodology used for the research of low carbon fuels (LCFs) in a direct injection (DI) compression ignition (CI) engine. The experimental facilities, the characteristics of the multicylinder engine, the fuel injection and air management systems, the Exhaust Gas Recirculation (EGR) system, and the control system are described in detail, laying the foundation for the study. The engine utilized in the experiments is the B16DTH, a commercial multicylinder engine, making it an ideal platform for assessing the performance of LCFs.

Accurate measurements of engine performance are crucial to the study, and therefore, the chapter elaborates on the measuring equipment, their working principle, and the methods employed to capture reliable data during our tests, emphasizing their importance in evaluating the engine's behaviour under various operating conditions.

The chapter introduces the seven distinct LCFs tested, highlighting their characteristic properties, and drawing upon previous research for correlations between fuel characteristics and performance. These insights provide valuable context for our investigation and aid in understanding the potential impact of different LCFs on engine performance and emissions.

To carry out the research, various theoretical tools are employed, among which the combustion diagnostics tool CALMEC plays a pivotal role. Alongside, relevant combustion indicators and parameters essential for the subsequent chapters are presented, which improve the understanding of the engine’s behaviour under LCF operation.

Both experimental and numerical methodologies are thoroughly discussed, with an emphasis on engine stationary operation. Possible sources of error are addressed to maintain the rigor of the study. The test matrix used to evaluate the LCFs is outlined, and the chapter distinguishes between two types of calibrations: drop-in and optimized. These calibrations will be the focus of the results in the forthcoming chapters. For optimized calibration, the concept of the design of experiments (DOE) is introduced, along with the explanation for adopting two-level factorial designs, providing a robust framework for optimization.

The chapter concludes by delving into the modelling of engine performance using linear models and linear optimization based on those models. This modelling approach enables to predict optimum conditions and validate them through

subsequent tests. By combining experimental data with numerical modelling, the aim is to gain deeper insights into the potential of LCFs for achieving more sustainable and efficient combustion in DI CI engines.

2 Experimental facilities

This section describes the experimental setup used to investigate the effect of LCFs on performance and emissions in a light-duty ICE. This includes a description of the engine, the fuel injection system, and the emissions measurement equipment; including a description of the data acquisition system used to measure engine performance and emissions, as well as the software used for data analysis. The experimental procedure is also described in detail, including the conditions under which the experiments were conducted.

2.1 Multicylinder engine description

The experimental section of the study will be carried on a B16DTH diesel engine, which is compliant with EURO 6 normative in its commercial version and it is equipped in a series of vehicles like the OPEL Astra J, Vauxhall Zafira Tourer 1.6 and other medium sized passenger cars. Details on the engine and its subassemblies are described in this section.

2.1.1 Engine description

The engine is a 1.6L 4-cylinder in-line diesel (B16DTH) engine provided with a high-pressure EGR system. Because the research focuses on assessing whether the LCFs could be used with minimal modifications into existing systems, almost no changes were made in the engine (scheme depicted in Figure 2). The engine can deliver up to 100 kWh at 4000 rpm with diesel as the use fuel. Table 1 shows the most relevant information for the engine.

Table 1. Engine characteristics

Engine type	4-stoke, 4-valves, direct injection
Number of cylinders (-)	4
Cylinder diameter (mm)	79.7
Stroke (mm)	80.1
Total displaced volume (cm3)	1598
Connecting rod length (mm)	140
Compression ratio (-)	15.5
Rated power (kw)	100 @ 4000 rpm
Rated torque (Nm)	320 @ 2000 rpm

The B16DTH is mainly made from aluminum, with an aluminum engine block, die-cast aluminum bedplate, an aluminum cylinder head and pistons; nonetheless connecting rods are made of forged steel. The piston bowl profile is shallow re-entrant type to facilitate combustion (Figure 1) and the pistons are cooled by under-skirt oil spraying. Each of the 4 cylinders has 4 valves which are actioned by a chain driven dual overhead camshaft.

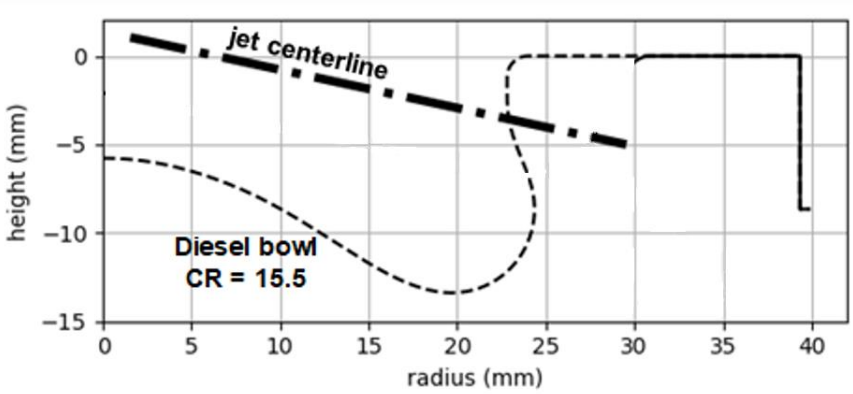

Figure 1. Piston bowl profile

2.1.2 Fuel injection system

The injection system relies on direct injection, as is typical for compression ignition diesel engines. During tests with the LCFs the fuel injection system (FIS) was maintained with stock specifications, with the fuel injected into the combustion chamber by high-pressure solenoid injectors, which are connected to a common rail with pressure regulator feed by a fuel lubricated high-pressure pump. Table 2 provides the main characteristics for the FIS.

Table 2. Injection system characteristics

Type of injector	Solenoid
Number of holes (-)	7
Hole diameter (μm)	141
Flow number (cc/30s)	340
Maximum injection pressure (bar)	2000

2.1.3 Air management and exhaust gas recirculation systems

One of the main reasons why current engines have reached high efficiencies is the air management system. The studied engine air management system is composed of a turbocharger with a variable geometry turbine (VGT) and a fixed geometry compressor. The VGT allows efficient operation through a wide range of mass flows according to its vane position. The ability to vary the flows in this way provides a degree of freedom which will be later taken advantage of during the calibration of the operation with LCFs, by allowing to correctly match mass flow variations and EGR concentrations. As for the calibration, it is important to characterize the EGR system as it has become a fundamental sub-system to provide an adequate tradeoff between NOx-soot and performance in ICEs. For this work the original high-pressure EGR route was maintained, where a portion of the exhaust gases is rerouted (and regulated with a valve) to a heat exchanger for reduction of the temperature to later be mixed with the fresh intake air coming from the compressor. These systems can be observed in Figure 2, represented by the blue, orange and red solid lines.

2.1.4 Engine control system

The engine control unit (ECU) was provided with a baseline diesel B7 calibration, developed by General Motors (GM) and PUNCH Torino (formerly GM Powertrain Torino). As will be later described in detail, this baseline calibration is used for drop-in tests to represent the scenario of the current automotive fleet. The ECU was open so with an INCA V5.2 virtual environment (dedicated tool for ECU tests, diagnostics and calibration of 128 electronically controlled systems in the vehicle [1]) the baseline calibration could be modified and optimized for the use of the engine with LCFs.

During this work 8 main parameters, for air management and injection control, were adjusted during the calibration optimization tasks. For the injection settings the injection pressure (IP), the start of injection (SOI), the volume (Vx) and dwell times (Dx) of the two pilot injections and the total mass injected (MI) were varied. The air mass quantity per cylinder cycle (Air) and boosting pressure (Boost) where controlled from the air management system; these last two variables in tandem regulate the amount of EGR that goes into the cylinder, where their reduction (particularly the Air) increases the amount of EGR by virtue of being linked to higher EGR valve aperture maps.

2.2 Test cell characteristics

The test cell configuration used in this study is represented in Figure 2. The test cell was equipped with a dynamometer, a gas analyzer, a smoke meter, a gravimetric fuel balance, pressure and temperature sensors, as well as controls and acquisition systems; these systems provided measurement of the main boundary conditions for the analysis and control of the engine during tests.

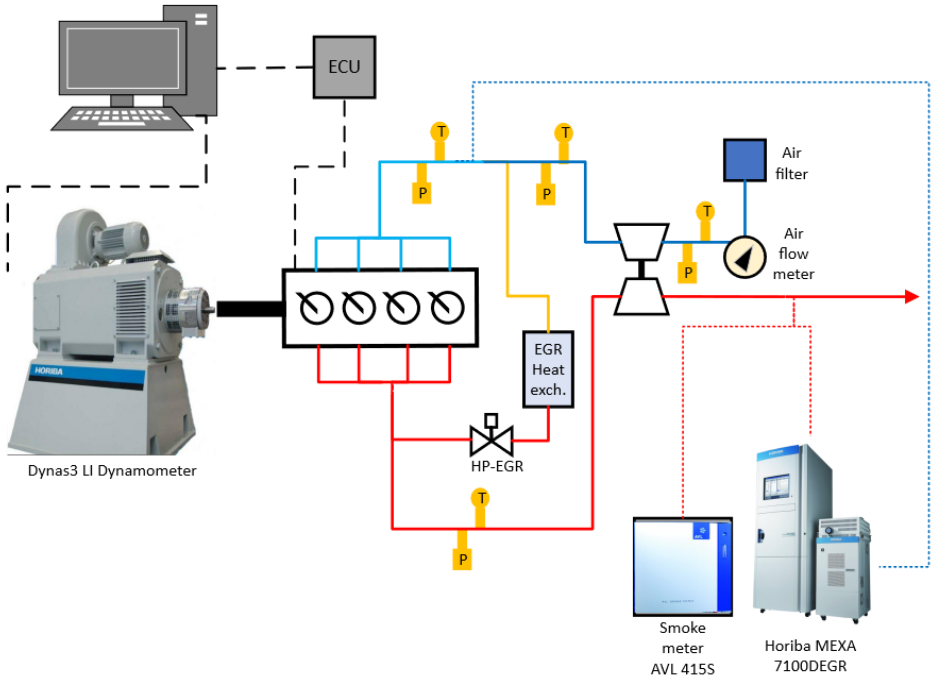

Figure 2. Test cell schematic

Table 3 provides a summary for the main instrumentation used during this study, while the next subsections will describe the working range, measurement principles and uncertainties associated with the sensors, in addition to the signal processing devices used.

Table 3. Test cell instrumentation summary

Variable	Device	Manufacturer/ model	Accuracy
Engine speed	Encoder	AVL / 364C	± 0.2 CAD
Instantaneous pressure	Piezoelectric transducer	AVL GH14p	±1% @ max. pressure
Intake/Exhaust pressure	Piezoresistive transducers	Kistler / 4045A	± 25 mbar
Temperature	Thermocouple	TC direct / type K	± 2.5 ºC
NOx, CO, HC, O_2 and CO_2	Gas analyzer	Horiba MEXA 7100 D-EGR	4%
FSN	Smoke meter	AVL 415SE	±0.025 FSN
Fuel mass flow	Fuel balance	AVL 733S	±0.12%
Air mass flow	Air flow meter	ABB/Sensyflow FMT700-P	±0.1%
Blow-by flow	Blow by flow meter	AVL 422	±0.1%
Torque	Dynamometer	Dynas3 LI 250	0-250 kW

2.2.1 Engine speed and torque regulation and measurement

For engine speed and torque regulation and measurement, the test rig was provided with a Horiba's Dynas3 LI 250 dynamometer [2]. This dynamometer guaranteed steady stationary conditions of engine speed and torque, preventing variations over time that could cause differences in the mass flow and other engines subsystems in a cycle-to-cycle basis. The dynamometer can support engines with power outputs up to 250 kW and torques up to 480Nm and 4980 rpm, which is more than enough to handle twice the maximum rated engine power and torque. Additionally, the dynamometer allows loading and motoring the engine which allows to assist during engine start and to characterize non-combustion operation.

The dynamometer allows to measure the reactive force of the device, by converting the mechanical energy generated by the engine into electrical energy. The Dynas3 LI in this study was calibrated at the start of the experimental campaign and checked

with calibrated weights periodically. For speed measurements, an additional optical AVL 364C encoder was installed on the crankshaft of the engine.

2.2.2 Average signal measurement

For steady-state measurements (as the ones carried out in this study) time-averaged measurements are useful to monitor and control boundary conditions, mainly as the signal dynamics are low.

The average pressure was measured with piezoresistive Kistler 4045A transducers, which have a measurement range of 0 to 10 bar and an accuracy of 25 mbar [3]. Conversely, temperature was acquired by means of both thermocouple thermos-resistive sensors. Thermocouples of type k were used with measurement range from 0 to 1100°C and precision of 2.5°C, while thermo-resistive Pt100 sensors have been used to measure the oil and water temperatures with a measuring range from -200 to +850°C, with a precision of 0.3°C.

2.2.3 Instantaneous signal measurement

The piezoelectric AVL GH14p sensor was used for the measurement of instantaneous pressure. This task is considered one of the most critical ones for combustion analysis and must provide signals with low thermal shock and support high pressure values. The sensor's measuring range covers from 0 to 250 bar, which is higher than the maximum pressure for the testing as the limit for pressure is 180 bar. Additionally, the thermal sensitivity change values are low as well as the cyclic temperature drift and thermal shock error [4]. The sensor is a direct mount sensor in combination with a glow-plug adaptor, therefore no drilling needs to be done to the cylinder head for its installation, only the replacement of one of the existing glow-plugs. A Kistler 5015A charge amplifier was used to pre-condition the signal before its acquisition. Instantaneous pressure transducers were also installed at the intake and exhaust of the engine, however the thermal and pressure requisites for this sensing devices is not as high as for the in-cylinder sensor, thus Kistler 4045A10 piezoresistive sensors were used.

2.2.4 Mass flow measurement

The air mass, fuel and blow-by values are important parameters that determine the combustion, and their measurement is dependent on the phase they are present in. The air mass flow was directly measured with an ABB's Sensyflow FMT700-P, this measurement instrument is independent of the operating temperature and pressure making it accurate at various operating conditions with a maximum range of 5000 kg/h [5]. Blow-by was measured with an AVL 422, which measures the leaking gas

volume from the engine between the piston and piston rings by the principle of and orifice measuring pipe and evaluation electronics [6].

The fuel mass flow was measured by a AVL 733S fuel balance which gravimetrically determines the fuel consumption of the engine by using a weighing vessel (that fills for each measurement) linked by a bending beam to a capacitive displacement sensor [7]. The range of the measurement is 0 to 150 kg/h and the measurement uncertainty is 0.12%. The measurement of the fuel consumption is also independent of the density of the fuel as only the mass is taken into consideration, which is positive considering that several fuels with different properties are measured in this study.

2.2.5 Emissions measurement

The Horiba Mexa 7100 D-EGR was the device used for the measurement of NOx, CO, HC, O_2 and CO_2, in addition to quantifying the EGR proportion. The species are quantified by a specific measurement principle each, which is summarized in Table 4, in addition to the range and measurement uncertainty.

Table 4. Horiba MEXA 7100 D-EGR components, measurement principles range, and associated uncertainty.

Component	Model	Principle	Range	Uncertainty
CO	AIA-31	NDIR	0-12 vol%	4%
CO_2	AlA-32	NDIR	0-20 vol%	4%
HC	FIA-01	FID	0-10000 ppmC	4%
O_2	MPA-01	MPD	0-25 vol%	4%
NOx	CLA-01	HCLD	0-10000 ppm	4%

Table 4 shows that four measurement principles are used to determine different engine-out species. The Non-Dispersive InfraRed detector (NDIR), the magneto-pneumatic detector (MPD), Heated chemiluminescence detector (HCLD) and the flame ionization detection (FID) principles, which will be briefly described in this section.

The NDIR principle separates broadband light into suitable wavelengths that can be absorbed by the gas of interest (CO and CO_2) to identify it. This signal is compared

to a reference signal in a neutral environment and the respective intensity reduction is proportional to the concentration values [8]. In the FID principle, a hydrogen flame (mix with synthetic air and helium) is used to ionize organic compounds containing carbon or unburned hydrocarbons (HC). The generation of ions is proportional to the concentration of organic species in the sample gas stream, which are detected by two electrodes used to provide a potential difference [9]. The detector in MPD uses a magnetic proportional flow rate system to measure O_2 because it has strong paramagnetic properties which modify a dumbbell position whose movement is opposed by a feedback system for which the opposing force is measured and translated into the oxygen concentration [10]. Finally, the NOx is measured using the HCLD principle which comprises the conversion of NOx to NO by a catalyst and they reacted with ozone to an excited state to produce an excited state of NO_2; then, the excited-state NO_2 emits light as it returns to its ground state which is proportional to the concentration of NOx in the sample [11].

The measured species are accounted for on either a wet or dry basis, depending on whether the exhaust gas water was removed from the sample before the analysis. For example, in the NDIR to measure CO and CO_2 the sample is dried to reduce the water before the measure. The European Commission in the regulation 2016/427 [12] indicates that for regulatory purposes emissions can be measured dry or wet, but if they are dried the drying device shall have minimal effect on the composition of the gas. Additionally, the regulation states that if emissions are measured dry, the concentrations shall be converted to a wet basis using Equation 1 and Equation 2.

$$c_{wet} = k_w \cdot c_{dry} \qquad \text{Equation 1}$$

$$k_w = \left(\frac{1}{1 + \alpha \times 0.005 \times \left(c_{CO_2} + c_{CO}\right) - \frac{1.608 \times H_a}{1000 + 1.608 \times H_a}} \right) \times 1.008 \qquad \text{Equation 2}$$

In the equations, c_{wet} is the wet concentration of a pollutant (in ppm or percentage), c_{dry} is the dry concentration of the pollutant and k_w is the dry-wet correction factor, which depends on the molar hydrogen ratio α, the dry CO and CO_2 concentrations (c_{CO_2} and c_{CO} in %), and the intake air humidity H_a in grams of water per kilogram of dry air.

After addressing raw emissions accordingly [12], instantaneous mass emissions are calculated following Equation 3

$$\dot{m}_{emission} = \left(x_i \cdot \frac{MW_{emission}}{MW_{exh}}\right) \cdot \dot{m}_{exh} \qquad \text{Equation 3}$$

where $\dot{m}_{exh}$ is the measured exhaust gas flow in g/s, x_i is the fraction of each component (in ppm or percentage), MW_i is the molecular weight of the emission and MW_{exh} is the molecular weight of the exhaust gas. Due to the differences in measuring principles and emission types, the specific case of each pollutant might be corrected by specific factors. Emissions can also be converted to brake or indicated power specific units by dividing the emission mass flow by the power (P) delivered by each operating condition. Then, the specific emissions (SX) are calculated following Equation 4

$$SX = \frac{\dot{m}_{emission}}{P} \qquad \text{Equation 4}$$

As shown in Figure 2, the Horiba Mexa 7100 D-EGR is connected to the exhaust by a probe located downstream of the turbo, where the sample is conducted to the measuring device by a warmed-up line that keeps the sample at 192°C to avoid hydrocarbon condensation. In addition to this, the intake is connected as well to the device by a probe after the EGR is integrated to measure the CO_2 concentration at the intake. Then, with the CO_2 concentrations at both the intake and the exhaust, the EGR proportion can be calculated by Equation 5.

$$EGR\ [\%] = \frac{CO_{2_{intake-dry}} - CO_{2_{ambient}}}{CO_{2_{exhaust-dry}} - CO_{2_{ambient}}} \times 100 \qquad \text{Equation 5}$$

2.2.6 Soot measurement

To provide a comparable quantity for the engine smoke measurement the AVL 415SE [13] was used. The device calculates soot by passing a fixed volume sample of the exhaust gases through a white paper filter (with a calibrated index of light reflection); in this process, the paper is blackened which later allows a reflectometer to correlate the degree of change of the light reflection with a value denoted Filter Smoke Number (FSN). The FSN ranges between 0 (completely white filter) and 10 (completely black paper), with a resolution of 0.001 FSN and a minimum detectable limit of 0.002 FSN.

The FSN can be converted into mass per volume of exhaust gas (mg/m^3) applying the correlation proposed by Christian et al. [14] shown in Equation 6

$$soot\ [mg/m^3] = \frac{1}{0.405} \cdot 4.95 \cdot FSN \cdot e^{(0.38 \cdot FSN)} \qquad \text{Equation 6}$$

Afterwards, the mass concentration of soot per mass of exhaust gas (mg/kg) can be calculated assuming constant density for the exhaust gas of 1.165 kg/m^3, which later serves as the basis to calculate the indicated soot as previously described.

Although the opacimeter measurement is commonly used, the particulate matter present in the exhaust can be underestimated with this device. The opacimeter measures smoke opacity from which mass concentration was calculated. The underestimation can be derived from the fact that its optical system is not accurate to quantify some species such as condensable organics. Currently, other measurement devices such as the Engine Exhaust Particle Sizer (EEPS) are preferred for their capacity to measure particle number and their size. Nonetheless, for the purpose of this study the FSN will serve as a sufficient initial comparison plane for the different fuels.

2.2.7 Data acquisition systems

Due to the large amount of data and parameters to be registered and their different origins, the test rig has three data acquisition systems with different sample frequencies and targets. The dynamometer was controlled by an in-house LABVIEW controller called SAMARUC, where the target was to maintain the engine speed, independently of the disturbances caused by the user; after which the engine load is modified by the amount of injected fuel. The SAMARUC controller, in addition to the dynamometer control, recorded temperature and pressure values from the sensors, and other important parameters during evaluations such as the integration of the flow measurements, gas analyzer and smoke meter readings at a sampling frequency of 10 Hz. During measurements the system registers all variables for 40 seconds and averages each one.

The instantaneous pressure and speed signals were interpolated to 0.2 CAD and recorded for 100 cycles with AVL's Indicom software to be later processed to evaluate the combustion with heat release analysis. This process requires a high sampling frequency which the software adapts to the specific engine speed recording always 720 CAD marks and calculating the time between marks.

3 Fuel properties and characteristics

During this work diesel-like LCF blends were tested to evaluate their performance and emissions. In this context, LCF will refer to fuels whose synthesis represents a lower CO_2 emission than diesel. Besides the potential environmental benefit of the fuels, the blend physical and chemical properties can also modify the combustion of the engine or be more prone to increase or decrease certain emissions. The LCFs blends are composed by the fuels described in Chapter 2 and their proportion will confer to a certain degree some of the properties of the single components. This section describes the composition, and the most relevant physical and chemical properties of the LCF blends used in the experiments.

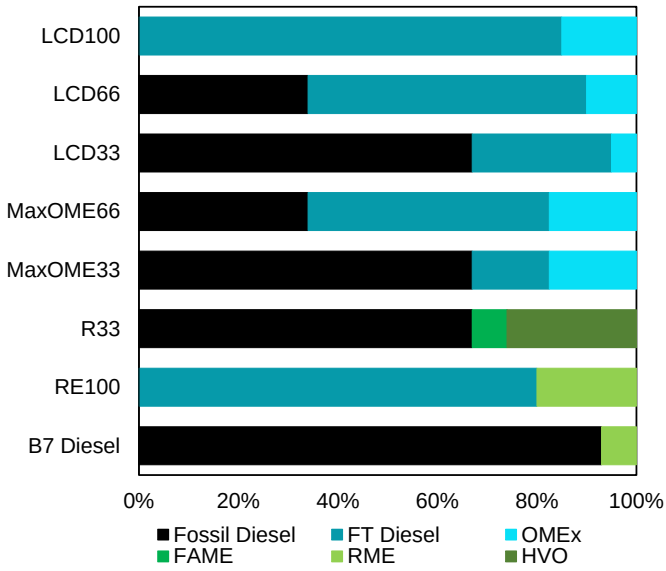

Figure 3. Low Carbon Fuel (LCF) blends volumetric composition

The LCF blends naming convention used in this work indicates the volumetric proportion of renewable fuel in the blend by the number at the end; thus, fuels with 100%, 66% and 33% renewable content by volume are tested and compared to diesel. Figure 3 shows the components of each of the blends and the reference diesel. The blends can be grouped by composition origin of the renewable proportion. Then, the LCD100, LCD66, LCD33, MaxOME66 and MaxOME33 all have the same main components (diesel, Fischer-Tropsch (FT) diesel and OMEx) with synthetic renewable proportion; while RE100 is a binary composition of FT diesel and RME and R33 a ternary blend of diesel, FAME and HVO fuel which are bio-originated.

Table 5 shows the main LCF blends' properties at standard conditions. The physical properties of the fuel have a significant impact on the injection characteristics and spray droplets aggregation of the fuel [15], while the chemical properties strongly affect the combustion characteristics.

Since OMEx has a low lower heating value (LHV), which is on average 19.2 MJ/kg; the fuel blends with a higher OMEx proportion will have a drop in their LHV. The fuel with the highest OMEx proportion in turn has a LHV that is 10.7% lower than diesel. Contrarily, the fuels which contain RME, FAME and HVO (with LHV of 37.2 MJ/kg for FAME and RME and 44 MJ/kg for HVO) have similar to diesel's LHV. Similarly, FT diesel has a LHV of 44 MJ/kg which allows to reach similar levels of the reference diesel. The low LHV of the OMEx containing blends is a direct consequence of the composition of the OMEx molecule, which could have almost half of its composition as oxygen [16]. This type of relation between one property of the blend and another is explored in Figure 4 (bivariate correlations between the properties shown in Table 5 for the LCF blends), and is closely linked to the fuel composition helping to explain some of the phenomena discussed in this work.

The representation in Figure 4 allows to evaluate the level of linear correlation or independence among the fuel properties. The Pearson correlation coefficient r, as calculated in Equation 7, is shown for each pair of properties. In the equation, x_i and y_i are the values of the x and y variables, while $\bar{y}$ and $\bar{x}$ are the mean values of x and y. A close to 1 coefficient indicates a stronger positive correlation between properties. Conversely, when it is closest to -1, a strong negative correlation is present. When the coefficient nears 0, no correlation is present, and the properties are said to be independent. The figure also shows *p-values*, which measure the probability of the obtained results occurring if the null hypothesis is true (in this case, the probability that there is no relationship between the fuel properties). Conventionally, the lower the p-value, the higher the statistical significance of the results; however, this should be interpreted with caution.

$$r = \frac{\sum(x_i - \bar{x})(y_i - \bar{y})}{\sqrt{\sum(x_i - \bar{x})^2 \sum(y_i - \bar{y})^2}} \qquad \text{Equation 7}$$

Table 5. Main fuel properties at standard conditions.

Fuel	Ref. Diesel	LCD 100	LCD66	LCD33	Max OME66	Max OME33	R33	RE 100
CN [-]	53.3	87	70	61.8	69.6	61	59	83.5
ρ@15ºC [g/ml]	0.834	0.821	0.825	0.827	0.841	0.845	0.821	0.799
Cloud Point [ºC]	-7	8	-6	-11	3	-10	-10	2
CFPP [ºC]	-20	-1	-9	-17	-1	-17	-24	-1
Flash Point [ºC]	61	66.5	61.5	60.5	61.5	55.5	67	>100
Lubricity, Wear scar D@60ºC [µm]	161	343	284	248	234	198	167	146
Sulfur [mg/ kg]	5.4	2.1	3.3	4.6	3.4	4.6	4.5	2.2
ν@40ºC [cSt]	2.861	2.075	2.23	2.461	2.074	2.218	2.906	2.898
Water content [%m/m]	0.008	0.015	0.013	0.011	0.014	0.013	0.012	0.009
HHV [MJ/ kg]	45.67	41.6	42.88	44.4	41.06	42.36	45.98	45.76
LHV [MJ/ kg]	42.81	38.67	39.96	41.48	38.24	39.55	43.04	42.73
C [% m/m]	85.78	76.05	79.48	82.89	76.49	79.58	85.4	83.64
H [% m/m]	13.45	13.81	13.78	13.74	13.3	13.23	13.84	14.2
O [% m/m]	0.77	10.14	6.75	3.36	10.21	7.18	0.76	2.16
FAME [%v/v]	7.1	<0.1	<0.1	<0.1	<0.1	<0.1	7	20
Total aromatics [%v/v]	20.1	0.2	8.1	14.5	8.2	14.5	13.6	0.2
AFR_{sto} [-]	14.36	12.97	13.50	14.02	12.84	13.30	14.45	14.31

	Cetane Number [-]	Density @ 15°C [kg/L]	Cloud Point [°C]	CFPP [°C]	Flash Point [°C]	Lubricity, wear scar diameter @ 60°C [µm]	Sulfur [mg/kg]	Viscosity @ 40ºC [mm2/s]	Water content [%m/m]	FAME content [%v/v]	Polycyclic aromatic content [%m/m]	Total aromatics [%m/m]	Carbon [%m/m]	Hydrogen [%m/m]	Oxygen [%m/m]	HHV [MJ/kg]	LHV [MJ/kg]
Cetane Number [-]	1.000																
Density @ 15°C [kg/L]	-0.591	1.000															
Cloud Point [°C]	0.853**	-0.319	1.000														
CFPP [°C]	0.881**	-0.317	0.901**	1.000													
Flash Point [°C]	0.595	-0.891**	0.423	0.456	1.000												
Lubricity, wear scar diameter @ 60°C [µm]	0.47	0.141	0.417	0.433	-0.377	1.000											
Sulfur [mg/kg]	-0.986***	0.595	-0.842**	-0.892**	-0.604	-0.443	1.000										
Viscosity @ 40°C [mm2/s]	-0.319	-0.517	-0.358	-0.479	0.51	-0.805*	0.315	1.000									
Water content [%m/m]	0.367	0.339	0.354	0.361	-0.417	0.757*	-0.394	-0.848**	1.000								
FAME content [%v/v]	0.235	-0.763*	0.148	0.117	0.907**	-0.695	-0.244	0.787*	-0.698	1.000							
Polycyclic aromatic content [%m/m]	-0.936***	0.625	-0.812*	-0.838**	-0.611	-0.392	0.977***	0.242	-0.406	-0.268	1.000						
Total aromatics [%m/m]	-0.987***	0.622	-0.824*	-0.87**	-0.634	-0.409	0.997***	0.281	-0.382	-0.275	0.975***	1.000					
Carbon [%m/m]	-0.552	-0.321	-0.613	-0.69	0.265	-0.771*	0.557	0.948***	-0.862**	0.588	0.496	0.527	1.000				
Hydrogen [%m/m]	0.554	-0.98***	0.237	0.244	0.789*	-0.029	-0.56	0.467	-0.263	0.642	-0.6	-0.585	0.31	1.000			
Oxygen [%m/m]	0.491	0.392	0.576	0.65	-0.322	0.751*	-0.495	-0.959***	0.859**	-0.623	-0.434	-0.464	-0.997***	-0.383	1.000		
HHV [MJ/kg]	-0.352	-0.525	-0.461	-0.547	0.449	-0.727*	0.356	0.98***	-0.847**	0.712*	0.293	0.323	0.974***	0.508	-0.988***	1.000	
LHV [MJ/kg]	-0.379	-0.499	-0.478	-0.566	0.428	-0.738*	0.383	0.98***	-0.852**	0.701	0.32	0.35	0.98***	0.482	-0.991***	1***	1.000

Figure 4. Bivariate correlation between relevant fuel properties. Significant values are represented as *p<0.05, **p < 0.01, ***p<0.001

In Figure 4, it can be observed that the LHV and the oxygen content are nearly perfectly correlated, which is similar to previous results for diesel fuel obtained with cetane improvers and oxygenates by Ullman et al. [17]. The representation also highlights the effect of properties where the variation within the population is small like the hydrogen mass content in the fuel which is related to the flash point of the fuel and the density. The work presented in [18] proposed a calculation method for the higher heating value (HHV) based on the viscosity of the fuel. This method yielded errors below 1% and showed a strong correlation between viscosity and the HHV, which resembles the correlation observed in this work.

Knowing which fuel properties are strongly correlated between them will also allow in future sections to provide analysis of the different engine responses with emphasis in fewer properties, as the presence of one effect can be derived from the correlations that exist with the selected properties like LHV, CN, density, viscosity and total aromatics (which can be considered sufficiently independent).

Figure 5 shows how are the fuel properties distributed in the tested LCF blends. In the diagram provided, each chart displays the chosen variable values using a consistent scale. This visual depiction facilitates the observation of a nearly exclusive correlation between aromatics and the proportion of fossil diesel within the fuel. Moreover, the utilization of fuel types such as HVO, OMEx, and FT diesels serves a dual purpose by acting as cetane improvers. Notably, the data also validates that an increase in the proportion of OMEx results in a reduction in the fuel's LHV.

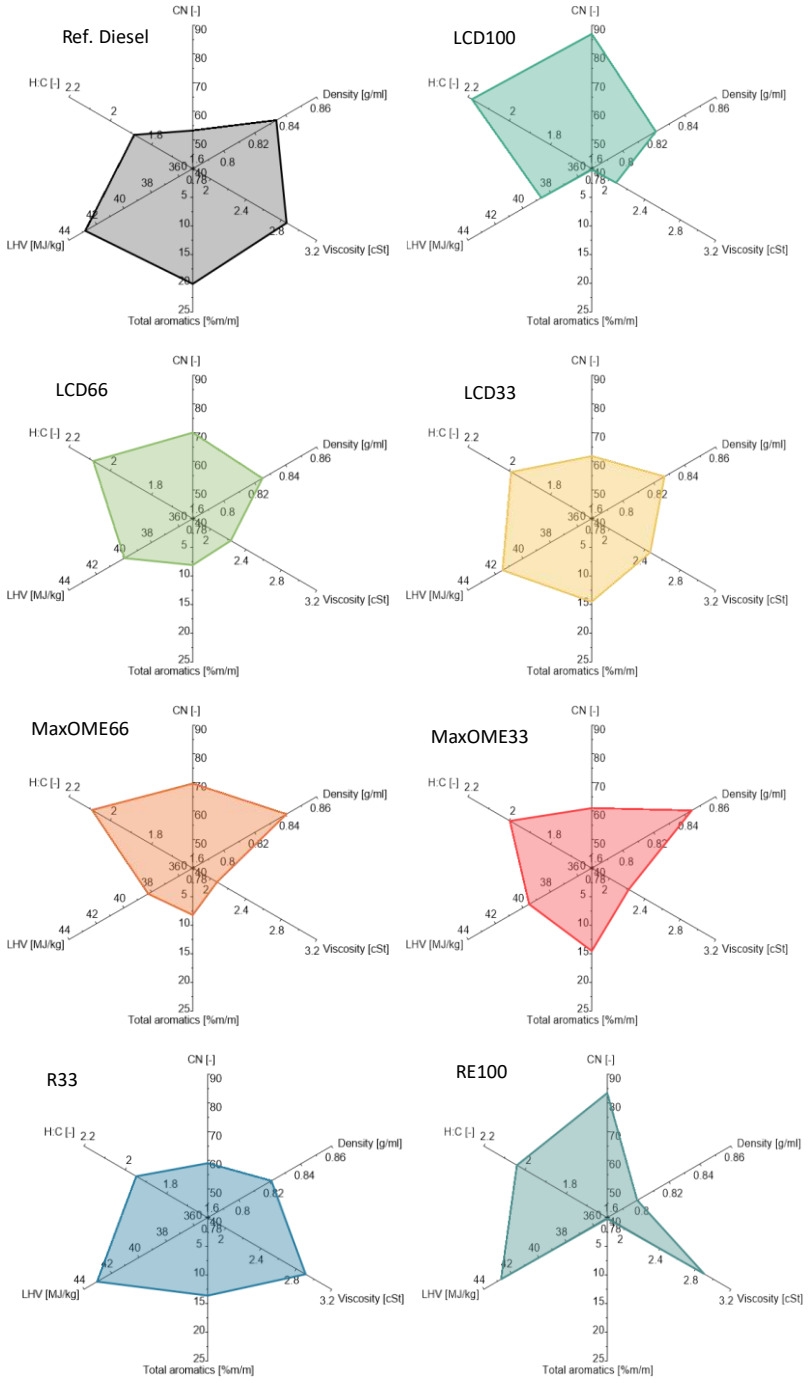

Figure 5. Balance of fuel properties for the studied LCF blends

4 Theoretical tools

The collected data needs to be post-processed to extract insightful observations from the experiments. This section describes the theoretical tools used for this purpose and the main equations that govern the observed phenomena.

4.1 Combustion diagnosis model

To study the combustion process in CI engines it is essential to have a thermodynamic model of diagnosis that allows to obtain from the instantaneous in-cylinder pressure parameters such as the total heat released (HRL) from the engine and its derivative the heat release rate (HRR). For this purpose, 0-dimensional and 1-dimentional models are often used. The basis for these models is the first law of thermodynamics, which is applied to the volume within the combustion chamber in the interval between the inlet valve closing (IVC) and the exhaust valve opening (EVO), hence the closed cycle of the engine.

During this study, CALMEC [19, 20, 21] was used as the combustion diagnosis. CALMEC is a tool developed within CMT-Motores Termicos (currently CMT-Clean Mobility and Thermofluids) which allows the calculations of the heat release by using the in-cylinder pressure, the average mass of air and fuel, and other boundary conditions like the intake and exhaust pressure and temperature. The energy balance follows the first principle of thermodynamics for open systems with the fuel energy as the input to the system and inefficiencies, blow-by, heat transfer and work are considered as outputs. This is presented in Equation 8.

$$\Delta HRL = m_{cyl} \cdot \Delta u_{cyl} + \Delta Q_w + p \cdot \Delta \mathrm{V} - (h_{f,inj} - u_{f,g}) \cdot \Delta m_{f,evap} + R_{cyl} \cdot T_{cyl} \cdot \Delta m_{bb} \qquad \text{Equation 8}$$

In Equation 8, the ΔHRL is the released thermal energy of the fuel assuming that its calorific value is constant throughout the combustion process; $m_{cyl} \cdot \Delta u_{cyl}$ is the sum of the variation of the internal energy of the trapped mass in the control volume as a function of the average temperature in the control volume per each time step; ΔQ_w is the heat transfer between the trapped gas and the piston, cylinder walls, cylinder head and valve surfaces; $p \cdot \Delta \mathrm{V}$ is the total work of the gas on the piston; $(h_{f,inj} - u_{f,g}) \cdot \Delta m_{f,evap}$ is the energy balance for the injection process; and $R_{cyl} \cdot T_{cyl} \cdot \Delta m_{bb}$ is the energy loss due to the blow-by flow.

Each of the terms in Equation 8 have specific characteristics and sub-models. For instance, the variation of the internal energy is calculated using specific correlations

for each species as presented by Lapuerta et al. [20]. The heat transfer term uses the Woschni model [22] with modifications based on the work of Payri et al. [23] for the coefficient of the instantaneous film coefficient between the gas and the cylinder walls and a nodal model for the wall temperature calculations [24]. Similarly, for the calculation of the instantaneous cylinder volume a mechanical deformation model is used which considers the gas pressure force as well as the inertial forces of the masses during the reciprocating piston movement.

It is important to consider that the models used in CALMEC use some assumptions for the calculation like uniform pressure in the combustion chamber, stoichiometric evolution of the gas mix (air, gaseous fuel and combustion products) and ideal gas behavior of the trapped mass. The use of these hypotheses are generally accepted and justified, nonetheless a detailed description can be found in the work of [21].

From the heat release analysis several combustion metrics to characterize the combustion, such as the ignition delay, CA10, CA50 and CA90 (respectively the crank angle degrees at which 10, 50 and 90% of the mass fraction is burned). Typically, the ignition delay is defined from 0-2% of the mass fraction burned (MFB), while the combustion duration tends to be estimated as the difference between CA90 and CA10 (CA90-CA10). To obtain these values the MFB is calculated by the normalization of the heat release profile by the total energy provided to the system.

4.1.1 Mean effective pressure

To evaluate the indicated engine characteristics (performance parameters calculated based on measurements and analysis of pressure variations inside the cylinder during the combustion process) 100 consecutive pressure cycles were used. For each of the cycles, the indicated mean effective pressure was calculated according to Equation 9, where V_{sweep} is the displaced volume by the piston during the stroke.

$$IMEP = \frac{\int_{-360}^{360} pdV}{V_{sweep}} \qquad \text{Equation 9}$$

The indicated mean effective pressure (IMEP), or more specifically the variability of the IMEP, allows to evaluate the engine cycle-cycle variability. For this the coefficient of variance of the IMEP is used (COV_{IMEP}) as calculated in Equation 10, where n is the number of total cycles considered, $IMEP_i$ is the IMEP at a given cycle, σ_{IMEP_i} is the standard deviation of the IMEP and $\overline{IMEP}$ is the mean IMEP of the

number of cycles. Generally, the combustion is considered stable when the value of COV_{IMEP} is below 5 %.

$$COV_{IMEP} = \frac{\sigma_{IMEP_i}}{\overline{IMEP}} = \frac{\sqrt{\frac{1}{n}\sum_{i=1}^{n}(IMEP_i - \overline{IMEP})^2}}{\overline{IMEP}} \quad \text{Equation 10}$$

The AVL's Indicom used during this study allows to evaluate this metric in quasi-real time, thus providing a verification of the combustion stability for the different tested LCF at different stages during the calibration.

4.1.2 Combustion efficiency

The brake thermal efficiency (BTE) of an engine is a measure of how effectively it converts the energy content of fuel into useful mechanical work. It is defined as the ratio of the useful work output to the energy input from the fuel. Mathematically, the BTE is calculated using Equation 11, where P_{brake} is the brake specific power and Q_{fuel} is the total energy from the injected fuel. The indicated thermal efficiency (ITE) is calculated in a similar manner, but instead $P_{indicated}$ is used.

$$BTE = \frac{P_{brake}}{Q_{fuel}} \quad \text{Equation 11}$$

An engine experiences a significant loss of energy due to incomplete combustion of fuel, exhaust gases, heat transfer and mechanical losses [25, 26, 27]. This inefficiency arises from various factors, such as fuel entrapment within cylinder gaps or partial oxidation of hydrocarbon molecules. To assess this energy loss accurately, exhaust emissions measurements provide valuable information. By employing an energy balance approach, it becomes possible to calculate the combustion efficiency. Equation 12 offers a means to determine combustion losses (η_{comb}) by dividing the energy from unburned species present in the exhaust from the total fuel energy entering the cylinder.

$$\eta_{comb} = \frac{(\dot{m}_{air} + \dot{m}_{fuel})(LHV_{CO}X_{CO} + LHV_{HC}X_{HC})}{Q_{fuel}} \quad \text{Equation 12}$$

The mass fractions of the exhaust species with non-zero heating values are represented by X. For the purpose of calculations, the most prevalent species considered are HC and CO (carbon monoxide). The heating values for each species

were obtained from literature sources: CO has a heating value of 10.1 MJ/kg and HC has a heating value of 42.5 MJ/kg [27].

Engine exhaust losses (η_{exh}) refer to the energy or power that is lost in the form of waste heat during the combustion process and subsequent expulsion of exhaust gases from the engine. Equation 13 shows how this magnitude is calculated in this work, and $h_{exh\ @\ T}$ is the enthalpy of the exhaust gases at the specified temperature.

$$\eta_{exh} = \frac{(\dot{m}_{air} + \dot{m}_{fuel})(h_{exh\ @\ T\ exhaust} - h_{exh\ @\ T\ amb})}{Q_{fuel}} \quad \text{Equation 13}$$

The mechanical losses (η_{mech}) are estimated as the difference between the ITE and the BTF. While the heat transfer losses (η_{cool}) are defined by Equation 14

$$\eta_{cool} = 1 - BTE - \eta_{exh} - \eta_{comb} - \eta_{mech} \quad \text{Equation 14}$$

4.2 Equivalent fuel consumption

One key factor regarding fuels with different LHVs is the evaluation of their efficiency. In that regard the brake specific fuel consumption (BSFC) which is a gravimetric measure of the fuel consumed is affected significantly by this difference. For the evaluation of the fuel efficiency then an equivalent BSFC (BSFCeq) is included for the comparison of the fuels as calculated in Equation 15. The BSFCeq normalizes the BSFC in reference to the LHV of the diesel fuel.

$$BSFC_{eq} = \frac{LHV_{LCF} \cdot \dot{m}_{LCF}}{LHV_{diesel} \cdot P} \quad \text{Equation 15}$$

5 Testing methodologies

This section describes the methods used to obtain the experimental results during the engine tests and the methods used to collect and analyze the data.

5.1 Stationary operation

The experiments in this study were conducted under stationary conditions. Engine stationary conditions refer to the state of an engine when it is operating at a stable and constant speed, without any significant changes in rotational speed or load. For engine performance evaluation and LCF blends comparison, stationary conditions allow the elimination of fluctuations for accurate, consistent and repeatable measurements of engine performance parameters such as power output, torque, fuel

consumption, and emissions. In addition, for calibration and optimization the stationary conditions allow for fine-tuning of the ignition timing, assessment of the combustion stability for a set of settings and optimize for efficiency and emissions.

To achieve stationary conditions in an engine some steps need to be taken before each test. Firstly, it must be ensured that the engine reaches its operating temperature (85±2°C during this study) this is done during a warm-up period where the engine runs with diesel. This ensures that all components within the engine such as the oil, coolant and metal parts are adequately heated and expanded to their normal operating conditions.

Once the engine is warm, for tests with the LCF blends, the diesel fuel is progressively replaced by switching the fuel source with a three-way valve. The FIS volume needs to be purged of diesel before testing, the criteria employed to verify this task and prevent diesel-LCF blends fixing the calibration settings for a constant setting demand (fixing the fuel mass, injection pressure, SOI, air and boost requirements) and then observing the variation in fuel measurement values, exhaust emissions and exhaust temperature. Once these are stabilized for at least 10 minutes the engine was running with only the LCF.

The next step for stationary testing includes the test's target speed and load stabilization which during this work will follow to different strategies: a drop-in strategy and a calibration-optimization strategy. Nonetheless, for both calibration cases the COV_{IMEP}, exhaust temperature, fuel consumption and emissions are stabilized before measurement.

It is important to note that achieving truly stationary conditions in an engine is challenging due to factors such as mechanical vibrations, system dynamics, and external disturbances. However, by carefully following the steps outlined above and employing proper control and measurement techniques variations have been minimized to the standards and relatively stable and repeatable engine stationary conditions have been achieved. For this reason, in addition to the steps for achieving stationary operation, additional considerations are taken before tests to avoid possible sources of error. As such, measurement equipment calibration is check before each test, and to guarantee that the engine is working properly a reference tests is always measured under the same conditions and parameters at the beginning and the end of testing [28].

5.2 Calibration types and test matrix

As mentioned, two types of calibrations are followed during this work. Drop-in tests consist of testing the fuel with the OEM's provided diesel B7 Euro 6 calibration while calibration-optimization tests involve modifying selected engine parameters to observe their effect over the combustion, performance and emissions of the engine. For both types of calibration all LCFs are evaluated under five different operating conditions which are selected due to their representativeness of the engine operation, based on the work Durrett and Potter [29]. These conditions include a low-speed low-load condition, two mid-load conditions, and two representative conditions for the peak power and peak torque. The engine speed and brake mean effective pressure (BMEP) targets are 1250 rpm @ 2 bar, 1500 rpm @ 14 bar, 2000 rpm @ 8 bar, 2000 rpm @max, and 3750 rpm @ max.

5.2.1 Drop-in calibration

To achieve the drop-in operation using the specified LCFs fuels, the dynamometer is used to set the engine speed and a pedal signal is transmitted to the ECU with the diesel B7 Euro 6 calibration until the desired load is attained. The pedal signal corresponds to a fuel requirement table that determines the amount of fuel to be injected, with higher pedal positions requiring greater amounts of fuel. This is particularly prevalent when assessing fuels with different LHVs, where the fuels with a lower LHV will require higher pedal demands than fuels with higher LHV as will be described in detail in chapter 4. A summary of the strategy can be seen in Figure 6.

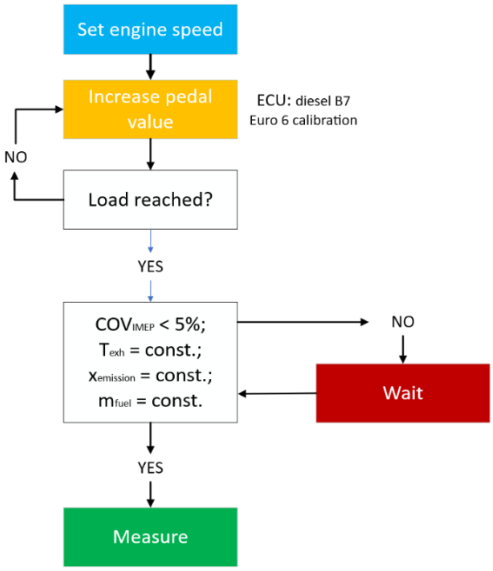

Figure 6. Schematic description of the drop-in calibration methodology

5.2.2 Calibration optimization

To achieve an optimized calibration in the engine, eight main parameters are modified, namely the SOI, injection pressure (Prail), volume (V1 and V2) and dwell time (D1 and D2) of the pilot injections, in-cylinder air mass quantity (AirM), and boosting pressure (PBoost). To determine which combination of these settings provides the best engine responses while fulfilling the targets specified in Table 6, a DOE methodology was applied. Then, models for each operating condition and fuel were created which were later used for selecting the optimum value using an algorithm of satisfaction restriction. The minimum targets -NOx, soot, maximum cylinder pressure (Pmax) and pressure rise rate (PRR)- guarantee that the working space for the calibration of the engine satisfy the minimum constraints for the hardware safety and emissions reduction with the baseline OEM ATS. In addition to these constraints, the fuel mass was varied minimally to remain within the load limits on each operating condition during screening tests and maintained constant during the DOE to not include the effect of the fuel mass demand in the analysis (hence the load at this stage could be outside the acceptable range). After the validation with the model, the mass could be adjusted to improve the fuel efficiency in each engine setting and LCF as the final step of the calibration.

Table 6. Minimum targets for the LCF calibration optimization

Operating condition	NOx (g/kWh)	Soot (FSN)	Pmax (bar)	PRR (bar/CAD)	Load (bar)	COV_{IMEP} (%)
1250 rpm @ 2 bar	0.2-1	2	<180	<8	1-3	5
1500 rpm @ 14 bar	3	3	<180	<8	13-15	5
2000 rpm @ 8 bar	0.7-2	2	<180	<8	7-9	5
2000 rpm @ 22 bar	4.5	3	<180	<8	20-24	5
3750 rpm @ max. load	5	3	<180	<8	max±2	5

6 Statistical modelling approach

A statistical modelling approach refers to a framework, wherein mathematical and probabilistic techniques are employed to represent, analyze, and make inferences about complex phenomena or relationships observed in data. This approach involves the formulation of mathematical models that capture the underlying structure or patterns in the data, with the aim of estimating and testing hypotheses, making predictions, and understanding the uncertainty inherent in the data-generating process. Statistical modelling encompasses a wide range of methodologies, including regression analysis, Bayesian modelling, and machine learning techniques, and it plays a crucial role in scientific research, data analysis, and decision-making across various domains by providing a structured and quantitative means to gain insights and draw conclusions from empirical observations.

6.1 Design of Experiments (DOE)

DOE is a systematic approach used in research to plan and conduct experimental work. In a DOE, experiments are designed before their execution to gather data more efficiently for its later analysis. Essentially, it provides a structure framework for understanding the relationship between the input parameters or factors (which in this work are the modified calibration settings) and the output response, while considering the interaction effects among factors. This allows researchers to identify

critical factors, determine optimal settings, and understand the underlying relationships and interactions.

In the context of ICEs, DOEs have been applied to optimize engine performance, fuel efficiency and emissions control [30, 31, 32]. DOEs have been used to investigate factors such as air-to-fuel ratio (AFR), SOI, CR, and other parameters to assess their impacts on the engine's responses. Ramalingan et al. [33], for example, used a Box-Behnken design and response surface methodology (RSM) to evaluate the effect of injection parameters and EGR over CI engine using lemongrass oil as a fuel and optimize the emissions, efficiency and fuel consumption. A Box-Behnken design is a quadratic design with treatment combinations at the midpoint of the edges of the input parameters and the center (Figure 7), which allows to select a subset of experiments and allows to account for the interaction between factors.

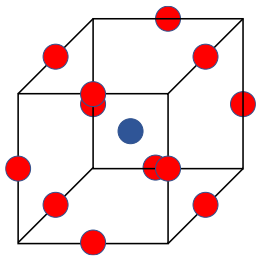

Figure 7. Three-dimensional Box-Behnken design representation

In the context of this work, it was important to generate a DOE methodology that allowed the evaluation of the selected 8 calibration parameters, considering the interactions between them and allowed to model a surface response in a simple manner given that for each of the LCF and operating condition a DOE had to be applied, meaning that 35 different LCF-operating condition combinations are to be evaluated with their own experiments. For this purpose, the following sections will detail the DOE and the specific considerations for the selection of a specific design.

When designing experiments using DOE, several principles should be considered to ensure the quality of the results. Replication and blocking during this study were addressed by taking three measurements from each experiment, in addition to randomly selecting some experiments from each group to be repeated another day. This in turn allows to verify the reproducibility and account for other potential sources of variability (like air humidity and ambient temperature).

6.1.1 Screening

For all the LCFs and operating conditions the drop-in calibration served as a baseline point from which to assess whether the engine can run or not with the fuel. But after this stage, to know the effect of the variation of the selected calibration parameters for a given operating condition and fuel screening tests were performed. These tests help to identify the most important factors. In addition, for this study, the screening tests were used to reduce the parameters to evaluate from eight to six while determining the maximum and minimum value limits for the SOI, Prail, V1, V2, D1, D2, AirM and PBoost that fulfill the constraints given in Table 6. The reduction to six calibration parameters at this stage will allow for execution of 2-k factorial designs (as will be explained in the next section) and the realization of a constrained optimization.

The screening tests in this work follow the form of Figure 8 for all 8 calibration parameters, where the grey circle represents the baseline point (drop-in calibration) and the red dots the maximum and minimum limits of a given parameter maintaining all other parameters equal to the baseline. The method is what is often called a classical "One at a Time" method were only one variable is evaluated. This approach does not allow to consider interactions between factors, but without any interactions provides the maximum values for the next stage of the DOE.

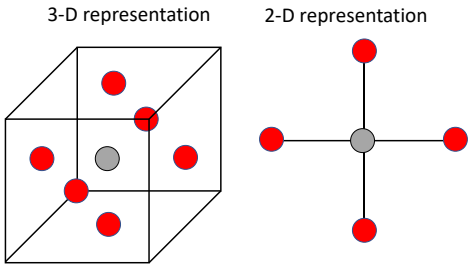

Figure 8. Three-dimensional and two-dimensional screening design representation

It is worth highlighting that the baseline point is not always in the center between the limits of a calibration parameter. And that to determine such calibration parameter limits, each individual parameter was varied (one step- at a time) and recorded until any which one of the constraints of Table 6 were surpassed with an additional step in the variation direction. Figure 9 shows a representation of this definition, where the grey dot (baseline calibration) is the step 0, while the parameter is increased (or decreased) until the constraint is surpassed with one additional step and the range is not symmetrical for the increase and decrease. Then the red dots (the last step before the constraint is surpassed) become the new parameter maximum

and minimum limits, ensuring safe operation of the engine, and reducing the potential of exceeding emissions. Another advantage of this screening, especially for the subsequent model creation, is ensuring that each of the parameters evaluated has a monotonous behavior (either increasing or decreasing) within the explored limits.

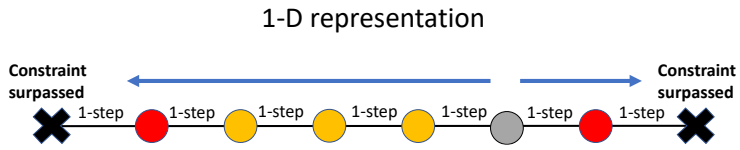

Figure 9. One-dimensional representation of the "one at a time" screening methodology for a single calibration parameter. The grey dot is the starting point

Not all operating conditions have a second pilot injection, and thus V2 and D2 are not evaluated in that condition (operating points 1500 rpm @ 14 bar, 2000 rpm @ 22 bar and 3750 rpm @ max. load) ending with only 6 calibration parameters. But, in the case where a second pilot injection exists the reduction of two variables was achieved by characterizing the effect sizes (BSNOx, FSN and BSFC) and discarding the two variables which had the lowest combined effect size.

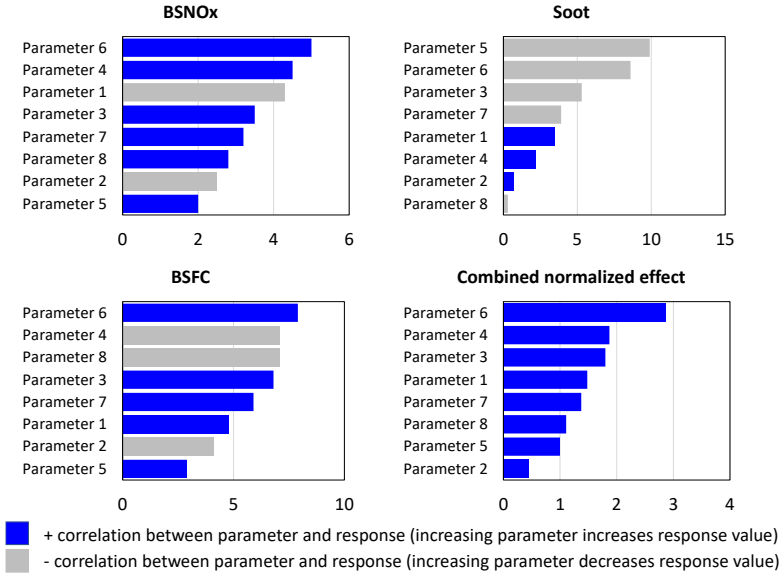

Figure 10. Representation of the effect sizing evaluation for the reduction of parameters from 8 to 6 for responses BSNOx, soot and BSFC with the combined normalized response (CNR)

The effect size was determined with the standardized response (SR), which is calculated as shown in Equation 16 and Equation 17. Here SE_i is the standard error of the response for the parameter i, σ_i the standard deviation and n the size of the sample, while y_1 is the response evaluated when the parameter value is x_1.

$$SE_i = \frac{\sigma_i}{\sqrt{n}} \qquad \text{Equation 16}$$

$$SR_i = \frac{\frac{y_2 - y_1}{x_2 - x_1}}{SE_i} \qquad \text{Equation 17}$$

Then each of the responses for each parameter i is normalized (NR) according to Equation 18, and then the combined normalized response (CNR) is calculated following Equation 19

$$NR_i = \frac{|SR_i - \min(|SR|)|}{\max(|SR|) - \min(|SR|)} \qquad \text{Equation 18}$$

$$CNR_i = \sum_{response} NR_{i_{response}} \qquad \text{Equation 19}$$

Figure 10 shows a visual representation of the effect sizing methodology for the number of parameters reduction. In the figure, an example case can be seen where the size of the effects for each parameter is present for BSNOx, BSFC and soot. The effects are ordered by the size of the absolute value, and the color (blue or grey) indicate respectively whether the parameter and the response have a positive or negative correlation. In this example case, “parameter 2” for example is consistently among the lowest value effect sizes; then, when the CNR is computed “parameter 2” is the lowest. In this example, during the next stages of the DOE “parameter 2” and “parameter 5” would not be evaluated as during the screening their effect size is not as large as for other parameters. The fact that these two parameters have the smallest effect size does not mean that they do not influence the combustion, only that they are not as dominant for the selected targets. Chapter 5 will show some of these results for the different LCFs.

6.1.2 Factorial tests

Factorial designs allow for simultaneous investigation of multiple factors and interactions (interdependency of effects). In factorial designs, if the effect of one factor changes depending on the value of another factor this will be captured. Factorial designs can include a variable number of levels, in this work the limits found during the screening tests described in Section 6.1.1 are the maximum and minimum levels (+1 and -1). Figure 11 shows a visual representation of this type of design in 2 and 3 dimensions.

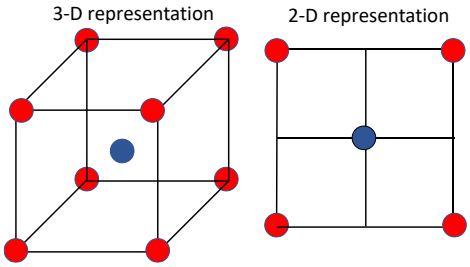

Figure 11. Three-dimensional and two-dimensional 2-k factorial design representation

Two types of factorial DOEs were used in this work: a 2-k factorial design with a central point [34] and a modified Plackett-Burman design [35]. One of the key reasons for selecting these designs is their simplicity and efficiency. The "2-k" notation signifies that the design involves k factors, each with two levels (typically low and high), making it easier to execute the experiments. The inclusion of a central point, which represents the mid-level values of the factors, allows for the estimation of main effects and interactions. In a complete factorial design with a central point, the number of experiments is calculated by the expression $n = k^y + 1$. In a 2-k factorial this expression is evaluated with k=2. For this work 6 parameters are varied, then $y = 6$. Finally, the number of runs or tests results in 65 when 6 factors are considered. The exponential nature of the design makes it so the addition of an additional parameter increases significantly the number of tests, because of this the decision of reducing the number of factors from 8 to 6 is justified as evaluating 8 factors with a full 2-k factorial design would result in 257 tests per engine operating condition, per LCF.

Although 65 operating conditions is an adequate number of tests to realize experimentally, some operating conditions, particularly at full load would cause considerable thermal and mechanical stress in the engine when sustained for prolonged periods of time. For these conditions (1500 rpm @ 14 bar, 2000 rpm @ 22 bar and 3750 rpm @ max. load), the “modified” Plackett-Burman design was

used was used with a shorter test matrix of 32 runs to be able to derive models to be used for the calibration of the engine in a similar way as the lower load conditions. Plackett-Burman designs are efficient screening designs that allow to explore a large number of factors with a relatively small number of experimental runs. In this design factor combinations are systematically selected based on balanced fractional factorial designs, being able to identify main effects with a high degree of orthogonality (guarantees that the effect of one factor or interaction can be estimated separately from the effect of any other factor or interaction in the model). The inclusion of additional central points in this design enhances its robustness to potential sources of variability and allows for the estimation of curvature in the response surface, which is particularly valuable when the relationship between factors and the response is nonlinear or when there might be unanticipated interactions among factors. The central points also provide a measure of experimental error.

6.1.3 Combined data

The data from the screening tests and the factorial DOEs was combined into a single dataset for the modelling tasks. The structure of this new dataset is represented in Figure 12 for 2 and 3 dimensions, although the experiments were carried out for 6 dimensions or input variables.

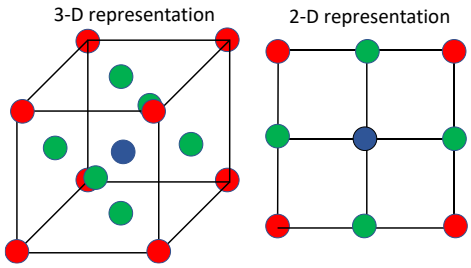

Figure 12. Three-dimensional and two-dimensional representation of the combined screening and 2-k factorial design

The data combination has both advantages and disadvantages for modelling, particularly considering the use of linear models in the next sections. The resulting dataset from the combination of DOEs has a larger size, providing more data points for analysis, while maintaining the systematic variation provided by the factorial DOE. By combining the two types of experiments, a more comprehensive view of the system behavior is obtained, capturing both main effects and interactions. However, it is important to mention that the two datasets may have different setups and error structures, leading to heterogeneity that can complicate modelling.

Similarly, a combined dataset with multiple factors and interactions may lead to complex models that are difficult to interpret.

6.2 Modelling

When factors evaluated during the DOE are quantitative (as in this work), a regression model representation can be used following Equation 20. In the equation, b_0 is the mean of the analyzed responses, b_i and b_{ij} the effect of the variables X_i and the interaction between $X_i X_j$, respectively.

$$Y = b_0 + \sum b_i X_i + \sum b_{ij} X_i X_j \qquad \text{Equation 20}$$

Models for each of the responses of interests were obtained (NOx, soot, fuel consumption, CA50, CA10, CA90 and torque) with 6 input parameters as mentioned in previous sections. The model for the torque and the CAX combustion parameters were used as checks for ensuring the operating condition is maintained within 5% threshold and that combustion is within desirable standards.

The quality of the models is evaluated through the fitted vs experimental values plot and the residuals plot, as observed in the example shown in Figure 13. The acceptance criteria for the model include an R-square value above 80%, an F-statistic that rejects the null hypothesis, and p-values below 0.05 for the included model factors, while simultaneously minimizing the number of factors (also known as the principle of parsimony).

The collected data is used to train a linear model, where the engine behaviours are represented as a linear combination of the calibration parameters. The fitted vs experimental values plot is a graphical representation of the model's predictive accuracy. It compares the model-predicted engine behaviours with the actual experimental observations. A high-quality model is expected to show a close alignment between the fitted values and the experimental data points, indicating that the model is accurately capturing the underlying relationships between the calibration parameters and engine responses. The residuals plot displays the differences between the predicted values and the actual experimental values. Residuals are essentially the errors made by the model during prediction. A good model will exhibit random scatter around the zero line, suggesting that the model's errors are unbiased and normally distributed. Systematic patterns or trends in the residuals plot indicate the presence of unaccounted factors or nonlinear relationships that may negatively impact the model's accuracy.

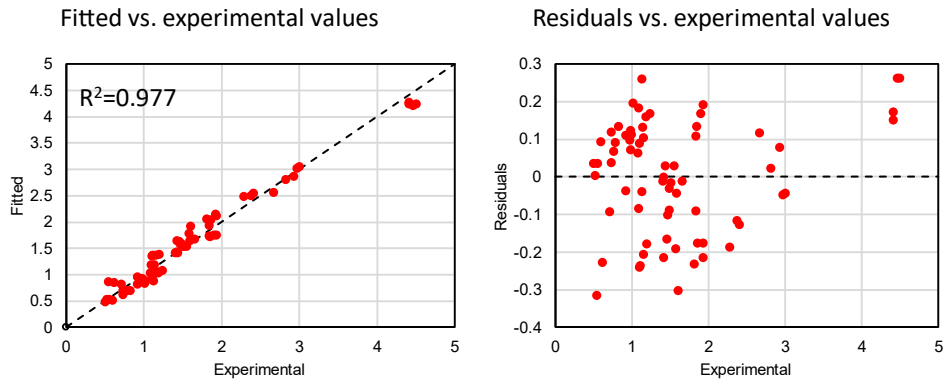

Figure 13. Example of fitted vs. experimental values (left) and residuals vs. experimental values (right) for the linear model of one of the responses of interest for a fixed operating condition with calibration settings captured in the combined dataset from the DOE and screening tests

Among the mentioned acceptance criteria for the models, the coefficient of determination (R-square) measures the proportion of variance in the dependent variable (engine behaviours) that can be explained by the independent variables (calibration parameters). An R-square value above 80% indicates that the model can explain a substantial portion of the variability in the engine responses, making it an acceptable model. The F-statistic is used to test the overall significance of the model. When the F-statistic yields a p-value below a predetermined significance level (typically 0.05), the null hypothesis, which suggests that all model coefficients are zero (i.e., the model has no predictive power), is rejected. A significant F-statistic demonstrates that the model is reliable and contributes valuable information. The p-values of individual model factors (calibration parameters) indicate their statistical significance. A p-value below 0.05 suggests that the inclusion of the corresponding calibration parameter in the model is warranted, as it significantly contributes to explaining the engine behaviours.

The models were constructed using stepwise regression [36, 37], which is an iterative process in which independent are selected (step-by-step) following the best fit with the acceptance criteria, until the best model is found. The method provides an automated way to select variables for inclusion in the model. It starts with no predictors in the model and iteratively adds or removes variables based on the specified criteria. With a high-dimensional parameter space (e.g., six calibration parameters), manually evaluating all possible combinations can be time-consuming and computationally expensive. Stepwise regression can efficiently explore different combinations and select the most relevant predictors. Additionally, the method can

also consider interaction terms between predictors, which in ICEs is important in capturing complex relationships among the calibration parameters. However, due to the limits of the method to find the "best" model, the models were manually revised to ensure good fulfilment of the criteria and evaluate if improvements could be made.

6.3 Optimization

After the models were obtained, they were used to find optimal calibrations for different responses. Namely, the "optimal condition" which is obtained by simultaneously minimizing the NOx, soot and fuel consumption; the "minimum NOx", the "minimum soot" and "minimum fuel consumption". For this purpose, linear optimization (or linear programming – LP [38, 39]) was used to achieve the best outcome. LP is a mathematical technique used to find the optimal solution to a problem while adhering to a set of linear constraints, in this sense for this study the goal is to minimize the objective function.

Mathematically, it can be expressed as:

$$Z = c_1x_1 + c_2x_2 + \cdots + c_nx_n \qquad \text{Equation 21}$$

$$\begin{gathered} a_{11}x_1 + a_{12}x_2 + \cdots + a_{1n}x_n \leq b_1 \\ a_{21}x_1 + a_{22}x_2 + \cdots + a_{2n}x_n \leq b_2 \\ \cdots \\ a_{m1}x_1 + a_{m2}x_2 + \cdots + a_{mn}x_n \leq b_m \end{gathered} \qquad \text{Equation 22}$$

$$x_1, x_2, \ldots, x_n \geq 0 \qquad \text{Equation 23}$$

Where Z is the objective function to be minimized; $c_1, c_2, \ldots, c_n$ are the coefficients of the input variables $x_1, x_2, \ldots, x_n$ to be selected; $a_{11}, a_{12}, \ldots, a_{1n}, \ldots, a_{mn}$ are the coefficients of the decision variables in the constraints b_1 to b_m.

Regression models are convenient for optimization because they allow to model and understand the relationships between the decision variables and the objective functions or responses. Having previously modelled outputs allows to predict the values of the responses for different sets of decision variables, enabling us to assess the impact of various scenarios on the optimization objectives.

The visual representation in Figure 14 is a scatter plot where each point represents a different combination of modelled results for fuel consumption, soot emissions (x-axis), and NOx emissions (y-axis). The color scale is used to indicate the fuel consumption, with different colors representing different levels of fuel consumption. In this plot, the bottom left axis represents a curve that does not reach the origin (0,0)

because it is physically impossible for the engine and calibration parameters to reach zero soot and NOx emissions simultaneously. This curve represents the feasible region, within which the engine can operate, points outside the colored are infeasible and outside the constraints given for NOx and soot emissions.

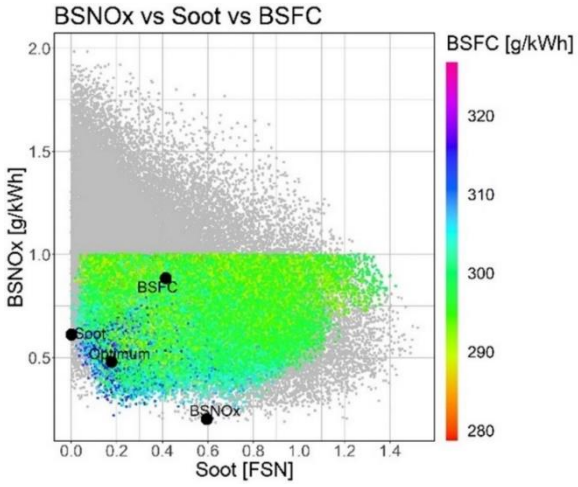

Figure 14. Soot, BSNOx and BSFC map from the linear regression models where the optimization function is applied based on given constraints to obtain the "optimum value", the lowest BSNOx, the lowest soot and the lowest BSFC within a fixed operating condition

The observed trend in the plot shows that as soot emissions increase along the x-axis, there is a clear reduction in NOx emissions along the y-axis. This suggests an inverse relationship between soot and NOx emissions, meaning that reducing soot emissions may lead to higher NOx emissions and vice versa. Additionally, the plot shows that fuel consumption tends to increase as we move towards the origin (0,0), representing the trade-off between reducing both soot and NOx emissions. The point labelled “optimum” near the origin correspond to a “optimal condition” where soot, NOx and fuel consumption are minimized. Similarly, the points for best NOx, best soot, and best fuel consumption can be observed.

This type of methodology was applied for all operating conditions across all tested LCFs, to later be able to compare the optimized calibrations for the LFCs between each other and compared to the drop-in calibration.

6.4 Validation

The developed models are validated using new experimental data from the predicted optimized operating conditions, these values were not used during training and allow to assess the models’ predictive capabilities. During this step it was checked whether

the models were overfitted, which occurs when a model performs well on the training data but poorly on new, unseen data.

Validation tests for BSFC, BSNOx, and soot were conducted to evaluate the accuracy of the predictive models. The objective is to ensure that the models provide a good approximation of the experimental data and that the prediction errors are within acceptable ranges. For all engine operating conditions, the fitted validation values are plotted against the experimental values (Figure 15).

For the BSFC the fitted vs. experimental plot shows a close alignment of data points, indicating that the model provides an excellent approximation of BSFC for various engine conditions. The error analysis reveals that for the majority of cases, the error in predicting BSFC is within the experimental error. Specifically, most of the cases show prediction errors below 5%. Even in the cases where there is a significant offset between the predicted and experimental values, the error remains below 15%. This suggests that the model is still reasonably accurate in capturing BSFC variations.

Similar to the BSFC validation, the fitted values (predicted BSNOx) are plotted against the experimental values of BSNOx for all engine operating conditions. The fitted vs. experimental plot demonstrates a strong agreement between the model's predictions and the experimental data for BSNOx emissions across various engine conditions. The analysis reveals that, in most cases, the prediction error for BSNOx is within the experimental error, with the majority of cases showing errors below 5%.

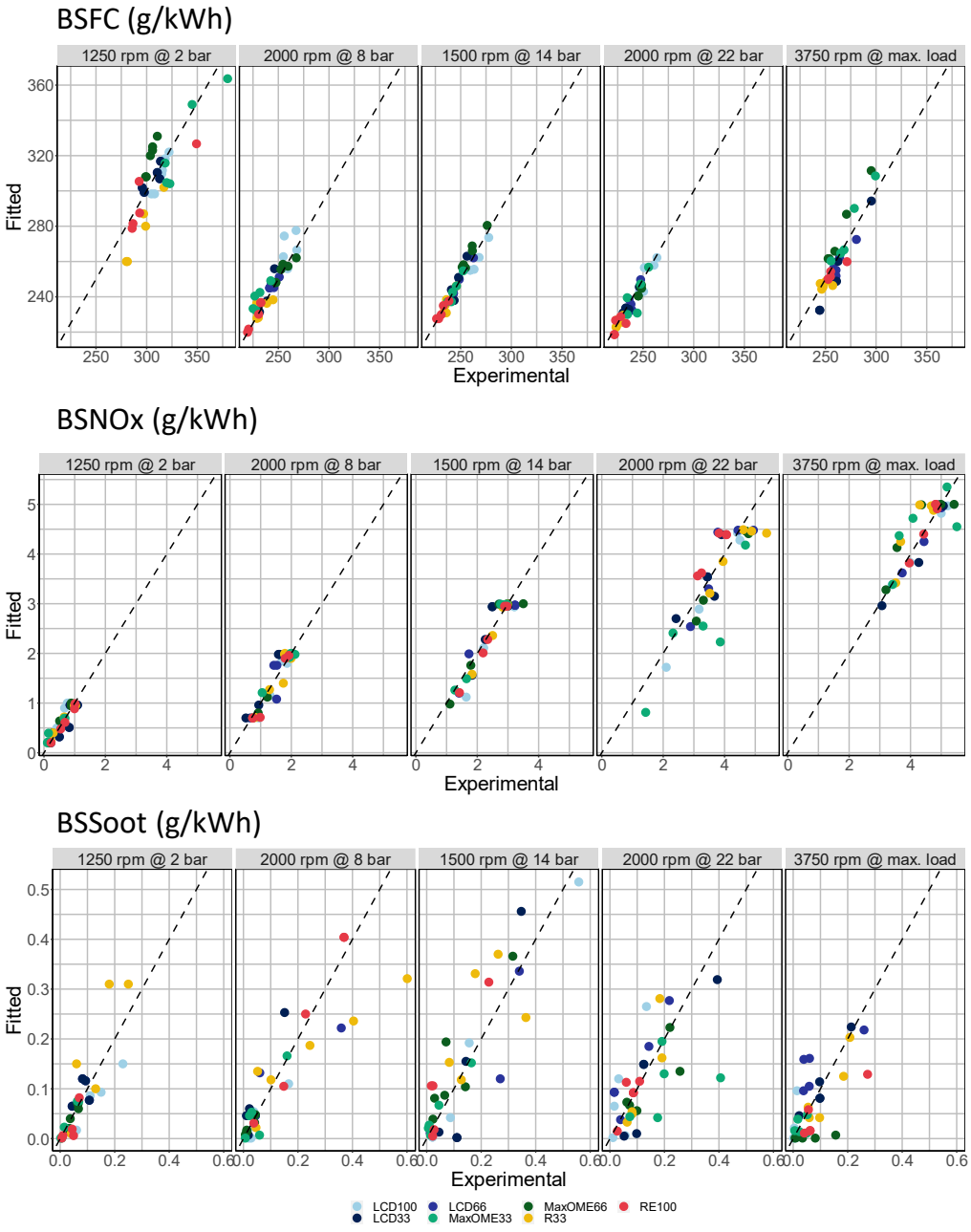

Figure 15. Fitted vs. experimental values for BSFC (top), BSNOx (middle) and BSSoot (bottom) in the validation dataset outside of the calibration data for the models

For soot, due to its low value and the large dispersion between measured data, the fitted vs. experimental plot shows a spread-out pattern. Despite the challenges posed by the low emission values and the variability in measurements, the fitted values from the model still manage to capture the general magnitude of the soot emission levels. Because of the previously mentioned reasons, the prediction error for soot might be higher (~8%) compared to BSFC and BSNOx, given the difficulty in precisely estimating low soot emissions. However, the fact that the model can still provide a reasonable estimation of soot despite its inherent uncertainties showcases its capability to capture the overall trend of soot emissions in different engine operating conditions.

7 Summary and conclusions

This chapter described the experimental setup used to investigate the effect of LCFs on performance and emissions in a light-duty ICE. The experimental setup includes details about the engine, fuel injection system, emissions measurement equipment, and data acquisition system. The engine used is a 1.6L 4-cylinder in-line diesel engine with a high-pressure EGR system. The fuel injection system relies on DI, and the air management system consists of a turbocharger with a VGT. The chapter explains the engine control system, test cell characteristics, and various sensors used to measure engine parameters. It also covers the measurement principles and instruments used for emissions analysis.

A description of the composition of the LCF blends used in the study and their physical and chemical properties is provided. The LCF blends are categorized based on their renewable fuel content, with different volumetric proportions of renewable components (e.g., Fischer-Tropsch diesel, RME, FAME, HVO, OMEx). The properties discussed include cetane number, density, cloud point, cold filter plugging point, flash point, lubricity, sulfur content, viscosity, water content, LHV, carbon content, hydrogen content, oxygen content, FAME content, and total aromatics content. The relationships between different fuel properties are analyzed using bivariate correlations. The section also introduces the concept of BSFCeq to compare the efficiency of fuels with different LHVs.

The chapter discusses the theoretical tools and equations used for post-processing and extracting insights from the experimental data collected during the engine tests.

The experimental and numerical methodologies for achieving stationary engine conditions and conducting tests with LCF blends are explained. Specific steps are taken to ensure the engine is at operating temperature, and the LCF blends are properly introduced and stabilized for testing. Additionally, measures are taken to

minimize sources of error and achieve relatively stable and repeatable engine conditions. Calibration of measurement equipment and reference tests are also performed to ensure data accuracy.

A detailed explanation of the calibration methodology and optimization process used in the study is provided. The methodology involves two types of calibrations: drop-in tests and calibration-optimization tests. The drop-in tests involve testing the fuel with the OEM's provided diesel B7 Euro 6 calibration, while the calibration-optimization tests involve modifying selected engine parameters to observe their effects on combustion, performance, and emissions.

The experiments are conducted under five different operating conditions representing various engine speeds and BMEP targets. These operating conditions are selected to be representative of the engine's typical operation. The responses of interest include NOx, soot, fuel consumption, and combustion parameters such as CA50.

The DOE methodology is applied to plan and conduct the experiments efficiently. A combination of a 2-k factorial design with a central point and a modified Plackett-Burman design is used to explore multiple factors and interactions while minimizing the number of experimental runs. The obtained data is then used to create regression models for each response of interest. These models represent the relationships between the calibration parameters and engine responses. Stepwise regression and modelling criteria are used to select the most relevant predictors and build the best-fit models. The optimization process involves using the regression models to find optimal calibrations for different responses. Linear programming is used for optimization, considering constraints such as minimum targets for NOx, soot, and maximum cylinder pressure. The models are validated using new experimental data from the predicted optimized operating conditions, and the accuracy of the models is assessed through fitted vs. experimental plots and error analysis.

8 References

[1] ETAS Driving Embedded Excelence, "INCA Software Products," ETAS Driving Embedded Excelence, [Online]. Available: https://www.etas.com/en/products/inca_software_products.php. [Accessed 30 September 2021].

[2] HORIBA, "DYNAS3 LI Low Inertia Series - AC Dynamometer," HORIBA, [Online]. Available: https://www.horiba.com/usa/products/detail/action/show/Product/dynas3-li-134/. [Accessed 31 May 2023].

[3] KISTLER, *Piezoresistive Absolute Pressure Sensors*, Winterthur: KISTLER, 2009.

[4] AVL, *PRESSURE SENSOR FOR COMBUSTION ANALYSIS (Datasheet)*, AVL, 2018.

[5] ABB, "Thermal mass flowmeter," ABB, 2023. [Online]. Available: https://new.abb.com/products/measurement-products/flow/thermal-mass-flowmeters/sensyflow-fmt700-p. [Accessed 31 May 2023].

[6] AVL, *AVL BLOW BY METER*, AVL, 2009.

[7] AVL, *AVL Fuel Balance*, Graz: AVL, 2009.

[8] T.-V. Dinh, I.-Y. Choi, Y.-S. Son and J.-C. Kim, "A review on non-dispersive infrared gas sensors: Improvement of sensor detection limit and interference correction," *Sensors and Actuators B: Chemical*, vol. 231, pp. 529-538, 2016.

[9] T. Holm, "Aspects of the mechanism of the flame ionization detector," *Journal of Chromatography A*, vol. 842, no. 1-2, pp. 221-227, 1999.

[10] C.-L. Tsai, C.-S. Fann, S.-H. Wang and R.-F. Fung, "Paramagnetic oxygen measurement using an optical-fiber microphone," *Sensors and Actuators B: Chemical*, vol. 73, no. 2-3, pp. 211-215, 2001.

[11] T. Collier, D. Gregory, M. Rushton and T. Hands, "Investigation into the Performance of an Ultra-fast Response NO Analyser Equipped with a NO2 to NO Converter for Gasoline and Diesel Exhaust NOx Measurements," *SAE Technical Paper,* no. 2000-01-2954, 2000.

[12] The European Commission, *Commission Regulation (EU) 2016/427 of 10 March 2016 amending Regulation (EC) No 692/2008 as regards emissions from light passenger and commercial vehicles (Euro 6) (Text with EEA relevance),* Official Journal of the European Union, 2016.

[13] AVL, *AVL Smoke Meter - Emission Measurement Instruments,* Graz: AVL, 2011.

[14] R. Christian, F. Knopf, A. Jasmek and W. Schindler, "A new method for the filter smoke number measurement with improved sensitivity," *MTZ Motortechnische Zeitschift,* vol. 54, pp. 16-22, 1993.

[15] M. Das, M. Sarkar, A. Datta and A. Kumar Santra, "Study on viscosity and surface tension properties of biodiesel-diesel blends and their effects on spray parameters for CI engines," *Fuel,* vol. 220, no. May, pp. 769-799, 2018.

[16] B. J., B. D. and A. Mitsos, "Production of Oxymethylene Dimethyl Ethers from Hydrogen and Carbon Dioxide - Part II: Modeling and Analysis for OME3-5," *Industrial and Engineering Chemistry Research,* vol. 58, pp. 556-5578, 2019.

[17] T. L. Ullman, K. B. Spreen and R. L. Mason, "Effects of Cetane Number, Cetane Improver, Aromatics, and Oxygenates on 1994 Heavy-Duty Diesel Engine Emissions," *SAE Technical Paper,* no. 941020, 1994.

[18] A. Demirbaş, "A direct route to the calculation of heating values of liquid fuels by using their density and viscosity measurements," *Energy Conversion and Management,* vol. 41, no. 15, pp. 1609-1614, 2000.

[19] F. Payri, P. Olmeda, J. Martín and A. García, "A complete 0D thermodynamic predictive model for direct injection diesel engines," *Applied Energy,* vol. 88, no. 12, pp. 4632-4641, 2011.

[20] M. Lapuerta, O. Armas and J. Hernández, "Diagnosis of DI Diesel combustion from in-cylinder pressure signal by estimation of mean thermodynamic

properties of the gas," *Applied Thermal Engineering*, vol. 19, no. 5, pp. 513-529, 1999.

[21] J. Martin, "Aportación al diagnóstico de la combustión en motores Diesel de inyección directa," *Doctoral Thesis, Universitat Politécnica de València, Departamento de Máquinas y Motores Térmicos*, 2007.

[22] G. Woschni, "A universally applicale equation for the instantaneous heat transfer coefficient in the internal combustion engines," *SAE Technical paper*, no. 670931, 1967.

[23] F. Payri, X. Margot, A. Gil and J. Martin, "Computational study of heat transfer to the walls of a DI diesel engine," *SAE Technical Paper*, no. 2005-01-0210, 2005.

[24] A. Torregosa, P. Olmeda, B. Degraeuwe and M. Reyes, "A concise wall temperature model for DI Diesel engines," *Applied Thermal Engineering*, vol. 26, no. 11-12, pp. 1320-1327, 2006.

[25] Z. Zhang, H. Liu, Z. Yue, Y. Wu, X. Kong, Z. Zheng and M. Yao, "Effects of Multiple Injection Strategies on Heavy-Duty Diesel Energy Distributions and Emissions Under High Peak Combustion Pressures," *Frontiers in Energy Research*, vol. 10, p. 857077, 2022.

[26] I. Taymaz, "An experimental study of energy balance in low heat rejection diesel engine," *Energy*, vol. 31, no. 2-3, pp. 364-371, 2006.

[27] J. Heywood, Internal Combustion Engine Fundamentals, McGraw-Hill Education, 2018.

[28] J. Benajes, J. Lopez, R. Novella and A. Garcia, "Advanced methodology for improving testing efficiency in a single-cylinder research diesel engine," *Exp Tech*, vol. 32, pp. 41-47, 2008.

[29] R. Durrett and M. Potter, "Renewable Energy to Power through Net-Zero-Carbon Fuels," in *THIESEL 2020 Conference on Thermo- and Fluid Dynamic Processes in Direct Injection Engines 8th-11th September 2020*, Valencia, 2020.

[30] S. Biswas, A. S. Segupta, D. Kakati, P. Chakraborti and R. Banerjee, "Parametric optimization of the CNG/ethanol-induced RCCI profiles in

biodiesel combustion through a robust design space foray," *Fuel*, vol. 332, no. Part 2, p. 126203, 2023.

[31] S. d'Ambrosio, D. Iemmolo, A. Mancarella and R. Vitolo, "Preliminary Optimization of the PCCI Combustion Mode in a Diesel Engine through a Design of Experiments," *Energy Procedia*, vol. 101, no. November, pp. 909-916, 2016.

[32] J. Sjoblom, J. Andric and E. Faghani, "Intrinsic Design of Experiments for Modeling of Internal Combustion Engines," *SAE Technical Paper*, pp. 2018-01-1156, 2018.

[33] S. Ramalingan, S. Gomathinayakam, V. Mani and S. Kachapalayam, "Analysis of optimising injection parameters and EGR for DICI engine performance powered by lemongrass oil using Box–Behnken (RSM) modelling," *International Journal of Ambient Enegry*, vol. 43, no. 1, pp. 6362-6379, 2022.

[34] D. Montgomery, Design and Analysis of Experiments, New York: John Wiley, 2019.

[35] Analytical Methods Committee, AMCTB No 55, "Experimental design and optimisation (4): Plackett–Burman designs," *Anal. Methods*, vol. 5, no. 8, pp. 1901-1903, 2013.

[36] P. Bruce and A. Bruce, Practical Statistics for Data Scientists, O'Reilly Media, Inc., 2017.

[37] G. James, D. Witten, T. Hastie and R. Tibshirani, An Introduction to Statistical Learning: With Applications in R, New York: Springer, 2013.

[38] G. Sierksma and Y. Zwols, Linear and Integer Optimization - Theory and Practice, Third Edition, New York: Chapman and Hall/CRC, 2015.

[39] A. Schrijver, Theory of Linear and Integer Programming, New York: John Wiley & Sons, 1998.

Chapter 4
Drop-in use of low carbon fuel blends in compression ignition engines

Contents

1 Introduction

Drop-in fuels are defined as alternative fuels that are interchangeable with conventional fossil counterparts without needing to modify elements of the engine hardware for its proper operation or even needing to update the calibration maps of the circulating fleets of vehicles. In Europe, since the years 2009 and 2011 commercially available diesel and gasoline have been introduced to the European Union with a proportion of up to 7% of FAME for the diesel fuel and up to 5% of ethanol for gasoline [1, 2]. For passenger and commercial vehicles, it was possible to use these new blended fuels commercially due to their properties being extremely similar to the previous fossil alternatives. Once these new blends became the standard, the vehicles fuel injection systems, additive composition and combustion parameters were gradually modified to reach optimum performance with the newer blends [3]; in contrast, there were reports in some vehicle models of issues like deposits in common-rail injectors, not necessarily attributable to aging, due to the small differences in the newer fuel blends [4, 5, 6, 7].

Fuels with high renewable proportions and other characteristic properties that can help mitigate emissions associated to combustion engines such as NOx and soot, as well as CO_2 emissions, are attractive to be evaluated as drop-in alternatives considering that massive adoption could be eased by removing barriers to entry like the need for vehicle modifications or fuel distribution systems [8, 9]. In addition, current engine control systems are better adapted to deal with the small differences between new renewable fuel blends and the current standard fuel [10, 11], guaranteeing a more reliable operation after the substitution. Nevertheless, using an existing calibration for a conventional fuel with a drop-in alternative fuel might lead to a scenario where the differentiating properties of the fuel, that can lead to the best performance increases and emissions reductions, are being misspent by not using a dedicated calibration (as will be seen in later chapters).

When contemplating an ideal drop-in low carbon fuel there are numerous considerations to be made. For a compression ignition engine it is desired that the fuel has a high LHV and CN, like diesel would, while at the same time maintaining a viscosity and density that allows the fuel injection system's pump, common-rail, and injectors to operate within their optimal design range. Biofuels have been the most prevalent alternative in this scenario as they fulfill the same quality standards as the fossil fuels they are replacing [12], as do some synthetic diesel fuels [13]. Other fuels, like highly oxygenated or alcohol fuels, although they can reach similar LHV, CN, density, and viscosity for the operation with the engine, maintaining similar or even improved performance and emissions [14]. However, the use of these

fuels can originate issues of reduced durability of the hardware components that need to be addressed, especially the fuel injection systems, due to increased corrosion and oxidation as has been previously reported [15].

Besides being relatively simple to implement as an energy carrier solution, few studies have really emphasized drop-in assessments of fuels for their application in internal combustion engines. In this chapter, this gap is bridged experimentally, evaluating seven low-carbon fuel blends under stationary conditions as drop-in alternatives. This chapter will focus solely on the engine effects of using the fuel, while future chapters will address other scenarios such as the lifecycle impacts of such fuels, and a brief discussion into the broad effects of adopting the use of low-carbon fuels.

2 Combustion, performance and emissions

Considering the advantages of using and selecting adequate drop-in fuels for the direct substitution of the current fossil ones in the engine, and the direct benefit in the simplicity of wide adoption of drop-in fuels both in terms of refueling station and consumer requirements. The drop-in potential of the chosen low-carbon fuel blends will be determined. First, the ability of the fuels to achieve drop-in operation will be assessed experimentally, as well as the characteristics of the combustion, emissions, and engine settings. For all the fuels the same calibration map used for conventional diesel will be tested using high reactivity fuels in a commercially available CI engine.

2.1 Engine settings: reaching drop-in operation

As described in Chapter 3, the drop-in tests are carried out for all the LCF and compared to a baseline diesel reference, which corresponds to the normal operation of the engine. The test matrix for the steady state operation of the engine is described also in Chapter 3 and is representative of the operation under the WLTP cycle. The operating conditions range from low-load low-speed conditions, mid-load, and two additional operating points that are proxy to the rated torque and rated power conditions. To reach the drop-in operation with the given fuels, the engine speed is set in the dynamometers and a pedal signal is sent to the ECU until the required load is achieved. The pedal signal is associated to a lookup fuel requirement table in mass, for which a higher pedal position demands a higher fuel to be injected. Because the LCF blends have different properties, and in particular differ in their LHV, fuels with lower LHV require a higher pedal signal than fuels with higher LHV (Figure 1) to reach the same engine load. In particular, the fuels with the lowest LHV (MaxOME66 and LCD100) – which have a reduction of nearly 10% in energy

density with respect to diesel – show an average increase in pedal position of 3%, reaching up to 7% for MaxOME66 at the highest load operating condition. From this, although the LHV has a significant influence in the pedal demand needed from the drop-in tests, the reduction in energy density does not directly translate to an equivalent increase in pedal, which will be explained by other fuel properties and their effect in the combustion characteristics that can compensate some of the lacking energy density with higher combustion efficiencies, for example.

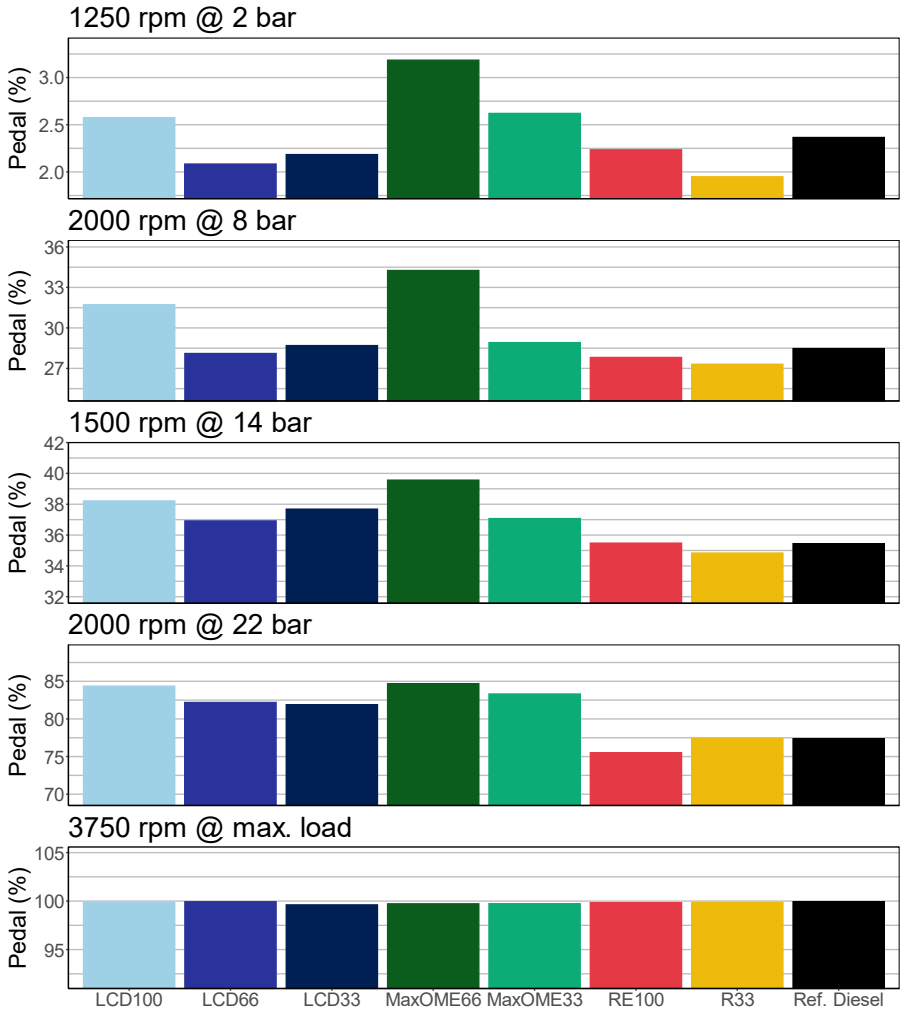

Figure 1. Pedal requirement for the different LCF blends at the tested operating conditions.

Keen observers might have noticed that the 3750 rpm @ max. load operating condition shows the same pedal for all the fuels, and might have wondered whether the rated power of the engine remains the same for all fuels. The answer to that question is no, the rated power varies similarly to the pedal variation with the fuel energy density. At the 3750 rpm @ max. load operating condition, the objective is to increase the maximum load to the maximum possible value that a given fuel allows with 100% pedal. In Figure 2, the effect of the fuel over the maximum pedal torque is observed. It can be seen how fuels with lower LHV, like LCD100 reach loads nearly 5% below the load achieved with diesel, while on the contrary RE100 can, with the same pedal, reach 4% higher loads. Surprisingly, while the MaxOME (33 & 66) fuels have some of the lower LHV, it is possible to reach almost the same rated power as with diesel. This is assumed to be related to the high OMEx proportion of the fuels which provides high oxygenation which favors better equivalence ratios for the combustion of the fuel. In the case of the RE100 fuel, although it has a similar LHV to diesel it is observed how the fuel yields a higher load for the same pedal signal, which could be also linked to the oxygen proportion of the fuel, which is 2.81 times higher than diesel.

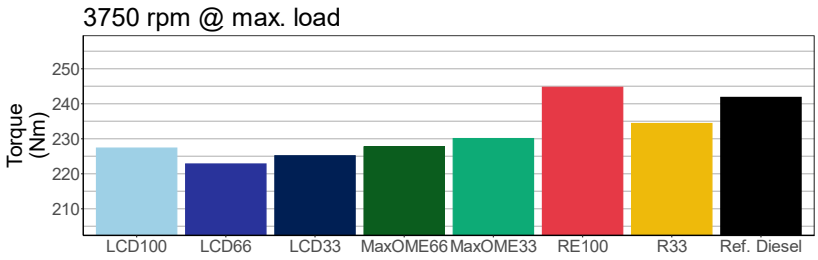

Figure 2. Achieved load for the different LCF blends at 3750 rpm and 100% pedal.

The baseline calibration map for diesel varies depending mainly on the set point for the pedal position and the engine speed, which in turn translates to a fuel mass demand map from which the other calibration settings – such as the injection pressure, quantity and timing for the injections, intake air mass, boost pressure and EGR proportion – have associated lookup tables. It is then logical that the cases with similar or the same pedal position will have similar calibration settings, as can be observed in Figure 3 and Figure 4; while as the pedal increases settings like the injection pressure will increase while the start of injection of the main injection (SOI M) will be advanced or delayed, as will the proportion and timing of the pilot injections. Because they have the largest differences in pedal position (because of their considerably lower LHV), the MaxOME66 and LCD100 fuels have the largest differences in their calibration.

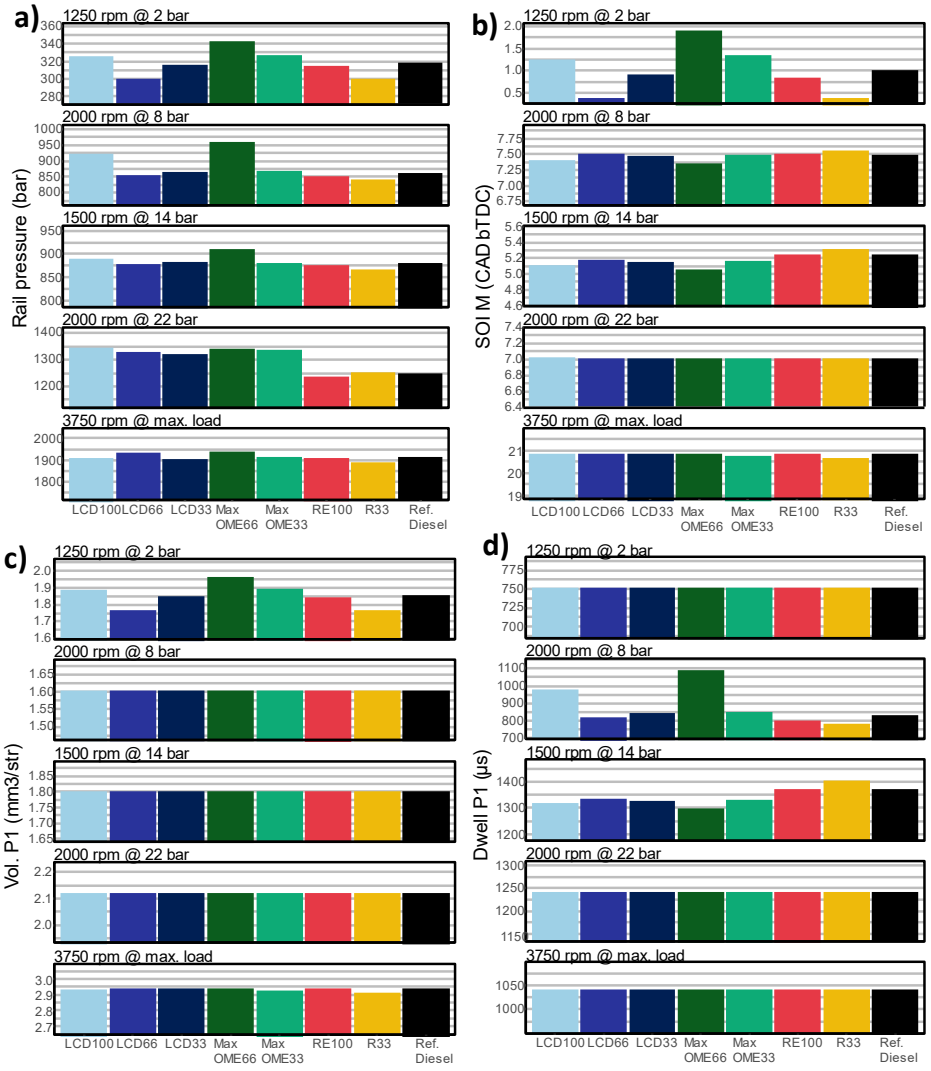

Figure 3. Injection settings for the different LCF blends under the drop-in calibration: (a) rail pressure; (b) start of injection of the main injection (SOI M); (c) volume of the first pilot injection (Vol. P1) and (d) dwell time between the first pilot injection and the main injection (Dwell P1).[1]

[1] In Figure 3 and Figure 4, calibration parameters that do not vary between fuels like the volume of the second pilot injection and its dwell time are not shown.

Although the changes in the calibrations settings under drop-in operation are mainly associated to the changes in fuel mass demand and their associated lookup values from the calibration maps, small corrections occur related to the fuel specific characteristics. For example, the charge renovation settings can be sensitive to the fuel even when the pedal position remains the same. The air mass and the EGR variation are then linked to the fuel because the turbocharger operation depends on the exhaust energy, which is dependent on the specific combustion characteristics of each fuel. Then, the admitted fresh air quantity is regulated to an extend by the turbocharger and later the desired set point is refined with the EGR valve, by opening or closing it to allow more or less fesh air. In this regard, it can be seen how the fuels with the highest oxygen concentrations allow around 2-4% more exhaust gas to recirculate even with higher pedal positions for which the calibration tables are designed to limit the amount of EGR to lower values.

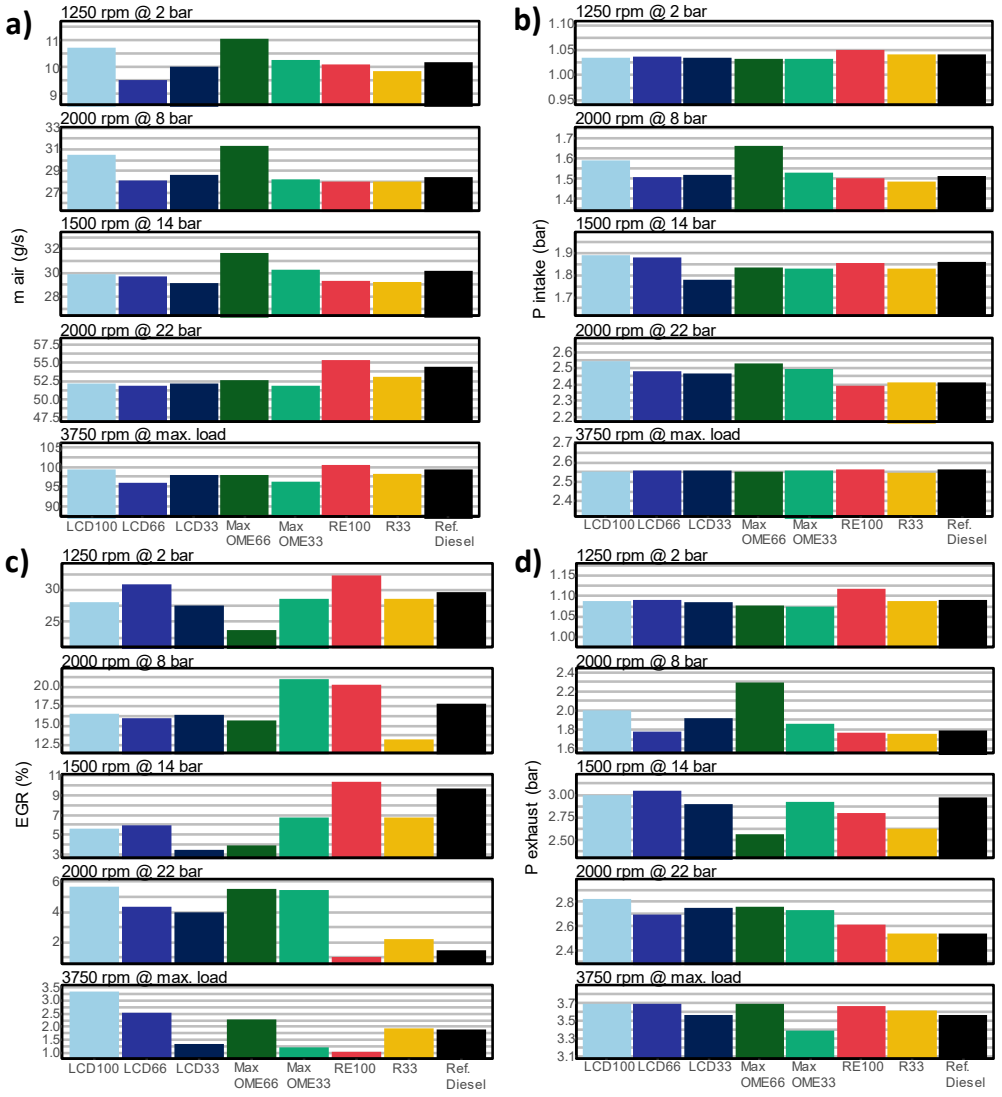

Figure 4. Charge renovation settings for the different LCF blends under the drop-in calibration: (a) air mass flow; (b) intake pressure and (c) EGR.

2.2 Combustion under drop-in calibration settings

In the previous section it was observed how changing the fuel changes the engine settings necessary to maintain the same load and speed as with diesel. Similarly, at the rated power condition it was seen how for the same engine settings the fuel drove the achievable load with a strong correlation with the LHV, but also with other properties like the oxygen content that allows higher loads with lower LHV, as it is thought to improve the local equivalence ratio.

Evaluating the combustion pressure indication provides useful information. The peak engine pressure, as seen in Figure 5, can be an important factor determining the performance and efficiency of an engine, as it is directly related to the amount of power produced and the amount of fuel consumed. When studying LCFs checking for the peak pressure will also provide insight into the thermal load and stress the engine will be subjected to. In the figure it is observed how the fuels with the highest oxygen content (LCD100 and MaxOME66) have higher peak pressures than diesel, which is especially prominent at the 3750 rpm-max. load condition. This higher oxygenation in the molecular structure means that, locally, the fuel will require less air to complete the combustion, resulting in a more efficient combustion process. For the purpose of addressing the feasibility of the adoption of LCFs as drop-in candidates, it should be mentioned that none of the fuels surpass the manufacturers recommended limit of 180 bar.

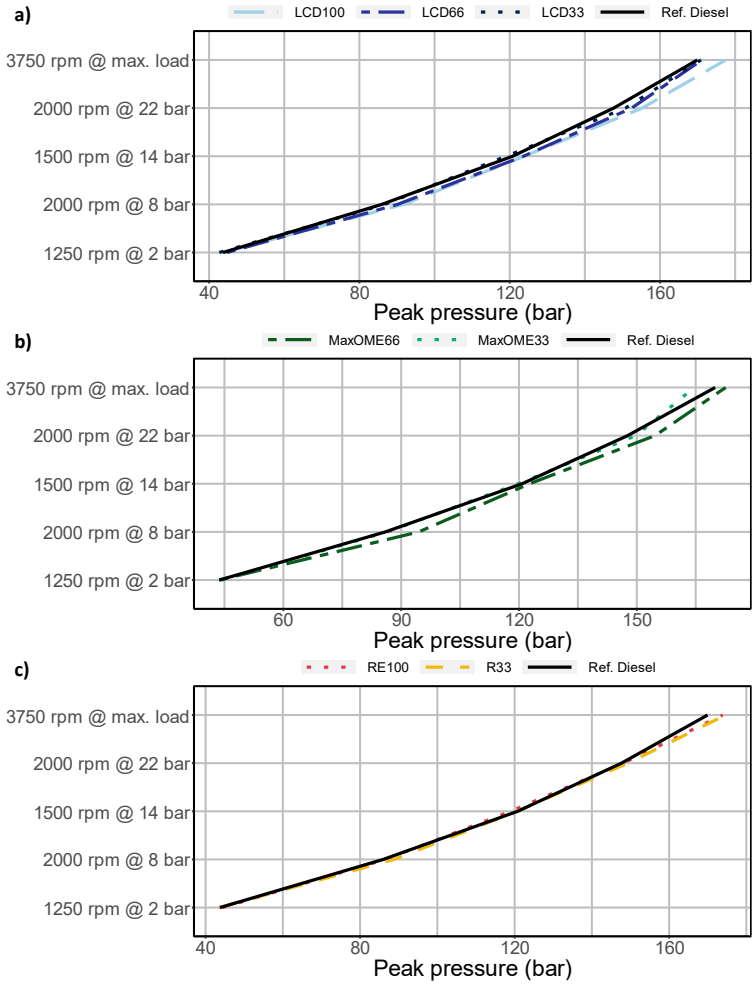

Figure 5. Peak pressure of Ref. Diesel compared with (a) LCD100, LCD66 and LCD33; (b) MaxOME66 and MaxOME33 and (c) RE100 and R33.

Combustion in internal combustion engines highly depends on the fuel-air mixture, the ignition delay, temperature, engine speed and load. Different fuels have different fuel-air interactions and ignition conditions depending on the chemical and physical properties of the fuel, which in turn modify the rate at which heat is released during the combustion. Figure 6 shows the heat release rate (HRR) at the 3750 rpm-maximum load condition. Because this operating point has similar calibration settings, it shows the LCFs effect on the combustion without the inclusion of large confounding effects. For all cases the pilot injection starts at 49.95 degrees before TDC (deg bTDC) and represents nearly 5% of the total injected energy. The low

temperature heat release (LTHR) is seen to occur earlier for the fuels with the highest CN of each group: the LCD100 (87 CN), MaxOME66 (69.6 CN) and RE100 (83.5 CN) which agrees with the extensively reported correlation between the CN and shorter ignition delays [16]. The main injection occurs at 20.8 deg aTDC after which a second LTHR occurs followed by the rapid increased of the high temperature heat release (HTHR). The peak of the HTHR shows a compensation for the LCD66, RE100 and MaxOME33 fuels, which had lower second LTHR but then have higher peaks than the rest of the fuels, likely product of a delayed start of combustion of the main injection (as can be also observed in Figure 8), which at higher temperatures and pressure conditions, once the combustion starts it is more intense.

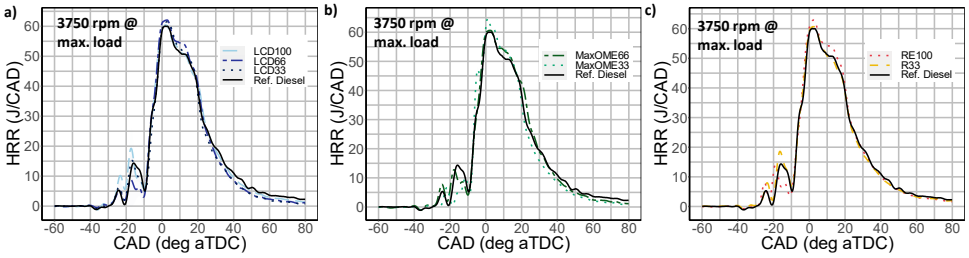

Figure 6. Comparison of the Heat release rate (HRR) of Ref. Diesel with (a) LCD100, LCD66 and LCD33; (b) MaxOME66 and MaxOME33 and (c) RE100 and R33 @ 3750 rpm and full load.

During the burnout stage, in which the remaining combustion products are burned, the fuels with a proportion of OMEx show a faster decrease, while the RE100 and R33 fuels show higher similarity to diesel. This faster burnout stage can be related to the higher oxygen proportion of the fuels, which overall increases the combustion temperature from TDC to around 60 deg aTDC (as is seen in Figure 7) and provides more oxygen for a complete combustion.

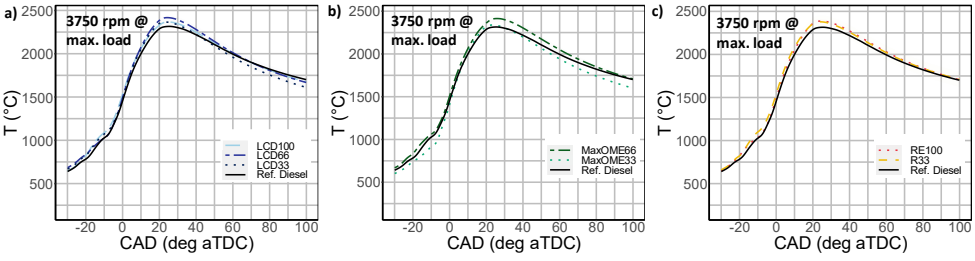

Figure 7. Comparison of the calculated in-cylinder temperature of Ref. Diesel with (a) LCD100, LCD66 and LCD33; (b) MaxOME66 and MaxOME33 and (c) RE100 and R33 @ 3750 rpm and full load.

To observe the combustion timing effects of the tested LCFs across all the operating conditions, Figure 8 shows the CA10, CA50 and CA90. These values provide a relative reference to the start of combustion (SOC), the combustion phase, and the end of combustion (EOC). At low and medium load the MaxOME66 is the clear outlier, having the most retarded SOC yet the earliest CA50, indicating that at these loads the LTHR is minimal and that the majority of the heat is released very fast during the premixed HTHR. For the 2000 rpm @ 22 bar condition it can be seen that the SOC and CA50 is close for all fuels, but that as the oxygen proportion increases so does the combustion duration decrease. Counterintuitively, at low loads the R33 fuel has one of the earliest CA10, even though it has one of the lowest CN (which would normally delay the combustion). This can be explained by the variations originated by the pedal position and the higher LHV of this fuel, where the pilot injection is injected considerably earlier than for the other fuels and thus when the ignition delay is observed, the fuel complies with the expected longer ignition delay.

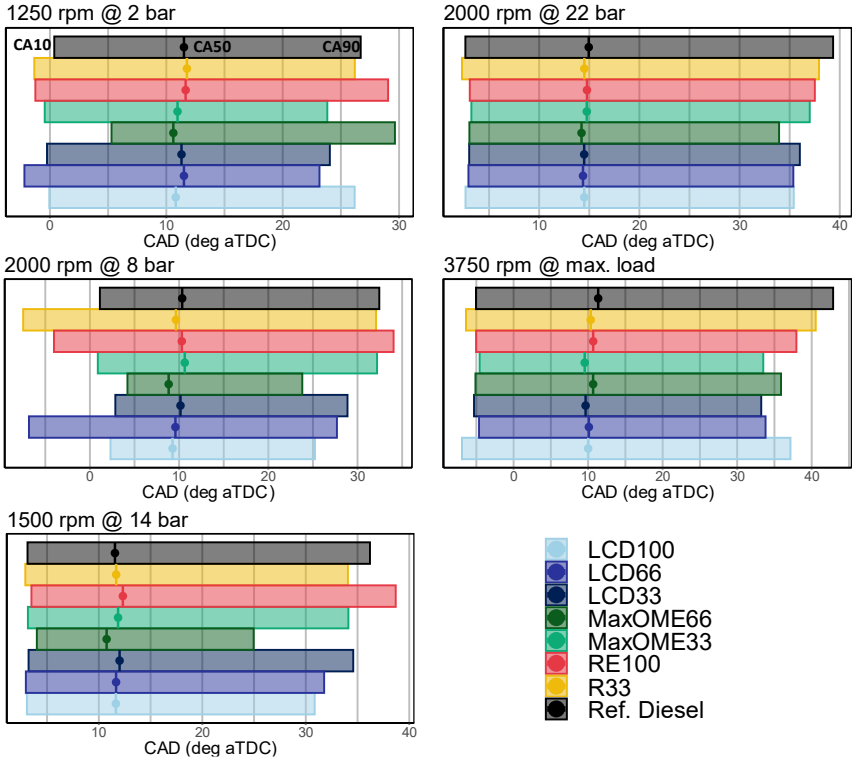

Figure 8. Combustion timing for the different LCF blends under the drop-in calibration. Each rectangle indicates the duration from CA10 to CA90, and the vertical line and point the CA50.

2.3 Performance and emissions of drop-in fuel operation

A drop-in fuel candidate to replace diesel must, besides being able to be burned in the engine, perform in such a way that regulated emissions can at least be as low as with the current diesel homologated vehicles and the fuel efficiency sufficiently high as to not represent a significant decrease in the vehicle milage.

2.3.1 Fuel energy utilization

The brake-specific fuel consumption (BSFC) and the equivalent brake-specific fuel consumption (BSFCeq) are shown in Figure 9 (a) and (b) respectively. The first represents the mass of fuel used to produce one kilowatt of power for one hour, while the second measure considers the LHV of the fuel and how would the fuel consumption would be if the fuel had the same LHV as diesel. Regarding the BSFC, the expected trends can be observed across all operating conditions: the fuels with the highest LHV have the lowest fuel consumption. When observing the BSFCeq it can be seen how fuels with low LHV have lower values than diesel. This effect is especially evident with the oxygenate fuels, and can be due to the fact the oxygenation of the fuel molecule improves the overall combustion efficiency. In the other direction, the fuels with higher LHV than diesel, still perform better than diesel when accounting the BSFCeq, also indicating a better efficiency.

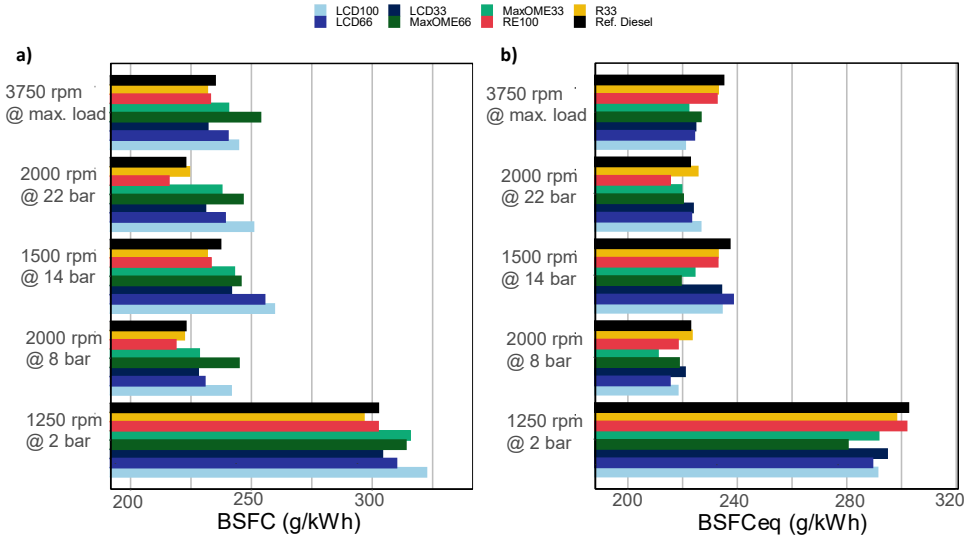

Figure 9. (a) Brake-specific fuel consumption (BSFC) and (b) equivalent BSFC (BSFCeq) for the different LCF blends under the drop-in calibration.

To explain some of the differences in fuel consumption and engine efficiency,

Figure 10 shows the energy distribution of diesel under the tested operating conditions (which has a similar general pattern to the tested LCFs), while Figure 11 shows more detail in the differences between fuels in terms of gross brake efficiency (GBE), combustion inefficiency and exhaust energy losses. In Figure 10, the GBE varies from 27% to 37%, while the rest of the energy is lost to different sinks like mechanical and pumping losses, heat transfer to the block, the exhaust or combustion inefficiencies (defined as the products of incomplete combustion). Because all fuels are tested within the same engine it can be assumed that mechanical and heat transfer losses will remain similar (with small variations due to the fuels in the work of components like the fuel pump and the turbocharger).

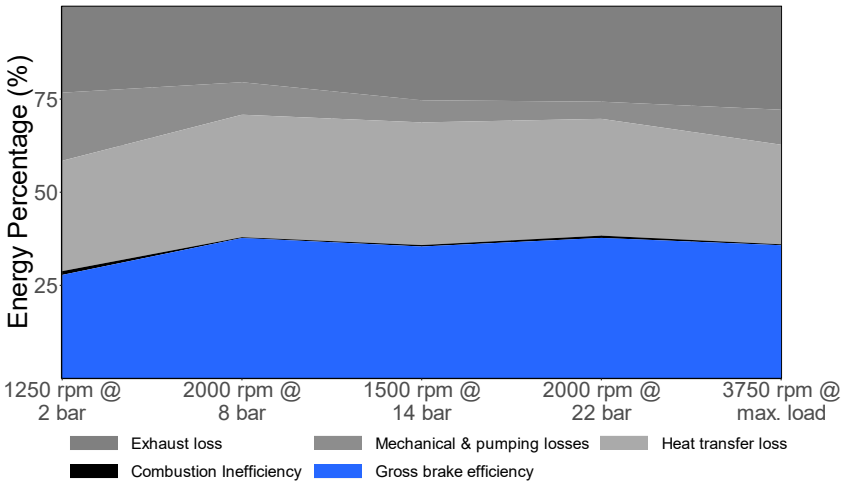

Figure 10. Energy distribution for Ref. Diesel under the drop-in calibration at the tested operating conditions

The GBE, combustion inefficiency and exhaust losses will vary significantly depending on the calibration settings and the LCF used, and they can represent up to 80% of the total fuel energy. In Figure 11 (a) the GBE is evaluated for all fuels, agreeing with the trends observed in the BSFCeq. The fuels with percentages of OMEx have 1-2.5% higher efficiencies than diesel, while the addition of FAME (as with the RE100) seems to equally improve the efficiency of the engine. Combustion inefficiency remains below 1% of the total fuel energy for the tested LCFs, and although some of the LCFs have higher values compared to diesel these losses are not of concerning magnitude and are within expectations. The exhaust energy losses,

on the other hand, show the biggest differences between fuels because exhaust gases contain a significant amount of energy, which is partially captured by the turbocharger, while some is required for the aftertreatment system (ATS), but a large portion remains unused. The exhaust energy depends as much on the combustion phasing, injection settings and subsequently on the fuel, and is one of the areas where a dedicated LCF calibration could aid achieve higher output power by unit of fuel energy injected.

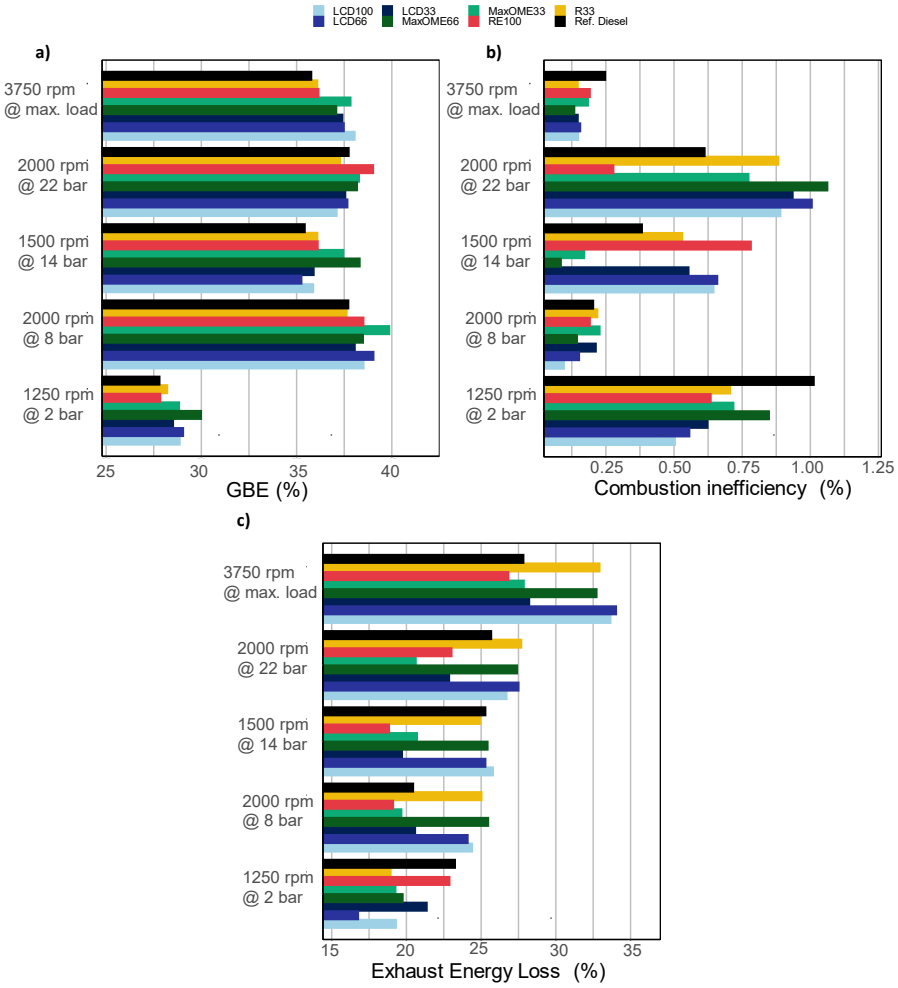

Figure 11. (a) Gross brake efficiency (GBE); (b) combustion inefficiency; and (c) exhaust energy loss for the different LCF blends under the drop-in calibration.

2.3.2 Criteria for the evaluation of pollutants

The final prerequisite for a diesel drop-in alternative is that pollutant emissions can be controlled, at minimum, equally as good as they are with the currently used diesel fuel. During this chapter the focus are the NOx, soot, HC and CO emissions which are all regulated in Europe under the Euro 6 normative (and soon under Euro 7).

NOx emissions depend greatly on the combustion temperature, the air-to-fuel ratio and ignition timing, which as has been observed so far vary depending on the fuel used. In addition, the amount of EGR has been prove to be instrumental in reducing NOx emissions by diluting the air-fuel mixture with the exhaust gases and thus reducing the peak combustion temperature; nonetheless, due to the nature of the drop-in tests, the calibration of this parameter is also changed by the differences in the fuel properties. Considering this, Figure 12 shows the brake-specific NOx (BSNOx) emissions for the LCFs. The higher pedal position of MaxOME66, which demanded a lower EGR in the calibration is directly correlated to a higher NOx emission at the three lower loads. Besides this extreme case, at the max. load and the 2000 rpm @ 22 bar operating condition the RE100 fuel also has nearly 1 g/kWh more than diesel, while showing moderate emissions at lower loads. The LCD fuels (100, 66, and 33) at high loads increase the NOx emissions as the OMEx proportion is decreased, while at low loads the effect is inversed. In this group of fuels, this effect could be explained by the variation of the OMEx proportion on each blend, which at low loads contributes to higher combustion temperatures by increasing the oxygen concentration, while at high loads the more complete combustion can reduce the formation of partially oxidized fuel compounds that can contribute to NOx emissions, as well as reduce the combustion temperature. A similar conclusion can be drawn for the MaxOME33 emissions. The fuels with bio-originated lipid blends do not show such consistent trends, with R33 generally promoting combustion at higher temperatures that result in higher NOx, while at low loads RE100 shows the opposed effect.

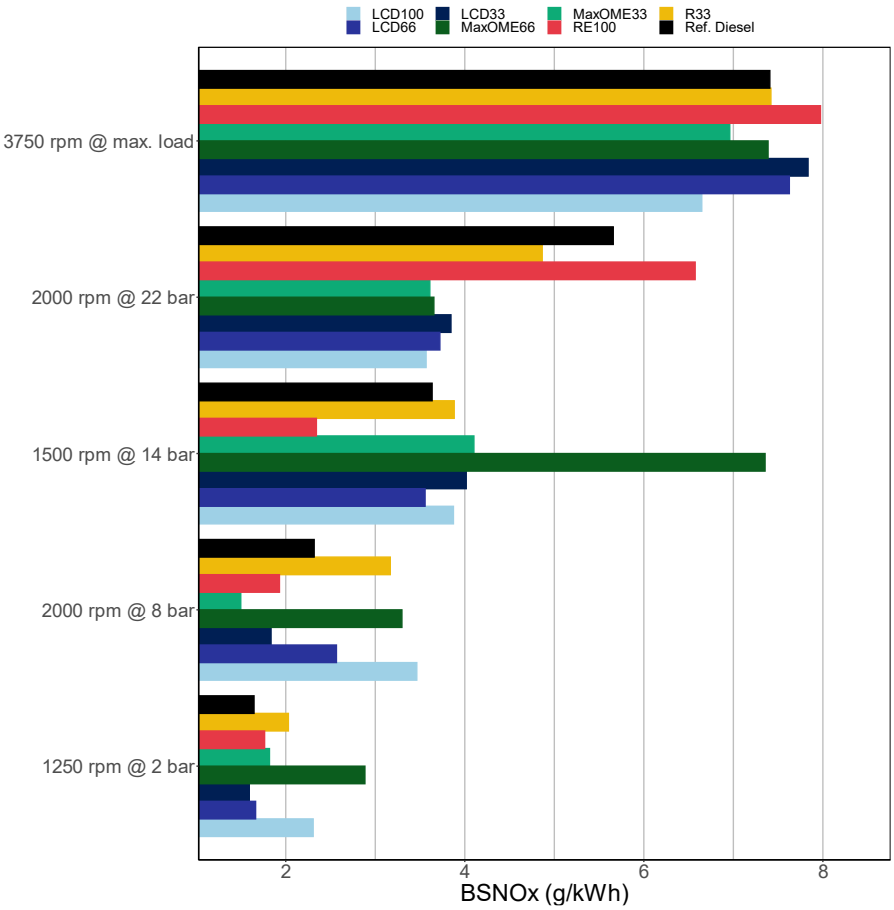

Figure 12. Brake-specific NOx emissions (BSNOx) for the different LCF blends under the drop-in calibration.

Soot emissions contribute to the formation of smog and air pollution, which can have negative impacts on the environment and human health. Regulating soot emissions from engines can help to minimize these negative impacts. Diesel particulate filters (DPFs), can capture and remove soot particles from the exhaust gases, reducing the amount of soot emissions released into the atmosphere, however the efficiency of this process will vary depending on the amount and size of the particles released and an excessive amount of soot can be prone to obstruct the filter, thus controlling the engine-out soot is a relevant criteria for a drop-in alternative. Contrarily to what is expected, under the drop-in calibration most of the OMEx containing fuels have higher soot emissions than diesel at the 2000 rpm @ 22 bar operating condition (Figure 13), which can in part be explained by the higher mass of fuel that has to be

injected to reach such load with the lower LHV fuel blends, creating rich local regions that increase the soot emissions. Under the rest of the operating conditions, however the OMEx containing fuels do present an improvement with respect to diesel or a similar value. Of the fuels tested, the R33 shows the worst case scenario in terms of drop-in soot emissions, which could be in part due to the calibration not being ideal for this fuel as the pedal position is lower, decreasing the amount of fresh air and reducing the injection pressure, which could increase the locally rich areas occurrence generating higher soot emissions. In any case, is worth noting that all LCFs have lower than 0.2 g/kWh.

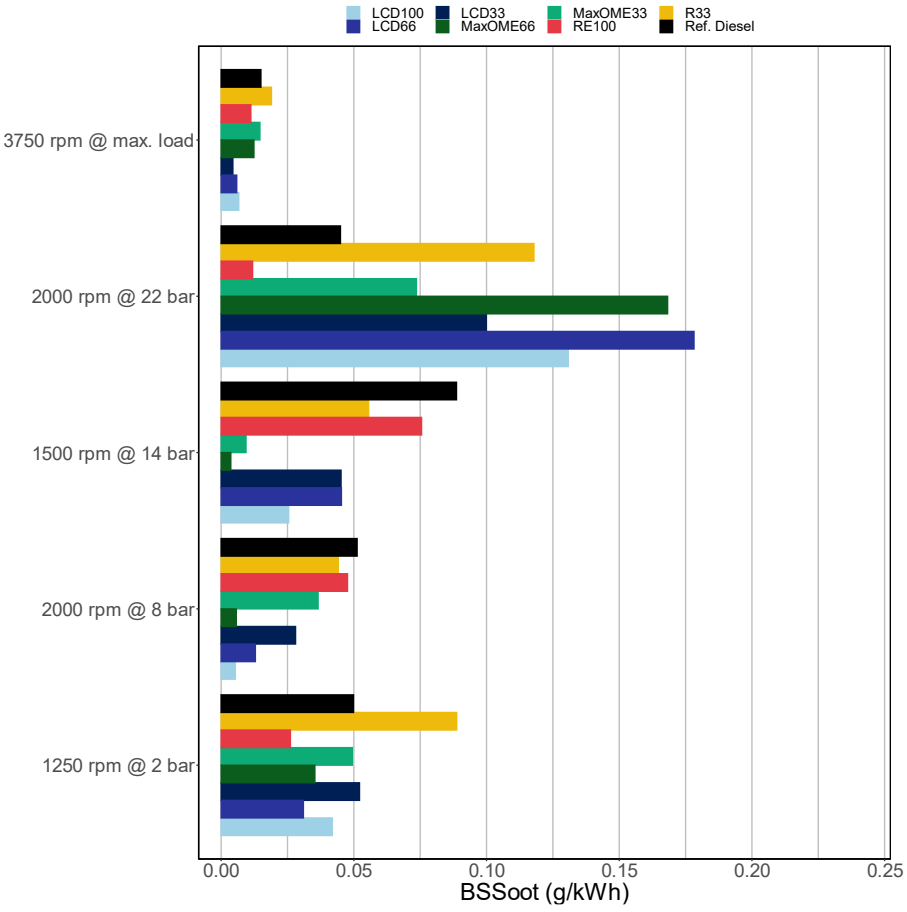

Figure 13. Brake-specific soot emissions (BSSoot) for the different LCF blends under the drop-in calibration.

Figure 14 shows the brake-specific HC and CO emissions. HC remain within diesel's levels (although the mass could increase up to 5% if the unburned hydrocarbon was considered as pure fuel instead of methane as described in previous chapters). On the other hand CO can be increased by up to 2.5 g/kWh at the 2000 rpm @ 22 bar and the 1500 rpm @ 14 bar operating conditions when testing fuels like the R33 and the LCDs. Is this high CO values that correlate directly to the higher observed combustion inefficiencies previously described. Although in some case, the tested LCFs can have higher CO and HC values, the level for these pollutants remains within reasonable diesel levels and thus with the already existent diesel ATS (like catalytic converters) could be significantly reduced before the tailpipe.

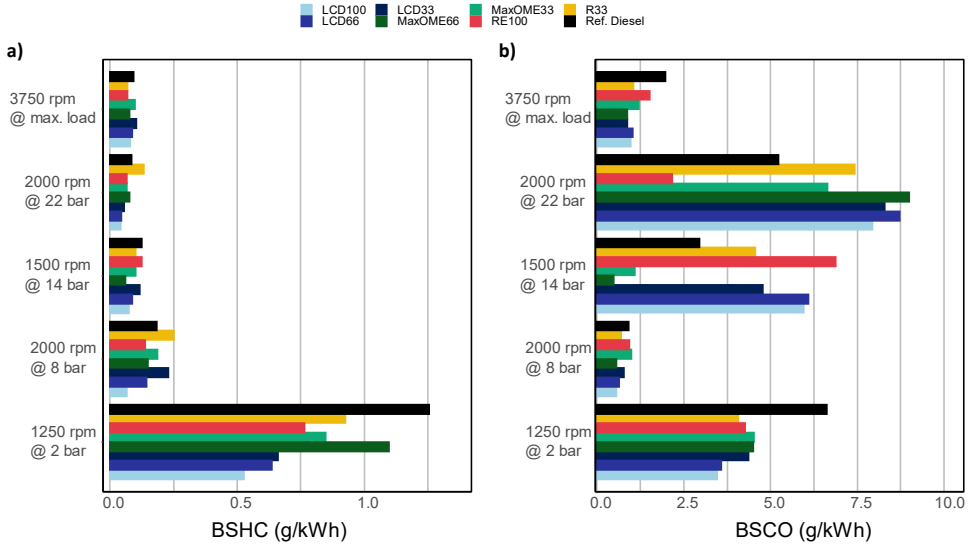

Figure 14. (a) Brake-specific HC emissions (BSHC) and (b) Brake-specific CO emissions (BSHC) for the different LCF blends under the drop-in calibration.

3 Unmeasured effects of the use of drop-in fuels

In this chapter the appropriateness of using LCFs as drop-in candidates for internal combustion is addressed, highlighting that the ideal drop-in fuel would not require to make significant changes to the vehicle, the fuel distribution system or end user considerations like additional safety measures when manipulating (for example in the case of refueling).

In the previous sections it has been demonstrated how all tested fuels are able to be used within a similar operation range to diesel's, with some even being more efficient in terms of fuel consumption or engine-out emission control. The criteria

used for this assessment considered exclusively what could be called ‘combustion effects’, disregarding the differences in wear and durability that the fuels might cause on different systems. Nonetheless, some negative effects were still observed during the tests of some of the selected LCFs, particularly in the fuel injection system.

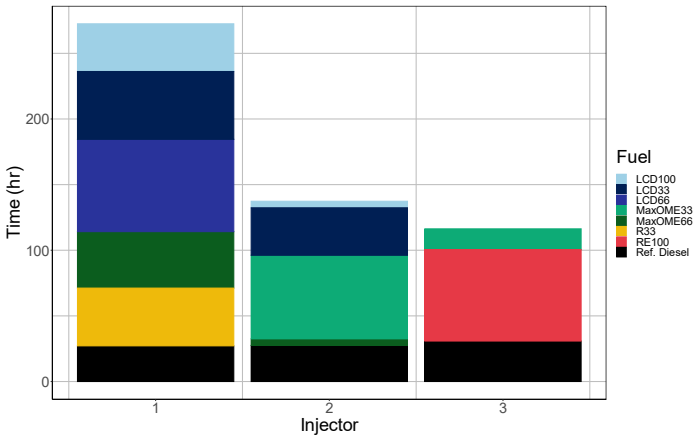

Figure 15. Injector usage summary including the operation time and the fuels used before breakage.

The following observations are anecdotal and rigorous dedicated durability and wear testing methodology should be implemented in the future. Nonetheless, it is interesting to comment that during testing it was found that oxygenated fuels had a higher tendency to reduce the durability of the common-rail, injectors and fuel pumps. Figure 15 shows the recorded injector operation time (which is similar to the distribution of use of the high-pressure pumps) with the tested LCFs. Because of the high injection pressure and presumably due to the differences in the fuel properties, the injectors were observed to be one of the most sensitive components to damage during testing with LCFs. A breakage pattern emerged specifically after around 40hrs of non-continuous operation with oxygenated fuels, which included problems like the injector not opening or closing as designed leading to missing injections or injection of unprecise fuel quantities. For comparison under normal operation with diesel a durability of over 150000 kilometers could be expected for an injector [17], many orders of magnitude more than what was observed during the study. The high-pressure fuel pump was another delicate component having to also use three sets in a total of 526 hrs (which would equate to only 52600 kilometers at a constant speed of 100 km/h). In addition, one of the common-rails and injectors was sent to the manufacturer for analysis after operation and breakage with MaxOME66 where corrosion was observed in functional components for both parts reassuring the

concern for the durability of components when using highly oxygenated fuels without improving the additivities formula or changing the hardware design.

The hardware durability observations in relation to the oxygenated fuels are directly linked to the lubricity wear scar diameter (WSD), which is also linked to the water content and the viscosity of the fuel. This was observed in the bivariate correlation between fuel properties shown in Chapter 3 and is summarized here in Figure 16. The WSD is a measure used to evaluate the lubricating properties of fuels, providing an indication of the fuel's ability to reduce friction and prevent wear between metal surfaces in engines and other mechanical systems. When fuel is used as a lubricant, such as in the fuel injection system (FIS) in this study, it forms a thin film between moving metal surfaces to minimize direct metal-to-metal contact. The WSD test measures the size of the wear scar produced on a flat metal specimen after it has been subjected to controlled sliding against another metal surface while being lubricated with the fuel being tested. In this context, the observations in Figure 16 empirically relate well to the usage time before injector breakage, with the oxygenated fuels, particularly the LCD100 showing the largest WSD.

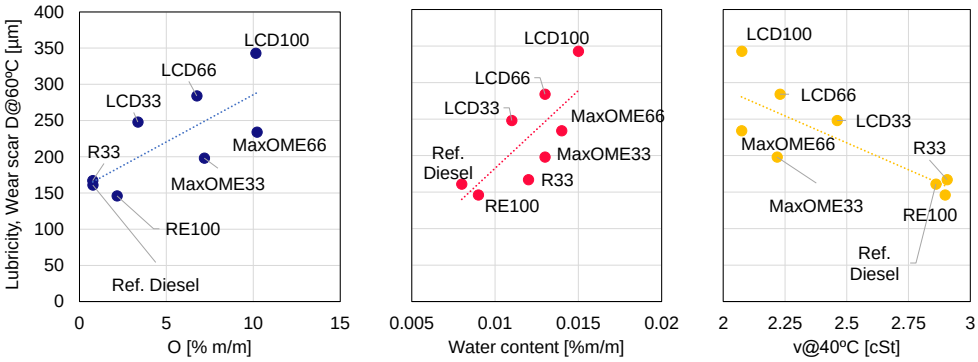

Figure 16. Relation between the wear scar diameter, the oxygen content, the water content and the viscosity of the fuels

What the previous empirical observations seem to indicate is that, although these LCF show excellent potential to be substitutes of fossil diesel in terms of combustion, some considerations still need to be made for the hardware it is going to be used in or the formulation of the fuels, to include additives that can mitigate some of the corrosion and oxidation associated issues that were observed. However, some fuels, like the RE100 and R33 are more ready to be directly applicable to existing vehicle floats.

4 Summary and conclusions

The drop-in potential of different low-carbon fuel blends was determined by assessing their ability to achieve drop-in operation and their characteristics of combustion, emissions, and engine settings. The test matrix for steady-state operation of the engine was representative of the operation under the WLTP cycle. The results showed that the fuels with the lowest LHV required a higher pedal signal to reach the same engine load, but the reduction in energy density did not directly translate to an equivalent increase in pedal. The rated power varied similarly to the pedal variation with the fuel energy density. The MaxOME fuels, despite having lower LHV, could reach almost the same rated power as diesel due to their high oxygen proportion.

The changes in the calibration settings under drop-in operation are mainly associated with changes in fuel mass demand, but small corrections occur due to fuel-specific characteristics. The air mass and EGR variation are linked to the fuel, as the turbocharger operation depends on the exhaust energy, which is dependent on the specific combustion characteristics of each fuel. The admitted fresh air quantity is regulated by the turbocharger and later refined with the EGR valve, which allows more or less fresh air.

In order for a drop-in fuel candidate to replace diesel, it must have similar or lower regulated emissions and fuel efficiency to diesel. The BSFC and BSFCeq were measured for different LCF blends under the drop-in calibration. The fuels with the highest LHV had the lowest fuel consumption and the fuels with low LHV had lower values than diesel when considering BSFCeq. The addition of FAME (as with the RE100) equally improved the fuel consumption and efficiency of the engine. Combustion inefficiency remained below 1% of the total fuel energy for the tested LCFs. The exhaust energy losses depend on combustion phasing, injection settings, and subsequently on the fuel, and is one of the areas where a dedicated LCF calibration could aid achieve higher output power by unit of fuel energy injected.

The LCFs tested in this study showed varying levels of NOx emissions, with MaxOME66 having the highest emissions due to its lower EGR calibration. Soot emissions can be controlled through the use of diesel particulate filters, but engine-out soot levels are also important to consider. OMEx containing fuels had higher soot emissions than diesel at high load conditions, but showed improvement at other operating conditions. HC levels remained within diesel levels, while CO emissions were increased in some LCFs, particularly R33 and LCDs. However, all LCFs tested

had CO and HC levels within reasonable diesel levels and could be reduced further with existing diesel ATS.

The chapter demonstrates that all tested LCFs are able to operate within a similar range to diesel under drop-in operation, with some being more efficient in terms of fuel consumption and engine-out emission control. However, negative effects were observed during testing, particularly in the fuel injection system. Oxygenated fuels were found to reduce the durability of common-rail injectors and fuel pumps. The study highlights the need for rigorous durability and wear testing and suggests that improvements in fuel additives or hardware design may be necessary to mitigate the corrosion and oxidation issues observed. Nonetheless, some LCFs, such as RE100, are more suitable for direct application to existing vehicle fleets.

5 References

[1] *Directive 2009/30/EC of the European Parliament and of the Council of 23 April 2009 amending Directive 98/70/EC as regards the specification of petrol, diesel and gas-oil and introducing a mechanism to monitor and reduce greenhouse gas emissions and amend,* Official Journal of the European Union, 2009.

[2] Directive 2009/28/EC (2009) of the European Parliament and of the Council of 23 April.

[3] O. I. Awad, R. Mamat, O. M. Ali, N. Sidik, T. Yusaf, K. Kadirgama and M. Kettner, "Alcohol and ether as alternative fuels in spark ignition engine: A review," *Renewable and Sustainable Energy Reviews,* vol. 82, no. 3, pp. 2586-2605, 2018.

[4] P. Lacey, S. Gail, J. Kientz, G. Benoist, P. Downes and Daveau, "Fuel Quality and Diesel Injector Deposits," *SAE Int. J. Fuels Lubr.,* vol. 5, no. 3, pp. 1187-1198, 2012.

[5] B. Ritcher, S. Crusius, U. Schümann and H. Harndorf, "Characterisation of Internal Deposits in Common-Rail Injectors," *MTZ Worldwide,* vol. 74, pp. 50-57, 2013.

[6] T. Pham Huu, K. Nguyen Duc, T. Nguyen The, T. Nguyen Duy and N. The Luong, "An experimental study on wear, deposits, performance, and emissions of bio-fueled motorcycle engines," *Energy Sources, Part A: Recovery, Utilization, and Environmental Effects,* vol. 45, no. 1, pp. 1309-132, 2023.

[7] A. Smith and R. Williams, "Linking the Physical Manifestation and Performance Effects of Injector Nozzle Deposits in Modern Diesel Engines," *SAE Int. J. Fuels Lubr.,* vol. 8, no. 2, pp. 344-357, 2015.

[8] A. Kumar Agarwal, "Biofuels (alcohols and biodiesel) applications as fuels for internal combustion engines," *Progress in Energy and Combustion Science,* vol. 33, no. 3, pp. 233-271, 2007.

[9] C. Bae and J. Kim, "Alternative fuels for internal combustion engines," *Proceedings of the Combustion Institute,* vol. 36, no. 3, pp. 3389-3413, 2017.

[10] C. Guido, C. Beatrice and P. Napolitano, "Application of bioethanol/RME/diesel blend in a Euro5 automotive diesel engine: Potentiality of closed loop combustion control technology," *Applied Energy,* vol. 102, pp. 13-23, 2013.

[11] M. D. Cárdenas, O. Armas, C. Mata and F. Soto, "Performance and pollutant emissions from transient operation of a common rail diesel engine fueled with different biodiesel fuels," *Fuel,* vol. 185, pp. 743-762, 2016.

[12] T. Kalnes, T. Marker and D. R. Shonnard, "Green Diesel: A Second Generation Biofuel," *International Journal of Chemical Reactor Engineering,* vol. 5, no. 1, 2007.

[13] S. Bezergianni and A. Dimitriadis, "Comparison between different types of renewable diesel," *Renewable and Sustainable Energy Reviews,* vol. 21, pp. 110-116, 2013.

[14] A. García, A. Gil, J. Monsalve-Serrano and R. Lago-Sari, "OMEx-diesel blends as high reactivity fuel for ultra-low NOx and soot emissions in the dual-mode dual-fuel combustion strategy," *Fuel,* vol. 275, p. 117898, 2020.

[15] M. H. Hassan and M. A. Kalam, "An Overview of Biofuel as a Renewable Energy Source: Development and Challenges," *Procedia Engineering,* vol. 56, pp. 39-53, 2013.

[16] K. Kim, W. Lee, P. Wiersema, E. Mayhew, J. Temme, C.-B. M. Kweon and T. Lee, "Effects of the cetane number on chemical ignition delay," *Energy,* vol. 264, p. 126263, 2023.

[17] C. Chase, C. Peterson, G. Lowe and P. Mann, "A 322,000 kilometer (200,000 mile) Over the Road Test with HySEE Biodiesel in a Heavy Duty Truck," *SAE Technical Paper,* no. SAE Technical Paper 2000-01-2647, 2000.

Chapter 5
Optimization of low carbon fuel blends calibration in compression ignition engines

Contents

1 Introduction

The use of low carbon fuels (LCFs) in internal combustion engines (ICE) has become an important research topic due to their potential to reduce greenhouse gas emissions and improve fuel efficiency. However, the use of LCFs presents some challenges, as their properties can differ significantly from those of conventional fuels. The modelling and optimization of a light-duty ICE using LCFs should be focal to extract the best performance from LCFs. The approach of the study involves adapting the calibration settings of the engine to better suit the properties of the LCFs and decrease NOx emissions. Furthermore, the impact of the LCFs on the engine's performance and emissions is evaluated with different calibrations to provide a thorough exploration of the coupling of the fuels and the engine. The aim of this study is to gain a deeper understanding of the advantages and obstacles associated with the utilization of LCFs in ICEs, and to establish effective techniques for enhancing their performance through calibration.

In chapter 4, the LCFs were tested under the drop-in calibration, proving it was possible. The engine could be operated without having to modify the reference diesel B7 calibration maps because of the high cetane index of the fuels, which easily allow their autoignition. In terms of the calibration settings under the drop-in scenario, changes in the mass requirements compared to diesel were a product of the fuels having a lower energy density by mass. Given the previously existing calibration of the ECU was done considering diesel B7, it is to be expected that a specific calibration from each of the LCF blends would allow to take more advantage of the distinctive properties of the fuels, particularly for the purpose of emissions reductions and maintaining diesel-like fuel consumption. This chapter centers on the different factors that have an effect over the responses of the engine with the different fuels, evaluating the possibilities from the broadest to the narrowest result of an optimized calibration for each of the LCFs. Each of the different analysis (see Figure 1) provides insights on the nuances of reaching an optimized calibration considering the characteristics of the fuel, until finally the optimization methodology described in Chapter 3 is used to find the calibration settings that provide the best result in terms of fuel consumption, NOx and soot emission while not exceeding the mechanical and efficiency constraints.

The first stage of the analysis allows to quantify the responses of the engine within the limits of the calibration settings, only limiting the available output by the mechanical constraints; these clusters are the available candidates for the optimized LCF operating condition. In the second stage, the scope of the operating conditions and settings are limited by the fixing of the CA50, equalizing the combustion

phasing and allowing to observe the responses assuming that the combustion is similar between the different LCFs. The third stage subsets the points by preserving the same calibration settings between fuels, showcasing the effect within the engine. By fixing conditions on stages two and three, the effects of the fuels can be better isolated, and this is the transversal knowledge generation that could be applied to other engines of the same type. Finally, on the fourth stage, the optimums for each LCF at each operating condition are found and compared to the drop-in calibration and to the diesel B7 operation.

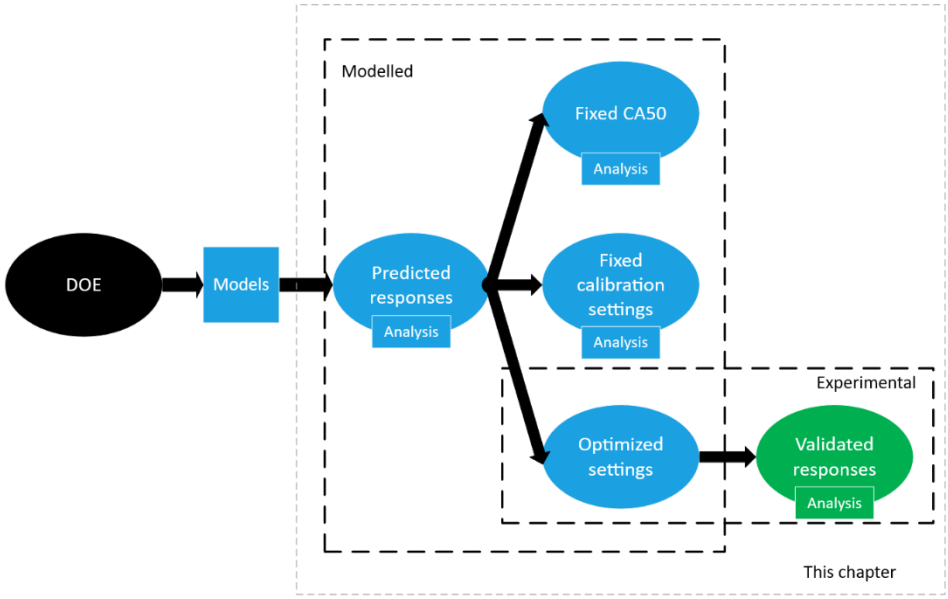

Figure 1. Schematic of the analysis approach of the chapter

To evaluate the responses and optimize the calibration of the engine, adjustments are made to eight key parameters: start of injection (SOI), injection pressure (Prail), volumes (V1 and V2), and dwell times (D1 and D2) for pilot injections, in-cylinder air mass quantity (AirM), and boosting pressure (PBoost). A design of experiments (DOE) approach was employed to identify the most effective combination of these settings, ensuring they meet targets for NOx, soot, load and COV_{IMEP} in terms of the desired outputs from the engine under stationary operation, as well as targets for maximum cylinder pressure (Pmax) and pressure rise rate (PRR) to ensure the safe operation of the engine and reduce the noise, vibration and harshness (NVH) of the engine.

2 Engine responses with DOE modelling

Chapter 3 introduced the DOE methodology as a systematic approach to plan and conduct experimental research efficiently. DOE structures experiments before execution to gather data for later analysis, understanding the relationships among input factors (modified calibration settings) and output responses. When working with quantitative factors in a DOE, regression models are a valuable representation, where the performance of the engine is expressed as a linear combination of calibration parameters. In this study, models were developed for various responses of interest, including NOx, soot, HC, CO, fuel consumption, BTE, and combustion parameters (CA50, CA10, CA90, and torque). And the validation process involved comparing fitted values from the models to experimental values and evaluating the prediction errors.

The developed models are used to represent the optimization space, which refers to the range or set of possible values within which the calibration is explored to later find the optimums. The value range of the calibration parameters is presented in Table 1. It is evident from the table that at different engine operating conditions each of the LCFs have a different minimum and maximum value that can fulfill the constraints presented in Chapter 3. For example, at the 1250 rpm @ 2 bar operating condition the majority of the LCFs have a large SOI range going to early injections near 7 to 10 CAD bTDC to late injections ranging from -6 to -3 CAD bTDC. The LCD100 has a narrower range of calibration for the SOI at that operating condition because the torque output with that fuel was highly sensitive to SOI variation being farther from the top dead center. Something similar occurs with all the calibration parameters, and larger calibration ranges indicate that the fuel is less sensitive to exceeding any of the constraints with that parameter. Regardless, as the fuels can be considered “diesel-like” fuels there is a clear overlap between the range of calibration parameters as the fuels have mostly high autoignition coefficients and relatively small difference in lower heating value (LHV) when compared with other low carbon fuels, like methanol with a CN of ~5 and LHV of 19.9 MJ/kg [1].

Table 1. Calibration ranges for the different fuels at the tested operating conditions

Fuel	Operating condition	LCD100	LCD66	LCD33	Max OME66	Max OME33	R33	RE100
Prail (bar)	1250 rpm @ 2 bar	[245; 350]	[255; 695]	[245; 355]	[270; 435]	[265; 480]	[250; 325]	[245; 405]
	2000 rpm @ 8 bar	[870; 1250]	[695; 1395]	[745; 1255]	[745; 1345]	[595; 1246]	[695; 1345]	[645; 1110]
	1500 rpm @ 14 bar	[545; 1390]	[495; 1090]	[690; 995]	[695; 1095]	[640; 1088]	[785; 945]	[740; 945]
	2000 rpm @ 22 bar	[620; 1565]	[780; 1590]	[780; 1525]	[875; 1475]	[975; 1625]	[885; 1260]	[780; 1350]
	3750 rpm @ max. load	[990; 1980]	[980; 1985]	[1185; 1935]	[980; 1980]	[1305; 1920]	[840; 1990]	[1085; 1910]
SOI (CAD bTDC)	1250 rpm @ 2 bar	[0.0; 3.0]	[-4.0; 10.0]	[-6.0; 5.0]	[-3.0; 7.0]	[-5.0; 11.0]	[-4.0; 7.0]	[-4.0; 5.5]
	2000 rpm @ 8 bar	[0.5; 11.0]	[-2.0; 18.0]	[-1.0; 14.0]	[1.5; 9.5]	[1.0; 14.0]	[2.0; 11.0]	[0.0; 11.0]
	1500 rpm @ 14 bar	[-8.0; 10.8]	[-2.0; 12.0]	[-3.0; 9.5]	[-2.0; 7.5]	[0.0; 9.5]	[-6.0; 10.0]	[0.0; 11.0]
	2000 rpm @ 22 bar	[0.0; 12.0]	[0.0; 11.0]	[2.0; 12.0]	[2.0; 12.0]	[1.0; 11.0]	[5.0; 11.0]	[1.0; 14.0]
	3750 rpm @ max. load	[10.0; 24.0]	[8.0; 23.0]	[12.0; 23.0]	[12.0; 23.5]	[10.0; 23.0]	[12.5; 22.0]	[10.0; 24.0]
PBoost (kPa)	1250 rpm @ 2 bar	[99.8; 105.4]	[99.3; 107.2]	[99.8; 105.6]	[99.0; 104.6]	[99.7; 104.5]	[102.2; 105.2]	[99.7; 105.6]
	2000 rpm @ 8 bar	[153.6; 173.6]	[139.1; 161.2]	[147.8; 160.3]	[149.7; 170.6]	[134.9; 160.1]	[139.5; 168.7]	[141.9; 160.2]
	1500 rpm @ 14 bar	[172.7; 198.0]	[169.9; 193.6]	[165.9; 183.5]	[171.1; 197.7]	[169.8; 189.4]	[161.8; 188.1]	[174.8; 187.6]
	2000 rpm @ 22 bar	[229.8; 258.2]	[219.6; 256.3]	[224.8; 255.4]	[229.9; 257.8]	[225.0; 257.2]	[192.5; 246.5]	[224.9; 257.1]
	3750 rpm @ max. load	[229.4; 256.5]	[219.7; 256.5]	[229.5; 256.4]	[229.5; 257.0]	[225.0; 256.7]	[234.6; 256.1]	[214.9; 256.3]
AirM (mg/cc)	1250 rpm @ 2 bar	[147.6; 283.4]	[187.9; 266.3]	[139.9; 276.4]	[152.0; 295.8]	[151.6; 282.4]	[178.0; 261.7]	[207.5; 280.0]
	2000 rpm @ 8 bar	[398.7; 544.8]	[396.9; 474.9]	[405.6; 502.0]	[417.7; 538.5]	[429.1; 502.1]	[406.8; 470.8]	[417.4; 487.9]
	1500 rpm @ 14 bar	[479.4; 783.0]	[609.3; 733.2]	[604.4; 718.9]	[602.9; 811.5]	[633.9; 761.6]	[609.3; 676.6]	[639.2; 690.4]
	2000 rpm @ 22 bar	[843.8; 921.0]	[819.0; 890.8]	[817.5; 880.8]	[818.5; 882.5]	[840.6; 905.5]	[674.1; 876.0]	[856.6; 961.0]
	3750 rpm @ max. load	[713.6; 829.7]	[679.8; 826.9]	[715.0; 826.4]	[717.2; 808.3]	[717.4; 825.8]	[728.6; 810.1]	[707.9; 857.8]
V1 (mm3)	1250 rpm @ 2 bar	[1.30; 5.00]	[0.90; 2.40]	[1.20; 3.00]	[1.65; 2.20]	[0.90; 2.60]	[0.90; 1.90]	[0.90; 4.00]
	2000 rpm @ 8 bar	[1.00; 3.00]	[1.00; 5.00]	[1.00; 2.80]	[1.00; 2.80]	[1.10; 2.00]	[0.90; 2.30]	[0.90; 4.50]
	1500 rpm @ 14 bar	[1.00; 5.00]	[1.00; 2.50]	[1.00; 4.00]	[1.00; 5.50]	[1.00; 4.00]	[1.00; 3.00]	[1.00; 3.00]

	2000 rpm @ 22 bar	[1.00; 2.20]	[1.20; 2.80]	[1.00; 3.00]	[1.20; 2.50]	[1.20; 3.00]	[1.15; 2.15]	[1.00; 2.70]
	3750 rpm @ max. load	[1.20; 5.00]	[1.50; 5.00]	[1.00; 4.00]	[1.50; 4.50]	[1.20; 4.50]	[1.50; 3.60]	[1.20; 4.50]
D1 (µs)	1250 rpm @ 2 bar	[678; 950]	[650; 800]	[700; 850]	[690; 770]	[700; 880]	[680; 765]	[600; 900]
	2000 rpm @ 8 bar	[650; 1500]	[400; 1000]	[830; 1300]	[750; 1600]	[780; 1200]	[510; 870]	[600; 850]
	1500 rpm @ 14 bar	[700; 1500]	[400; 1500]	[750; 1400]	[500; 1500]	[600; 1600]	[500; 1435]	[500; 1500]
	2000 rpm @ 22 bar	[500; 1700]	[700; 1500]	[600; 1500]	[1000; 1500]	[600; 1600]	[995; 1500]	[700; 1400]
	3750 rpm @ max. load	[500; 1400]	[500; 1500]	[540; 1200]	[500; 1200]	[600; 1500]	[950; 1150]	[600; 1400]
V2 (mm3)	1250 rpm @ 2 bar	[0.90; 3.20]	[0.80; 3.50]	[0.80; 3.00]	[0.80; 1.90]	[0.80; 2.60]	[0.80; 3.00]	[0.80; 4.00]
	2000 rpm @ 8 bar	-	[0.00; 5.00]	-	-	[0.00; 1.30]	[0.00; 2.40]	[0.00; 2.00]
	1500 rpm @ 14 bar	-	-	-	-	-	-	-
	2000 rpm @ 22 bar	-	-	-	-	-	-	-
	3750 rpm @ max. load	-	-	-	-	-	-	-
D2 (µs)	1250 rpm @ 2 bar	[650; 900]	[600; 800]	[700; 900]	[620; 765]	[610; 950]	[630; 790]	[600; 900]
	2000 rpm @ 8 bar	-	[400; 1000]	-	-	[600; 700]	[500; 700]	[400; 1000]
	1500 rpm @ 14 bar	-	-		-	-	-	-
	2000 rpm @ 22 bar	-	-		-	-	-	-
	3750 rpm @ max. load	-	-		-	-	-	-

Figure 2, Figure 3 and Figure 4 show the modelled space for the BSFC, BSNOx, soot and CA50 variables at the 2000 rpm @ 8 bar operating condition, which will serve to explain the general behavior of the different fuels, while Figure 5 shows the relation between the responses at the maximum power setting of the engine. The 3750 rpm @ max. load condition also allows us to observe how the available optimization space is reduced as the load increases. The modelled spaces are created by the combinatory of the calibration parameters at least with 7 levels after, taking a random sample of 900,000 different combinations. The limits of the calibration settings were found during the screening phase described in Chapter 3. The sampled combinations are then evaluated with each of the calibrated models for BSFC, BSNOx, soot and CA50. Then, once the modelled values are obtained, the modelled torque, PRR and peak pressure are confirmed to ensure the conditions reach the necessary power requirements and the safety limits can be fulfilled.

The fuels were grouped by composition, thus LCD fuels (LCD100, LCD66 and LCD33) are within one group, MaxOME fuels (MaxOME66 and MaxOME33) are in another group and R33 and RE100 are grouped together due to their biofuel content. The figures show the pairwise relationship among four variables: BSFC, BSNOx, soot, and CA50. Each variable appears both on the X and Y axes of the scatter plots. The data points (different colors) are grouped according to the fuel type used. The distribution of each fuel for all variables is shown in the main diagonal. The figures also indicate the correlation between each pair of variables for the whole set of fuels (specified as “Corr:”) and each specific fuel (specified by the name of the fuel). In this sense, a strong correlation will be determined by a correlation coefficient between 0.7 and 1 ($0.7 < r < 1$), a moderate one by a correlation coefficient between 0.3 and 0.7 ($0.3 < r < 0.7$), a weak correlation by a correlation coefficient between 0 and 0.3 ($0 < r < 0.3$) and no correlation indicated by 0; depending on the whether the values are negative or positive the correlation will be negative or positive. The stars (*) shown in the figures represent statistical significance levels with more stars indicating a very low p-value.

The calibration ranges described in Table 1, were controlled during the experiments. The EGR is not a directly controlled parameter, however it is a consequence of the variation of the air mass parameter and the boost pressure. The effects of the EGR on the emission control of ICEs, the fuel consumption and the combustion phasing are extensively discussed [2, 3, 4]. EGR lowers peak combustion temperatures and reduces the oxygen concentration of the intake air. Considering this, due to the differences in calibration settings, particularly the airmass and the boost pressure, it is expected that the EGR will vary as well, and it will play a significant role in the variation of the responses being studied. This observation was confirmed during the

experiments as the lower air mass requirements and lower boost pressures increased the EGR percentage, and with that greatly improved the NOx emissions. For the LCD fuels these observations have been previously stated in published work by the author [5]. It is also true that at lower loads the EGR quantities are proportionally higher, and thus the effect of the different fuels is in fact not as evident due to the EGR quantities define the combustion phasing.

2.1 Low-to-medium-load engine performance

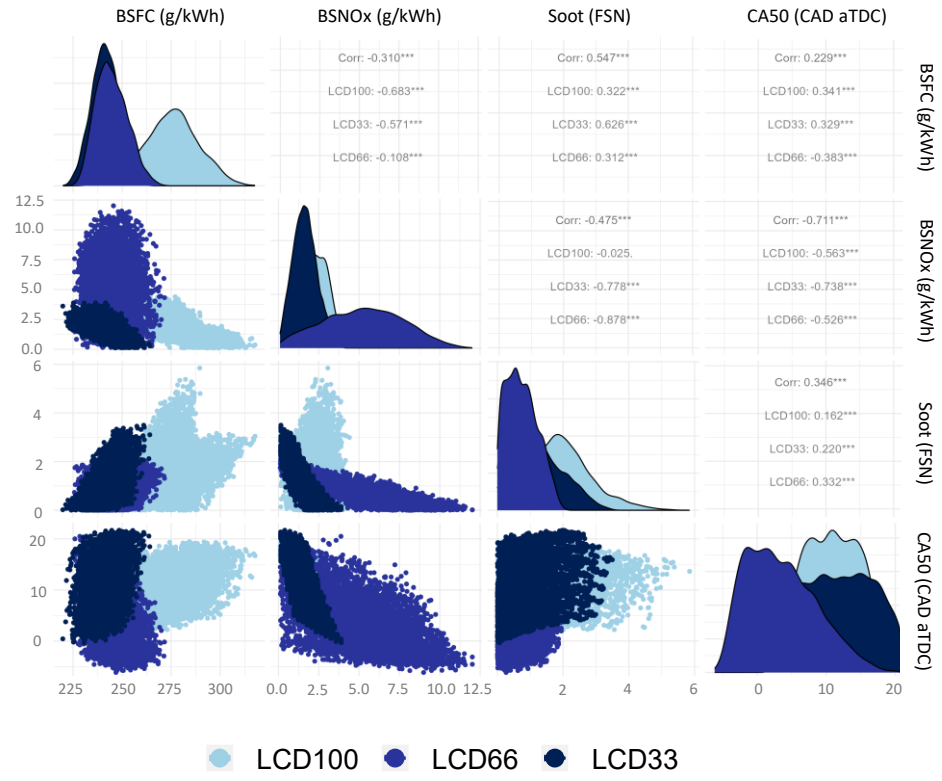

Figure 2. Correlation matrix of the optimization space for the BSFC, BSNOx, Soot and CA50 for the LCD100, LCD66 and LCD33 fuels at the operating condition 2000 rpm @ 8 bar. Significant values are represented as *p<0.05, **p < 0.01, ***p<0.001.

The LCD group of fuels has a tri-component composition of OMEx, Fischer-Tropsch (FT) diesel, and fossil diesel (in the case of the LCD66 and the LCD33). For the LCD group in Figure 2, the median fuel consumption of LCD100 makes a dramatic increase compared to the LCD66 and LCD33 although for the operating condition all three fuels can reach values as low as 225 g/kWh. The higher overall

BSFC for the LCD100 can be explained by the difference in its LHV. In terms of correlations with the BSFC, there is a moderate correlation with the BSNOx, soot and CA50 for the LCD100 and LCD33 fuels, while the LCD66 has a low correlation between the BSNOx and the BSFC. Additionally, the median BSNOx is nearly 4 g/kWh higher than for the other two fuels. The low correlation and larger NOx for the LCD66 is evidenced by the more symmetrical distribution of the emissions which might have originated from a combination of the large range of calibration parameters seen in Table 1 allowable with this fuel.

The relation between the BSNOx and soot emissions is decidedly strong for the LCD33 and LCD66, and the range for soot emissions does not surpass 4 FSN. The LCD100, on the other hand, has a higher maximum range of soot emissions, while the BSNOx emissions are mostly contained below 5 g/kWh. Although the LCD100 has the highest possible soot emissions, the NOx-soot tradeoff of the fuel is the most favorable with more values in the lower range for both pollutants. In relation to the CA50, at this operating condition correlations are rather moderate. LCD100 and LCD33 show a minimum CA50 of 0° bTDC, while the earlier injection limit for the LCD66 in tandem with its higher CN allow the combustion to be phased earlier. This 2-D model representations show in advance how after optimizing the resulting point will be below the 2 g/kWh mark for BSNOx and the under 1 FSN mark for soot, while at the same time maintaining a fuel consumption under 250 g/kWh.

While in Figure 2 there was a strong overlap in the fuel consumption between the LCD fuels, no such overlap is observed for Figure 3 in the BSFC. In fact, when observing the BSFC-BSNOx trade-off it is seen that for a given value of BSNOx, the maximum BSFC for the MaxOME33 is the minimum BSFC for the MaxOME66. Following the logic where the LHV explains this difference is a good starting point as the MaxOME33 has a LHV of 39.55 MJ/kg while the MaxOME66 has a LHV of 38.24 MJ/kg. Nonetheless, if this were the only reason for the difference in fuel consumption, the difference between the LCD fuels would be larger (difference between the maximum and minimum LHV of the LCD group is 2.81 MJ/kg, which is larger than the difference of 1.31 MJ/kg of the MaxOME fuels). Because of this, it makes sense to also look at the oxygen content and the CN to further explain the fuel consumption because of changes in the combustion.

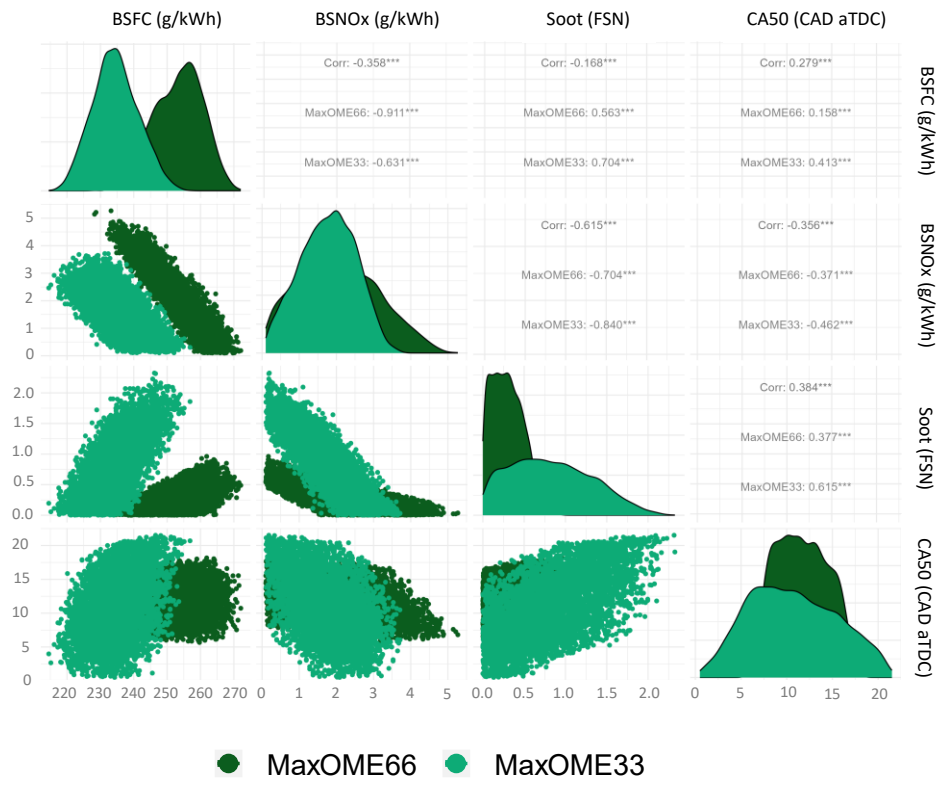

Figure 3. Correlation matrix of the optimization space for the BSFC, BSNOx, Soot and CA50 for the MaxOME66 and MaxOME33 fuels at the operating condition 2000 rpm @ 8 bar. Significant values are represented as *p<0.05, **p < 0.01, ***p<0.001.

Soot emissions for the MaxOME fuels, due to its high proportion of OMEx and the imposed calibration limits, is low across all operating conditions. In the observed 2000 rpm @ 8 bar, the emissions reach a maximum of 2 FSN and the higher proportion of oxygen in the MaxOME66 seen to have a positive effect in reducing the soot emissions. BSNOx emissions for the MaxOME33, nonetheless are lower, mainly in the cases where the combustion occurs earlier. The range of CA50 for the MaxOME66 is comparatively more reduced, going from 5 to 15 CAD aTDC, compared to the 0 to 20 CAD aTDC of the MaxOME33.

Figure 4. Correlation matrix of the optimization space for the BSFC, BSNOx, Soot and CA50 for the R33 and RE100 fuels at the operating condition 2000 rpm @ 8 bar. Significant values are represented as *p<0.05, **p < 0.01, ***p<0.001.

Comparing the R33 and the RE100 in Figure 4, although the lower limit of the BSFC for the operating condition is the same for both fuels R33 has a higher BSFC and higher BSNOx emissions, while both fuels have a similar distribution of the CA50 and soot emissions. These two fuels are the most dissimilar of the compared groups, with RE100 having a CN of 83.5 and the R33 of 59. Thus, if the CN is a typical indicator of the autoignition capability of a fuel, it could be expected that the RE100 with a higher CN, would have an earlier combustion, yet this is not the case: the median CA50 of the R33 is between 5 and 10 CAD aTDC while for the RE100 the median is at a later timing. These two fuels also have a difference in the oxygen proportion, with the R33 being close to the fossil diesel reference at 0.76%m/m while the RE100 has a 2.16 %m/m. In this case, the difference in the oxygen level could compensate the apparent difference in the CN, with the larger oxygen content

promoting a less rapid combustion that can burn slowly, which in turn can explain the small benefits in soot and NOx, as the oxygen likely decreases the combustion temperature (reducing NOx) and allows a more favorable mixture in the cylinder even in the regions with high fuel concentrations as the fuel has its own oxygen content.

2.2 High-load engine performance

As the load increases, the range of calibration settings that can maintain the safety constraints and the operation range of components like the turbocharger and the common-rail is reduced. Because of this, the calibration at maximum load operating conditions is defined in part for the mechanical limits of the engine. Figure 5, shows the pairwise relations between the selected responses for the 3750 rpm @ max. load operating condition. At this load the BSFC-BSNOx-Soot tradeoffs are considerably closer to a line described, with a strong negative correlation between each for all the studied LCFs. At this load the extensively reported NOx-soot tradeoff of diesel engines can be observed, with most of the fuels reaching a NOx emission of nearly 5 g/kWh when the soot emissions reach a value of 1 FSN, being the fuel with the most favorable emission outcome at the load condition the LCD66 which can reach emissions as low as 2 g/kWh at the 1 FSN level.

One possible explanation for this is the fact that at a higher LHV the fuel mass necessary to reach the operating condition is smaller; thus, a more favorable air-to-fuel ratio (AFR) can be reached without the need to increase the air demand and put the turbocharger (which at this operating point is working at its limits) under more strenuous conditions. In the fuel properties table in Chapter 3, it can be seen how the fuels that have a higher oxygen proportion in their composition have lower stoichiometric AFR (AFR_{sto}), which at lower loads improves the efficiency of the charge renewal system allowing to somewhat mitigate the increase of the fuel consumption product of a higher LHV as the turbine needs to produce less work because the air demand is lower. However, at full load the engine needs a large mass of fuel to reach the necessary torque, thus in this condition the equivalence ratio is richer for the OMEx containing fuels and the turbine experiences higher losses as the air mass demand needs to increase to optimize the AFR.

Similar soot values can be reached with RE100 and R33, the fuels that contain OMEx (all the fuels in the LCD and MaxOME groups) have significantly reduced soot emissions (~3 FSN) compared to the ones that do not contain OMEx. Although there are differences between all the fuels in terms of consumption and emissions the CA50 values remain consisted for the operating condition, where maintaining

the value between 5 and 25 CAD aTDC avoids undesirable effects like an extreme PRR and peak pressures above 180 bar.

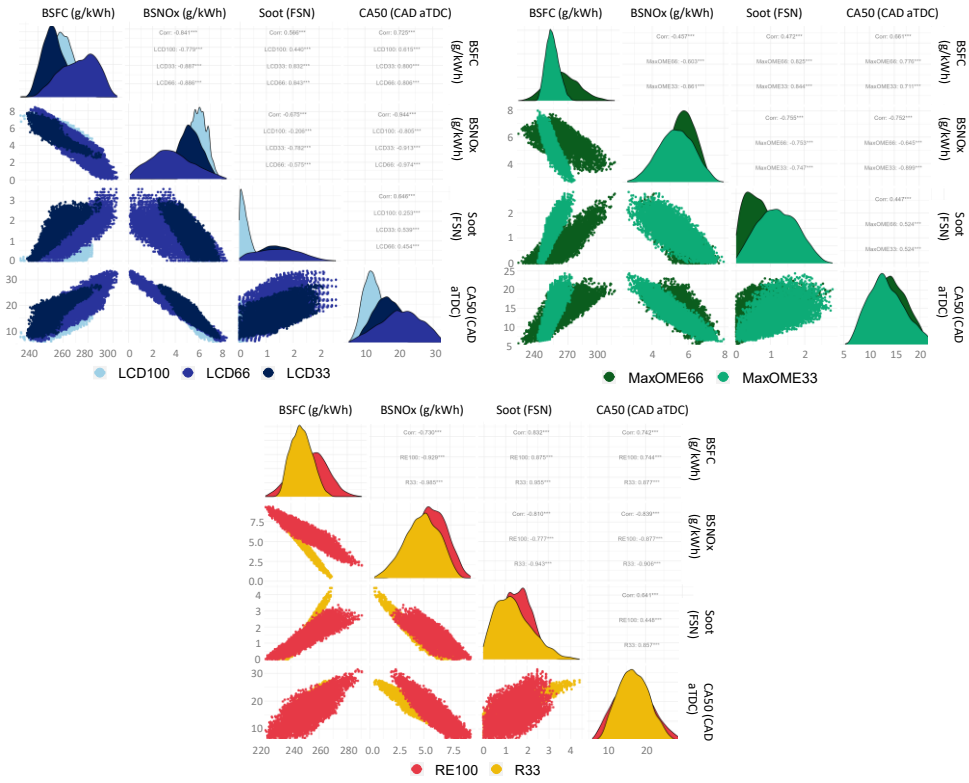

Figure 5. Correlation matrix of the optimization space for the BSFC, BSNOx, Soot and CA50 at the operating condition 3750 rpm @ max. load. Significant values are represented as *p<0.05, **p < 0.01, ***p<0.001.

Notably, the seven LCFs can reach BSFC values that are comparable to diesel, showing some of the advantages of using fuels that are close to diesel both in terms of the autoignition capabilities and that can achieve the EN 590 and ASTM D 975. While the variations, operational limits, and benefits in terms of emissions are linked to the characteristic properties of each fuel, having again highlighted the benefits in terms of emissions of using oxygenated fuels. Although the areas for the different responses generated by the models are useful to see the general performance of the fuel, they provide a too general comparison where the specific potential of the fuel is not easily observed at the lowest BSFC-BSNOx-soot condition. This topic will be addressed in the following sections by means of equalizing the CA50, as well as the setting for the different fuels. The fuels with higher LHV, like the RE100 and the

R33, have a smaller lower limit of BSFC, without necessarily increasing too much either the NOx or soot emissions compared with the other fuels.

3 Fixed combustion phasing analysis

Keeping the whole range of operation of the modelled LCFs provides too broad a comparison and does not allow us to directly explain all the differences in the combustion of the fuels because all the fuels have both different setting and combustion phasing. For this reason, in this section the CA50 at each operating condition is fixed. The idea behind this is ensuring the combustion of the fuels have a similar phasing, and thus the effects on the other responses (fuel consumption, NOx and soot) will not be affected by the size of this effect. Table 2 shows the selected CA50 for each operating condition, which has an admissible span of 2 CAD.

Table 2. Selected CA50 range for each operating condition

Operating condition	CA50 range (deg aTDC)
1250 rpm @ 2 bar	9-11
2000 rpm @ 8 bar	9-11
1500 rpm @ 14 bar	14-16
2000 rpm @ 22 bar	14-16
3750 rpm @ max. load	14-16

3.1 Fuel consumption impact

To observe the effect of the fuels at constant CA50 conditions, boxplots are used as a visualization tool to explore the distribution of the BSFC, BSNOx and soot. Figure 6 shows the distribution of the BSFC. In the plot, the box represents the interquartile range (IQR), which contains the middle 50% of the data. The bottom edge of the box is the Q1 (25th percentile), and the top edge is the Q3 (75th percentile). The whiskers extend from the box to the minimum and maximum values within a certain range. This range is typically calculated as 1.5 times the IQR. Any data points beyond the whiskers are considered outliers and are plotted individually as points.

In Figure 6 as the OMEx content in the fuels increased, so did the BSFC. This relationship can be attributed to the fact that fuels with higher OMEx concentrations tend to exhibit lower LHVs due to oxygenation. Consequently, these oxygenated fuels necessitate a larger volume to produce the same power output, resulting in elevated BSFC values. However, intriguingly, we observed an exception at the lowest load operating condition with MaxOME33, where it deviated from the expected behavior compared to MaxOME66. This anomaly might be attributed to unique combustion properties of MaxOME33 under these specific conditions, potentially the larger aromatic content (a reduction of CN) of the MaxOME33 can play a role in the reduction of the fuel economy by increasing the combustion delay as has been reported to occur [6, 7].

A significant reduction in BSFC occurred when fuels had lower OMEx content, particularly in the RE100 and R33 fuels. This reduction is consistent with the overarching principle that fuels with lower OMEx content possess higher energy content, translating to reduced fuel consumption in the CI engine. These findings underscore the advantages of using fuels with properties more akin to traditional diesel fuels, supporting their potential as viable alternatives for CI engines.

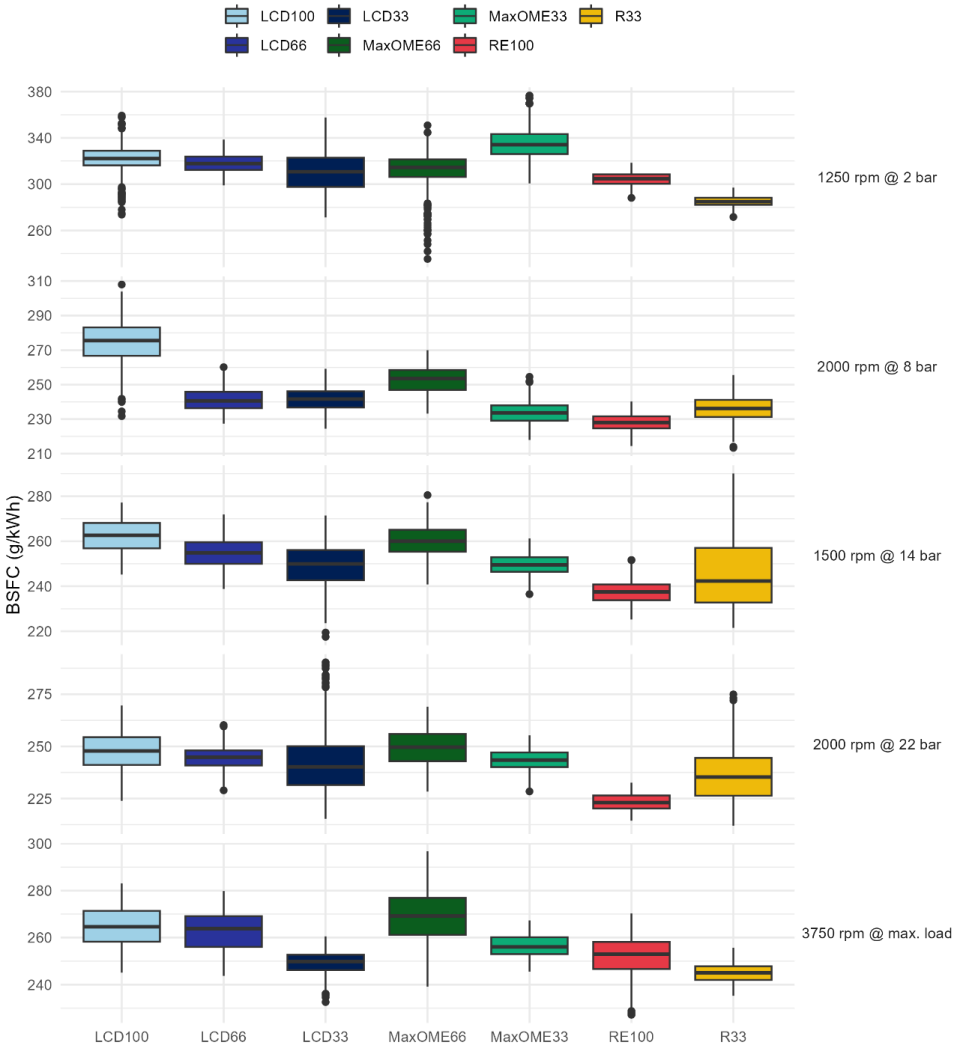

Figure 6. BSFC at different loads under fixed CA50 values

3.2 NOx emissions impact

The NOx emissions results with fixed CA50 are not as straightforward as the fuel consumption, and do not seem to provide a clear trend by fuel. For most operating conditions, the fuels that contain OMEx have a similar Q1 limit (with some exceptions in the LCD66 fuel), while RE100 and R33 can have either higher or lower values depending on the operating condition. Typically, delaying the CA50 to reduces the combustion temperature [8] especially when delaying the CA50 by means of increasing the EGR [9]; this can limit the thermal NOx pathway.

In this study, to maintain the same CA50 for the different fuels the input conditions of the model are then changed to achieve this goal. In that sense, to equate the on average earlier CA50 of the LCD100 and the R33 to the later average values of the other fuels, most of the conditions to reach the target CA50 for the LCD100 and R33 have a larger preference for lower intake air masses and lower injection pressures; however as the fuels are significantly different between them, the median NOx emissions for R33 is higher at lower loads while at higher loads, as the LCD100 needs large intake air masses to reach an appropriate AFR the benefit in NOx emissions of having larger EGR quantities and colder combustions is not perceived.

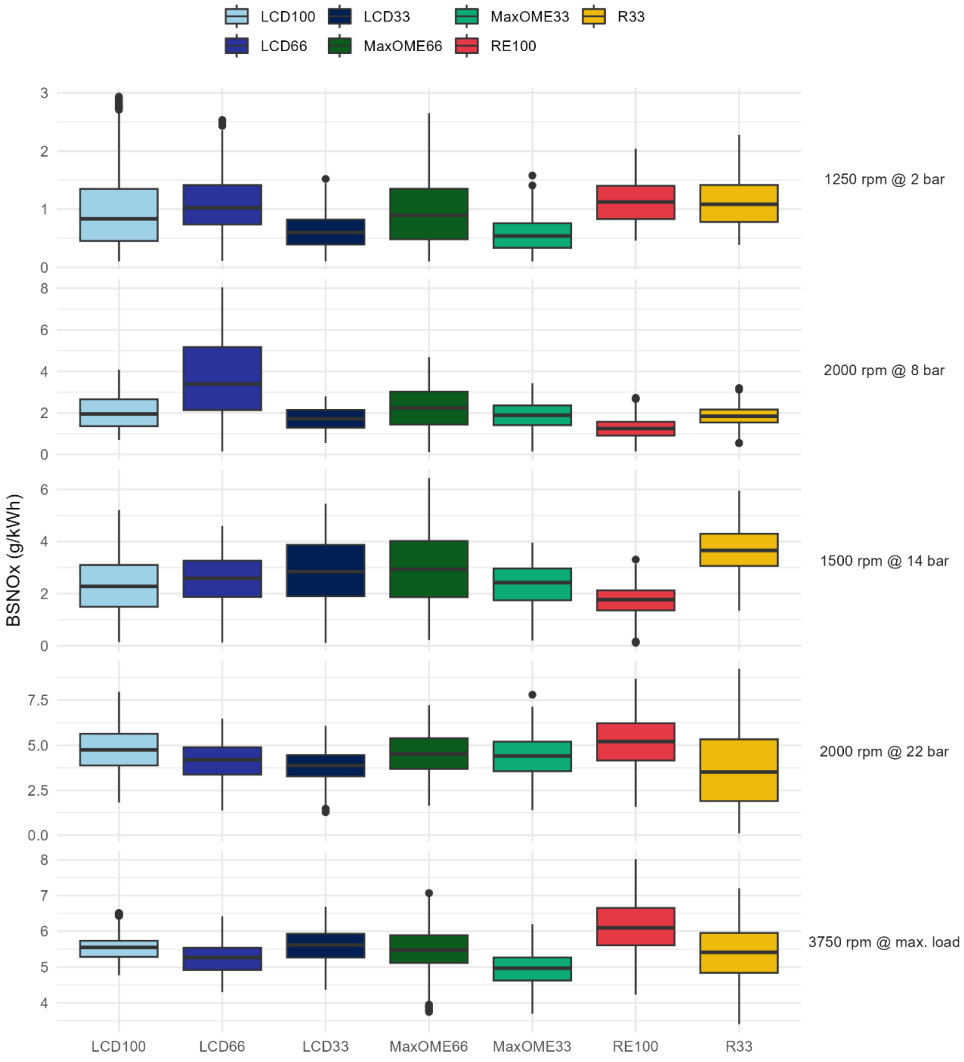

Figure 7. BSNOx emissions at different loads under fixed CA50 values

3.3 Soot emissions impact

Soot emissions at fixed CA50 values are compared in Figure 8. Apart from extreme cases, there is no discernible advantage in terms of soot emissions at fixed CA50 when comparing oxygenated and less oxygenated fuels, especially when they contain several proportions of OMEx. The variations in soot emissions across different fuels exhibited a significant overlap, spanning a range of over 2 FSN for all fuels and operating conditions. This extensive overlap in soot emissions underscores the complexity of the combustion process and the multitude of factors at play.

It has been reported how soot emissions increases as the CA50 is delayed [10]; the combustion tends to be more diffusive and there are regions in the cylinder with extremely high equivalence ratios. The delay in CA50 is indicative of a more diffusive combustion process, characterized by regions within the cylinder experiencing extremely high equivalence ratios. These fuel-rich regions are susceptible to incomplete combustion due to oxygen limitations. When the CA50 is held across all fuels, the different calibration parameters have a significant impact on the soot emissions. The wide range of calibration settings capable of achieving the same CA50 value contributes to the substantial variability in soot emissions observed for most fuels, ranging from as low as 0 FSN to as high as 7 FSN. Notably, the fuel with the highest oxygen content and the lowest carbon content, namely MaxOME66, consistently exhibited the lowest median soot emissions. This can be attributed to the fuel's ability to achieve a balanced combustion process, even under conditions of lower air mass, leading to more complete oxidation and reduced soot formation.

Building upon the comparison between LCD100 and R33 fuels, which was originally highlighted for the NOx emissions section, elucidates the relationship between extreme differences in fuel properties and soot emissions. As anticipated, the R33 fuel exhibits greater soot emissions in contrast to the LCD100 fuel. This difference can be primarily attributed to the lower carbon content of the LCD100 fuel, which necessitates less oxygen for the complete oxidation of its molecules during combustion, even in regions of the cylinder with higher concentrations of fuel. The inverse relationship between carbon content and soot emissions underscores the critical role of fuel composition in shaping the combustion process and its emissions characteristics, emphasizing the potential for tailored fuel formulations to mitigate soot formation in internal combustion engines.

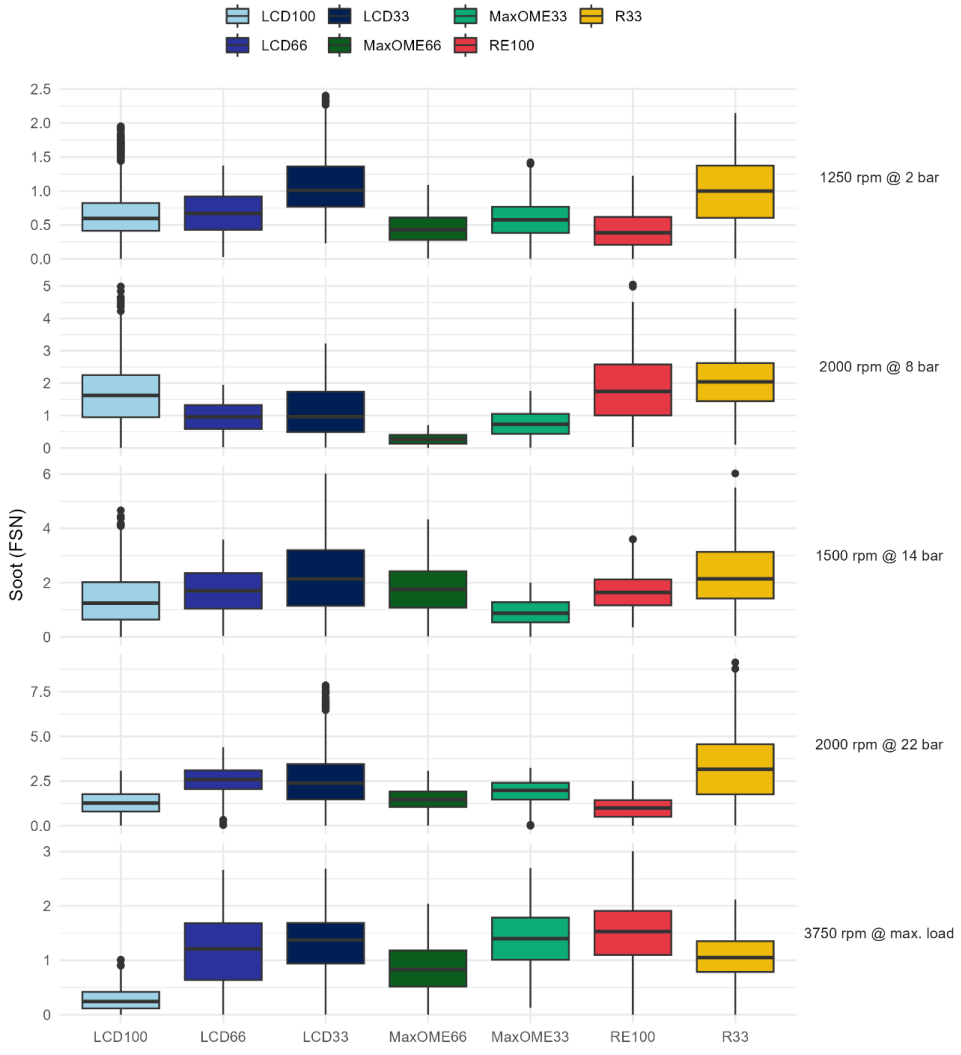

Figure 8. Soot emissions at different loads under fixed CA50 values

4 Fixed calibration settings analysis

Having validated linear models for all the operating conditions and all the tested LCFs allows us to compare the responses of the engine under different controlled scenarios. One of such scenarios is the iso-setting comparison, which allows to account for the effect of the engine calibration on the different responses of interest. This approach was proposed in the 2022 work by the author in SAE Powertrains, Fuels & Lubricants Conference & Exhibition [11].

Table 3. Iso-setting calibration setting levels.

Setting	1250 rpm @ 2 bar	2000 rpm @ 8 bar	1500 rpm @ 14 bar	2000 rpm @ 22 bar	3750 rpm @ max. load
Rail Pressure [bar]	-30; 0; +30	-60; 0; +60	-200; 0; +100	-350; 0; +350	-500; 0; +500
SOI [deg aTDC]	-3.5; 0; +3.0	-2.5; 0; +2.5	-2; 0; +2	-2.5; 0; +2.5	-5; 0; +5
Air [mg/cc]	-25; 0; +25	-25; 0; +25	-20; 0; +20	-20; 0; +20	f(Boost)
Boost [kPa]	-2; 0; +2	-5; 0; +5	-5; 0; +5	-10; 0; +10	-12.5; 0; +12.5
Total cases [-]	81/fuel	81/fuel	81/fuel	81/fuel	27/fuel

An iso-setting approach aims to isolate the effects of the fuels themselves, disregarding variables like injection settings and intake air conditions that could introduce complications. Given that optimal calibrations for injection timing and AFR differ across fuels due to distinct physical and chemical properties (fuel properties in Chapter 3), three tiers of rail pressure, SOI, intake air mass, and boost pressure are used in this study. Consequently, all feasible combinations of these

parameters are explored, resulting in 81 cases for each fuel and operational circumstance except for the 3750 rpm @ max. load point, where 27 cases are established for each fuel due to the air mass quantity being contingent on the boost pressure. Table 3 reflects the distinct levels associated with each iso-setting combination, while Figure 9 represents a simplified schematic of the parameter combinatory process.

Although the pilot injections were varied during the DOE process described in Chapter 3, to prevent an exponential surge in the number of case permutations, and considering their relatively lesser influence compared to the aforementioned factors, the pilot injection quantities and dwell times are held constant.

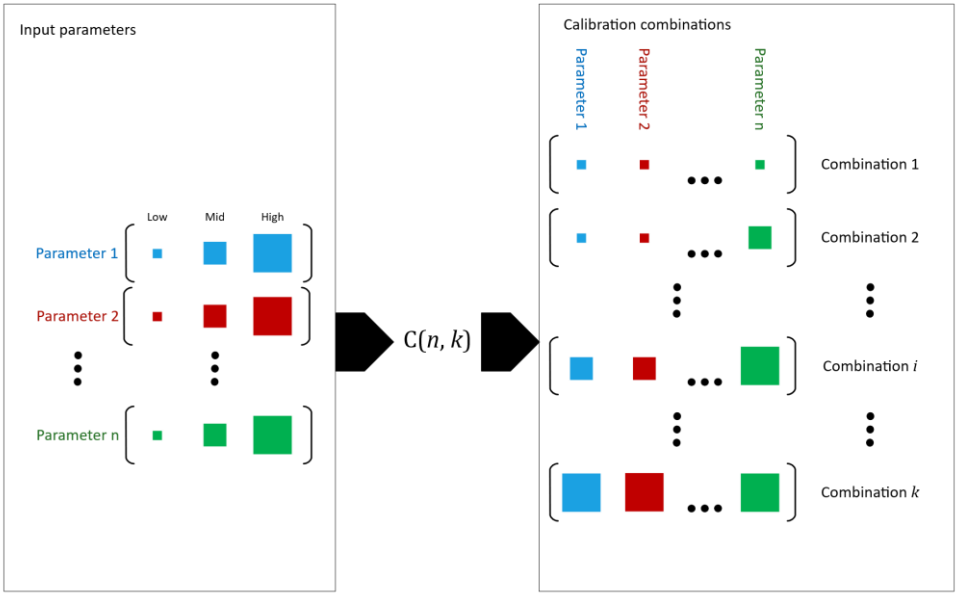

Figure 9. Schematic of the combinatorics used during the iso-settings analysis

4.1 Required fuel mass

It was mentioned in Chapter 3 that during the DOE the fuel mass was kept constant to avoid incorporating the effect of the fuel demand into the experiments analysis. As one of the constraints shown in Chapter 3 is the load, the maximum level for each operating condition is given by the maximum setting value obtained with the lowest setting value LCF that would allow to remain within the load limits at constant fuel mass (determined experimentally). A similar condition was applied to determine the minimum level of each of the calibration settings.

Figure 10 shows the effect of the LHV, cetane number (CN), density, viscosity, total aromatics and O-C ratio in the fuel mass levels for each operating condition. It is well known at this point that the LHV is one of the determining factors in the quantity of fuel necessary to reach a specific load at a given speed. The trend for higher LHV resulting in lower fuel masses is easily observable in the figure, especially at the high engine loads. The LHV represents the amount of energy released when a unit mass of fuel is completely burned under constant pressure conditions, and the combustion products (such as water vapor) are allowed to condense to their liquid state, thus it is a measure of the energy density of the LCFs, which explains why the trend is more noticeable when the engine's power output is higher.

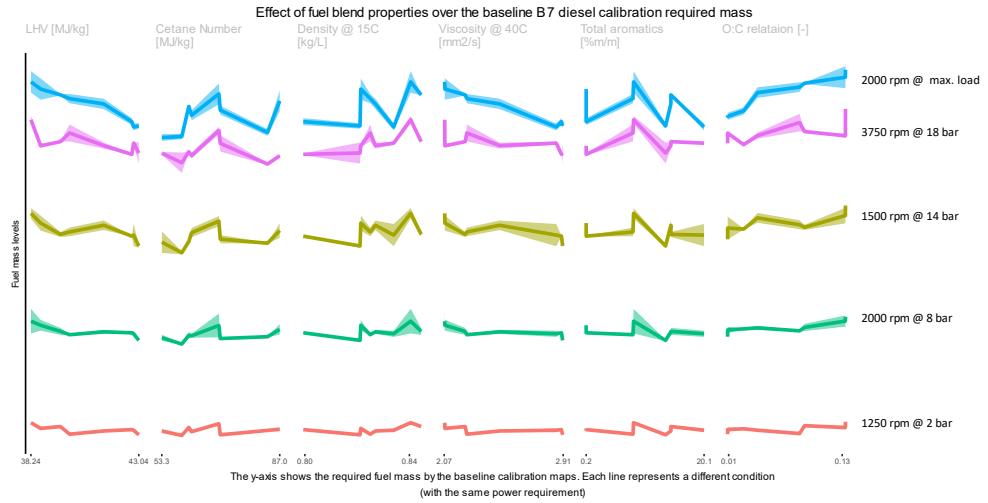

Figure 10. Effect of fuel blend properties over the normalized required fuel mass at different engine conditions

In Figure 10, trends are also observed for the viscosity and the O-C relation, where the viscosity is effect on the fuel mass is extremely similar to the LHV's. This can be explained by the O-C proportion, as fuels with higher O-C have higher oxygen proportions and thus lower carbon content. The viscosity of a fuel is primarily influenced by its chemical composition and molecular structure [12], a lower carbon content can change the size and shape of its molecules, thus with lower carbon content generally have smaller and simpler molecules which can move more freely past each other, leading to lower friction and thus lower viscosity. Similarly, a larger oxygen proportion content fuels generally have lower LHVs because the oxygen contributes to the overall mass of the fuel without adding as much energy.

At lower loads, the trends are not seen as constant because of the combustion stoichiometry, which again, can be linked to the O-C proportion of the fuels. In fuels with oxygenated compounds, the oxygen can participate in the combustion process and affect the overall stoichiometry (ratio of fuel to oxygen) required for complete combustion. This can influence the heat released during combustion allowing for fuels with lower LHV, but higher O-C to have lower fuel consumption in some cases (in combination with other properties like the CN and the aromatic content).

4.2 Fuel consumption impact

Figure 11 illustrates the impact of fuel blend properties on the BSFC across the five examined operating conditions. Absolute differences are used to express the results. Each of the grey lines represents a combination of iso-settings, while a bolder black line indicates the linear correlation. The corresponding correlation coefficients are also depicted within the figure.

Upon initial inspection, regardless of the engine´s power target, a negative correlation between LHV and BSFC is evident. However, this correlation is notably weak (-0.21) at the 3750 rpm @ max. load condition. This reduction in correlation strength is believed to stem from the tradeoff between LHV and oxygen proportion in the fuel. At this specific operating condition, fuels with higher oxygen proportions benefit from improved combustion due to the capacity for better oxidation, particularly in A/F mixing scenarios.

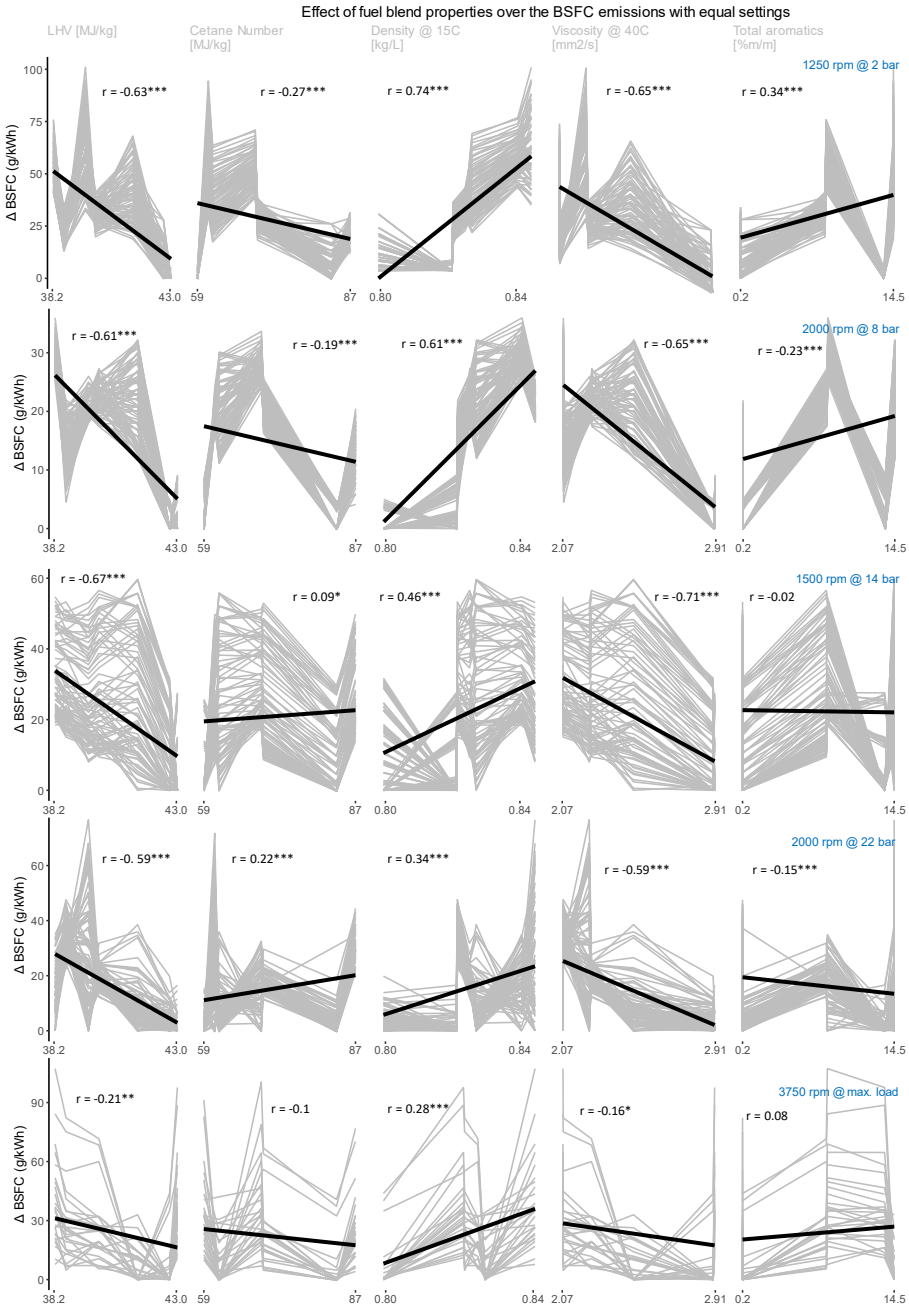

Figure 11. Effect of fuel blend properties over the BSFC at different engine conditions for cases with equal settings. Significant values are represented as *p<0.05, **p < 0.01, ***p<0.001.

For the CN, linear correlations with BSFC are notably feeble (below 0.2), and their direction varies depending on the operating condition. Analyzing the iso-setting lines, particularly at low and medium loads, it is apparent that fuel consumption rises when the CN falls within the range of 59 to 71, and it decreases beyond that threshold. However, testing a broader array of cetane numbers within those ranges is necessary to adequately validate this hypothesis.

The pattern associated with the aromatic content effect is similar. The weak correlations here can be attributed to substantial variations, such as over 20 g/kWh for the same 0.2 %m/m aromatics content of LCD100 and RE100, as well as 14.5 %m/m of MaxOME33 and LCD33. This would indicate that the fuel's aromatic content will not play a hugely significant role in the BSFC of the engine.

Contrastingly, the impact of density on BSFC exhibits a stronger correlation compared to the other considered factors. This correlation remains positive across all engine operating conditions, which might appear counterintuitive. Yet, considering that denser fuels (MaxOME33 and MaxOME66) possess lower LHV values, the direction of this relationship potentially finds explanation. An intriguing observation is how the correlation coefficient decreases as engine power increases. One conceivable hypothesis for this phenomenon is that at lower loads, characterized by lower injection pressures and less turbulent in-cylinder conditions, higher fuel density curtails fuel penetration into the cylinder [13] more than in the case of lower density fuels.

Figure 12 shows the BSFC distributions for the LCF blends with iso-settings. In the presented charts, quartiles (defining the box boundaries), the median (depicted as a horizontal black line within the boxes), and the range encompassing maximum and minimum data values (represented by vertical whiskers) are included. The charts are organized in ascending order, so fuels positioned further to the left exhibit lower values. Notably, a horizontal dashed line marks the reference diesel value with the baseline B7 ECU calibration.

In Figure 12, the expected trend emerges, fuels with higher LHV generally exhibit lower BSFC, aligning with the previously observed strong correlation between this property and fuel consumption. This trend is particularly evident in the case of R33 and RE100, which consistently demonstrate lower fuel consumption values, sometimes even surpassing those of the diesel reference. This trend might be weakly linked to the presence of FAME, which tends to increase the CN [14] potentially increasing the combustion efficiency; and the lower density of these fuels which slightly reduces the fuel mass for the same volume. An exception occurs in the 3750 rpm @ max. load operating condition for R33 diesel, where its fuel consumption is

higher than that of other samples. Considering the prior results (Figure 11), which indicated weak correlations between individual variables and engine load/speed, this anomaly is likely tied to a combination of factors. These factors include slightly lower CN, diminished oxygen content proportion, and marginally higher viscosity of the fuel. These aspects contribute to a delayed start of combustion, generating localized richer zones that slow down combustion, alongside an injection spray that lacks diffusion. These combined effects hinder the achievement of the same efficiency as seen with other fuels.

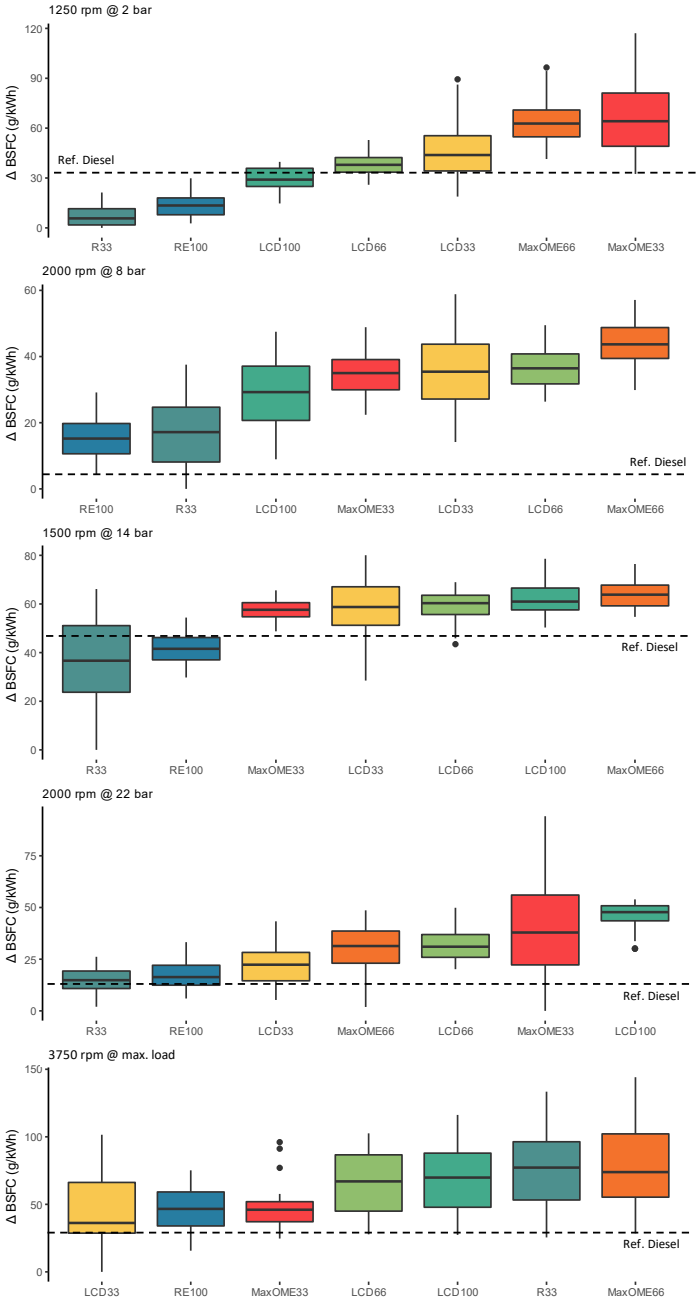

Figure 12. BSFC at different engine conditions with equal engine settings.

4.3 NOx emissions impact

The impact of fuel properties on BSNOx emissions is illustrated in Figure 13. Notably, correlations between various fuel properties and BSNOx emissions are either weak or absent. This phenomenon can be partly attributed to the emission constraints outlined in Chapter 3, which restrict the achievable emission ranges. Although the iso-settings criterion is employed to mitigate this limitation and highlight inter-fuel effects, even under the same calibration, resulting NOx emissions appear to lack a clear dependence on any single fuel property.

NOx emissions in ICEs are influenced by a combination of fuel properties rather than a single property due to the complex and interdependent nature of the combustion process. The combustion of fuel in an engine involves a series of chemical reactions that are affected by various factors, which in turn can be influenced by the properties of the fuel. For example, the stoichiometric A/F ratio will change depending on the fuels' oxygen content, and in combination with the calibration this can lead to leaner mixtures which can reduce the combustion temperature, leading to lower NOx [15]. Contrarily, excessive oxygen availability can also lead to higher flame temperatures and increased NOx formation [16]. Further exploration into chemical kinetic modelling of the fuels could offer deeper insights into their individual effects on NOx emissions.

The iso-setting lines effectively demonstrate how changes in calibration influence BSNOx variations. These calibration changes lead to a range of BSNOx variation for the same fuel and operating condition, extending from 0.25 g/kWh at low loads to more than 4 g/kWh in scenarios like the 1500 rpm @ 14 bar operating condition. Markedly, BSNOx emissions exhibit high sensitivity to changes in injection pressure – both increases and decreases – and demonstrate a reduction in NOx emissions as the SOI is delayed. The variation in injection pressure plays a pivotal role in influencing NOx emissions. When injection pressure is increased, there is a propensity for more efficient atomization and mixing of the fuel with air. This enhanced atomization promotes a more complete combustion process, which, under certain conditions, can lead to higher combustion temperatures. These elevated temperatures can subsequently result in increased production of NOx. Additionally, when the SOI is delayed – meaning that the fuel injection occurs closer to the top dead center (TDC) of the piston's compression stroke – there is more time for air-fuel mixing to take place before ignition. This extended mixing duration results in a more homogeneous mixture in the combustion chamber. Consequently, when ignition occurs, the combustion process is distributed more uniformly, leading to lower peak temperatures and subsequently reduced NOx formation.

Figure 14 provides insight into the BSNOx distribution for the LCF blends. Due to the imposed testing limitations, the majority of LCF blends tend to exhibit lower BSNOx emissions compared to the reference diesel across most load conditions. However, an exception arises at the 1500 rpm @ 14 bar operating condition, where the median value diverges from this trend. Nevertheless, the 25th quartiles of most fuels remain below that of diesel for this emission metric, and all minimum values are lower than diesel.

Despite the lack of significant correlations observed when scrutinizing individual fuel properties, a discernible classification emerges in Figure 14. Specifically, MaxOME33, LCD33, and RE100 (in that sequence) tend to occupy positions with the lowest NOx emissions for various operating conditions, excluding the 3750 rpm @ max. load scenario. Discrepancies in the primary fuel compositions of the three mentioned LCF blends, impede making assertions about direct causal relationships with NOx emissions. Instead, these observations prompt a deeper exploration of the chemical mechanisms governing combustion.

Furthermore, the distribution of NOx emissions for the 3750 rpm @ max. load condition exhibits substantial similarity across fuels. Only the RE100 fuel displays significant deviations towards higher values. This could potentially be attributed to the combination of a relatively higher CN and a high LHV in RE100, which may lead to elevated diffusion combustion peaks. This pattern is not replicated in the case of LCD100.

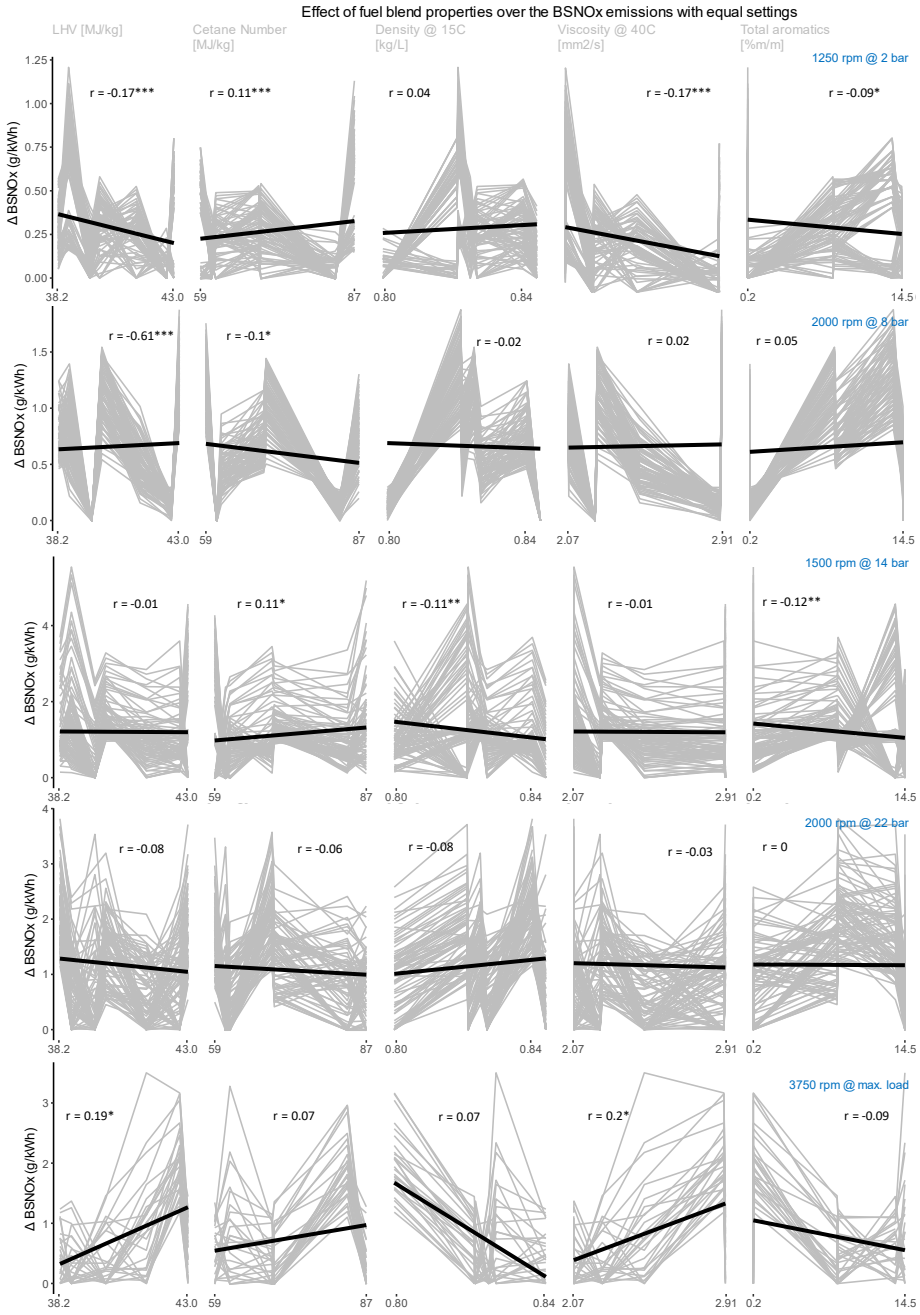

Figure 13. Effect of fuel blend properties over the BSNOx at different engine conditions for cases with equal settings. Significant values are represented as *p<0.05, **p < 0.01, ***p<0.001.

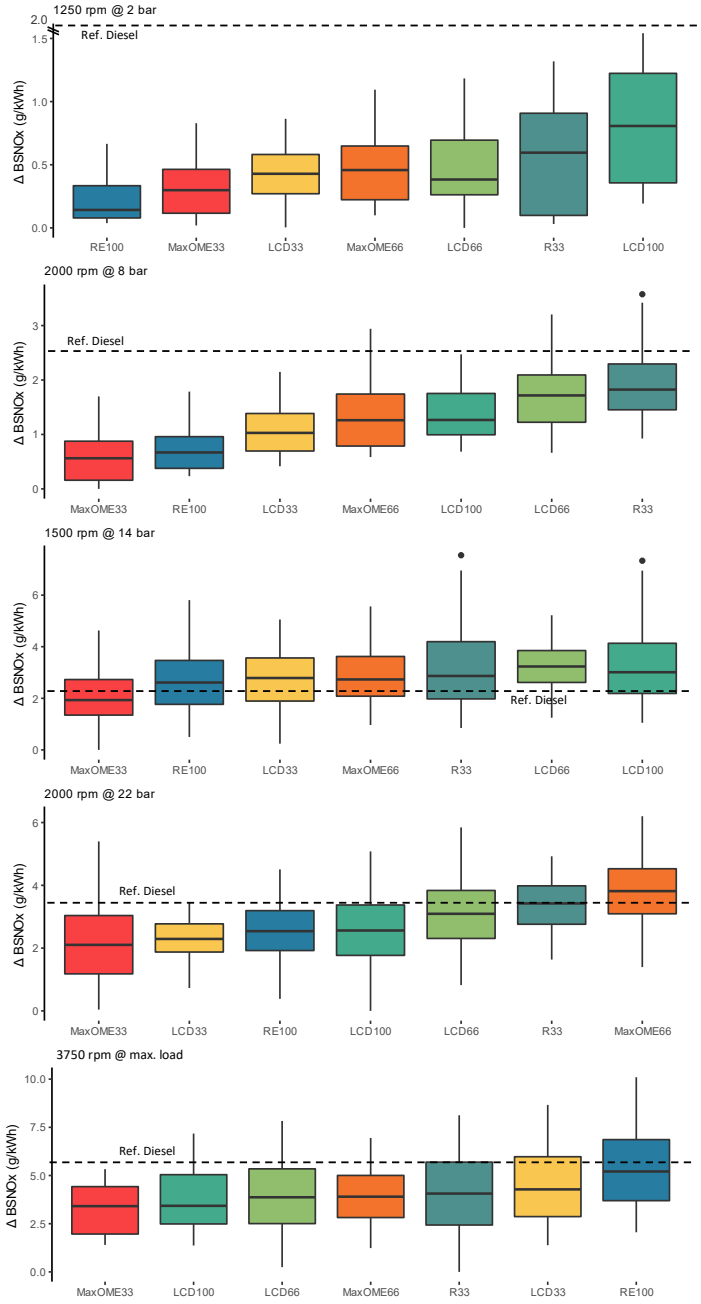

Figure 14. BSNOx at different engine conditions with equal engine settings.

4.4 Soot emissions impact

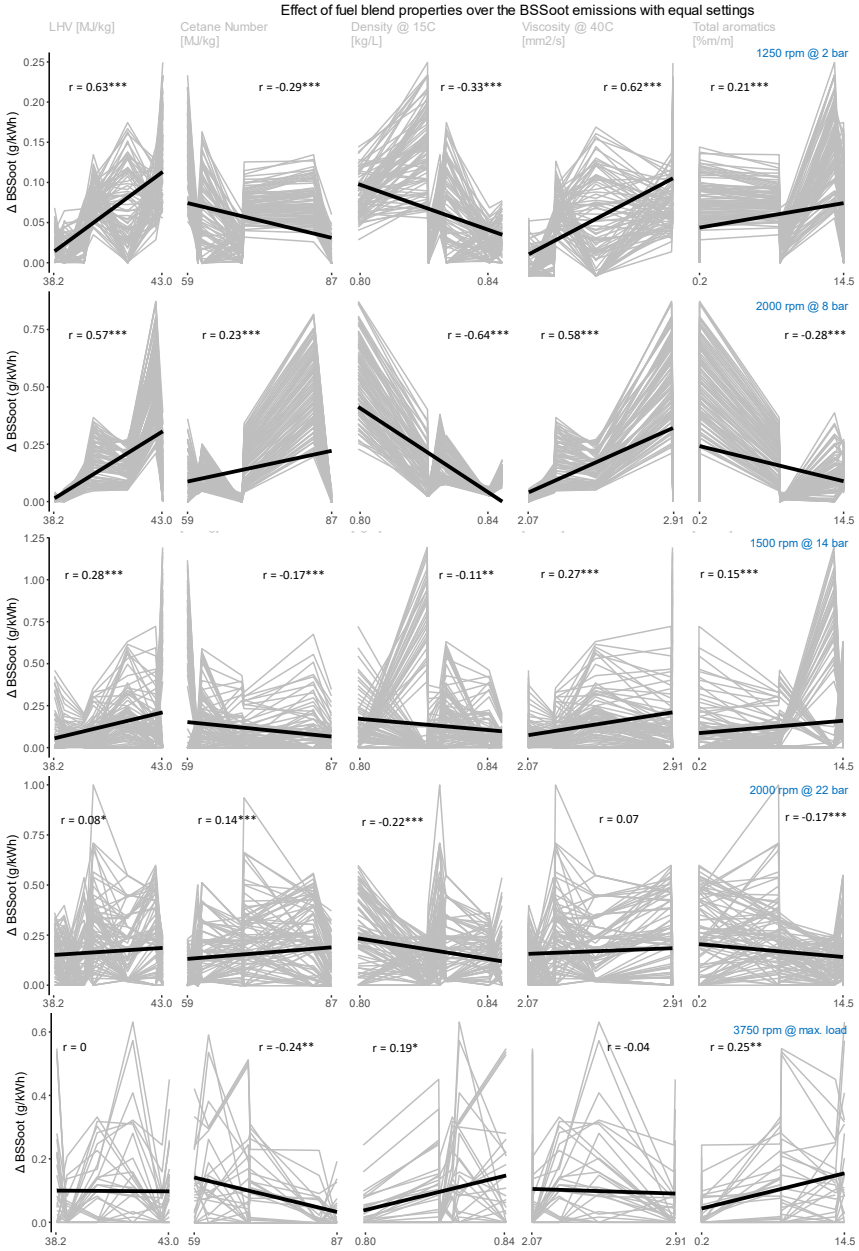

Figure 15. Effect of fuel blend properties over the BSSoot at different engine conditions for cases with equal settings. Significant values are represented as *p<0.05, **p < 0.01, ***p<0.001.

In contrast to the BSNOx emissions, the BSSoot emissions (as shown in Figure 15) do exhibit a discernible relationship with the studied fuel properties, particularly noticeable at low to medium engine loads.

One noteworthy trend is the influence of the LHV of the fuel on BSSoot emissions. An increase in the LHV of the fuel is associated with elevated BSSoot emissions from the engine. However, it's important to recognize that the LHV is effectively reflecting the oxygen content in the fuel. Thus, the observed relationship might be more accurately interpreted as follows: as the oxygen content in the fuel increases (thus reducing the LHV), there is a reduction in soot emissions. This effect becomes particularly pronounced in fuels with higher concentrations of oxygenated compounds such as OMEx.

An additional observation pertains to the impact of the fuel's physical properties, specifically density and viscosity. At low engine loads, viscosity shows a strong correlation with BSSoot emissions. During these operating conditions, fuels with lower viscosity could contribute to faster breakage of fuel droplets upon injection, facilitating improved mixing of fuel and air. Similarly, fuels with higher density could enhance spray penetration [17], thereby enhancing the mixture. These effects align with the notion that efficient mixing is crucial for reducing soot emissions. However, at higher engine loads, where thermodynamic conditions favor more homogeneous combustion, the effects observed at lower loads become dampened, with the dominant impact being on BSFC.

Interestingly, the absence of a clear-cut effect of fuel aromatics on both NOx and soot emissions coincides with prior research findings [18]. This phenomenon suggests that the aromatic property can influence emissions by various mechanisms, leading to outcomes that can either increase or decrease soot and NOx emissions. For instance, although aromatics might enhance soot precursors, the ignition delay facilitated by these compounds aids in forming a more homogeneous mixture, which subsequently burns more completely at lower temperatures.

The collective influence of various fuel properties on BSSoot emissions is represented in Figure 16. The patterns observed in Figure 15 can be seamlessly extrapolated to these results, with the impact of the proportion of oxygenated compounds in OMEx, characterized by the absence of C-C bonds, being evident.

A notable outlier in Figure 16 is RE100. Across most engine loads, RE100 exhibits low NOx emissions but relatively high levels of soot emissions. However, this trend changes at the highest power condition, where RE100 demonstrates lower soot emissions compared to the other fuels. In both the cases of RE100 and R33, it's plausible that these fuels, which possess higher LHVs, require lower fuel masses to attain the required power output. Consequently, the A/F ratio in these situations tends to leaner mixtures than other tested fuels, which can contribute to variations in emissions behaviour. The intricate interplay of fuel properties, particularly the proportion of OMEx, in shaping BSSoot emissions. This further emphasizes the multifaceted nature of emissions formation in combustion processes, where multiple factors interact to determine the resulting emissions profile.

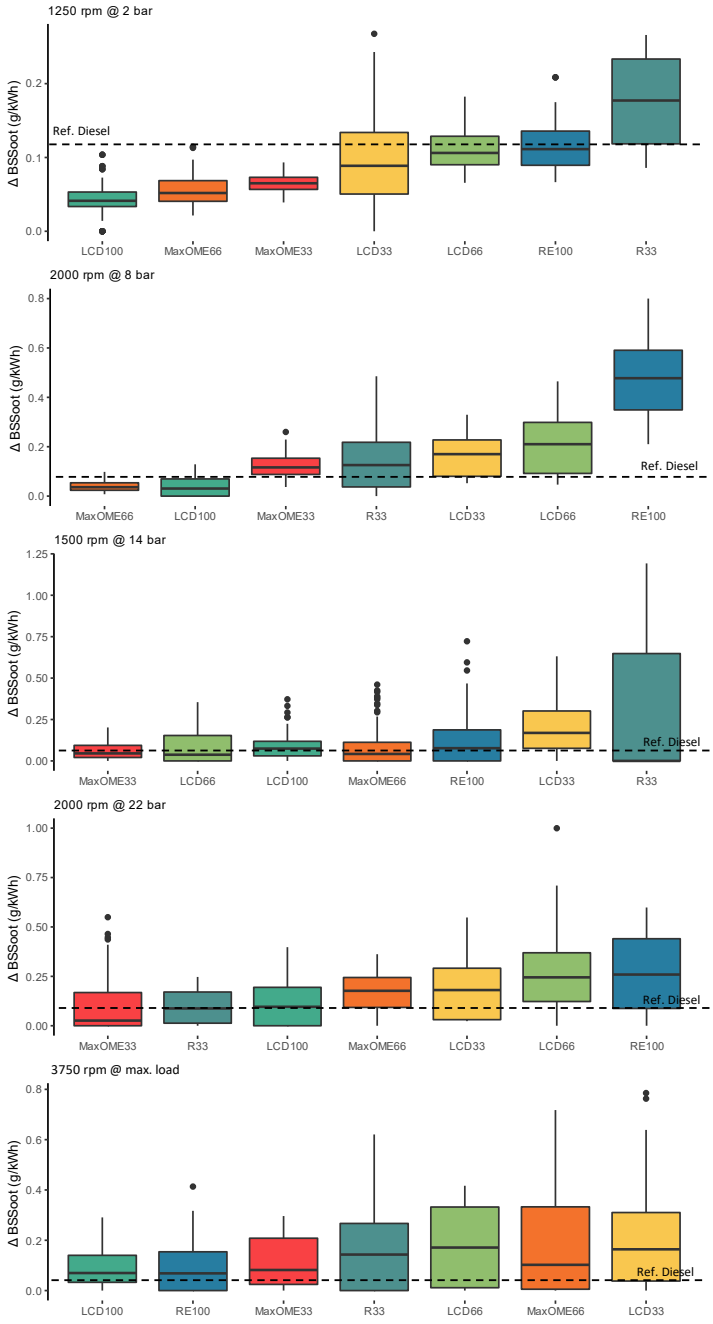

Figure 16. BSSoot at different engine conditions with equal engine settings.

5 Experimental optimized responses analysis

Due to their close to diesel autoignition potential, the tested LCFs can be evaluated under direct drop-in conditions (Chapter 4) and with optimized calibrations tailored to each specific fuel type. As mentioned during Chapter 3 and Chapter 4, the settings under drop-in conditions primarily depend on the LHV of the fuel and its influence on the lookup values of the open-loop control system. Conversely, other fuel characteristics, such as elevated oxygen content, can be leveraged during the optimization process to reduce NOx emissions without adverse effects on soot levels.

In Figure 17, both the drop-in calibration (represented by bars) and the optimized calibration (represented by dots) yield comparable brake-specific fuel consumption levels to the conventional diesel reference for most LCFs, with a few exceptions like the low LHV fuels MaxOME66 and LCD100. Notably, the optimized calibration slightly elevates the BSFC at medium-to-high loads. The calibration proposed in Chapter 3 calibration targets significantly lowering NOx emissions, which favors combustion strategies that delay the SOI and reduce injection pressure, thereby decreasing in-cylinder combustion temperatures. However, these changes also affect combustion efficiency.

At the 1250 rpm and 2 bar operating condition, where fuel consumption is typically higher and drop-in NOx emissions are lower, the optimization leads to fuel consumption reductions across all tested LCFs. This enhancement in low-load operation could offer substantial advantages in fuel economy, especially in urban driving scenarios characterized by low engine loads and speeds. The environmental effect of this will be seen in the life cycle analysis that will be discussed in Chapter 6.

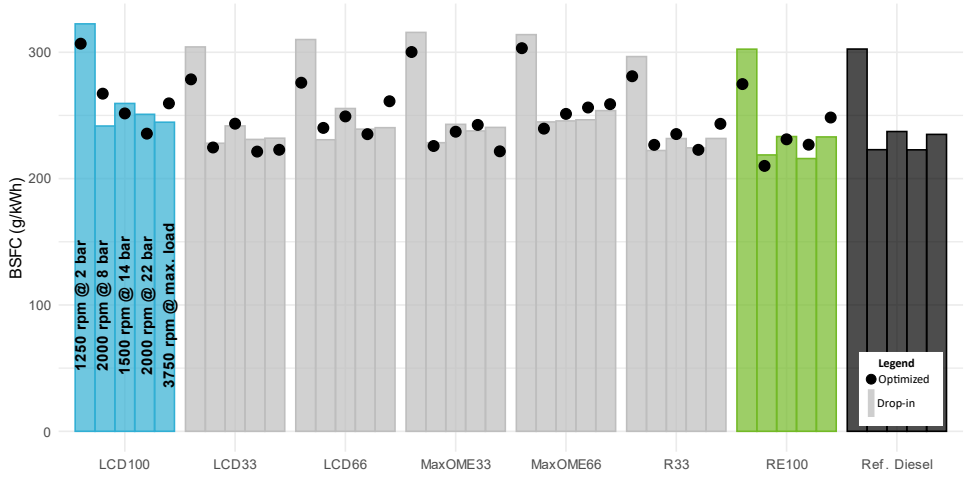

Figure 17. BSFC comparison for the optimized vs. drop-in calibration

One of the primary objectives of the optimization was to achieve a significant reduction in NOx emissions while maintaining comparable or lower soot levels than the diesel baseline, ensuring the proper functioning of the stock diesel particulate filter (DPF). This NOx-soot tradeoff is depicted in Figure 18. Due to variations in calibration settings and fuel properties, NOx emissions under drop-in calibration are generally higher than those of diesel across various operating conditions and LCFs. Nevertheless, the calibration optimization can result in reductions of up to 3 g/kWh in most conditions. Like with the BSFC, the low-load, low-speed region sees significant improvements, but the 3750 rpm @ max. load condition also benefits greatly (a reduction of more than 2 g/kWh for all fuels). The calibration to reach such low NOx levels is given by a combination of the fuel properties, which allows to generally increase the EGR without increasing the soot emissions, as well as delaying the SOI and reducing the injection pressure (see Appendix).

While NOx emissions can be reduced through dedicated calibration for all LCFs, it is in the tradeoff with soot emissions that fuels with high oxygen content (high OMEx proportion fuels) shine as the preferable option. As observed in Figure 18 for the OMEx-containing fuels, it was possible to simultaneously reduce NOx emissions and maintain soot levels consistently below diesel. However, for non-OMEx-containing fuels (RE100 and R33), which possess longer-chain hydrocarbons, the optimization results in higher soot levels compared to drop-in calibration and, in most cases, higher than diesel. Notably, these elevated soot levels still fall within acceptable limits in the engine exhaust, staying below 1.5 FSN for the 1250 rpm at

2 bar condition and below 2.5 FSN for other conditions (the operational limit recommended by the manufacturer).

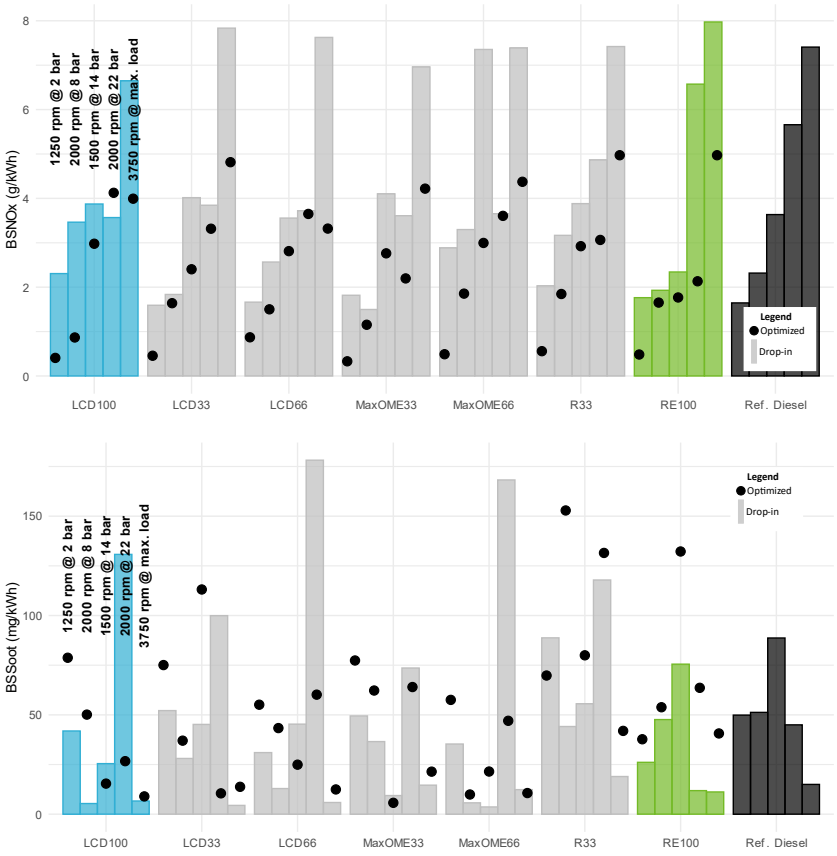

Figure 18. BSNOx (top) and BSSoot (bottom) comparison for the optimized vs. drop-in calibration

When examining unburned HC and CO emissions, it's worth noting that the lowest load conditions tend to exhibit the worst emissions due to low cylinder pressure and temperature The optimization methodology did not consider these emissions (CO and HC) beyond exceeding a certain threshold, which is the reason the optimized values exceed the drop-in ones. Additionally, at low load conditions, there's a likelihood of poorer mixing and quenching near the cylinder walls [19]. Regardless, for both calibration scenarios, the LCFs generally produce lower emissions than diesel under these low-load conditions, except for the optimized R33, where reduced injection pressure and SOI retarding contribute to worsened combustion (though BSFC may be reduced).

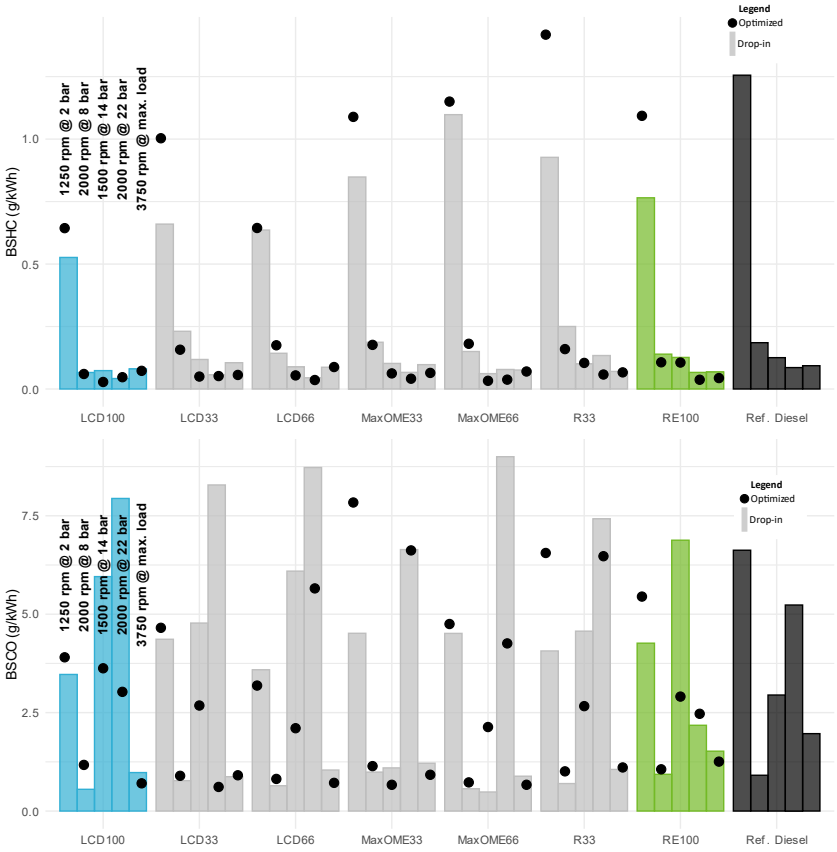

Figure 19. BSHC (top) and BSCO (bottom) comparison for the optimized vs. drop-in calibration

At higher loads and speeds, HC emissions with LCFs improve, especially with the optimized calibration, although differences between calibrations are minimal. Interestingly, there doesn't appear to be a clear correlation between the calibration strategy used and specific fuel properties regarding CO emissions, as was seen when the calibration settings were fixed in Section 4. Nonetheless, CO emission values remain within the same range as those of a diesel engine, ensuring compatibility with exhaust temperatures and the potential for oxidation by an Aftertreatment System (ATS).

6 Summary and conclusions

This chapter outlines a four-stage analysis of the use of LCFs under specific calibrations and combustion phasing, leading to their operation optimization. In the first stage, the analysis quantifies engine responses while operating within the calibration settings' limits, considering only mechanical constraints as limiting factors. This stage identifies clusters of data points representing the available candidates for optimized LCF operating conditions. The second stage narrows down the scope of operating conditions and settings by fixing the Combustion Phasing (CA50) to ensure uniform combustion timing across different LCFs. This step allows for a more controlled comparison of engine responses under similar combustion conditions. The third stage further refines the analysis by preserving the same calibration settings across different fuels, providing insights into how different fuels affect engine performance while holding other variables constant. This stage is crucial for isolating the specific effects of different LCFs within the engine. In the fourth and final stage, the analysis seeks to identify the optimal operating conditions for each LCF at different settings and compare them to drop-in calibration and diesel B7 operation. This stage provides valuable insights into the potential benefits and trade-offs of using LCFs compared to traditional diesel fuels.

6.1 Low-to-medium load and high load performance

This section discusses a detailed analysis of engine performance and emissions characteristics under various operating conditions and with different fuels. The analysis is based on the use of different fuels, categorized into LCD fuels (LCD100, LCD66, and LCD33), MaxOME fuels (MaxOME66 and MaxOME33), and R33 and RE100, each with its unique composition. The key findings and observations include:

- Among LCD fuels, LCD100 exhibits higher fuel consumption due to its lower LHV, with moderate correlations between BSFC, BSNOx, soot, and CA50. LCD66 shows lower correlations between BSNOx and BSFC but has higher median BSNOx emissions. The NOx-soot tradeoff is favorable for LCD100, despite higher soot emissions.
- For MaxOME fuels, MaxOME66 has lower BSFC than MaxOME33 due to differences in LHV, oxygen content, and CN. Soot emissions are low across all operating conditions for MaxOME fuels, with MaxOME66 showing a positive effect on reducing soot emissions. MaxOME33 has lower BSNOx emissions, mainly when combustion occurs earlier.

- Comparing R33 and RE100, R33 has higher BSFC and BSNOx emissions, despite similar CA50 and soot emissions distributions. The difference in CN and oxygen content suggests that oxygen levels compensate for the CN difference, resulting in favorable soot and NOx emissions for RE100.
- As engine load increases, the calibration settings become narrower, and engines operate closer to their mechanical limits. This underscores the importance of carefully calibrating engines for high-load conditions to ensure safety and performance.
- The study confirms the well-known NOx-soot tradeoff in diesel engines, where reducing one emission often results in an increase in the other. However, some LCFs, such as LCD66, exhibit more favorable emission outcomes at maximum load.
- Fuels with higher LHVs require less mass to reach the operating condition, leading to improved AFR at lower loads. Oxygenated fuels, with higher oxygen content, also show benefits in terms of charge renewal efficiency at lower loads.
- Despite differences in consumption and emissions, the book highlights that various LCFs can achieve BSFC values comparable to diesel, especially fuels with higher LHVs like RE100 and R33.

6.2 Fixed combustion phasing

The study focuses on maintaining a fixed CA50 at each operating condition to ensure similar combustion phasing among different LCFs. This approach allows for a more direct comparison of fuel effects on other parameters like fuel consumption, NOx, and soot emissions.

- The relationship between the oxygen-to-mass ratio content in fuels and BSFC is confirmed. As OMEx content increases, BSFC tends to rise. This outcome is primarily due to fuels with higher OMEx concentrations having lower LHVs, which require a larger fuel volume to produce the same power output. However, there is an exception observed with MaxOME33 at the lowest load condition, possibly due to its unique combustion properties.
- LCFs with lower OMEx content, such as RE100 and R33, show significantly reduced BSFC values, indicating their potential as more efficient alternatives for compression ignition engines. These fuels possess higher energy content compared to oxygenated fuels, leading to lower fuel consumption.
- The relationship between fuel properties and NOx emissions is not as straightforward as BSFC. Fuels containing OMEx exhibit similar limits for

NOx emissions, with some exceptions in the LCD66 fuel. Adjusting input conditions to maintain the same CA50 for different fuels shows variations in NOx emissions, depending on load and fuel properties.

- Soot emissions at fixed CA50 values show complex relationships across different LCFs. There is no distinct advantage in terms of soot emissions when comparing oxygenated and less oxygenated fuels, especially when only OMEx proportions vary. The wide range of calibration settings capable of achieving the same CA50 contributes to substantial variability in soot emissions for most fuels. MaxOME66, with the highest oxygen content and the lowest carbon content, consistently exhibits the lowest median soot emissions due to its ability to achieve balanced combustion.

6.3 Fixed calibration settings

The study employs an iso-setting approach to isolate the effects of different LCFs on various engine responses. This approach allows for a direct comparison of how fuel properties influence engine performance and emissions.

- Fuel properties such as LHV, CN, density, viscosity, total aromatics, and O-C ratio significantly impact the fuel mass levels required to reach specific loads and speeds. Higher LHV generally leads to lower fuel masses, especially at high engine loads, reflecting the energy density of LCFs. The viscosity and O-C ratio also influence fuel mass, with lower carbon content and higher oxygen proportions leading to lower fuel masses.
- The impact of CN and aromatic content on BSFC is weak, with varied correlations depending on the operating condition. While there are trends suggesting BSFC rises with CN below 71. Aromatic content appears to have a limited role in affecting BSFC.
- Density shows a stronger correlation with BSFC across all engine operating conditions compared to other factors. Denser fuels tend to exhibit higher BSFC, potentially due to reduced fuel penetration into the cylinder, particularly at lower loads.
- NOx emissions display weak correlations with individual fuel properties. The complexity of NOx formation in internal combustion engines involves multiple interdependent factors, making it challenging to attribute emissions solely to one property. Combustion stoichiometry and oxygen content influence NOx emissions, with leaner mixtures and higher oxygen proportions potentially leading to reduced NOx.
- Soot emissions show a more discernible relationship with fuel properties, particularly at low to medium engine loads. Higher LHV is associated with

elevated soot emissions, with the oxygen content playing a crucial role. Fuels with higher oxygenated compound concentrations tend to exhibit lower soot emissions, especially at low loads, where efficient mixing is crucial.

6.4 Optimized calibration

The study evaluates the performance of tested LCFs under direct drop-in conditions and with optimized calibrations tailored to each specific fuel type.

- The optimization, which targets lower NOx emissions, may slightly elevate BSFC in certain conditions. The optimized calibration generally results in BSFC levels comparable to conventional diesel reference for most LCFs. However, some low LHV fuels like MaxOME66 and LCD100 exhibit higher BSFC with the optimized calibration, particularly at medium-to-high loads.
- At low engine loads and speeds, where fuel consumption is typically higher, the optimization leads to fuel consumption reductions across all tested LCFs. This improvement in low-load operation can be advantageous for fuel economy, especially in urban driving scenarios with low engine loads and speeds.
- The optimization successfully reduces NOx emissions, with reductions of up to 3 g/kWh across various conditions and fuels. The tradeoff between NOx and soot emissions varies, but fuels with high oxygen content (high OMEx proportion) can simultaneously reduce NOx emissions and maintain lower soot levels below diesel.
- Under low-load conditions, HC and CO emissions may be higher due to low cylinder pressure and temperature. However, LCFs generally produce lower HC and CO emissions than diesel under low-load conditions, except for the optimized R33, where reduced injection pressure and SOI retarding contribute to worsened combustion.
- At higher engine loads and speeds, HC emissions with LCFs tend to improve, especially with the optimized calibration. There doesn't appear to be a clear correlation between the calibration strategy and specific fuel properties regarding CO emissions. Nonetheless, CO emission values remain within the range of a diesel engine, ensuring compatibility with exhaust temperatures and potential oxidation by an ATS.

7 References

[1] A. García, J. Monsalve-Serrano, C. Micó and M. Guzmán-Mendoza, "Parametric evaluation of neat methanol combustion in a light-duty compression ignition engine," *Fuel Processing Technology,* vol. 249, no. October, p. 107850, 2023.

[2] M. H. M. Yasin, R. Mamat, A. F. Yusop, P. Paruka, T. Yusaf and G. Najafi, "Effects of Exhaust Gas Recirculation (EGR) on a Diesel Engine fuelled with Palm-biodiesel," *Energy Procedia,* vol. 75, no. August, pp. 30-36, 2015.

[3] B. Rajesh Kumar and S. Saravanan, "Effect of exhaust gas recirculation (EGR) on performance and emissions of a constant speed DI diesel engine fueled with pentanol/diesel blends," *Fuel,* vol. 160, no. November, pp. 217-226, 2015.

[4] E. Öztürk and Ö. Can, "Effects of EGR, injection retardation and ethanol addition on combustion, performance and emissions of a DI diesel engine fueled with canola biodiesel/diesel fuel blend," *Energy,* vol. 244, no. Part B, p. 123129, 2022.

[5] A. García, J. Monsalve-Serrano, D. Villalta and M. Guzmán-Mendoza, "Parametric assessment of the effect of oxygenated low carbon fuels in a light-duty compression ignition engine," *Fuel Processing Technology,* vol. 229, no. October, p. 107199, 2022.

[6] G. Karavalakis, D. Short, D. Vu, R. Russell, M. Hajbabaei, A. Asa-Awuku and T. D. Durbin, "Evaluating the Effects of Aromatics Content in Gasoline on Gaseous and Particulate Matter Emissions from SI-PFI and SIDI Vehicles," *Environ Sci Technol,* vol. 49, no. 11, pp. 7021-7031, 2015.

[7] Y. Qian, Y. Qiu, Y. Zhang and X. Lu, "Effects of different aromatics blended with diesel on combustion and emission characteristics with a common rail diesel engine," *Applied Thermal Engineering,* vol. 125, no. October, pp. 1530-1538, 2017.

[8] M. Elkelawy, E. Shenawy, S. A. Mohamed, m. M. Elarabi and H. A.-E. Bastawissi, "Impacts of EGR on RCCI engines management: A

comprehensive review," *Energy Conversion and Management: X*, vol. 14, no. May, p. 100216, 2022.

[9] J. Han, H. Bao and L. Somers, "Experimental investigation of reactivity controlled compression ignition with n-butanol/n-heptane in a heavy-duty diesel engine," *Applied Energy*, vol. 282, no. January, p. 116164, 2021.

[10] H. Guo, W. S. Neill and B. Liko, "An Experimental Investigation on the Combustion and Emissions Performance of a Natural Gas - Diesel Dual Fuel Engine at Low and Medium Loads," in *Proceedings of the ASME 2015 Internal Combustion Engine Division Fall Technical Conference*, Houston, TX, USA, 2015.

[11] A. Garcia, J. Monsalve-Serrano, D. Villalta, M. G. Guzman-Mendoza, P. Gaillard, R. Durrett, A. Vassallo and F. C. Pesce, "Evaluation of the Effect of Low-Carbon Fuel Blends' Properties in a Light-Duty CI Engine," *SAE Int. J. Adv. & Curr. Prac. in Mobility*, vol. 5, no. 3, pp. 1094-1106, 2022.

[12] P. Hellier, M. Talibi, A. Eveleigh and N. Ladommatos, "An overview of the effects of fuel molecular structure on the combustion and emissions characteristics of compression ignition engines," *Proceedings of the Institution of Mechanical Engineers, Part D: Journal of Automobile Engineering*, vol. 232, no. 1, pp. 90-105, 2018.

[13] J. J. Lópuz, J. García-Oliver, A. García and V. Domenech, "asoline effects on spray characteristics, mixing and auto-ignition processes in a CI engine under Partially Premixed Combustion conditions," *Applied Thermal Engineering*, vol. 70, no. 1, pp. 996-1006, 2014.

[14] S. M. Miraboutalebi, P. Kazemi and P. Bahrami, "Fatty Acid Methyl Ester (FAME) composition used for estimation of biodiesel cetane number employing random forest and artificial neural networks: A new approach," *Fuel*, vol. 166, no. February, pp. 143-151, 2016.

[15] A. A. Al-Harbi, A. J. Alabduly, A. M. Alkhedhair, N. B. Alqahtani and M. S. Albishi, "Effect of operation under lean conditions on NOx emissions and fuel consumption fueling an SI engine with hydrous ethanol–gasoline blends enhanced with synthesis gas," *Energy*, vol. 238, no. Part A, p. 121694, 2022.

[16] D. Agarwal, S. Sinha and A. K. Agarwal, "Experimental investigation of control of NOx emissions in biodiesel-fueled compression ignition engine," *Renewable Energy*, vol. 31, no. 14, pp. 2356-2369, 2006.

[17] S.-w. Lee, D. Tanaka, J. Kusaka and Y. Daisho, "Effects of diesel fuel characteristics on spray and combustion in a diesel engine," *JSAE Review*, vol. 23, no. 4, pp. 407-414, 2002.

[18] J. Reijinders, M. Boot and P. de Goey, "Impact of aromaticity and cetane number on the soot-NOx trade-off in conventional and low temperature combustion," *Fuel*, vol. 186, no. December, pp. 24-34, 2016.

[19] S. Saxena and I. D. Bedoya, "Fundamental phenomena affecting low temperature combustion and HCCI engines, high load limits and strategies for extending these limits," *Progress in Energy and Combustion Science*, vol. 39, no. 5, pp. 457-488, 2013.

8 Appendix

8.1 Optimization calibration settings

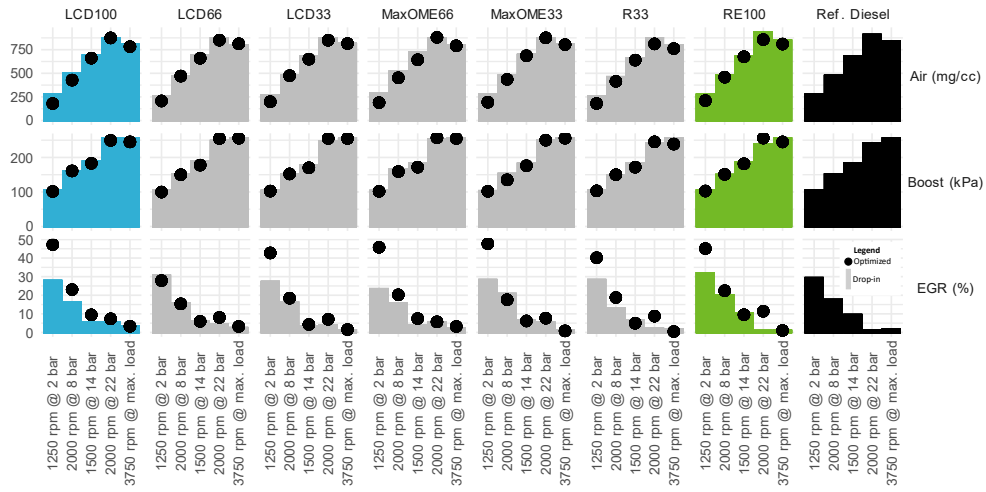

Figure 20. Air management system setting for the drop-in and optimized calibration

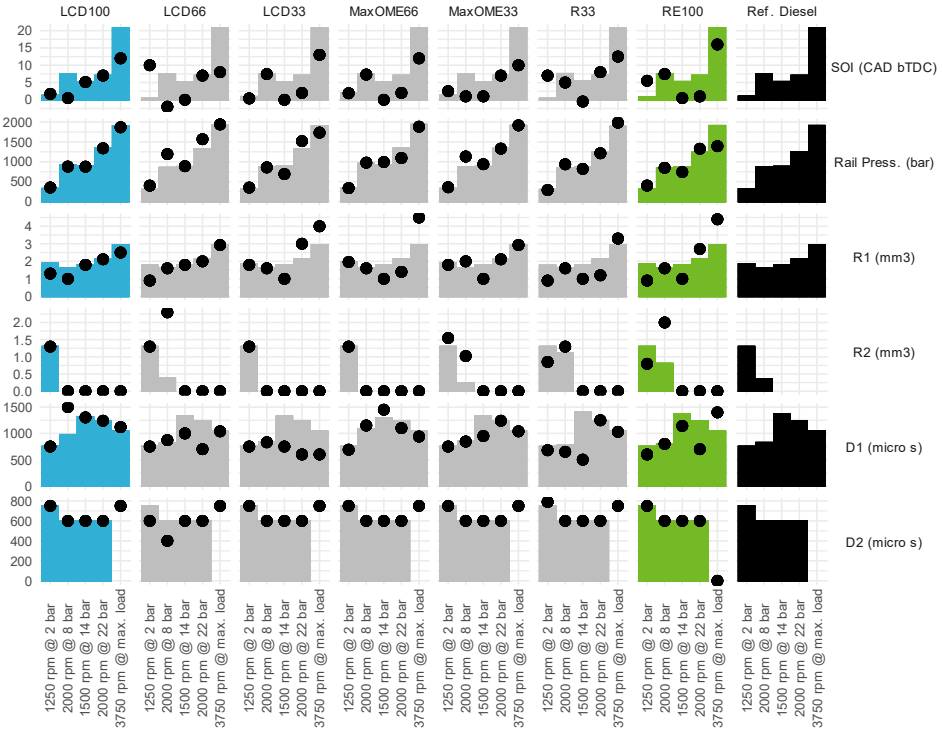

Figure 21. Injection settings for the driop-in and optimized calibration

Chapter 6
Life Cycle Analysis of Low Carbon Fuels for Light-Duty Combustion Engine Vehicles

Contents

1 Introduction

Previous chapters have reviewed the reduction of pollutant emissions from the engine associated with the properties of different fuel blends and the benefits of the production pathways of low carbon fuels (LCFs). However, the full environmental impacts of using LCFs in light-duty combustion engine vehicles has not yet been extensively addressed. Quantifying the magnitude of these impacts can be useful for policymakers and stakeholders in the transportation sector to make informed decisions about transitioning exclusively to the use of electric vehicles or otherwise adopting LCFs as an energy resource for road transport. For that reason, this chapter highlights the environmental impact of using internal combustion engine vehicles (ICEV) with LCFs and the importance of considering the entire life cycle of the fuels used, particularly compared to the current baseline for compression ignition vehicles. This is achieved by performing a life cycle analysis (LCA), considering different types of representative ICEVs for a usage period of 10 years.

When discussing the environmental effect of ICEVs, and even electric vehicles (EVs), there is a tendency by industry experts and policy makers to focus almost exclusively on greenhouse gas (GHG) emissions coming from the vehicle tailpipe to compare their global warming potential (GWP). Although, it is necessary to assess the GWP due to the negative consequences of increasing the global average temperature above the 2°C critical threshold [1, 2, 3, 4], centering the attention exclusively on tailpipe emissions could hinder the observation of the whole landscape, and lose sight of impacts not directly attributed to the tailpipe emissions of vehicle use. In fact, LCAs for both EVs and ICEVs consistently show that 20-40% of the GHG of the vehicle lifecycle come from the manufacturing of the vehicle, while 60-80% of the GHG is directly attributed to the usage and energy production of the vehicle, especially when the energy production is derived from fossil sources for either EVs or ICEVs [5, 6, 7, 8]. Furthermore, while EVs generally show lower GHG emissions and are attributed a higher contribution to reaching net zero emissions for the 2050 timeline [9], some current localized LCA studies where the energy mix consist of non-renewable sources can show higher GHG impacts for EVs than for ICEVs [10].

The transport and energy sectors have been two of main GHG emitters for the past 20 years both in Europe and globally [11, 12, 13], with cars contributing the most to the emissions (45.1% of the transport sector in 2018) [14]. LCFs directly target the reduction of the high GHG emissions from the transport sector by considering the whole lifecycle of the fuel, whose production is designed to potentially act as a CO_2 sink at some stages [15, 16]. The prospective carbon offsetting capabilities of LCF

production probe the evaluation of more than just the tailpipe emissions of the vehicle, but a more complete overview. An LCA can allow the assessment of different impacts to methodologically quantify possibly detrimental effects to not only the environment, but also to human health, society, and the economy. This broader evaluation of an LCA, in addition, offers a more balanced comparison between different types of vehicles like EVs and ICEVs. Therefore, by examining the full lifecycle of a vehicle, an LCA can identify areas where environmental improvements can be made regarding the selection of technologies for the future of transportation.

As previously mentioned, depending on the energy mix for the EV, its lifecycle GWP will be smaller or larger. Similarly, if LCFs are produced with renewable energy sources and technologies like carbon capture and utilization (CCU) [17, 18, 19], the case could occur that an ICEV running on LCFs could potentially have a lower GWP than an EV, especially if the EV is charged in an electric grid with large proportions of fossil sources (as was the case in Europe in 2021 [20]). In addition, the LCA provides the comparison stage for things like non-renewable material depletion, water and soil contamination, and societal and economic impacts. The evaluation of these additional impacts for vehicles allows to include in the perspective activities like raw materials mining; which have increased in scale in recent years, particularly for EVs battery production which cannot be measured in GWP [9, 21], but have real consequences like unethical mining practices [22].

An LCA of an ICEV can evaluate the environmental impact of the fuel production, vehicle manufacturing, and end-of-life (EOL) disposal. Similarly, an LCA of an EV can assess the impact of the battery production, electricity generation, and vehicle manufacturing. Then, it is possible to compare both vehicles as substitute products that fulfill the same function of transportation, identify the most significant contributors to the environmental impact and prioritize efforts to reduce emissions to reach the climate goals.

1.1 Life cycle analysis: fundamentals and conventions for evaluating the impact of road vehicles

LCAs are a widely accepted methodology for evaluating the impact of products from the raw material extraction (frequently defined as *cradle*) to the end-of-life disposal (*grave*), or an intermediate stage between the two (often labelled as *gate*). Its methods and procedures are consolidated on the ISO 14040 [23] and 14044 [24]; where the first describes the principles and framework, and the second specifies requirements and provides guidelines and methodologies for the individual phases

of the LCA. Under the ISO standards there are four stages in an LCA: definition of the goal and scope; lifecycle inventory (LCI); lifecycle impact assessment (LCIA); and interpretation, reporting and review. Additionally, the limitations and restrictions of the method are considered, mainly related to reducing results to a single score or that applying weights should not be allowed for comparative assertions [25].

1.1.1 Goal and scope definition

The goal and scope definition stage of an LCA, as the name indicates, involves the statement of the purpose and scope of the LCA, including the system boundaries, functional unit (FU), and impact categories to be considered. The study should be clearly defined and reflect the intended application of the result, clearly identifying the simplifications, assumptions and limitations to provide transparency regarding the reliability of the results. This definition is important as the data used might be incomplete or uncertain, especially since industries (and commonly in the automotive industry) would rather avoid publishing information about their technical processes. Defining assumptions and limitations can also help to ensure that the results of the LCA study are appropriately interpreted and applied, and are not generalized beyond their reach.

The system boundaries define the physical, procedural, temporal, and geographical limits of the product or process being studied. This can affect the results of the LCA by leading to an incomplete or inaccurate assessment of the different impact if, for example, certain stages of the life cycle or portions of the product system are excluded, and the exclusions are not accounted for during the analysis. The system boundaries clarify the list of activities related to the different stages of the selected product or process, and the exchanges between the process chain and the environment [26]. For passenger vehicles, the system boundaries usually include the vehicle lifecycle and the fuel life cycle (or battery life cycle in the EV case) [27, 28, 29, 30]. Typically, the vehicle life cycle includes the manufacturing, operation, and maintenance stages for a cradle-to-gate analysis; and vehicle disposal can also be included for a cradle-to-grave analysis. On the other hand, the fuel life cycle analysis is constituted by a well-to-wheel (WTW) analysis where the energy pathway and its projection for different scenarios tends to be the focus [31, 32].

The FU is the unit of measurement for the product or process being studied, and it is used as a basis for comparison in the LCA study. The FU should be meaningful to the intended application of the study, and accurately reflect the environmental impacts of the product or process. In the case of road transport, the functional unit selected tends to be 1 km, considered as the average driven by a vehicle under the

conditions specified in the scope. This average 1 km can be associated with real driving conditions or a homologation cycle. For example, many European studies consider the Worldwide harmonized Light-duty vehicles Test Cycles (WLTC) to calculate the impacts corresponding to 1 km [33, 5, 34, 35, 5]; this has the advantage of being standardized and easy to reproduce for many vehicle models and types. Other studies, like [33, 36], also use real driving (simulated or measured) to quantify the 1 km FU.

The impact categories are the environmental issues or areas of concern that are considered in the LCA study. Common impact categories include GWP, acidification potential (AP), eutrophication potential (EP), water consumption potential (WCP), ozone depletion potential (ODP), human toxicity potential (HTP), and particulate matter formation potential (PMFP) [37]. GWP is the most common evaluation for vehicle LCAs, considering the potential contribution of greenhouse gases, such as carbon dioxide, to climate change. The other impact categories like AP, EP, ODP, HTP, PMFP and WCP respectively consider: the potential for acid rain formation, which can damage ecosystems and infrastructure; the potential for excess nutrients, such as nitrogen and phosphorus, to cause harmful algal blooms and other ecosystem imbalances; the potential for certain chemicals, such as chlorofluorocarbons (CFCs), to deplete the protective ozone layer in the atmosphere; the potential for chemicals to cause adverse health effects in humans, such as cancer or developmental effects; the emissions of small particles, which can contribute to air pollution and respiratory problems; and the amount of water used throughout the vehicle life cycle, including in manufacturing and use. These categories are relevant to the passenger vehicles as they reflect the environmental concerns that can be associated with the vehicle manufacturing and energy emissions.

Correctly defining the system boundaries, FU and impact categories allows for the correct setting of the input and output flows to the various products or services within a system. The allocation process involves assigning the environmental impacts of the system to each individual product to their reference unit (economic value, mass, duration, energy, etc.). Allocation can retroactively contribute to the definition of the system boundaries by determining which products or services are included in the study and defining the preferred reference unit for the system flows.

1.1.2 Lifecycle inventory (LCI)

In this stage, data is collected and compiled for all inputs and outputs of the product or process, including raw material extraction, manufacturing, use, and end-of-life disposal. The inventory provides the necessary data and information to quantify the environmental impacts associated with the product or service studied.

The LCA will be more detailed and accurate if all material and anergy flows for a process or product are considered, however, this is rarely a possible scenario. The data from an LCI is often sourced from various databases, which can be incomplete, outdated, or inaccurate. These inaccuracies can come from the geographical coverage, the technological information for the involved processes and the representativeness of the dataset for the modelled scenario [26]. Some software tools like ecoinvent [38, 39], SimaPro [40] and Sphera's GaBi [41] are widely accepted and provide simplified models and databases for an extensive number of industrial process and materials, which are also geographically allocated, however due limitations in the data acquisition from industries the models often include approximations that can be sources of errors and generate important differences between two tools for the same process [42]. For the transportation industry the Greenhouse Gases, Regulated Emissions and Energy Use in Technologies (GREET) model developed by the Argonne National Laboratory [43] is often used and accepted in LCAs; this model contains emissions for vehicle component, battery and fluid manufacturing, as well as the summary of the resources and processes considered at the different stages [44]. Similarly, the GaBi tool is widely used, particularly for the fuel's inventories [18].

The databases facilitate the accounting for the input and output flow balances, often contain data that is difficult to obtain through other means, such as energy consumption and emissions data for specific processes or technologies, and provide a level of standardization for comparing similar studies and products. Nonetheless, to guarantee the accuracy of the results, measuring and modelling the difference process and components in the flows can provide a more detailed understanding of the impacts of the specific system studied.

1.1.3 Lifecycle impact assessment (LCIA)

The LCIA stage involves assessing the potential environmental impacts of the data collected in the LCI in relation to the FU, across the impact categories selected in the scope definition [45]. The impact categories are evaluated to determine the magnitude and significance of the environmental impacts. Several methodologies exist for the LCIA, like the ReCiPe2016 [37], CML [46] and the Product Environmental Footprint (PEF) and Organisation Environmental Footprint (OEF) methods from the European Commission [47]. These methodologies contain different characterization factors (indication of the environmental impact per unit of stressor) for each impact category and the flows associated in a process, and ways of interpreting the results.

Characterization factors can be derived at the midpoint or endpoint. The distinction between the two lies in where the characterization factor is located along the impact pathway. Midpoint factors have a stronger relation to the environmental flows and a relatively low uncertainty (besides the previously described sources of error), while the endpoint characterization, although with higher uncertainty, provides better information on the environmental relevance of the flows [48, 49, 37].

The LCIA stage of an LCA is a critical step in quantifying and characterizing the potential environmental impacts of a product or process. It involves converting the LCI data into impact indicators and providing guidelines for interpreting the environmental impacts resulting from it.

For transportation vehicles the focus tends to global warming or GWP regarding the midpoint indicators, mainly because the reach of the damage pathways into the endpoint indicators extends to both consequences for human health and ecosystem damage. However, given the resource intensive nature of energy production (both electricity and fuels) and of vehicle manufacturing the consideration into other midpoint impact categories like resource depletion, land and water use are worth considering. This material impact in tandem with the decarbonization in transportation was explored in the work of [9], finding a tradeoff between the increase in the demand of raw material like nickel, cobalt, and manganese with the potential CO_2 reduction of EVs when observing the transition from ICEVs to EVs. Or the work of [27], which in addition to the GWP also studied the AP and cumulative non-renewable energy demand (CED) for vehicles with combustion (hydrogen, CNG and gasoline), hybrid and fuel-cell electric powertrains; concluding that for GWP and CED, all vehicles fueled only with hydrogen show the best performance, while an unfavorable performance was identified for the CNG car; and that the FC powertrain has the highest AP potential.

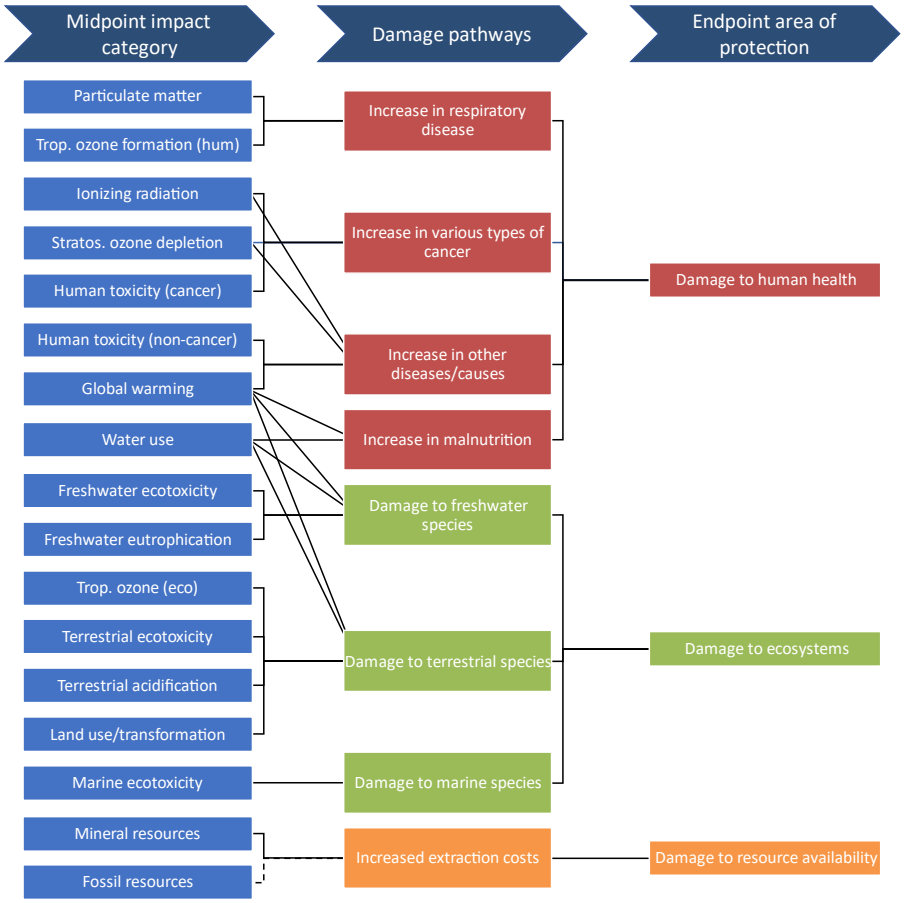

Figure 1. Overview of the impact categories that are covered in the ReCiPe2016 method and their relation to the areas of protection (figure adapted from [37])

1.1.4 Interpretation, reporting and review

In the final stage, the results of the impact assessment are interpreted and analyzed to draw conclusions that can guide informed decisions relating to the environmental impacts assessed, preferably leading to the least environmental burden [26]. The environmental impacts identified in the previous stages (goal and scope, LCI, and LCIA) are assessed and evaluated in the context of the study's objectives.

To carry out the interpretation of LCA results, a range of expert knowledge is needed. This includes knowledge of the product or process being studied, the relevant environmental impacts, and the social and economic context in which the product or process is used. Additionally, expertise in data analysis, statistics, and

risk assessment may also be required, as well as knowledge of environmental regulations and policies.

For the transportation sector a wide range of experts from different backgrounds have made contributions in LCAs that have helped guide some of the decisions and regulations; transportation engineers, can provide insights into the technical aspects of the vehicle system being studied, such as the design and performance of the powertrain; energy experts provide knowledge about the energy sources used, such as the production and consumption of different types of fuels, and their associated environmental impacts; environmental scientists usually have a large understanding into the long-term effects of the environmental impacts observed and can determine specific thresholds that should not be surpassed to prevent negative environmental and health consequences; and policy makers take the LCA results in the context of regulatory and policy frameworks, which will later inform some of the objectives for future developments.

1.2 Study contributions, novelty, and implications

The current study will employ a comprehensive LCA approach to assess the environmental impacts of ICEVs using LCFs, which considers the entire life cycle of the fuels used and the manufacturing and maintenance of the vehicle. The study will reveal whether even with LCFs, ICEVs still have significant environmental impacts across several impact categories, including GWP, WCP, fossil depletion, and human health. The study highlights the importance of using LCFs to reduce the environmental impact of ICEVs, especially in terms of GWP, but also highlights the limitations of LCFs in reducing other environmental impacts. The findings could have important policy and industry implications in the current transition scenario for transportation, stressing the urgent need for more sustainable and low-carbon transportation systems.

2 Materials and methods

The LCA in this study involves the modelling of a complete vehicle and energy pathways for manufacturing, maintenance, and operation. This requires data collection, modelling, and analysis. Starting from the engine data measured and analyzed in chapters 3 and 4, the CO_2 emissions associated to the use of the vehicles with the different LCFs are estimated, while the additional impacts of the different fuels and vehicles throughout their entire lifecycle, including production, transportation, and road use are modelled for characteristic vehicles carrying the engine evaluated in previous chapters. The analysis is not intended to compare a

specific vehicle; it is intended to be representative of the passenger vehicle class and the impacts of LCFs as energy carrier options for road transportation.

2.1 Goal and scope of the LCA

The goal of this LCA study is to evaluate the environmental impact of replacing fossil diesel with a LCFs; assuming the LCFs are produced in a way that their renewable portions act as CO_2 sinks (see Table 6). Specifically, the study aims to identify the most significant factors contributing to the overall assessment results, including both the vehicle manufacturing stage and the maintenance and utilization stage of the car. The LCA analysis will provide a comprehensive understanding of the net environmental impact change resulting from the adoption of the tested LCFs.

2.1.1 Vehicles definition

Three segments of ICEVs from the passenger class will be studied: mini, hatchback and sedan. It is assumed that the ICEVs studied can be powered with the LCFs with the same maintenance regime as the car that carries the stock engine, without the occurrence of the previously described FIS issues that would increase the rate for part replacements. Additionally, it should be mentioned that only one vehicle per segment is studied and vehicle float behavior is not considered. The main characteristics of the vehicles can be seen in Table 1.

Table 1. Vehicle and driving strategy characteristics

		Segment		
Parameter	Unit	Mini	Hatchback	Sedan
Front area	m2	2.42	2.47	2.52
Drag coefficient	-	0.324	0.284	0.228
Vehicle weight	kg	937	1164	1503
Wheel radius	m	0.29155	0.319	0.3225
Differential ratio	-	3.2	3.2	3.2
Transmission type	-	Manual	Manual	Manual
Gear shift-up	rpm	2200	2200	2200
Gear shift-down	rpm	1200	1200	1200

2.1.2 Cradle-to-road methodology

This study follows the ISO 14040 and 14044 standards for LCAs [23, 24], and considers the life cycle of the selected vehicles from the extraction of raw materials to the end of its useful life on the road. The methodology covers the extraction of raw materials, production, distribution, use, and maintenance phases, as well as the energy sources used during the vehicle's operation. The cradle-to-road (or cradle-to-gate) approach considers the different components of the road vehicle, such as the body, powertrain, and chassis, as well as the fuel and energy sources used during the use phase.

Each of the vehicles are evaluated for the equivalent of 120000 km, which is the estimated distance travelled by car in 10 years in Europe, considering the yearly travelled distance ranges from 8000 to 15000 km depending on the country [50]. The EOL was decided not to be included in this study because there is a lack of consistent data on the end-of-life phase across different countries and the challenges associated with assessing the environmental impacts of end-of-life treatment [27, 51, 52]. Moreover, a vehicle with a mileage of 120000 km could considered to be in good state and may continue to operate for many years to come by keeping a maintenance regime and replacing single components as they break.

2.1.3 Functional unit, energy flow and system boundaries

The functional unit in this study is defined as 1 km traveled by each vehicle. Because the EOL of the vehicle is not being evaluated, 1 km represents a fair comparison point between vehicles and fuels across the different phases in the life cycle of the vehicle. The vehicles will be compared in the scenario of being manufactured in Europe with the energy mix of 2023, and as previously mentioned used for a period of 10 years, covering 1200 km each year.

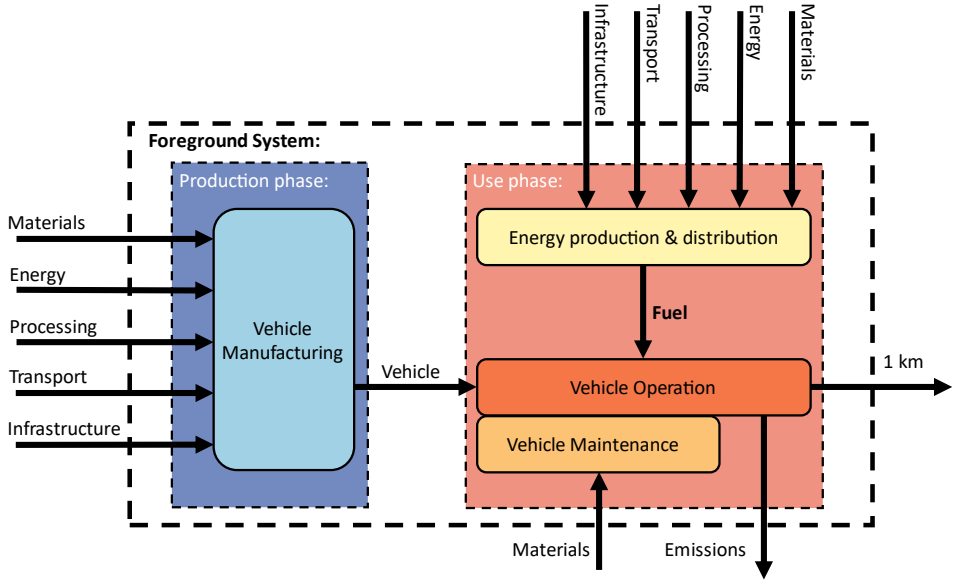

Figure 2. Vehicle system boundaries and elementary flows during the cradle-to-road process

Because the study is aimed at evaluating the impact of using LCFs, the fuel and vehicle life cycles converge in the vehicle operation phase, when the vehicle tank is filled with fuel, and this is used to move the vehicle [29]. Figure 2 shows the general system boundaries and flows that will be used for the different vehicles and the output of the 1 km FU. The vehicle operation consists of tank-to-wheel analysis (TTW), that for this project will be represented by the WLTC to obtain the values of emissions and fuel consumption per km. Additionally, the vehicle maintenance takes the same considerations as the vehicle manufacturing for energy and localization and assumes the recommended manufacturing replacement regime for the main upkeep elements, like oil, cooling fluid and tyres.

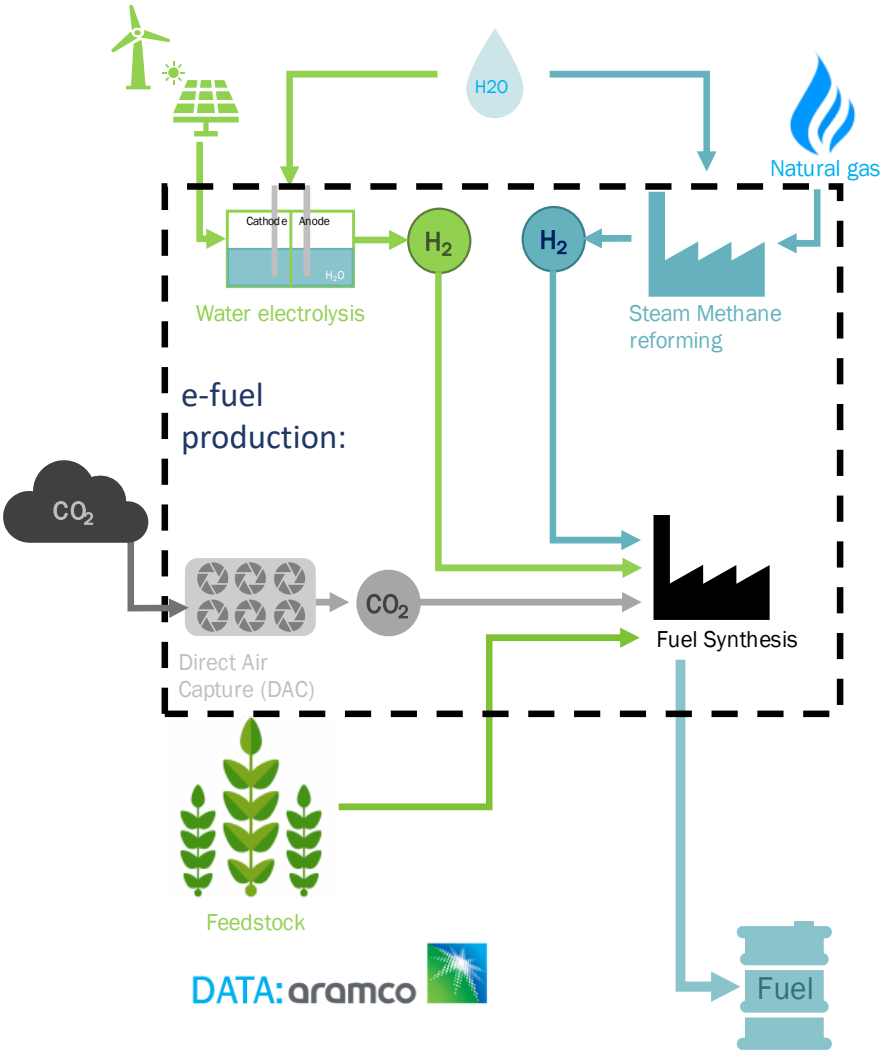

Figure 3. Schematic for the LCF production assuming renewable sources of energy and raw components

The energy production and distribution phase correspond to the so-called well-to-tank (WTT) of the fuel. The simplified schematic of this stage is observed in Figure 3, including the considerations for the raw material and energy procurement from renewable sources. It is highlighted by the figure how the LCFs studied in this work are ideated to be renewable (with the exception of the reference diesel). Previous chapters provide more detail into the different pathways and energy flows that allow to produce LCFs that reduce the carbon footprint compared to fossil fuels.

2.1.4 Impact categories

Results for this study will be presented for five characterization factors: GWP, TAP (terrestrial acidification potential), PMFP, HOFP (human ozone formation potential) and WCP. The impact categories are chosen based on their significance in terms of environmental impacts and their relevance to the automotive industry. GWP is considered a critical impact category due to the contribution of vehicles to GHG emissions and climate change. TAP is explored due to the emissions of acidic pollutants (like NOx) during the life cycle of the vehicle, which can contribute to soil acidification. PMFP and HOFP were chosen due to the impact of vehicle emissions on human health. Finally, WCP is considered due to the significant water use associated with the production and use of cars and their fuels, which can have significant environmental impacts and negative consequences on human health (as seen in Figure 1).

The Hierarchist (100 years) midpoint level ReCiPe2016 method is used for this study using OpenLCA v1.11.0 for the calculations [53]. Table 2 provides a concise description of various impact categories, including the typical emissions that contribute to each effect and the category indicators used to express the effects based on a reference substance. The equivalent potential for each of the flows can be seen in [37].

Table 2. Impact categories overview

Characterization factor	Abb.	Description	Accounted flows (ex.)	Unit
Global Warming Potential	GWP	how much a GHG contributes to global warming	CO_2, N_2O, CH_4, SF_6, $CHCL_3$, CF_4, CFCs, HCFCs, CH_3Br	kg CO_2-eq
Terrestrial Acidification Potential	TAP	potential of a substance to cause acidification in the environment	NOx, SO_2, NH_3, HNO_3, $H2SO_4$, H_3O_4P	g SO_2-eq

Fine Particulate Matter Formation Potential	PMFP	a substance's potential to contribute to the formation PM2.5	NH_3, NOx, SO2, PM2.5	kg PM2.5-eq
Human Ozone Formation Potential	HOFP	potential of a substance to contribute to the formation of ozone in the lower atmosphere	NOx, VOCs, C_6H_6, C_4H_{10}, $C_4H_{10}O$, C_3H_6, C_5H_8, C_4H_6, …	Kg NOx-eq
Water Consumption Potential	WCP	potential of a substance or process to consume freshwater resources	Water (undetermined source)	m^3

2.2 Life cycle inventory

The inventory for the LCA is divided into the vehicle manufacturing, energy production and distribution, vehicle operation and vehicle maintenance stages. The vehicle manufacturing stage includes all processes involved in the production of the vehicle, such as the manufacturing of components and assembly. The energy production and distribution stage include the production of fuel, without accounting for transportation to refueling stations. The vehicle operation stage encompasses the use of the vehicle, including the combustion of fuel, as well as the associated emissions and energy consumption during use. Finally, the vehicle maintenance stage includes all activities required to maintain the vehicle such as replacement of parts and fluids.

2.2.1 Vehicle manufacturing

The summary of the inventory data for vehicle manufacturing are presented in Table 3. The vehicle component weights were retrieved from technical datasheets released by manufacturers and vehicle media content where different parts are weighted [54, 55, 56], to be later averaged by segment. The main data sources for the elementary flows of the vehicle manufacturing (by weights and composition materials) are based

on the GREET 2022 model [29] and ecoinvent 3.9 database [38]. The extended LCI for the vehicle manufacturing can be looked at in section 6.1 of the Appendix.

It can be observed from Table 3 that the powertrain system is kept the same for all three vehicles. Because the powertrain system remains constant, when observing the LCIA GWP of the vehicle manufacturing in ratio of CO_2-eq per component (Figure 4), it can be seen that as the vehicle segment increases in size (in order: Mini, Hatchback and Sedan) the CO_2 proportion corresponding to the chassis and body of the vehicle increase as well. Generally, it is observed that the sub-assemblies with larger masses have higher CO_2 impacts; nonetheless the electronics subassembly (which includes the ECU and infotainment system) represents a large proportion of CO_2 although not being as large in mass. For the case of the electronics, it is reported that due to the number of rare materials needed for their manufacturing the upstream CO_2 results in larger proportions by weight of final product [57, 38].

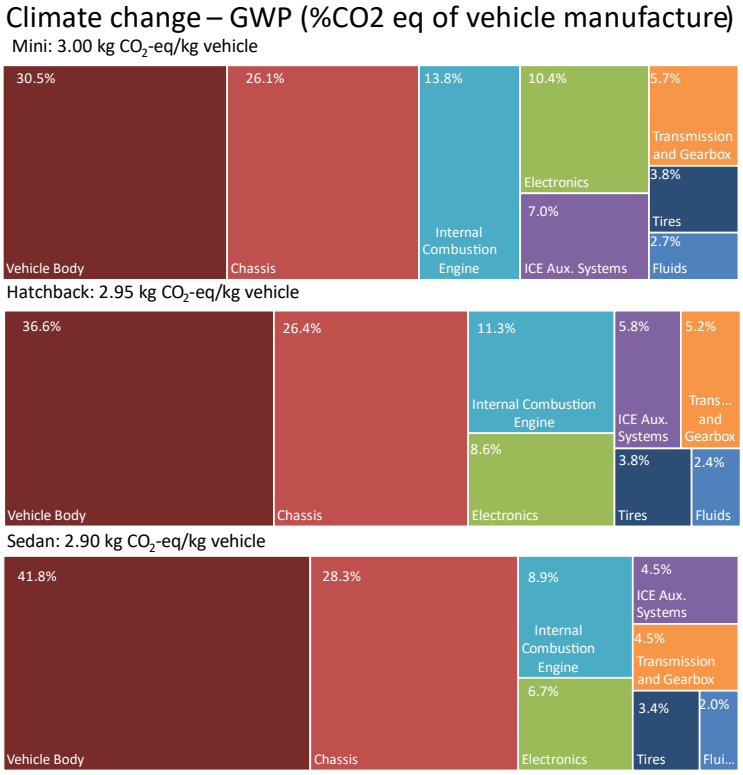

Figure 4. GWP distribution for the vehicle manufacturing material stage (without assembly energy)

Table 3. Summarized inventory data for the vehicle manufacture

Phase	Comp.	Item	Unit	Mini	Hatchback	Sedan
Production		Vehicle	kg	937.0	1164.0	1503.0
Production	Glider	Vehicle Body (interior, exterior & glass)	kg	338.20	494.32	716.63
		Chassis (unibody)	kg	230.25	284.64	386.80
		Electronic Components & Wires	kg	8.18	8.18	8.18
		Windshield Fluid	kg	2.76	2.76	2.76
		Tires	kg	32.40	39.56	44.76
		Adhesives	kg	6.14	8.14	9.14
Production	Drivetrain	Powertrain System (ICE)	kg	140.06	140.06	140.06
		Alternator	kg	6.21	6.21	6.21
		Starter motor	kg	3.20	3.20	3.20
		Fuel System	kg	16.23	16.23	16.23
		Exhaust System	kg	27.52	27.52	27.52
		Transmission System/Gearbox	kg	70.00	77.33	84.66
		Engine Control Unit	kg	1.30	1.30	1.30
		Lead-Acid Battery	kg	12.40	12.40	12.40
		ICE Cooling System	kg	21.81	21.81	21.81
		Engine Oil	kg	4.94	4.94	4.94
		Power Steering Fluid	kg	2.00	2.00	2.00
		Brake Fluid	kg	0.91	0.91	0.91
		Transmission Fluid	kg	5.29	5.29	5.29
		Engine/Powertrain Coolant	kg	7.20	7.20	8.20
Production	Assembly	Electricity	mmBtu	2.68	3.33	4.30
		Natural Gas (NG)	mmBtu	5.16	6.42	8.28

The vehicles' GWP (including the assembly) are within the ranges observed in the literature for ICEVs (Table 4), with 3.81 kg CO_2-eq, 3.76 kg CO_2-eq, and 3.71 kg CO_2-eq respectively for the Mini, Hatchback and Sedan. This is explained in part by the changes in the energy mix used for the process and materials and the location for the manufacture, as well as the lack of explicit data by vehicle manufacturers to be able to accurately replicate the correct inventory inputs and outputs in the LCI; with many in the vehicles in the literature modelled after the 2000 LCA of a Golf A4 [58].

Table 4. Vehicle manufacture GWP in kg CO_2-eq/kg vehicle from selected literature

ICEV	Vehicle weight (kg)	GWP (kg CO_2-eq/kg vehicle)	Location	Year *as publication date	Source	Comment
Diesel	1750	3.67	Europe	2022	[59]	SUV
CNG	1330	3.77	Europe	2021	[27]	
H2-ICE	1380	4.69	Europe	2021	[27]	H2 increases fuel system complexity and weight
H2-Gaoline	1335	4.01	Europe	2021	[27]	H2 increases fuel system complexity and weight
Petrol	1280	6.30	Spain	2021	[5]	
Diesel	1373	6.40	Spain	2021	[5]	
Diesel	1059	7.54		2020	[60]	
Petrol	1050	8.30		2020	[60]	
ICEV	1395	4.53	Hong Kong	2020	[61]	
ICEV	1395	4.62	Europe	2012	[62]	diesel & gasoline

2.2.2 Vehicle maintenance

For the vehicle maintenance, the materials and energy resources considered as inputs and outputs follow the typical scheduled service of a passenger vehicle. The EOL is not considered for the elements replaced during maintenance operations, although for components like oil it is well known that a poor EOL management can cause considerable environmental harm [63]. The replacement is considered for a period of 10 years or 120000 km and the LCI for the different components is described in Table 5, fractional portions are assigned to the end of the defined life cycle.

Table 5. Summarized inventory data for the vehicle maintenance

Component	Distance for replacement (km)	Total weight (kg)	Replacements
Brake fluid	40000	2.7	3
Engine coolant	4500	192.2-216.3	26.7
Engine oil	4500	131.9	26.7
Lead acid battery	40000	24.8	2
Transmission fluid	40000	15.9	3
Tires	30000	129.6-158.2-179.0	4
Windshield fluid	4500	73.7	26.7

2.2.3 Energy production and distribution

The energy production and distribution in this study is comprised of all the processes used to produce and transport the fuel, or WTT. The term is used to describe this portion of the fuel life cycle because it encompasses all the processes that occur before the fuel enters the vehicle's fuel tank. Table 6 shows the well-to-tank carbon intensity (WTT CI) for the different fuels assuming completely renewable energy sources and raw materials as provided by Aramco's GaBi Model and references [18, 64]. Although the assumption of completely renewable energy sources and raw materials for the calculation of the WTT CI for different fuels might not be entirely realistic in the current context, it still provides an overview of the target objective for the fuel technology, especially for the 2050 energy context. Water usage and other process emissions (other than CO_2) that affect the selected impact categories for the fuel were retrieved from [29, 38, 18] based on the single components of the fuels (diesel, RME, FAME, HVO, FT-diesel and OMEx).

Table 6. Well-to-tank carbon intensity for the different fuels assuming completely renewable energy sources and raw materials from Aramco's Gabi Model and [18, 64, 65]

		Components						
Fuel Name	Unit	Diesel	RME	FAME	HVO Waste Oil	FT Diesel	OMEx	Fuel Total
Ref. Diesel	gCO_2/MJ	18.9x 0.93	-27.8 x0.07	-	-	-	-	15.83
LCD100	gCO_2/MJ	-	-	-	-	-68.2x 0.85	-79.0x 0.15	-69.22
LCD66	gCO_2/MJ	18.9x 0.34	-	-	-	-68.2x 0.56	-79.0x 0.10	-37.14

LCD33	gCO_2/MJ	18.9x 0.67	-	-	-	-68.2x 0.28	-79.0x 0.05	-8.17
MaxOME66	gCO_2/MJ	18.9x 0.34	-	-	-	-68.2x 0.48	-79.0x 0.18	-36.65
MaxOME33	gCO_2/MJ	18.9x 0.67	-	-	-	-68.2x 0.16	-79.0x 0.18	-5.85
R33	gCO_2/MJ	18.9x 0.67	-	-67.9x 0.07	-59.7x 0.26	-	-	-6.70
RE100	gCO_2/MJ	-	-27.8 x0.20	-	-	-68.2x 0.80	-	-60.34

It is important to highlight, that if completely renewable energy sources and raw materials are not used for the fuel production, the fuel could have higher carbon intensities than the reference diesel, and thus the advantages over their life cycle will not be perceived. The potential repercusions of this assumption would deem void the purpose of LCFs, thus for further sections the analysis will be centered on the completely renewable case.

For the inventary, the WTT of each of the fuels is obtained by multipliying the fuel consumption (in MJ of fuel) obtained during the vehicle operation phase by the carbon intensity of the fuel.

2.2.4 Vehicle operation: WTT, TTW & WTW

To explore the differences in the envrionmental impact of the LCFs, a preliminary evaluation of the LCIA will be done for the vehicle use phase. A stationary analysis will be done to compare the potential CO_2 emissions by operating point and later a driving cycle assessment will be done for the final LCIA.

Exhaust emissions for the LCA are modelled considering the engine-out results measured for the the drop-in and optimized calibrations showed in previous chapters. The TTW CO_2 emissions are calculated assuming complete combustion, thus all HC and CO emissions are accounted for in the CO_2 emissions. For the complete combustion calculations, equations 1 and 2 are used. k_{CO_2} is the coefficient for one unit mass of CO_2 per one unit mass of fuel based on the m/m proportion of carbon $y_{C_{fuel}}$ in the fuel; M_C and M_{O_2} are, respectively, the molar massses of carbon and oxygen; and m_{CO_2} and m_{fuel} are the CO_2 and fuel mass.

$$k_{CO_2} = y_{C_{fuel}} \cdot \left(\frac{M_C + M_{O_2}}{M_C}\right) \qquad \text{Equation 1}$$

$$m_{CO_2} = k_{CO_2} \cdot m_{fuel}$$ Equation 2

Partially, the high efficiency of diesel oxidation catalysts (DOC), which can achieve above 90% efficiency [66, 67], supports the hypothesis that complete oxidation of fuel after the engine is feasible. This consideration is also one of the more stringent CO_2 scenarios, although speciation of the unburned HC could have increased impact factors in some of the evaluation categories. For example, in GWP methane (CH_4) has an impact factor of 34 kg CO_2-eq/kg and, for HTPc, formaldehyde has a 57.4 kg 1,4-DCB-eq/kg impact factor; nonetheless ongoing work in the research group indicates that for the tested LCFs the proportion of the uHC for these species does not surpass values of 2-5% and 2-9%, respectively and depending on the operating condition. Table 7 displays the final TTW CI under the assumption of complete combustion.

Table 7. Tank-to-wheel carbon intensity for the different fuels assuming complete combustion

Fuel Name	Tank-to-wheel carbon intensity (g_{CO2}/g_{fuel})
Ref. Diesel	3.15
LCD100	2.79
LCD66	2.91
LCD33	3.04
MaxOME66	2.80
MaxOME33	2.92
R33	3.13

Sulfur oxide emissions are modelled assuming all sulfur in the fuel is converted to sulfur dioxide (SO_2), and exhausted from the vehicle [68]. And nitrous oxides (N_2O) are modelled according to ongoing Fourier-transform infrared spectroscopy (FTIR) measurements from the research group. Non-exhaust emissions (road wear, tyre wear and brake wear [38]) are not modelled in this study, concentrating instead in the engine emissions which better showcase the differences between the evaluated LCFs. Stationary impact of LCFs in an internal combustion engine

It should be commented that to increase the allocation in the PMFP impact category for the TTW in the vehicle usage phase, all the soot emissions are modelled as PM2.5. The soot emissions were considered without an aftertreatment system, but

with the inclusion of one would be lower. Similarly, as NH_3 emissions were not recorded during experiments, values for this pollutant were approximated from the diesel case shown in [69], which uses an Euro 6b vehicle with a 2L engine and complete aftertreatment system (three-way catalyst (TWC); diesel oxidation catalyst (DOC); diesel particle filter (DPF); selective catalytic reduction (SCR)).

2.2.4.1 Driving cycle impact of LCFs in an internal combustion engine

The vehicle described in Section 2.1.1 is modelled in GT-Power to evaluate different driving cycles and their effect in the total emissions and fuel consumption, and later in terms of the GHG impact and other impact categories of interest. As peviously said, the vehicle emissions will be reported in terms of engine-out instead of taking into account the effect of aftertreatment systems (ATS), characterizing the worst-case scenario for emissions. This approach is justified as it provides a conservative estimate of the vehicle's environmental impact.

The vehicles are evaluated under the WLTC, which is a laboratory tests included in the current European standard for characterization of fuel consumption, pollutant emissions and CO_2 for light duty vehicles [70] which complements the Real Driving Emissions (RDE) test of Euro 6 and recent Euro 7 [71]. The cycle was selected because it covers different driving characteristics (as seen in the vehicle speed profile in Figure 5) that allows to observe a large range of the vehicle operating conditions.

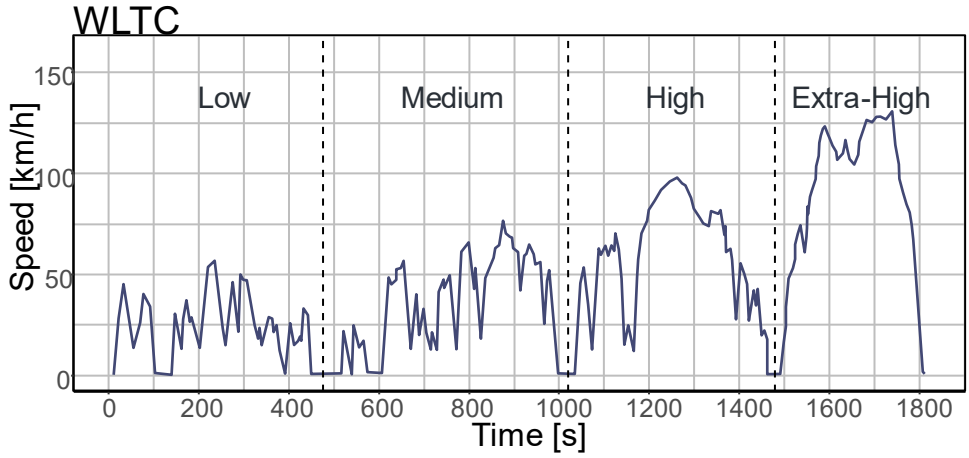

Figure 5. Speed profile for the class 3b WLTC

For the GT-Power simulations, engine maps for the fuel consumption and emissions must be introduced. During this work, engine maps[1] were measured exclusevely with diesel due to the inavailbility of sufficient quntities of LCFs for such tests. As such, a novel methodology was formulated [72, 73] and employed to estimate a simplified engine map using data obtained from the five stationary operating conditions that were optimized and measured. Given the range of loads and speeds for the tested operating conditions, they can be considered representative of the engine operation. This methodology allows for the incorporation of LCFs into engine simulations and the consequent evaluation of their performance characteristics.

The simplified engine map is obtained by first discretazing the diesel's engine map into equally sized bins of speed and load. The dimension of the speed bin is 150 rpm and covers the range from 1000 rpm to 4000 rpm (similarly to the measured speeds of the diesel map), while the load is separated every 5 bar of BMEP. The 5 bar of BMEP bin is selected because it is a sufficiently large size to capture significant changes in the engine's responses in terms of fuel consumption and emissions, while remaining narrow enough to differentiate between individual operating conditions. This also provides that not two operating conditions from the 5 point set fall inside the same load ribbon across the whole map.

Using the measured operating conditions as centroids, multiple bins are consolidated to form larger bins to encompass all operating conditions. The minimum bin sizes at this stage are 2000 rpm and 10 bar of BMEP. Due to the distribution of the measured points predominantly below 2000 rpms, the upper speed bin size limits are defined by the nearest adjacent boundary (in this case at 3000 rpm). During this stage, overlapping may be exhibited between regions and is desired for the later stages of the methodology.

To resolve the overlap between bins and to assign a unique area to each centroid, the regions that overlap are split into two at the diagonal of the overlapping area, resulting in the delimitation of five separate regions within the engine map. At this stage, although there are five regions that represent a significant proportion of the engine map, the map is not completely defined as there remains an unassigned region. To determine how will this area be represented in the simplified map, the closest defined areas are extended direction of the unassigned area until reaching the limits of the map. Then resulting area overlaps are resolved as previously explained.

[1] Engine maps in this work consist of 42 stationary operating conditions. Measurements are taken every 500 rpm (from 1000rpm to 4000rpm) at 10, 25, 50, 75 and 100% of the maximum engine load at any given speed.

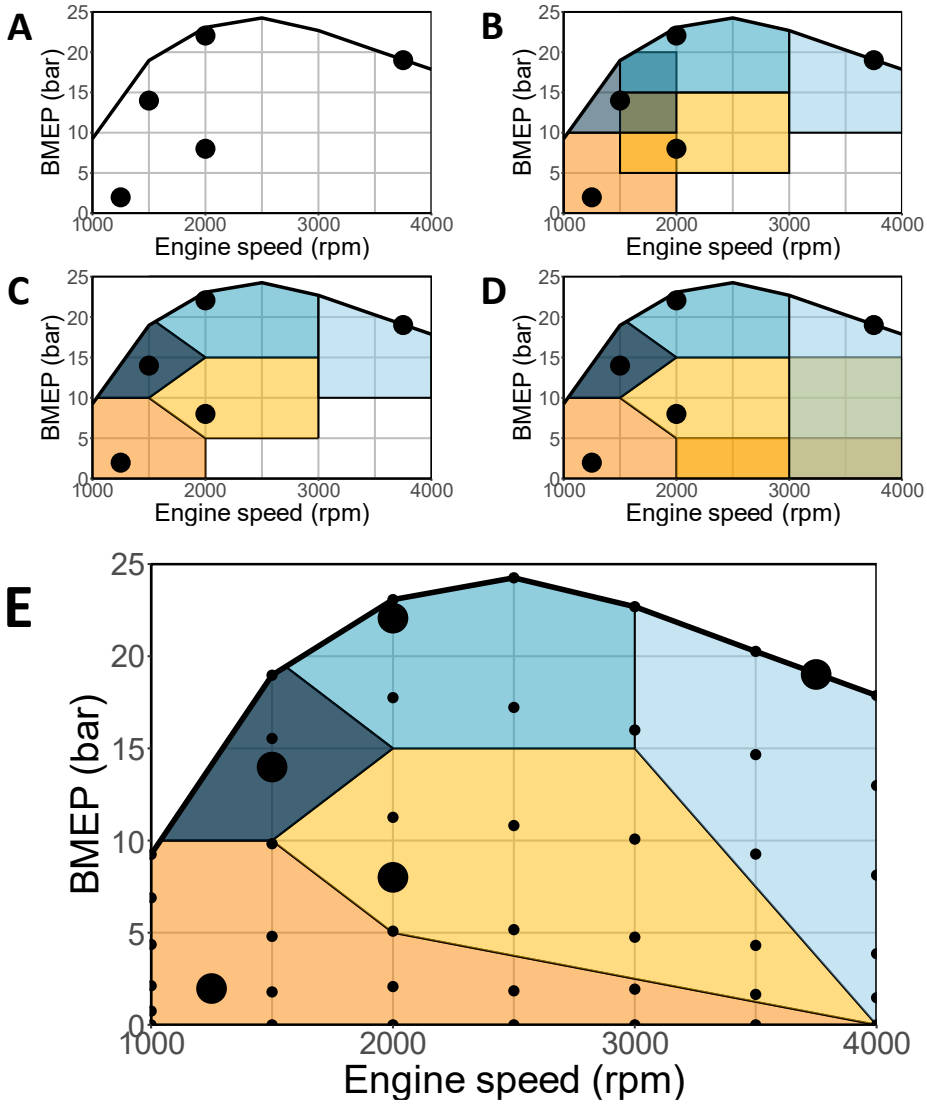

Figure 6. Engine map discretization schematic

This approach effectively allows for the assignment of unique areas to each of the centroids and facilitates a simplified understanding of the engine's operating characteristics with only a few measured and distributed operating conditions. Once the five engine areas are defined the fuel consumption and emissions of the larger engine map are associated with the value of the centroid to which they correspond,

while the operating conditions that happen to fall in the interphase between areas is assigned the average of the adjacent centroids. The summary of the methodology described can be observed in Figure 6.

Finally, a BSFC criteria is applied for the reference diesel to each of the operating points inside each region. The BSFC criterium is considered because fuel usage has one of the most significant CO_2 impacts and exceeding the proposed limit would yield higher inaccuracies when estimating the driving cycle results. As can be seen in Figure 7, in most of the map the difference does not exceed 30% and a significant portion remains under 15% difference. The only regions where the BSFC exceeds 30% difference are near the extremes of the maps at low loads. Something to consider is that the simplified map seems to generally estimate higher BSFC values, which later will result in higher total CO_2 estimation, showing a probable worse case than what would happen with the complete map.

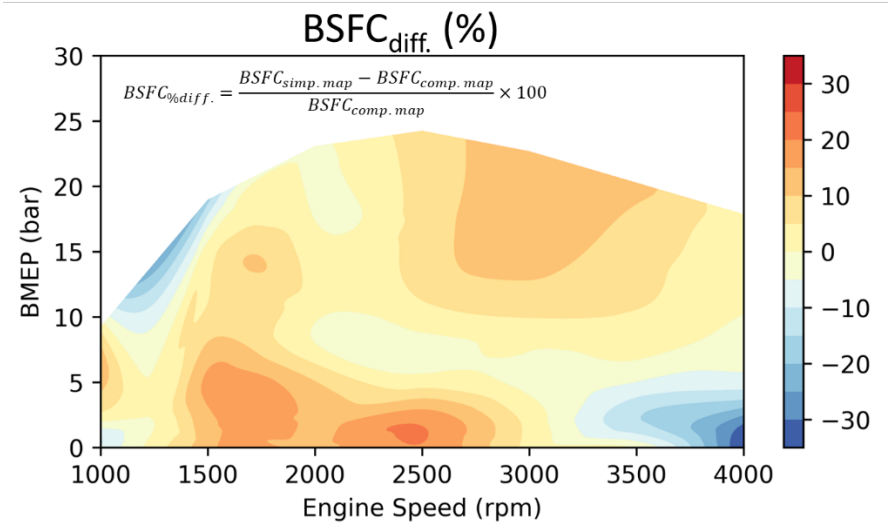

Figure 7. BSFC difference between the complete and simplified engine maps for the reference diesel fuel

To provide a reference for the brake-specific emissions included in the LCI the variation between the complete engine map and the simplified engine (Equation 3) map is shown in Figure 8. In the equation, BSE is the brake-specific emission considered.

$$BSE_{diff.} = BSE_{simp.\ map} - BSE_{comp.\ map} \qquad \text{Equation 3}$$

For the NOx emissions it is observed that from nearly 2 bar to around 12 bar of BMEP and under 3000rpm the simplified map underpredicts the observations of the complete map by an average of 1.5 g/kWh, while above 3000 rpm an overestimation of nearly 3g/kWh is ocurring. The NOx differences are significative as targeting NOx reduction is one of the key objectives of this thesis, additionally, NOx are one of the emissions that affect the PMFP and TAP characterization factors. Because of this, a corrective coefficient will be implemented after the driving cycles in the total cycle NOx emissions (Table 8) in order to provide representative results of the engine-out criteria during the LCA. A similar treatment, is done for the soot emissions.

Other approaches, like cluster analysis [74] and kernel interpolation [75], were considered but given the high correlation between speed, load and the resulting emissions and the fuel consumption responses, as well as the limited sample of operating conditions for the LCFs, the described simplified spatial distribution approach was selected. The engine map simplification is then applied to the seven LCFs tested under both the drop-in calibration and the optimized calibration. This simplified engine map characterization, although easy to implement, serves to provide an estimate of the emissions potential considering different engine power demands that could be obtained during driving conditions, while simultaneously providing an evaluation standard to compare the effect LCFs considering different types of vehicles.

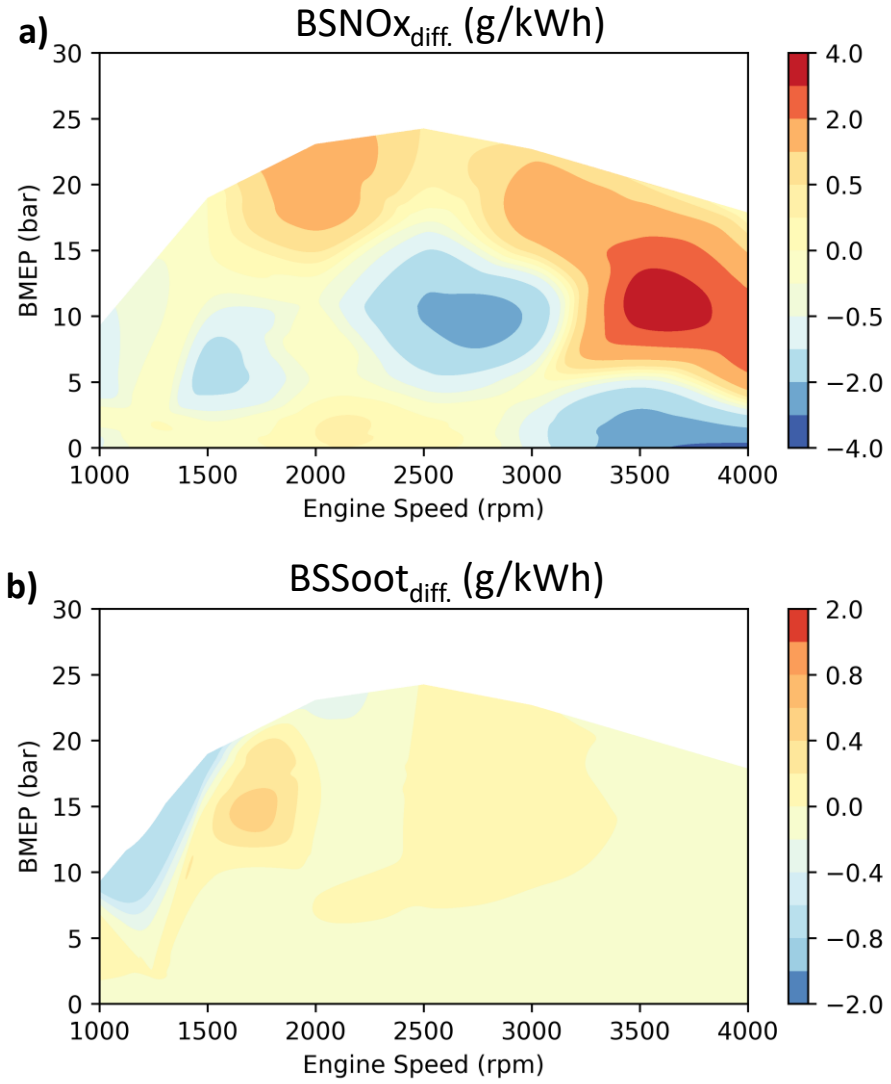

Figure 8. Difference in the BSNOx between the complete and simplified engine maps for the reference diesel fuel

2.2.4.1.1 GT-Power vehicle modelling

The simplified engine maps were used in a GT-Power model to estimate the driving cycle results for the vehicles in the mini, hatchback and sedan segment. GT-Power is a 1D engine simulation software that is widely used in the automotive industry to simulate engines and vehicles for performance and emissions analysis [76]. The

schematic shown in Figure 9 illustrates the model characteristics and the different subassemblies to represent the different vehicle systems. Each of the subassemblies is customized according to the vehicle characteristics and gear changing strategies described in Table 1, to simulate the behavior of the vehicles as a complete system.

The complete engine map for the reference diesel and the simplified engine maps for the fuel consumption and emissions are inputted into the "Engine" object. This module preprocesses the introduced maps by performing a grid interpolation to create continuous data look-up tables in terms of the load, speed, fuel consumption and emissions that will be used to reach the power demands during the driving cycle. In turn, the "Vehicle" module contains the vehicle information in terms of weight, wheelbase, tires, drag and area, rolling resistance and system strategies. In addition, the module also includes the passenger and cargo information, which in this work is defined as a single driver of 75 kg of weight.

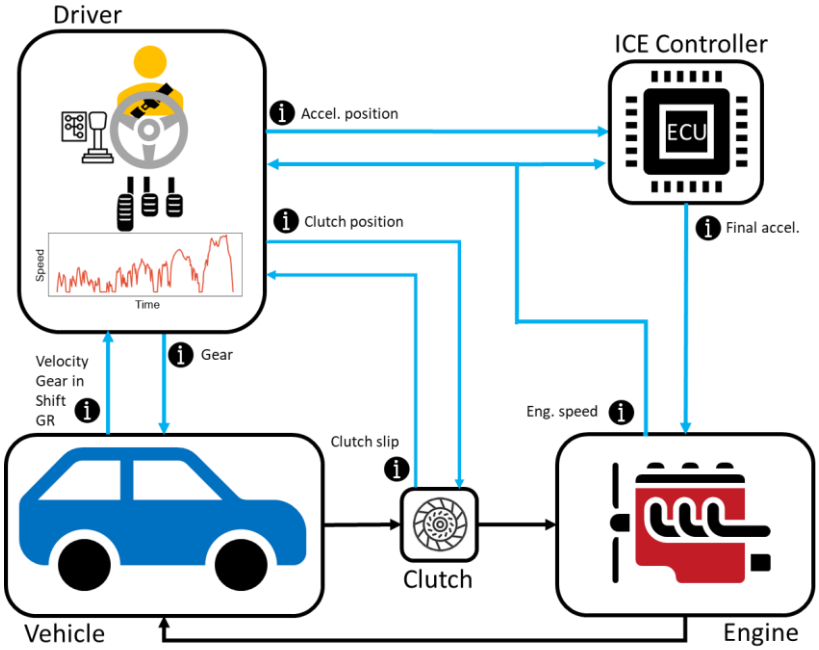

Figure 9. GT-Power vehicle model schematic

The "Driver" object simulates the control system for the accelerator pedal. Specifically, it is a PID controller that adjusts the position of the accelerator in response to the speed and load demands. This allows the engine to maintain the desired speed or power output during the cycle simulation for all the vehicles, fuels

and calibrations modelled. To adhere to the vehicle speed and load profiles of the driving cycle, the driver mode was configured for speed targeting. The simulation model then computes the BMEP and engine speed at each time step.

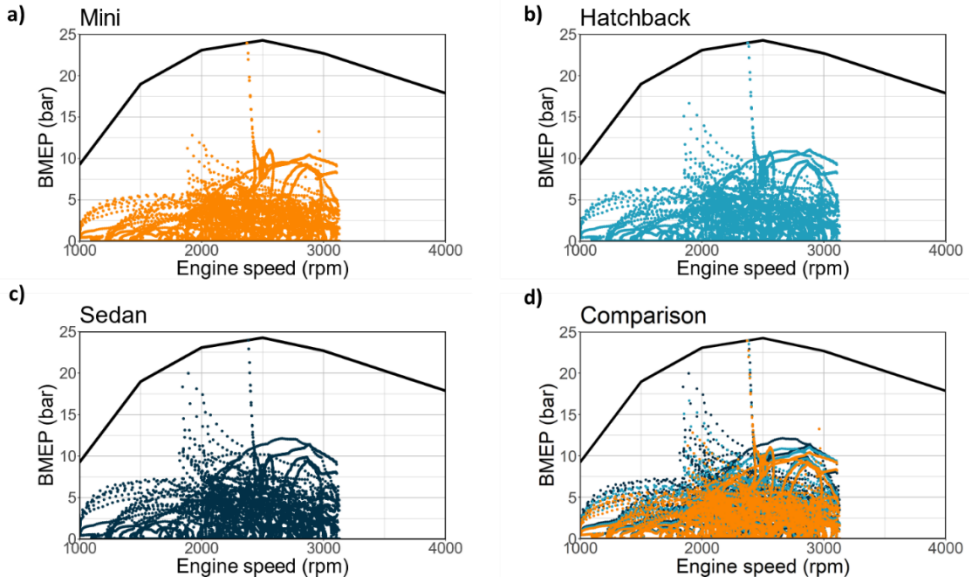

Figure 10. Distribution of the engine operating conditions during the WLTP cycle for different vehicle segments: a) Mini segment, b) Hatchback segment, c) Sedan segment and d) comparison between segments

Figure 10 shows the distribution of the engine operating conditions during the WLTP cycle for the selected vehicle segments. Because during the simulation the shifting strategy is maintained constant between vehicles, the engine speed is similar for the three cases, while the small differences observed in the load can be associated to the vehicle weight, drag coefficient and friction. The sedan, being the heaviest vehicle, has a higher engine load demand (easily observable near the 1800 rpm region). These engine operating condition patterns remain constant across fuels, as the load and speed required from the engine is independent of the fuel.

Based on the analysis of the operating conditions in the WLTP cycle, it can be concluded that the simplified cycle will overestimate fuel consumption by approximately 10%, as the average difference in BSFC in the region of the map under 3000 rpm suggests. Additionally, the simplified cycle will likely underestimate NOx emissions. As previously noted, the higher fuel consumption predicted by the simplified map represents a worst-case scenario, meaning that the resulting CO_2 LCA estimations will be more conservative than the probable real-

world scenario. As such, no correcting coefficient will be applied to the fuel consumption results, nonetheless for the NOx and soot emissions if the total WLTC value is inferior for the simplified map, a corrective coefficient will be applied to all fuels.

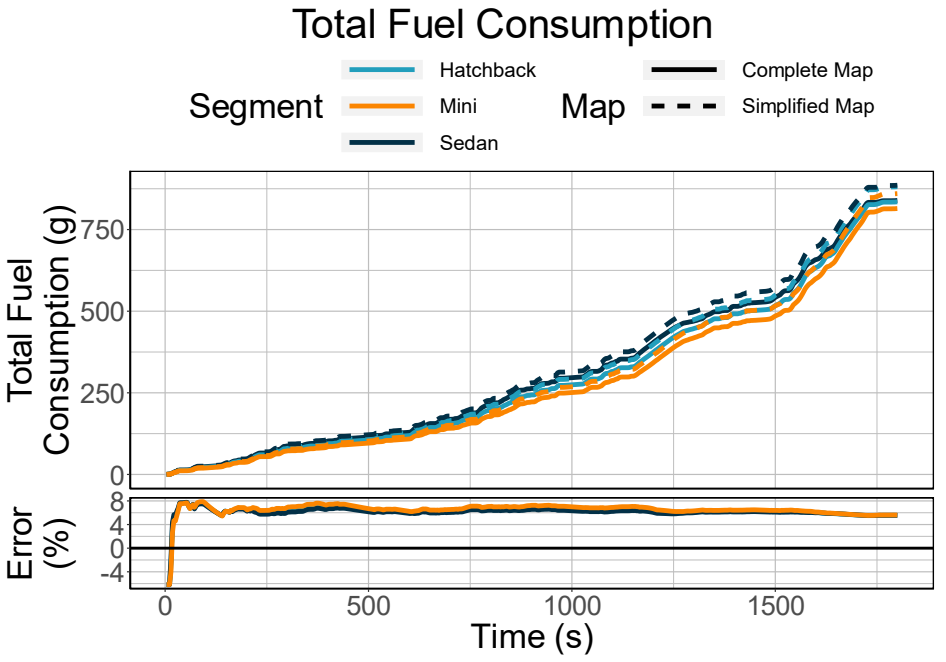

Figure 11. Cycle fuel consumption comparison between the complete and simplified engine map

Figure 11 shows the cumulative fuel consumption during the WLTC for both the complete and simplified map with the diesel reference fuel. In the top of the figure, it can be seen how the simplified map (dashed lines) is constantly higher than the complete map; while the bottom of the figure shows the error which at the end of the cycle is nearly 5.5% for the three vehicles (calculated as the difference between the simplified map and the complete over the value of the complete map).This higher fuel consumption value for the simplified map fulfills the requirement from the LCA of selecting conservative estimations for fuel consumption and might compensate some of the known underestimation of these types of laboratory cycles and simulations with respect to real driving values [36].

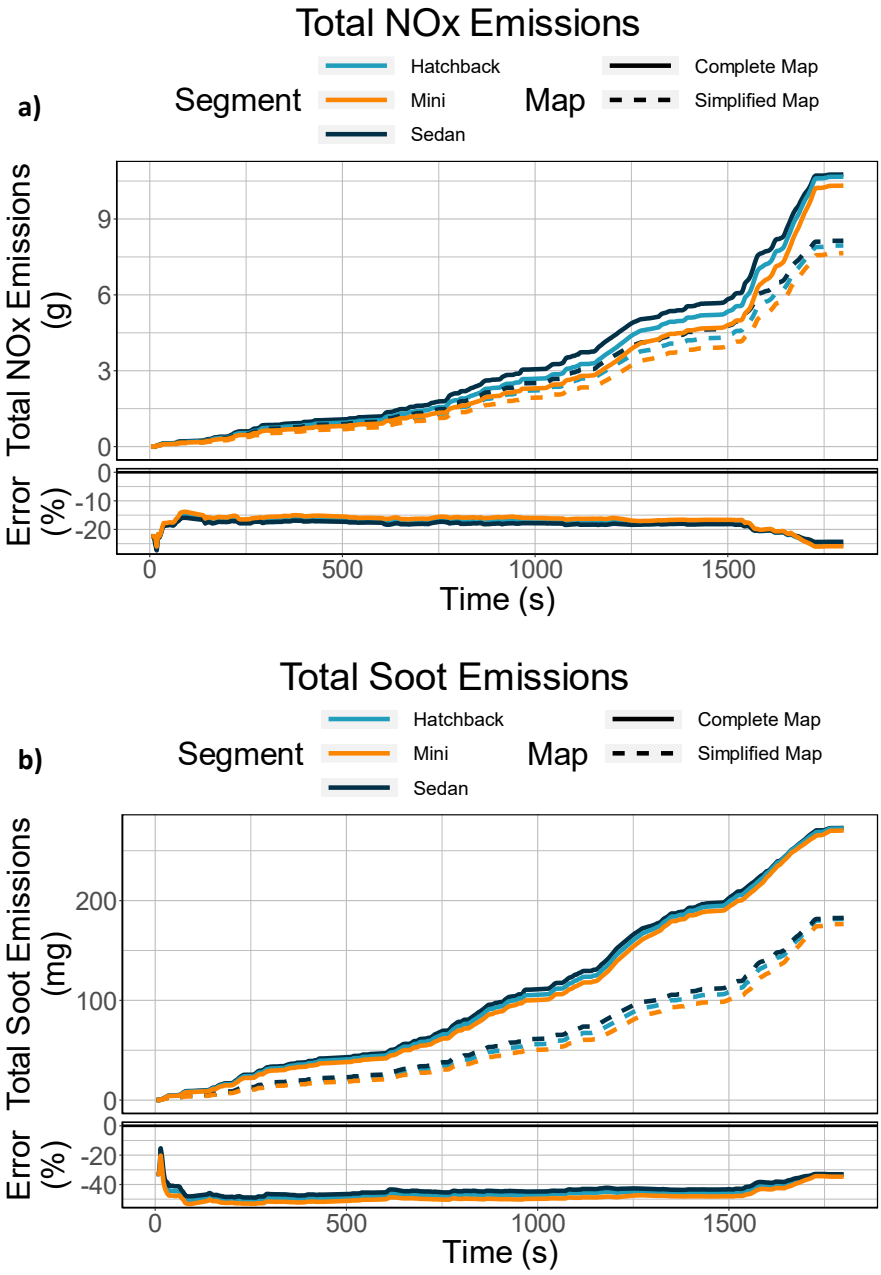

Figure 12. Cycle NOx (a) and soot (b) emissions comparison between the complete and simplified engine map

Figure 12 shows the cumulative NOx and soot emissions for the cycle. Where it can be seen that while the complete map has a total of nearly 10.5 g of NOx and 260 mg of soot at the end of the cycle, the simplified map underestimates the results by around 25% for the NOx emissions and 33% for the soot emissions. This cycle error is what is corrected for the LCI of the use phase regarding the emissions following Equation 4; where $c_{correction}$ is the coeffient of correction which is applied depending on the vehicle as described in Table 8.

$$E_{cycle} = c_{correction} \cdot E_{simplified\ map} \quad \text{Equation 4}$$

It should be recalled that the emission correction is to ensure the occurrence of the worst case scenario during the LCA, especially as reported efficiencies for DPFs and SCR range from 70-95% [77, 78], which could make the real driving emissions be lower than the results from the complete map.

Table 8. Emission correction coefficients for the WLTP cycle using simplified engine maps

	Segment		
Emission	Mini	Hatchback	Sedan
NOx	1.26	1.26	1.24
Soot	1.35	1.33	1.33

3 Impact assessment of low carbon fuel use in light-duty vehicles

The outcomes from the three modelled vehicles are evaluated for engine-out stationary conditions, driving cycle WTW and finally the cradle-to-road LCA. The LCIA methodology presented in the previous sections was used to calculate the environmental impact indicators, including GWP, TAP, PMFP and WCP. The results provide valuable insights into the environmental performance of each vehicle segment and highlight the key findings and implications for the use of LCFs in ICEVs.

3.1 Stationary assessment

For the stationary results, Figure 13 and Figure 14 show the TTW and WTW CO_2 emissions for the five operating conditions tested and optimized in previous chapters. The results are presented for both a drop-in and an optimized calibration. TTW differences are relatively small between fuels, this is because although the fuels that have the least proportion of carbon should have a smaller TTW CO_2

footprint, in previous chapters it was observed that this property increased considerably the fuel consumption; thus, limiting the potential CO_2 reduction at this stage. Nonetheless, all the tested LCFs show smaller TTW CO_2 for the drop-in calibration and in the optimized for NOx reduction calibration only a small increased with respect to diesel is obtained for very few operating conditions and fuels.

It is also observed on Figure 13, how the lowest load operating condition has the highest TTW CO_2 emissions, which as seen in Figure 6 E is translated into the higher overall cycle emissions given the representativeness of the operating point in the simplified engine map.

WTW CO_2 emissions show the benefit of including larger proportions of renewable content in the fuel. The reduction of WTW CO_2 is proportional to the WTT CI (Table 6). The fuels with the larger renewable content (RE100 and LCD100) show the biggest reduction with respect to diesel, with LCD100 having values as low as 27.3 g/kWh of CO_2 for the drop-in calibration. Nonetheless, none of the fuels reach carbon neutrality.

Stationary results for NOx and soot emissions are not included in this section due to them being presented and discussed in previous chapters.

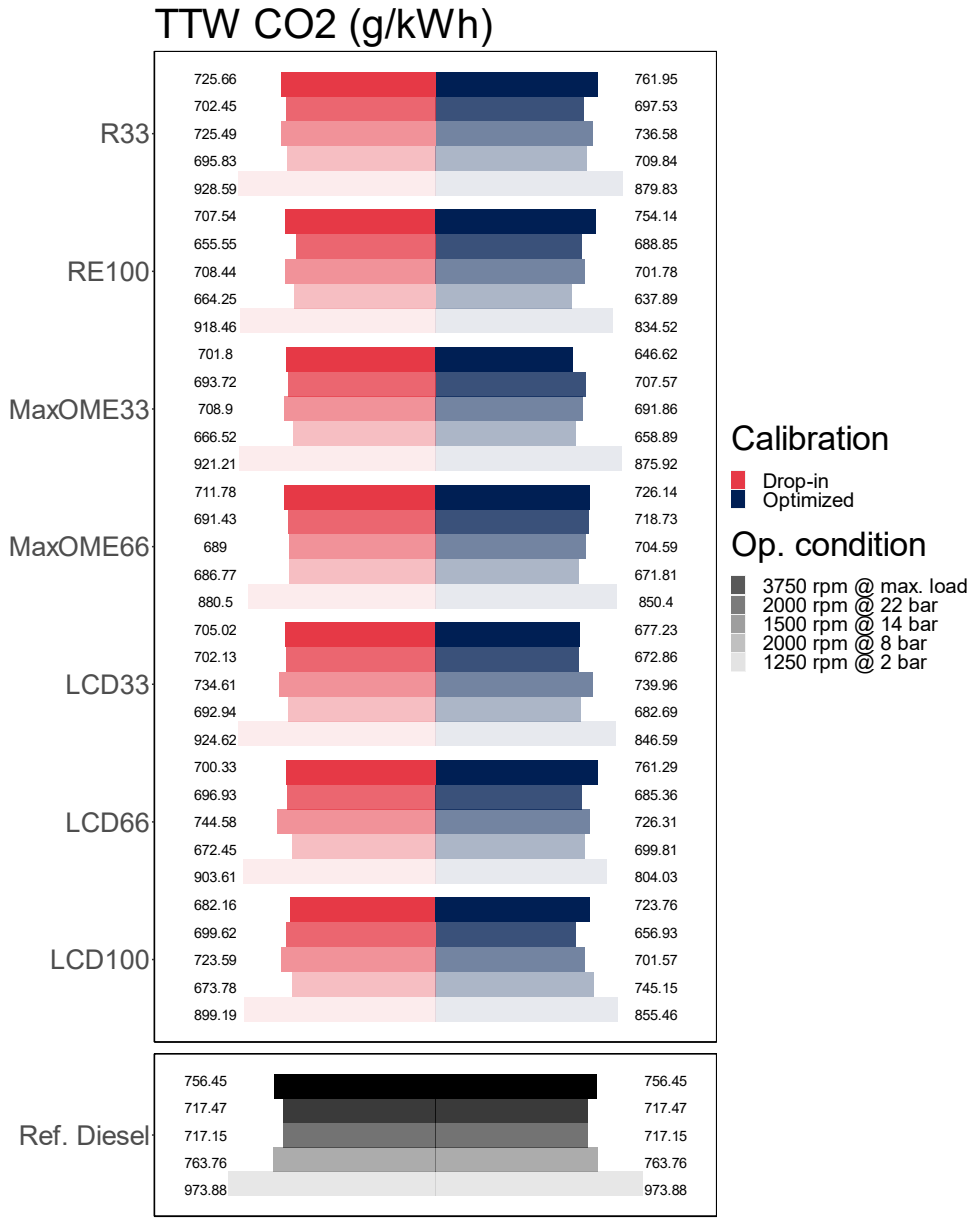

Figure 13. TTW CO_2 emissions for the stationary operating conditions

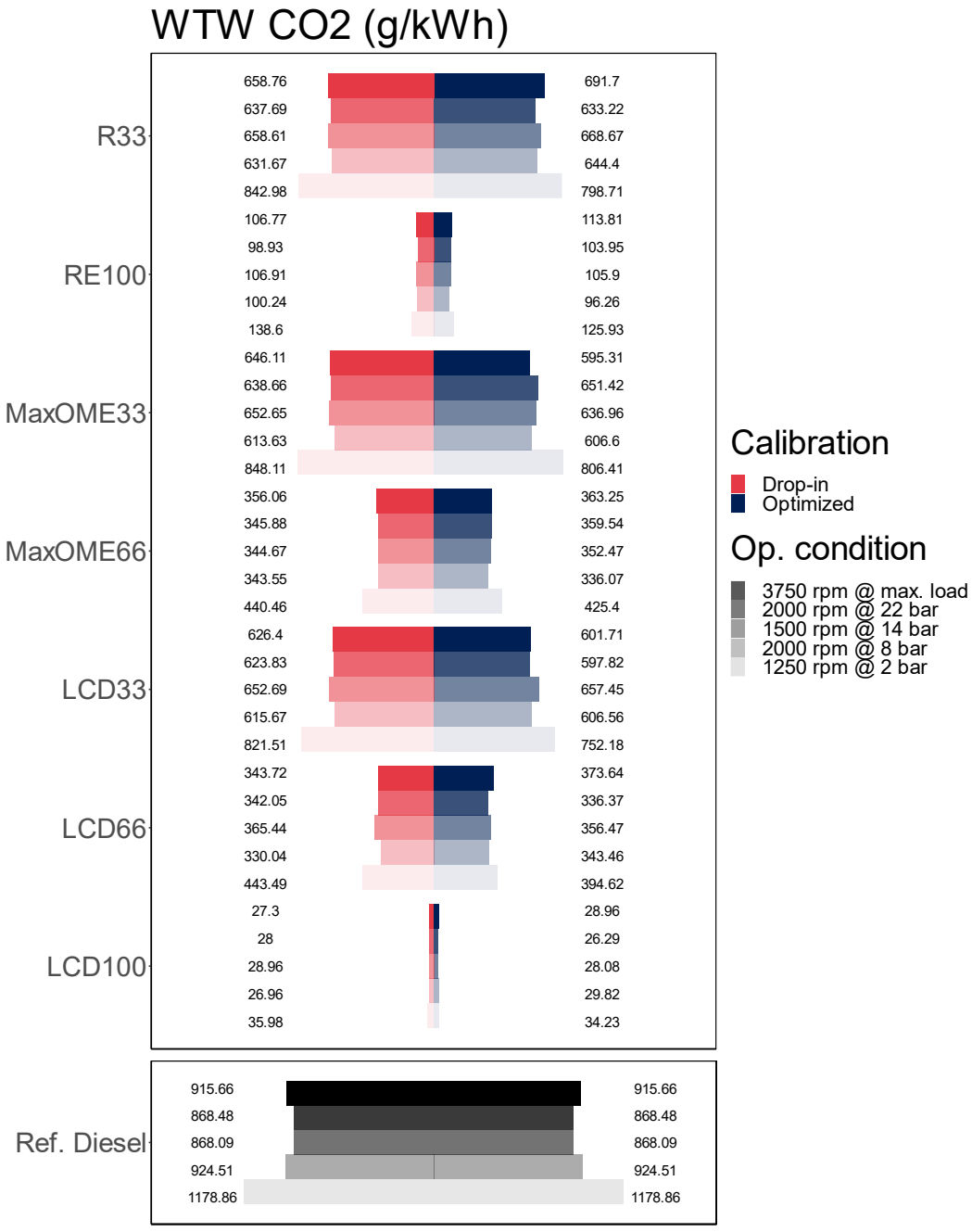

Figure 14. WTW CO_2 emissions for the stationary operating conditions

3.2 Driving cycle assessment

The WLTC results are presented in this section under the 1 km FU, except for the fuel consumption which is presented as L/100 km per industry standard.

As described previously, the fuels with the lowest carbon content show increased fuel consumption due mainly to their lower energy density (Figure 15). This is notable for the MaxOME66 and the LCD100, which have respectively a near 10% and 7% increase with respect to the diesel reference. Regarding the type of vehicle, it also needs to be commented that size matters, with smallest vehicle showing a better fuel efficiency than the larger vehicles, as the hatchback and the sedan have similar fuel consumption values regardless of the difference in their vehicle weight. The similarity in the fuel consumption of the hatchback and the sedan might be explained by the relation of the drag coefficient to the weight of the vehicle, which is more favorable for the sedan.

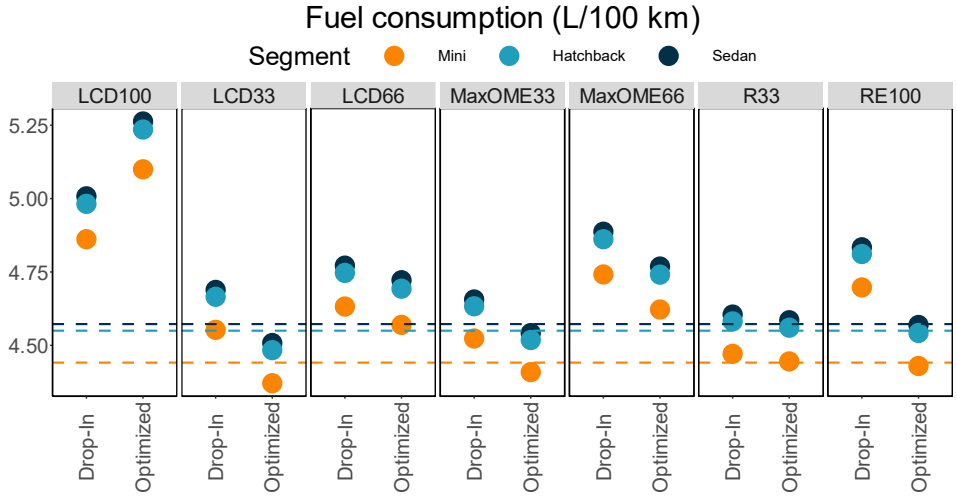

Figure 15. Vehicle operation fuel consumption in liters per 100 km. The dashed lines represent the reference diesel result

Directly conditional on the fuel consumption, Figure 16 shows the WTT, TTW and WTW CO_2 emissions for the cycle. These emissions, like the stationary results show higher improvement the higher the carbon negativity of the fuel production is. Again, with the LCD100 and the RE100 showing values that are close to 0 g/km, but not quite reaching the target. Regardless of not being net 0, in WTW CO_2 emissions all fuels show a reduction, independently of the vehicle and calibration, of at least 40 g/km of CO_2 with respect to the diesel reference.

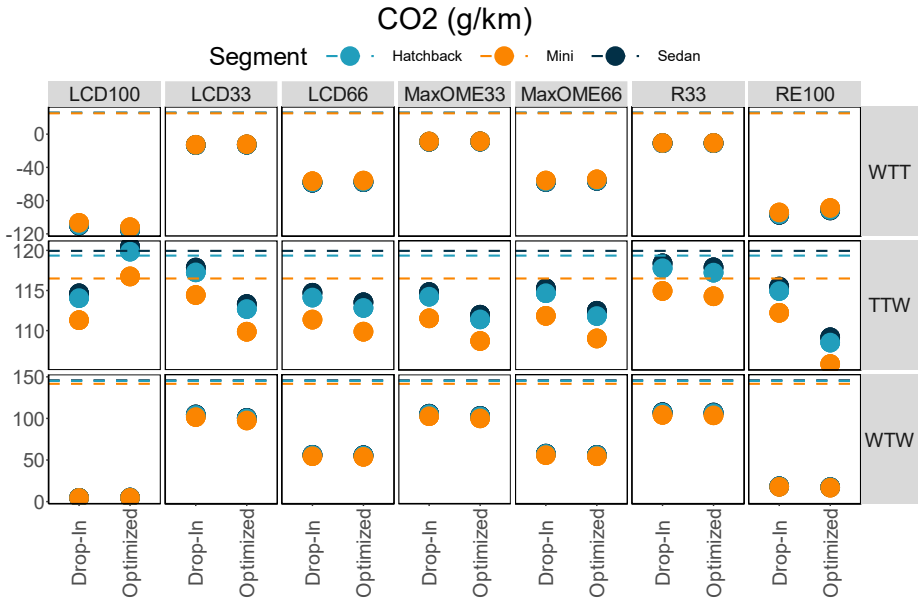

Figure 16. Vehicle operation CO_2 emissions per km. The dashed lines represent the reference diesel result

The NOx emissions in Figure 17 show the highest dependence to the calibration used during the cycle, with the optimized calibration decreasing the cycle NOx emissions for most of the LCFs by nearly half. The vehicle selection, in turn, has a slight impact on the cycle NOx emissions with the weight of the vehicle being directly proportional to the NOx result, the magnitude of the effect is considerably smaller with respect to the calibration effect. Later, when assessing the impact categories with NOx emissions contributions this too will be reflected.

In terms of NOx, not all LCFs have benefits with respect to diesel. Particularly, during the drop-in calibration due to LHV being significantly lower than diesel's, fuels like the LCD100 and the MaxOME66 have unbefitting engine settings (Chapter 4) that are related to increases in NOx emissions.

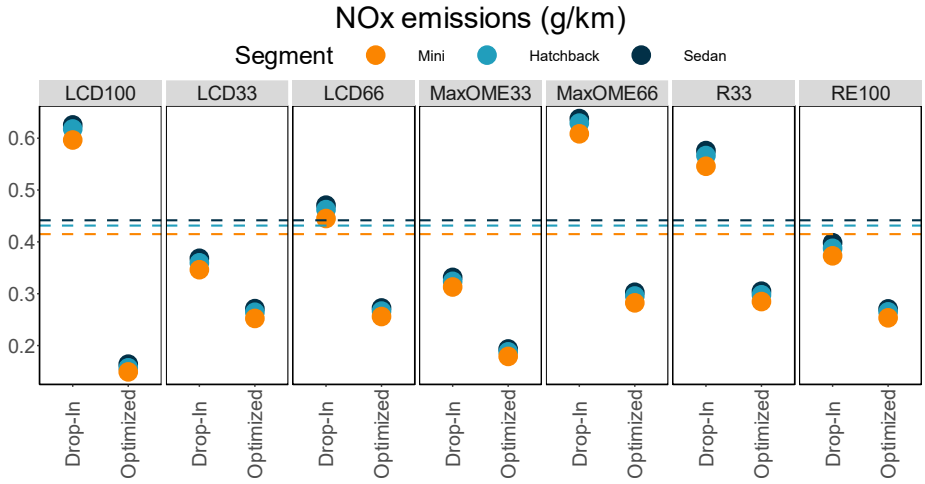

Figure 17. Vehicle operation NOx emissions per km. The dashed lines represent the reference diesel result

Finally, the soot emissions also show high dependency on the used calibration, with the optimized calibration outputting higher emissions. It is worth noting that even without the consideration of a DPF, soot values are relatively low. The LCD100 and MaxOME66 fuels reach admissible Euro 6 limits (5 mg/km) without the addition of an ATS for the drop-in calibration and MaxOME66 fulfilling this condition even for the optimized calibration. Only the R33 fuel emits higher soot masses than diesel for both calibrations, which as seen in previous chapters might be a combination of the higher LHV of the fuel with a low oxygen content.

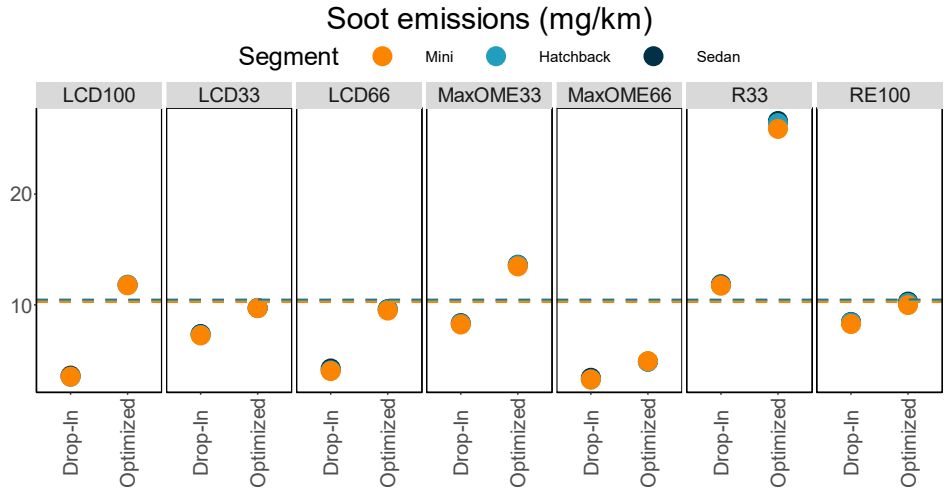

Figure 18. Vehicle operation soot emissions per km. The dashed lines represent the reference diesel result

3.3 Cradle-to-road impact assessment

This section, following the interpretation stage of the ISO 14040 and ISO 14044, provides a detailed account of the outcomes obtained from the LCA, including the environmental impacts and potential trade-offs associated with the vehicle's life cycle. The focus of the section is to present a comprehensive picture of the environmental performance of the vehicle under the selected impact categories (GWP, TAP, PMFP, HOFP and WCP), and draw insights on the sustainability profile of the tested LCFs as fuel replacement for ICEVs.

The yearly progression of the GWP impact category can be seen in Figure 19 for the three studied vehicle segments with the evaluated LCFs and diesel as the baseline reference. On the 0^{th} km only the vehicle's manufacturing has a CO_2eq footprint, while as the years progress an almost perfectly linear increase can be seen for all the 45 fuel-vehicle cases. Only minuscule non-linear increases can be observed between at 30000^{th} km, 60000^{th} km and the 90000^{th} km, which correspond to the tire replacements, while the rest of the maintenance duties cause almost negligible GWP increases as their periodicity is higher and their impact lower. Then, the linear increase is mainly due to the impact of the vehicle use or the WTW, which was calculated assuming no changes in the fuel production technology and no efficiency losses or malfunction from the ICEV, therefore the WTW is maintained constant though the years.

In Figure 19 and Figure 20 the benefits of renewable fuels, and more so, of the carbon negativity of the fuel production process can be observed. The trends are independent of the vehicle, the LCD100 and RE100 fuels have the smallest GWP impact, with the LCD100 emitting almost 2 Ton CO_2eq less in year 10 than the RE100. This difference is important because both fuels are completely renewable, but -8.88 gCO_2/MJ WTT CI less of the LCD100 in the aggregated impact of 10 years is translating into a significantly smaller amount of CO_2eq than the RE100. The partially renewable fuels, have smaller differences between the ones with the same proportion of renewable content; the fuels with 66% of renewable content (MaxOME66 and LCD66) having similar composition have almost identical GWP at the end of the 10 years, and the ones with 33% renewable content (MaxOME33, LCD33 and R33) only show a difference of less than 1% of the total CO_2eq mass.

Observing Figure 20, and the proportional effect of the different phases of the foreground system it is interesting to note that for the LCD100 and the RE100 more than half of the total GWP comes from the vehicle manufacturing and maintenance stages, and in fact for the LCD100 results (46-64 gCO_2eq/km depending on the vehicle segment) are lower in CO_2eq than those reported by Tesla in 2021 for their electric Model 3Y personal use vehicle in Europe (61.8 gCO_2eq/km for the solar charged and 79.5 gCO_2eq/km for the grid charged) [79]. Even the inclusion of N_2O (which has an GWP impact factor of 298 kg CO_2eq/kg) in the vehicle use LCI only increases the final WTW GWP by a maximum of 0.16 tons of CO_2eq for the RE100 and a median of 0.11 tons of CO_2eq for the rest of the fuels, which is around 1-2% of the life cycle GWP.

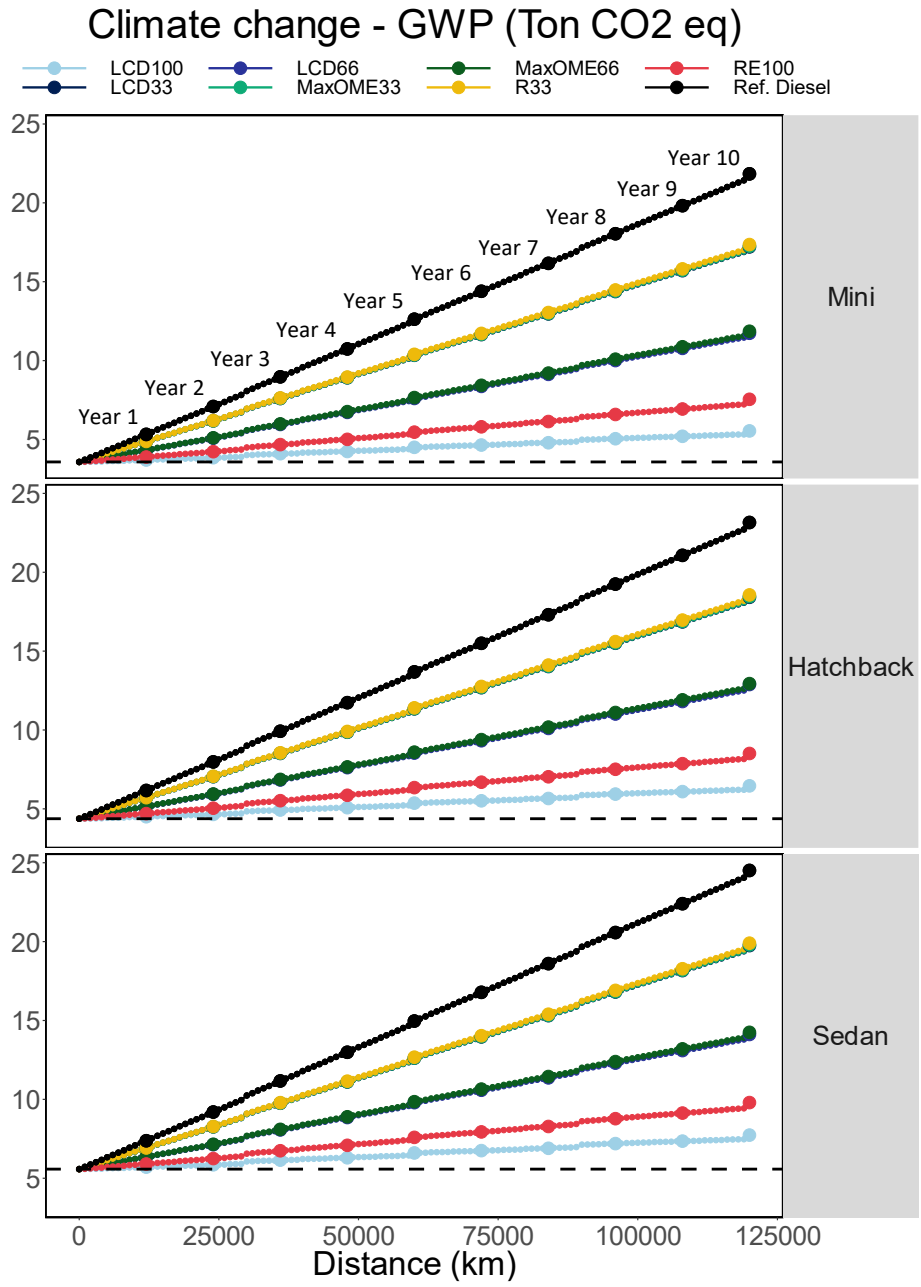

Figure 19. Life cycle GWP for three vehicle segments manufactured in 2023 using LCFs for 10 years or 120000 km

All the diesel fueled vehicles surpass the 180 gCO_2eq/km mark, while as the renewable proportion increases the ranges are 141-166 g gCO_2eq/km for the 33% renewable content LCFs; and the 66% renewable content LCFs have 97-117 gCO_2eq/km GWP impacts. Besides the LCD100, the only other fuel that reaches comparable values to an electric vehicle is the RE100 with a range of 62-82 g/km for the lightest to heaviest segment.

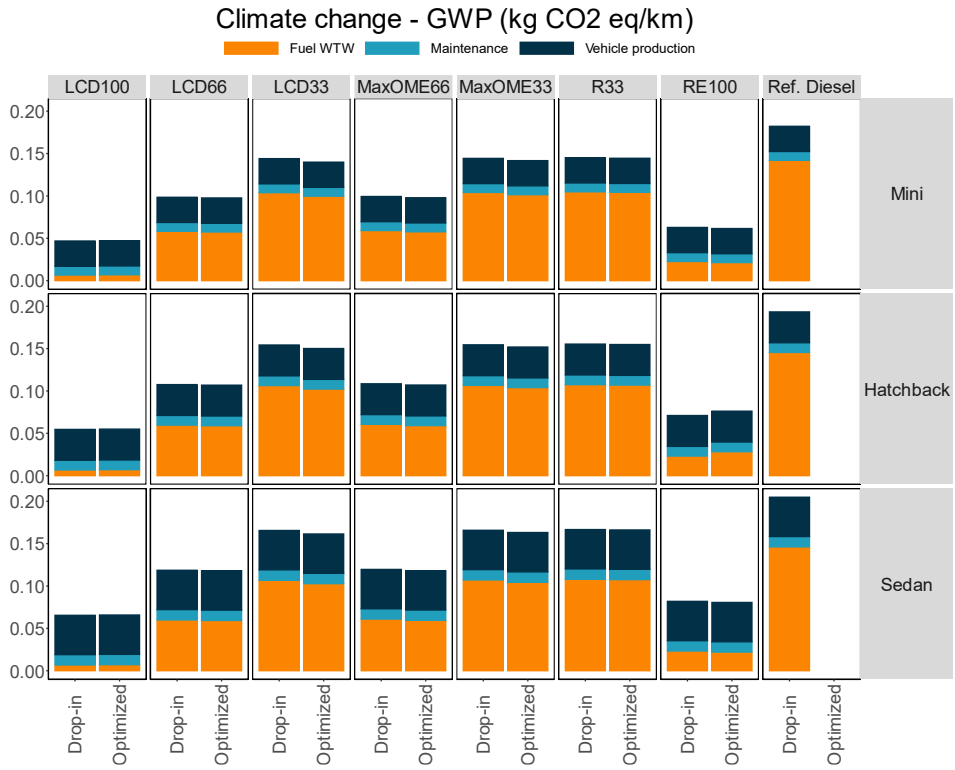

Figure 20. Summarized life cycle GWP for three vehicle segments manufactured in 2023 using LCFs for 10 years or 120000 km

For LCFs, considering more than just the reduction in CO_2eq between one fuel and the other can be highly important. As it was mentioned, LCFs can take advantage of CCU technologies for their reductions in GWP. Nonetheless it has been found, for 2012 technology, that the decrease in GWP derived from the use of CCU technologies can be linked with increases in other impact factors like AP, EP and HTP by as much of 150% from scenarios of not including CCU [80]. And that depending on the CCU technology used its GWP reduction will vary [81]. Then considering whether LCF produced using these technologies (like FT-diesel and

OMEx) can increase some impact factors becomes an important question in this study.

The TAP impact category affects the threshold for the deviation from the optimum acidity level of the soil for different plant species, which might cause changes in the species occurrence [82]. In other words, this could reduce crop yields, decrease soil fertility, and change the composition of plant and animal communities, which directly affect human life. Being the major acidifying species NOx, NH_3 and SO_2 [37], the evaluation of this impact criteria for diesel ICEVs is worth exploring considering that NOx emissions are one of the major problematics of diesel vehicles and NH_3 can be a product of a poorly managed aftertreatment system.

Figure 21 shows the TAP for the vehicles and the LCFs. The TAP values are comparable in magnitude with literature results [30, 60]. There seems not to be a fuel renewability degree specific trend, but with the fuels that emit more engine-out NOx. The WTW represents the gross of the SO2-eq emissions, which mainly come from the vehicle's TTW because for the WTT for the LCFs is mainly negative and for diesel is relatively small (0.03%). NOx, although having an impact factor of 0.36 kg SO_2eq/kg, are the main contributing flow at the TTW stage, which is why it is logical to see the strong favorable effect the optimized calibration has on the terrestrial acidification. The small sulfur content of modern fuels, makes the direct emissions of SO_2 from the vehicle use phase, relatively small and non-concerning with a maximum of 0.4 mgSO_2eq/km (or 0.1% of the SO_2eq emissions), while NH_3 adds up to 0.04 gSO_2eq/km.

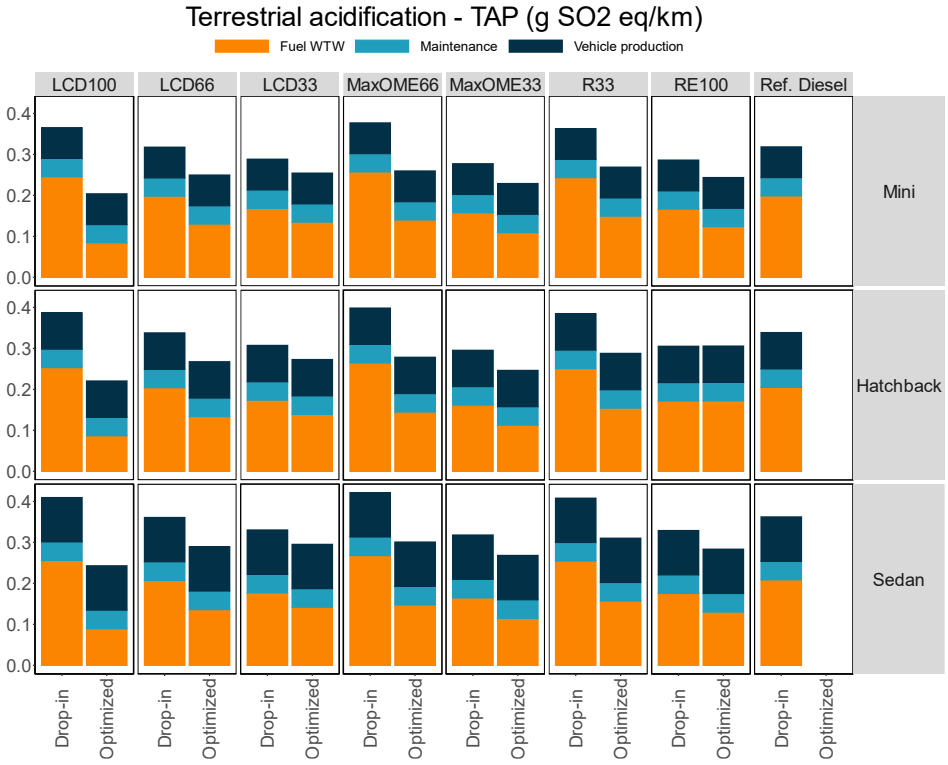

Figure 21. Summarized life cycle TAP for three vehicle segments manufactured in 2023 using LCFs for 10 years or 120000 km

A high PMFP impact factor has negative consequences to human health and the environment such as respiratory and cardiovascular diseases, like asthma, bronchitis, and heart attacks. Fine particulate matter (PM2.5) can penetrate deep into the lungs and even enter the bloodstream, causing inflammation, oxidative stress, and damage to the respiratory and cardiovascular systems [83]. Similar to NOx emissions, PM is one of the main known tradeoffs of diesel engines and, coincidentally, for the modelling of PMFP NOx emissions are also considered as a value choice flow [37]. This is the reason that even though soot emissions increased for the optimized calibration (Figure 18), the results from this impact factor are still lower than for the drop-in calibration. This could suggest an interesting change of paradigm for diesel ICEVs, where giving priority during calibration to the reduction of NOx emissions could have a larger positive impact than simply finding a balance between the NOx-soot tradeoff.

As with the TAP impact factor, there is no evident benefit from the use of renewable fuels, but a great benefit from choosing lower NOx calibration. Here, nonetheless is

worth restating that the LCA TTW emissions are modelled without ATS, and its addition would reduce the results here presented, as results for all LCFs would be closer to the 29 mg PM2.5-eq/km reported by [5], and not only the calibrated case for the LCD100.

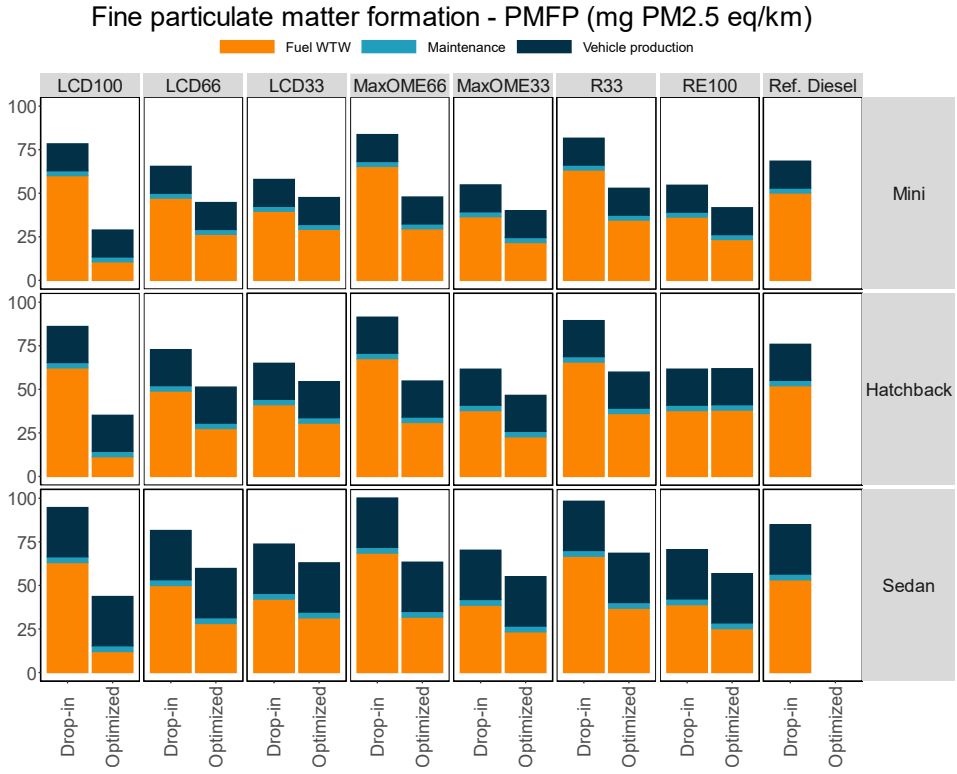

Figure 22. Summarized life cycle PMPF for three vehicle segments manufactured in 2023 using LCFs for 10 years or 120000 km

Ozone is formed through the photochemical reactions of NOx and Non-Methane Volatile Organic Compounds (NMVOCs), and its formation can inflame airways and damage lungs, making it a health hazard for humans [83]. The impact of ozone on human health is measured by the HOFP impact category through NOx-eq. Because of this, as with the other highly NOx dependent impact categories, the TTW stage of WTW is the single most contributing stage and is highly linked to the used vehicle engine calibration. And, contrarily to the previous impact categories, the impact of the vehicle manufacture and maintenance could be considered negligible in comparison to the WTW.

Although the renewable content has little effect on the impact factor; low-sooting fuel properties should be commended as alternative fuels are explored. Fuels like the LCD100 and MaxOME66, because they produce negligible soot due to their high OMEx (high oxygen) content, allow to reach calibrations with really low levels of NOx without sacrificing much the soot emissions; an advantage that later during the LCA study proves to increase the potential for the reduction of negative impact factors that can damage the environment and human health.

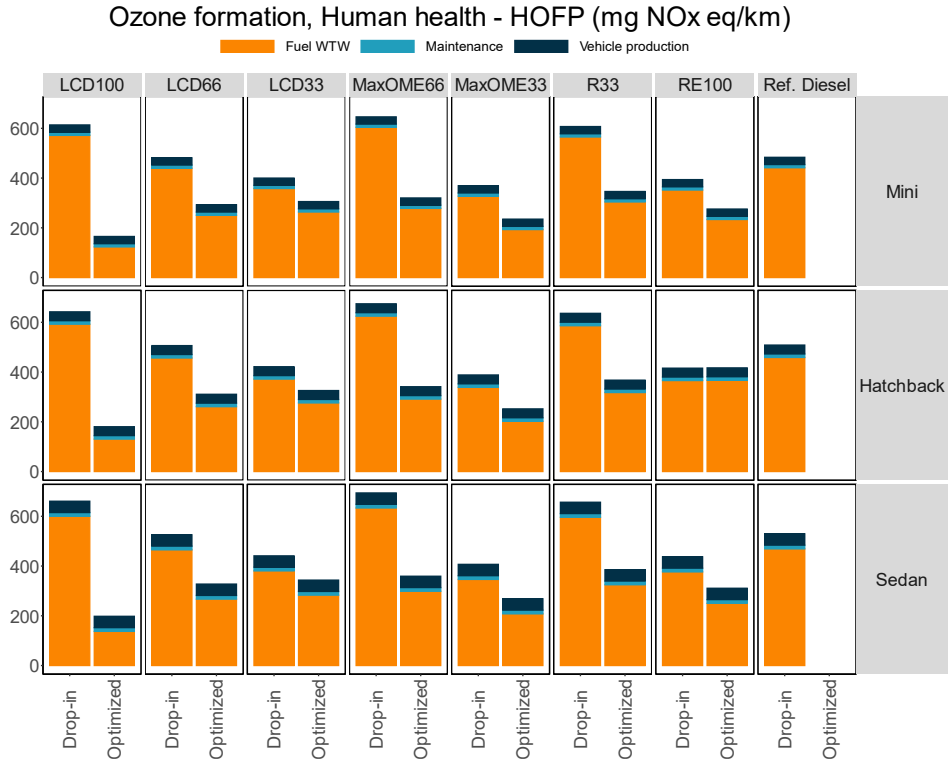

Figure 23. Summarized life cycle HOFP for three vehicle segments manufactured in 2023 using LCFs for 10 years or 120000 km

The final impact category to evaluate in this LCA study is the WCP, for which high values can reduce the availability of water resources for drinking, irrigation, and other essential uses, particularly in regions with water scarcity. High water consumption can also lead to reduced flow and quality of freshwater ecosystems, which can affect aquatic biodiversity and the ability of ecosystems to provide critical ecosystem services. In addition, competition over water resources can lead to conflicts between different users, including between farmers, industries, and urban areas.

For WCP, the origin of the LCF is of high importance. In Figure 24, synthetic LCFs with completely renewable, 66% and to some degree 33% renewable content show representative reductions with respect to the reference diesel. However, for the fuels with higher proportions of bio-diesel, particularly HVO waste oil show the importance of considering more than just the carbon footprint when regarding biofuels. Biofuel production can involve water-intensive activities such as irrigation, harvesting, and processing of biomass feedstocks. In contrast, the production of synthetic fuels typically involves less water-intensive processes, such as gasification, reforming, and Fischer-Tropsch synthesis.

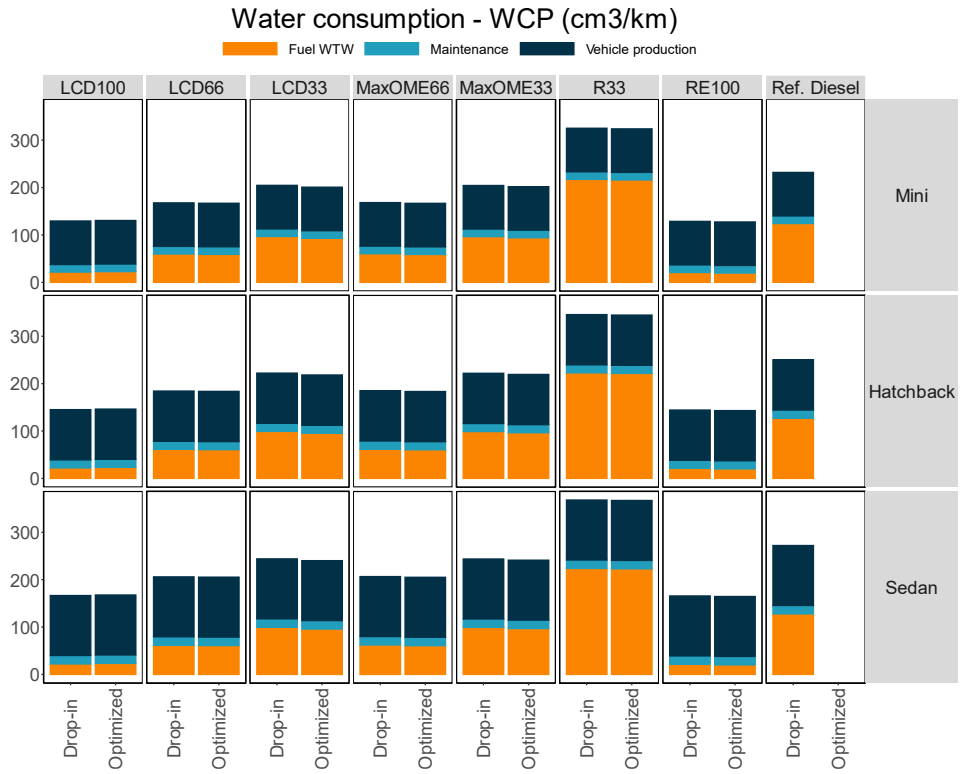

Figure 24. Summarized life cycle WCP for three vehicle segments manufactured in 2023 using LCFs for 10 years or 120000 km

The impact of the vehicle manufacturing should not be discarded for the WCP, as for all the LCFs with synthetic origin the manufacturing and vehicle maintenance stages represent nearly 50% of the total impact of the category. This can also be extended to EVs, which can have a mean WCP of 550 cm3/km depending on the origin of the electricity generation used [84]. The higher WCP of EVs have been

previously reported when compared with gasoline and diesel ICEVs of the same segment (nearly 4.4 times more) [85].

4 Summary and conclusions

LCAs are an important tool for evaluating the environmental impacts of products and processes. However, the results of LCAs are sensitive to a range of factors, including the origin of the data used, the scenarios evaluated, and other difficult-to-quantify uncertainties. Despite these challenges, the current study aimed to reduce these sources of error to the best of its capacity. One of the biggest challenges in conducting LCAs is the reluctance of industries to freely share data, which can lead to errors in the LCA results. In the case of the automotive industry, the main source of error is thought to be associated with the LCI of the vehicles and the fuel production. The error is considered reduced during the vehicle use phase as the vehicle use was modelled with in-house experiments presented in previous chapters. Besides the uncertainties, the diesel results agree with previous baselines found in the literature, particularly for the often-evaluated GWP, which indicates that the current LCA is in line with the current industry evaluations.

The objective of this study was to evaluate the environmental impacts of seven LCFs under three different vehicle segments and compare them to a diesel reference not only to assess the positive impact of reducing the carbon footprint of the fuel usage and production, but to also assess often ignored impacts that can also have large consequences on human health and the environment. The main conclusions that can be extracted from this study are summarized in this section, however, independently of the impact category it can be generalized that the smaller the vehicle the smaller the environmental impact.

4.1 Global Warming Potential – GWP

This study has provided valuable insights into the GWP impacts of ICEVs over their lifespan, considering various fuel types of variable renewable content. The main conclusions for the GWP of ICEVs from this study are:

- The yearly life cycle GWP impact of vehicles increases almost linearly with use, with only minor non-linear increases observed during tire replacements at 30,000th km, 60,000th km, and 90,000th km.
- The use of renewable fuels, particularly those with carbon-negative production processes, can significantly reduce the GWP impact of vehicles over their lifespan.

- Partially renewable fuels with the same proportion of renewable content have similar GWP impacts.
- Vehicle manufacturing and maintenance stages have a significant impact on the GWP, and diesel-fueled vehicles have a higher GWP impact than those fueled by renewable fuels.
- Among the evaluated fuels, the LCD100 and RE100 fuels have the smallest GWP impact, with the RE100 fuel reaching comparable values to an electric vehicle.
- The inclusion of N_2O in the vehicle use LCI has a negligible impact on the GWP of the evaluated fuels.
- For the LCD100 and RE100 fuels, more than half of the total GWP comes from the vehicle manufacturing and maintenance stages.
- The GWP impact of the LCD100 fuel is lower in CO_2eq than that reported by Tesla in 2021 for their electric Model 3Y personal use vehicle in Europe, indicating the potential for renewable liquid fuels to have a comparable environmental impact to electric vehicles.

4.2 Terrestrial acidification – TAP; fine particle matter formation – PMFP & human health ozone formation – HOFP

During this study it was emphasized tht it is important to consider more than just the reduction in CO_2eq when evaluating the environmental impact of different fuels using LCAS because technologies that can result in GWP can also lead to increases in other impact factors. As such the TAP, PMFP and HOFP impact categories were evaluated, and the main conclusions are:

- The TAP, PMFP and HOPF impact categories were found to be highly dependent on NOx emissions, which are a major problem with diesel ICEVs.
- The choice of lower NOx calibration can have a significant positive impact on these impact categories.
- The use of low-sooting fuel properties should be considered when exploring alternative fuels, as they can increase the potential for the reduction of negative impact factors linked with NOx emissions by providing an extra degree of freedom for the calibration by eliminating the concerns for soot formation.

4.3 Water consumption – WCP

The final impact category assessed was water consumption because it is regarded as one the main necessary resources for life, and whose misuse and contamination

would bring negative effects for the environment and human health. The main conclusions for the study are:

- The production of biofuels, which have been considered a potential solution for reducing greenhouse gas emissions, can also contribute to high WCP if not produced sustainably.
- It is essential to consider not only the carbon footprint but also the water footprint of biofuels, which involves water-intensive activities such as irrigation, harvesting, and processing of biomass feedstocks.
- The impact of vehicle manufacturing and maintenance should not be disregarded as they can represent a significant portion of the total impact on the WCP.

5 References

[1] W. Steffen, J. Rockström, K. Richardson, T. M. Lenton, C. Folke, D. Liverman, C. P. Summerhayes, A. D. Barnosky, S. E. Cornell, M. Crucifix, J. F. Donges, I. Fetzer, S. J. Lade, M. Scheffer, R. Winkelmann and H. J. Schellnhuber, "Trajectories of the Earth System in the Anthropocene," *Proceedings of the National Academy of Sciences*, vol. 115, no. 33, pp. 8252-8259, 2018.

[2] N. Wunderling, R. Winkelmann, J. Rockström and e. al., "Global warming overshoots increase risks of climate tipping cascades in a network model," *Nature Climate Change*, vol. 13, pp. 75-82, 2023.

[3] V. Masson-Delmotte, P. Zhai, H.-O. Pörtner, D. Roberts, J. Skea, P. Shukla, A. Pirani, W. Moufouma-Okia, C. Péan, R. Pidcock, S. Connors, J. Matthews, Y. Chen, X. Zhou, M. Gomis, E. Lonnoy, T. Maycock, M. Tignor and T. Waterfield, "Global Warming of 1.5°C. An IPCC Special Report on the impacts," IPCC, 2018.

[4] UN General Assembly, *United Nations Framework Convention on Climate Change : resolution / adopted by the General Assembly*, UN General Assembly, 1994.

[5] G. Puig-Samper Naranjo, D. Bolonio, M. F. Ortega and M.-J. García-Martínez, "Comparative life cycle assessment of conventional, electric and

hybrid passenger vehicles in Spain," *Journal of Cleaner Production,* p. 125883, 2021.

[6] B. Sen, N. C. Onat, M. Kucukvar and O. Tatari, "Material footprint of electric vehicles: A multiregional life cycle assessment," *Journal of Cleaner Production,* vol. 209, pp. 1033-1043, 2019.

[7] E. Karaaslan, Y. Zhao and O. Tatari, "Comparative life cycle assessment of sport utility vehicles with different fuel options," *Int J Life Cycle Assess,* vol. 23, p. 333–347, 2018.

[8] L. La Picirelli de Souza, E. E. Silva Lora, J. C. Escobar Palacio, M. H. Rocha, M. L. Grillo Renó and O. J. Venturini, "Comparative environmental life cycle assessment of conventional vehicles with different fuel options, plug-in hybrid and electric vehicles for a sustainable transportation system in Brazil," *Journal of Cleaner Production,* vol. 203, pp. 444-468, 2018.

[9] C. Zhang, X. Zhao, R. Sacchi and F. You, "Trade-off between critical metal requirement and transportation decarbonization in automotive electrification," *Nature Communications,* vol. 14, p. 1616, 2023.

[10] K. Petrauskienė, M. Skvarnavičiūtė and J. Dvarionienė, "Comparative environmental life cycle assessment of electric and conventional vehicles in Lithuania," *Journal of Cleaner Production,* vol. 246, p. 119042, 2020.

[11] H. Ritchie, M. Roser and P. Rosado, "CO_2 and Greenhouse Gas Emissions," OurWorldInData.org, 2020. [Online]. Available: https://ourworldindata.org/co2-and-greenhouse-gas-emissions. [Accessed April 2023].

[12] European Commission, "Shedding light on energy in the EU," Eurostat, Publications Office, 2023.

[13] IEA, "CO2 Emissions in 2022," IEA, Paris, 2023.

[14] H. Ritchie, "Cars, planes, trains: where do CO2 emissions from transport come from?," Our World in Data, 06 October 2020. [Online]. Available: https://ourworldindata.org/co2-emissions-from-transport. [Accessed 11 April 2023].

[15] M. Bui, C. S. Adjiman, A. Bardow, E. J. Anthony, A. Boston, S. Brown, P. S. Fennell, S. Fuss, A. Galindo, L. A. Hackett, J. P. Hallett, H. J. Herzog, G. Jackson, J. Kemper, S. Krevor, G. C. Maitland, M. Matuszewski, I. S. Metcalfe, C. Petit, G. Puxty, J. Reimer, D. Reiner, E. Rubin, S. Scott, N. Shah, B. Smit, J. Trusler, P. Webley, J. Wilcox and N. Mac Dowell, "Carbon capture and storage (CCS): the way forward," *Energy & Environmental Science*, vol. 11, no. 5, pp. 1062-1176, 2018.

[16] D. L. Sanchez, J. H. Nelson, J. Johnston, A. Mileva and D. M. Kammen, "Biomass enables the transition to a carbon-negative power system across western North America," *Nature Climate Change*, vol. 5, pp. 230-234, 2015.

[17] M. Pérez-Fortes, J. C. Schöneberger, A. Boulamanti and E. Tzimas, "Methanol synthesis using captured CO2 as raw material: Techno-economic and environmental assessment," *Applied Energy*, vol. 161, pp. 718-732, 2016.

[18] E. Commission, J. R. Centre, M. Prussi, M. Yugo and L. De Prada, "JEC well-to-tank report V5 : JEC well-to-wheels analysis : well-to-wheels analysis of future automotive fuels and powertrains in the European context," Publications Office, 2020.

[19] S. Schemme, R. Can Samsun, R. Peters and D. Stolten, "Power-to-fuel as a key to sustainable transport systems – An analysis of diesel fuels produced from CO2 and renewable electricity," *Fuel*, vol. 205, pp. 198-221, 2017.

[20] Eurostat, "Gross and net production of electricity and derived heat by type of plant and operator," 04 04 2023. [Online]. Available: https://ec.europa.eu/eurostat/databrowser/view/nrg_ind_peh/default/table?lang=en. [Accessed 11 04 2023].

[21] R. B. Kaunda, "Potential environmental impacts of lithium mining," *Journal of Energy & Natural Resources Law*, vol. 38, no. 3, pp. 237-244, 2020.

[22] B. E. Murdock, K. E. Toghill and N. Tapia-Ruiz, "A Perspective on the Sustainability of Cathode Materials used in Lithium-Ion Batteries," *Advance Energy Materials*, vol. 11, no. 39, p. 2102028, 2021.

[23] International Organization for Standardization, *ISO 14040:2006 environmental management - life cycle assessment - principles and framework,* Geneva: ISO, 2006.

[24] I. O. f. Standardization, *ISO 14044:2006 environmental management - life cycle assessment - requirements and guidelines,* Geneva: ISO, 2006.

[25] M. Finkbeiner, A. Inaba, R. Tan, K. Christiansen and H.-J. Klüppel, "The New International Standards for Life Cycle Assessment: ISO 14040 and ISO 14044," *The International Journal of Lifecycle Assessment,* vol. 11, pp. 80-85, 2006.

[26] H. H. Khoo and R. B. H. Tan, Life cycle assessment: New developments and multi-disciplinary applications, New Jersey: World Scientific, 2022.

[27] D. Candelaresi, A. Valente, D. Iribarren, J. Dufour and G. Spazzafumo, "Comparative life cycle assessment of hydrogen-fuelled passenger cars," *International Journal of Hydrogen Energy,* vol. 46, pp. 35961-35973, 2021.

[28] O. Winjobi, J. C. Kelly and Q. Dai, *Life-cycle analysis, by global region, of automotive lithium-ion nickel manganese cobalt batteries of varying nickel content,* 2022.

[29] M. Q. Wang, *GREET 1.5 - transportation fuel-cycle model - Vol. 1 : methodology, development, use, and results. Office of Scientific and Technical Information (OSTI),* 1999.

[30] D. A. Notter, M. Gauch, R. Widmer, P. Wäger, A. Stamp, R. Zah and H.-J. Althaus, "Contribution of Li-Ion Batteries to the Environmental Impact of Electric Vehicles," *Environmental Science & Technology,* vol. 44, no. 17, pp. 6550-6556, 2010.

[31] M. F. Torchio and M. G. Santarelli, "Energy, environmental and economic comparison of different powertrain/fuel options using well-to-wheels assessment, energy and external costs – European market analysis," *Energy,* vol. 35, no. 10, pp. 4156-4171, 2010.

[32] J. Desantes, R. Novella, B. Pla and M. Lopez-Juarez, "Impact of fuel cell range extender powertrain design on greenhouse gases and NOX emissions in automotive applications," *Applied Energy,* vol. 302, p. 117526, 2021.

[33] A. García, J. Monsalve-Serrano, S. Martinez-Boggio and R. Soria Alcaide, "Carbon footprint of battery electric vehicles considering average and," *Energy*, vol. 268, p. 126691, 2023.

[34] J. Desantes, R. Novella, B. Pla and M. Lopez-Juarez, "Impact of the Powertrain Sizing on Cradle-to-Grave Emissions and Fuel Cell Degradation in a FCV with a Range-Extender Architecture," *SAE Technical Paper*, no. 2022-01-0681, 2022.

[35] Ö. Andersson and P. Börjesson, "The greenhouse gas emissions of an electrified vehicle combined with renewable fuels: Life cycle assessment and policy implications," *Applied Energy*, vol. 289, p. 116621, 2021.

[36] U. Tietge, P. Mock, V. Franco and N. Zacharof, "From laboratory to road: Modeling the divergence between official and real-world fuel consumption and CO2 emission values in the German passenger car market for the years 2001–2014," *Energy Policy*, vol. 103, pp. 212-222, 2017.

[37] M. A. Huijbregts, Z. J. Steinmann, P. M. F. Elshout, G. Stam, F. Verones, M. Vieira, M. Zijp, A. Hollander and R. van Zelm, "ReCiPe2016: a harmonised life cycle impact assessment method at midpoint and endpoint level," *The International Journal of Life Cycle Assessment*, vol. 22, pp. 138-147, 2017.

[38] G. Wernet, C. Bauer, B. Steubing, J. Reinhard, E. Moreno-Ruiz and B. Weidema, "The ecoinvent database version 3 (part I): overview and methodology. The International Journal of Life Cycle Assessment," *The International Journal of Life Cycle Assessment*, vol. 21, p. 1218–1230, 2016.

[39] J. N. A. H.-J. D. G. D. R. Frischknecht R., H. T., H. S., H. R., N. T., R. G. and S. M., "The ecoinvent database: Overview and methodological framework," *International Journal of Life Cycle Assessment*, vol. 10, pp. 3-9, 2005.

[40] Pré, "PRé: enabling fact-based sustainability," 2023 PRé Sustainability B.V. , [Online]. Available: https://pre-sustainability.com/about/about-pre/. [Accessed 12 April 2023].

[41] Sphera, "LCA for Experts (GaBi)," Sphera, [Online]. Available: https://sphera.com/life-cycle-assessment-lca-software/. [Accessed 12 April 2023].

[42] I. T. Herrmann and A. Moltesen, "Does it matter which Life Cycle Assessment (LCA) tool you choose? – a comparative assessment of SimaPro and GaBi," *Journal of Cleaner Production,* vol. 86, pp. 163-169, 2015.

[43] A. Burnham, M. Q. Wang and Y. Wu, "Development and applications of GREET 2.7 -- The Transportation Vehicle-CycleModel," 2006.

[44] J. Kelly, J. Han, Q. Dai and A. Elgowainy, "Update of Vehicle Weights in the GREET ® Model," 2017.

[45] T. Li, H. Zhang, Z. Liu, Q. Ke and L. Alting, "A system boundary identification method for life cycle assessment," *The International Journal of Life Cycle Assessment,* vol. 19, pp. 646-660, 2013.

[46] J. Guinée, M. Gorrée, R. Heijungs, G. Huppes, R. Kleijn, A. d. Koning, L. v. Oers, A. Wegener Sleeswijk, S. Suh, H. Udo de Haes, H. d. Bruijn, R. Duin and M. Huijbregts, Handbook on Life Cycle Assessment: Operational Guide to the ISO Standards, Boston: Kluwer Academic Publishers, 2002.

[47] *Commission Recommendation (EU) 2021/2279 of 15 December 2021 on the use of the Environmental Footprint methods to measure and communicate the life cycle environmental performance of products and organisations,* Official Journal of the European Union, 2021.

[48] M. Goedkoop, R. Heijungs, M. Huijbregts, A. De Schryver, J. Struijs and R. van Zelm, *ReCiPe 2008: A life cycle impact assessment method which comprises harmonised category indicators at the midpoint and endpoint levels. First edition. Report i: Characterization,* the Netherlands: Ruimte en Milieu, Ministerie van Volkshuisvesting, Ruimtelijke Ordening en Milieubeheer, 2009.

[49] M. Z. Hauschild and M. A. J. Huijbregts, "Chapter 1. In Life cycle impact assessment," in *Introducing life cycle impact assessment*, Springer, 2015.

[50] Odyssee-Mure, "Sectoral Profile - Overview," Enerdata, [Online]. Available: https://www.odyssee-mure.eu/publications/efficiency-by-sector/overview/. [Accessed 20 April 2023].

[51] A. Funazaki, K. Taneda, K. Tahara and A. Inaba, "Automobile life cycle assessment issues at end-of-life and recycling," *JSAE Review*, vol. 24, no. 4, pp. 381-386, 2003.

[52] S. Karagoz, N. Aydin and V. Simic, "End-of-life vehicle management: a comprehensive review," *Journal of Material Cycles and Waste Management*, vol. 22, pp. 416-442, 2020.

[53] GreenDelta, "OpenLCA," [Online]. Available: https://www.openlca.org/.

[54] ChrisFix, "How Much Weight can you REMOVE from your Car? (Weight Reduction)," Youtube, 5 June 2021. [Online]. Available: https://www.youtube.com/watch?v=MCiNGmwopx4. [Accessed 29 March 2023].

[55] S. Dudes, "How Much Weight Can You REMOVE From Your Car?," Youtube, 12 March 2022. [Online]. Available: https://www.youtube.com/watch?v=RSJuXoQwPsg. [Accessed 29 March 2023].

[56] R. a. Race, "Clio RS 182 - Weight Reduction For Extra Speed - Budget Track Car Build Project pt.6," Youtube, 9 November 2017. [Online]. Available: https://www.youtube.com/watch?v=bG09BbxNpxA. [Accessed 29 March 2023].

[57] M. Pilotto Cenci, T. Scarazzato, D. Dotto Munchen, P. C. Dartora, H. M. Veit, A. Moura Bernardes, P. R. Dias and ç, "Eco-Friendly Electronics—A Comprehensive Review," *Advanced Materials Technologies*, vol. 7, no. 2, p. 2001263, 2021.

[58] G. W. Schweimer and M. Levin, "Life Cycle Inventory for the Golf A4," Volkswagen AG, Wolfsburg, 2000.

[59] A. García, J. Monsalve-Serrano, S. Martinez-Boggio and S. Tripathi, "Techno-economic assessment of vehicle electrification in the six largest

global automotive markets," *Energy Conversion and Management,* vol. 270, p. 116273, 2022.

[60] A. Temporelli, M. L. Carvalho and P. Girardi, "Life Cycle Assessment of Electric Vehicle Batteries: An Overview of Recent Literature," *Energies,* vol. 13, no. 11, p. 2864, 2020.

[61] M. Shafique, A. Azam, M. Rafiq and X. Luo, "Life cycle assessment of electric vehicles and internal combustion engine vehicles: A case study of Hong Kong," *Research in Transportation Economics,* vol. 91, p. 101112, 2022.

[62] T. R. Hawkins, B. Singh, G. Majeau-Bettez and A. Hammer Strømman, "Comparative Environmental Life Cycle Assessment of Conventional and Electric Vehicles," *Journal of Industrial Ecology,* vol. 17, no. 1, pp. 53-64, 2012.

[63] M. Collins, K. Schiebel and P. Dyke, "Life Cycle Assessment of Used Oil Management (ERM)," Environmental Resources Management, 2017.

[64] A. Soler, V. Gordillo, W. Lilley, P. Schmidt, W. Werner, T. Houghton and S. Dell'Orco, "E-Fuels: A techno-economic assessment of European domestic production and imports towards 2050," Concawe, Brussels, 2022.

[65] M. Prussi, M. Yugo, L. De Prada, M. Padella, R. Edwards and L. Lonza, "JEC Well-to-Tank report v5, EUR 30269 EN," Publications Office of the European Union, Luxembourg,, 2020.

[66] J. Benajes, A. Garcia, J. Monsalve-Serrano and R. Sari, "Evaluating the Efficiency of a Conventional Diesel Oxidation Catalyst for Dual-Fuel RCCI Diesel-Gasoline Combustion," *SAE Technical Paper,* no. 2018-01-1729, 2018.

[67] A. Srinivasacharya Ayodhya and K. Gottekere Narayanappa, "An overview of after-treatment systems for diesel engines," *Environmental Science and Pollution Research,* vol. 25, pp. 35034-35047, 2018.

[68] A. Simons, "Road transport: new life cycle inventories for fossil-fuelled passenger cars and non-exhaust emissions in ecoinvent v3," *The*

International Journal of Life Cycle Assessment, vol. 21, pp. 1299-1313, 2016.

[69] R. Suarez-Bertoa, P. Mendoza-Villafuerte, F. Riccobono, M. Vojtisek, M. Pechout, A. Perujo and C. Astorga, "On-road measurement of NH3 emissions from gasoline and diesel passenger cars during real world driving conditions," *Atmospheric Environment,* vol. 166, pp. 488-497, 2017.

[70] P. Mock, "World-Harrmonized Light-Duty Vehicles Test Procedure," The International Council on Clean Transportation, 2013.

[71] European Commission, Directorate-General for Internal Market, Industry, Entrepreneurship and SMEs , *Proposal for a REGULATION OF THE EUROPEAN PARLIAMENT AND OF THE COUNCIL on type-approval of motor vehicles and engines and of systems, components and separate technical units intended for such vehicles, with respect to their emissions and battery durabili*, 2022.

[72] A. García, J. Monsalve-Serrano, D. Villalta and M. Guzmán-Mendoza, "Optimization of low carbon fuels operation on a CI engine under a simplified driving cycle for transportation de-fossilization," *Fuel,* vol. 310, no. Part A, p. 122338, 2022.

[73] A. García, J. Monsalve-Serrano, D. Villalta and M. Guzmán-Mendoza, "Impact of low carbon fuels (LCF) on the fuel efficiency and NOx emissions of a light-duty series hybrid commercial delivery vehicle," *Fuel,* vol. 321, p. 124035, 2022.

[74] C.-F. Tsai, W.-C. Lin, Y.-H. Hu and G.-T. Yao, "Under-sampling class imbalanced datasets by combining clustering analysis and instance selection," *Information Sciences,* vol. 477, pp. 47-54, 2019.

[75] T. Mühlenstädt and S. Kuhnt, "Kernel interpolation," *Computational Statistics & Data Analysis,* vol. 55, no. 11, pp. 2962-2974, 2011.

[76] Gamma Technologies, LLC, "GT-POWER," Gamma Technologies, LLC, 2020.

[77] M. Okubo and T. Kuwahara, "Chapter 4 - Operation examples of emission control systems," in *New Technologies for Emission Control in Marine Diesel Engines*, Butterworth-Heinemann, 2020, pp. 145-210.

[78] B. Rossomando, E. Meloni, G. De Falco, M. Sirignano, I. Arsie and V. Palma, "Experimental characterization of ultrafine particle emissions from a light-duty diesel engine equipped with a standard DPF," *Proceedings of the Combustion Institute,* vol. 38, no. 4, pp. 5695-5702, 2021.

[79] Tesla, "Impact Report," Tesla, 2021.

[80] P. Zapp, A. Schreiber, J. Marx, M. Haines, J.-F. Hake and J. Gale, "Overall environmental impacts of CCS technologies—A life cycle approach," *International Journal of Greenhouse Gas Control,* vol. 8, pp. 12-21, 2012.

[81] A. Dutta, "Life Cycle Assessment Strategies for Carbon Capture and Utilization Processes," in *Life Cycle Assessment*, WORLD SCIENTIFIC, 2022, pp. 55-75.

[82] K. Hayashi, M. Okazaki, N. Itsubo and A. Inaba, "Development of damage function of acidification for terrestrial ecosystems based on the effect of aluminum toxicity on net primary production," *The International Journal of Life Cycle Assessment,* vol. 9, pp. 13-22, 2004.

[83] J. Lelieveld, J. Evans, D. Giannadaki and A. Pozzer, "The contribution of outdoor air pollution sources to premature mortality on a global scale," *Nature,* vol. 525, pp. 367-371, 2015.

[84] N. Cihat Onat, G. M. Abdella, M. Kucukvar, A. A. Kutty, M. Al-Nuaimi, G. Kumbaroğlu and M. Bulu, "How eco-efficient are electric vehicles across Europe? A regionalized life cycle assessment-based eco-efficiency analysis," *Sustainable Development,* vol. 29, no. 5, pp. 941-956, 2021.

[85] E. Karaaslan, Y. Zhao and O. Tatari, "Comparative life cycle assessment of sport utility vehicles with different fuel options," *The International Journal of Life Cycle Assessment,* vol. 23, pp. 333-347, 2018.

[86] European Commission, "European Platform on LCA | EPLCA," European Commission, 29 June 2018. [Online]. Available:

https://eplca.jrc.ec.europa.eu/ELCD3/datasetDownload.xhtml. [Accessed 2023 March 29].

[87] "Amazon," Amazon, [Online]. Available: https://www.amazon.com/. [Accessed 29 April 2023].

6 Appendix

6.1 Life cycle inventory for the vehicle manufacturing

6.1.1 Glider

Item	Material Comp.	Unit	Value (unit/kg item)	Mini	Hatchback	Sedan	Source
Vehicle Body (BIW, interior, exterior & glass)		kg	0.7263	338.20	494.32	716.63	[29]
	Steel (avg.)	kg	0.0122	245.64	359.03	520.50	[38]
	Wrought Aluminum	kg	0.0047	4.13	6.04	8.76	[38]
	Copper wire	kg	0.0460	1.58	2.31	3.34	[38]
	Glass	kg	0.1672	15.57	22.76	32.99	[38]
	Plastic (avg.)	kg	0.0075	56.55	82.65	119.83	[38]

	Styrene-butadiene Rubber	kg	0.0002	2.54	3.72	5.39	[38]
	Zinc	kg	0.0359	0.06	0.09	0.13	[38]
	Others	kg	0.9951	12.13	17.72	25.69	[38]
Chassis (unibody)		kg	0.7223	230.25	284.64	386.80	[29]
	Steel	kg	0.0748	166.32	205.60	279.40	[38]
	Cast Iron	kg	0.0132	17.22	21.29	28.93	[38]
	Forged Iron	kg	0.0274	3.04	3.76	5.11	[38]
	Wrought Aluminum	kg	0.1395	6.31	7.80	10.60	[38]
	Styrene-butadiene Rubber	kg	0.0088	32.11	39.70	53.94	[38]
	Plastic (avg.)	kg	0.0034	2.02	2.49	3.39	[38]
	Copper wire	kg	0.0006	0.78	0.97	1.31	[38]
	Brass	kg	0.0031	0.15	0.18	0.24	[38]
	Zinc	kg	0.0020	0.72	0.89	1.21	[38]
	Magnetite	kg	1.0000	0.46	0.57	0.77	[38]
Electronic Components & Wires		kg	0.0187	8.18	8.18	8.18	[30]
	Light Emitting Diode (LED)	kg	0.6075	0.15	0.15	0.15	[86]
	Cable connectors and wires	kg	0.3738	4.97	4.97	4.97	[38]

	Electronics	kg	1.0000	3.06	3.06	3.06	[38]
Windshield Fluid		kg	0.5000	2.76	2.76	2.76	[29]
	Distilled water	kg	0.5000	1.38	1.38	1.38	[29]
	Methanol	kg	1.0000	1.38	1.38	1.38	[29]
Tires		kg	0.6670	32.40	39.56	44.76	[29]
	Styrene-butadiene Rubber	kg	0.3330	21.61	26.39	29.85	[38]
	Steel (avg.)	kg	1.0000	10.79	13.17	14.91	[38]
Adhesives	Plastic (avg.)	kg	0.7263	6.14	8.14	9.14	[29]

6.1.2 Drivetrain

Item	**Material Comp.**	**Unit**	**Value (unit/kg item)**	**Mini**	**Hatchback**	**Sedan**	**Source**
Powertrain System (ICE)		kg	1.0000	140.06	140.06	140.06	[29]
	Steel (avg.)	kg	0.5443	76.23	76.23	76.23	[38]
	Cast Aluminum	kg	0.1938	27.14	27.14	27.14	[38]
	Wrought Aluminum	kg	0.0077	1.07	1.07	1.07	[38]
	Cast Iron	kg	0.0027	0.38	0.38	0.38	[38]

	Forged Iron	kg	0.0005	0.07	0.07	0.07	[38]
	Plastic (avg.)	kg	0.1846	25.85	25.85	25.85	[38]
	Copper wire	kg	0.0665	9.31	9.31	9.31	[38]
	Platinum-PGM	kg	0.0000	0.00	0.00	0.00	[38]
Alternator		kg	1.1649	6.21	6.21	6.21	[27, 87]
	Steel (avg.)	kg	0.6667	4.14	4.14	4.14	[38]
	Aluminum (avg)	kg	0.1661	1.03	1.03	1.03	[38]
	Copper (avg)	kg	0.1661	1.03	1.03	1.03	[38]
	Copper wire	kg	0.1661	1.03	1.03	1.03	[38]
Starter motor		kg		3.20	3.20	3.20	[27, 87]
	Steel (avg.)	kg	0.6667	2.13	2.13	2.13	[38]
	Aluminum (avg)	kg	0.1661	0.53	0.53	0.53	[38]
	Copper (avg)	kg	0.1661	0.53	0.53	0.53	[38]
	Copper wire	kg	0.1661	0.53	0.53	0.53	[38]
Fuel System (injection, fitting & tank)		kg	1.0000	16.23	16.23	16.23	[30]
	Steel (avg.)	kg	0.0960	1.56	1.56	1.56	[38]
	Aluminum (avg)	kg	0.0960	1.56	1.56	1.56	[38]

	Polyethylene sulfide	kg	0.1919	3.12	3.12	3.12	[38]
	Polyethylene, HDPE	kg	0.6161	10.00	10.00	10.00	[38]
Exhaust System		kg	1.0000	27.52	27.52	27.52	[30]
	Steel (avg.)	kg	0.2666	7.34	7.34	7.34	[38]
	Aluminum (avg)	kg	0.2666	7.34	7.34	7.34	[38]
	Ceramic	kg	0.2333	6.42	6.42	6.42	[38]
	Metal oxide	kg	0.2000	5.50	5.50	5.50	[38]
	Synthetic Rubber	kg	0.0333	0.92	0.92	0.92	[38]
	Precious metal (Pt)	kg	0.0002	0.00	0.00	0.00	[38]
Transmission System/Gearbox		kg	1.0000	70.00	77.33	84.66	[29]
	Steel (avg.)	kg	0.3047	21.33	23.56	25.80	[38]
	Cast Iron	kg	0.2306	16.14	17.83	19.52	[38]
	Forged Iron	kg	0.0407	2.85	3.15	3.45	[38]
	Cast Aluminum	kg	0.3229	22.60	24.97	27.33	[38]
	Plastic (avg.)	kg	0.0506	3.54	3.91	4.28	[38]
	Styrene-butadiene Rubber	kg	0.0506	3.54	3.91	4.28	[38]
Engine Control Unit	ECU	kg	1.0000	1.30	1.30	1.30	[27]
Lead-Acid Battery		kg	1.0000	12.40	12.40	12.40	[27]
	Polypropylene	kg	0.0610	0.76	0.76	0.76	[38]
	Polyphenylene sulfide	kg	0.1180	1.46	1.46	1.46	[38]
	Lead (avg.)	kg	0.7210	8.94	8.94	8.94	[38]
	Sulfuric Acid	kg	0.0790	0.98	0.98	0.98	[38]
	Glass Fiber	kg	0.0210	0.26	0.26	0.26	[38]
ICE Cooling System		kg	1.0000	21.81	21.81	21.81	[27]
	Steel (avg.)	kg	0.1498	3.27	3.27	3.27	[38]
	Aluminum (avg)	kg	0.1000	2.18	2.18	2.18	[38]

	Polyethylene, HDPE	kg	0.0997	2.17	2.17	2.17	[38]
	Ethylene Glycol	kg	0.3505	7.64	7.64	7.64	[38]
	Polyphenylene sulfide	kg	0.2000	4.36	4.36	4.36	[38]
	Synthetic Rubber	kg	0.1000	2.18	2.18	2.18	[38]
Engine Oil	Gasoline blend stock	kg	1.0000	4.94	4.94	4.94	[29]
Power Steering Fluid	Gasoline blend stock	kg	1.0000	2.00	2.00	2.00	[29]
Brake Fluid	Gasoline blend stock	kg	1.0000	0.91	0.91	0.91	[29]
Transmission Fluid	Gasoline blend stock	kg	1.0000	5.29	5.29	5.29	[29]
Engine/Powertrain Coolant		kg	1.0000	7.20	7.20	8.20	[29]
	Distilled water	kg	0.5000	3.60	3.60	4.10	[29]
	Ethylene Glycol	kg	0.5000	3.60	3.60	4.10	[29]

Chapter 7
Conclusions and suggestions for future work

Contents

1 Introduction

Throughout this thesis, the role that low carbon fuels (LCFs) play in addressing the pressing challenges of climate change and air quality deterioration, particularly within the context of the transportation sector, has been explored. As the global community grapples with the imperative to reduce greenhouse gas (GHG) emissions and transition towards more sustainable energy sources, the adoption of LCFs emerges as a promising solution to mitigate the environmental impact of internal combustion engines.

The investigation has encompassed the examination of various LCFs, their production pathways, combustion characteristics, and their environmental impacts through a life cycle analysis (LCA). The intricacies of engine performance, emissions reduction, and the overall feasibility of LCFs as a viable alternative to conventional fossil fuels in compression ignition (CI) engines has been explored.

In this chapter, the implications of the work for the future of transportation are detailed, the limitations of the study are addressed and recommendations for further research and practical implementation of LCFs in light-duty CI engines are provided.

2 Summary and conclusions

Addressing carbon emissions in the transportation sector is a key step in mitigating the catastrophic effects of climate change. There is an urgent need to reduce carbon emissions, with a particular focus on the transport and energy sectors, which have consistently been major contributors to GHG emissions.

In the literature review, LCFs are presented as a promising solution to reduce the carbon footprint of internal combustion engine vehicles (ICEVs) while leveraging production with renewable energy sources. These fuels have the potential to significantly decrease carbon emissions during their production, making them a valuable energy storage medium when coupled with renewable energy generation. However, addressing tailpipe emissions with LCFs remains a critical challenge that requires ongoing research and development efforts.

Various aspects of using LCFs for decarbonizing the transportation industry are highlighted. Two biodiesel fuels, FAME and RME, made from different sources and produced through transesterification are discussed. While they may have higher tailpipe CO2 emissions than conventional diesel, their overall life cycle CO2 emissions can be more favourable. Engine tests reveal varying effects on emissions and engine durability. HVO, another biofuel, offers advantages like better cold-

weather performance and reduced emissions. FT diesel, synthesized from feedstocks, also reduces emissions. Oxymethylene dimethyl ethers (OMEx) show promise in reducing soot emissions but have drawbacks in fuel consumption and hardware compatibility. Blending LCFs can enhance combustion efficiency, improve hardware compatibility issues and reduce emissions. Adapting vehicles and optimizing engine components for LCFs is crucial to extract the maximum energy from the fuel. However, transitioning to non-fossil LCFs faces challenges related to production costs, energy input, infrastructure, and potential environmental impacts.

This thesis aimed to evaluate ways to reduce emissions from CI engines, particularly through LCFs blends of HVO, FAME, OMEx and FT diesel. These LCF blends are classified based on their renewable fuel content, which involves varying volumetric proportions of the discussed renewable components. In turn, the blends have an amalgamation of the properties of the different LCFs in their composition based on the proportion of each one, also offering varying environmental benefits and challenges.

The research examined the LCF properties and their potential to reduce emissions in ICEVs. Additionally, it analysed the environmental impact of different vehicle types using LCFs. Several key research domains are identified, including addressing tailpipe emissions, assessing LCF feasibility as diesel replacements, understanding the relationship between fuel properties and emissions, optimizing engine performance with LCFs, and considering emissions control strategies. Durability and environmental impact assessments were also crucial aspects of this study.

The engine employed for this thesis was a 1.6-liter, 4-cylinder, in-line diesel engine equipped with a high-pressure Exhaust Gas Recirculation (EGR) system. The fuel injection system relies on Direct Injection (DI), and the air management system incorporates a turbocharger featuring Variable Geometry Turbocharging (VGT). Experimental and numerical methodologies were employed to achieve stable engine conditions and conduct tests with LCF blends. Specific measures were taken to ensure that the engine reaches the desired operating temperature, and that LCF blends are introduced and stabilized correctly for testing.

The calibration methodology and optimization process employed encompasses two types of calibrations: drop-in tests and calibration-optimization tests. The former entails testing the fuel with the original equipment manufacturer's (OEM) provided diesel B7 Euro 6 calibration, while the latter involves modifying specific engine calibration parameters to observe their impacts on combustion, performance, and emissions. The experiments were conducted under five distinct operating conditions that represent various typical driving conditions, in addition to rated power and rated

torque measurements. The targets for the calibration include NOx emissions, soot emissions, fuel consumption, and combustion parameters like CA50.

A Design of Experiments (DOE) methodology was used which allowed to explore multiple factors and their interactions while minimizing the number of experimental runs. The data obtained from these experiments was subsequently used to construct regression models for each parameter of interest. These models highlight the relationships between calibration parameters and engine responses. Lastly, the models are validated using new experimental data acquired under the predicted optimized operating conditions.

2.1 Drop-in use of low carbon fuel blends in compression ignition engines

In this study, the suitability of various LCF blends for drop-in operation (defined as the direct use of the fuel without modifying neither the calibration nor the engine components) was assessed by examining their combustion characteristics, emissions, and engine settings. The testing revealed that fuels with lower lower heating value (LHV) required a higher pedal signal to achieve the same engine load. However, the reduction in energy density didn't translate directly into increased pedal use. The rated power behaved similarly to the pedal variation based on fuel energy density. Notably, MaxOME fuels, despite their lower LHV, could nearly match diesel's rated power due to their high oxygen content.

Engine control unit (ECU) calibration adjustments in drop-in operation mainly related to fuel mass demand, with minor corrections tied to fuel-specific attributes. Air mass and EGR changes were influenced by the fuel, given that turbocharger operation relies on exhaust energy, which varies with each fuel's combustion characteristics.

For a drop-in fuel candidate to replace diesel, it should exhibit similar or lower regulated emissions and fuel efficiency. Brake specific fuel consumption (BSFC) and equivalent BSFC (BSFCeq) were measured for the different LCF blends. Fuels with higher LHV boasted lower BSFC, while those with lower LHV had higher values compared to diesel. Considering BSFCeq the lower LHV fuels did not have an extreme penalty. The addition of FAME, as in RE100, improved both fuel consumption and engine efficiency. Exhaust energy losses depended on factors like combustion timing and injection settings, suggesting a dedicated LCF calibration could boost output power per unit of injected fuel.

NOx emissions levels varied among the LCFs tested, with MaxOME66 showing the highest emissions, primarily due to its lower EGR calibration. Soot emissions could be managed with diesel particulate filters, but engine-out soot levels also mattered. Fuels containing OMEx exhibited higher soot emissions than diesel under high load conditions but showed improvement in other operational conditions. Unburned hydrocarbon (HC) levels remained within diesel levels, while carbon monoxide (CO) emissions increased in certain LCFs, notably R33 and LCD fuels. Nevertheless, all LCFs maintained CO and HC levels within reasonable diesel limits, which could be theoretically further reduced with existing diesel Aftertreatment Systems (ATS).

The study reveals that all tested LCFs can operate within a range comparable to diesel under drop-in operation, with some being more efficient in terms of fuel consumption and engine-out emission control. However, negative effects on the fuel injection system were observed, particularly in the durability of common-rail injectors and fuel pumps. This underscores the need for rigorous durability and wear testing, suggesting potential improvements in fuel additives or hardware design to address observed corrosion and oxidation issues. Nevertheless, some LCFs, like RE100 and R33, appear more suitable for direct use in existing vehicle fleets.

2.2 Optimization of low carbon fuel blends calibration in compression ignition engines

A comprehensive four-stage analysis is presented aimed at optimizing the operation of LCF by carefully examining their performance under specific calibrations and combustion phasing. In the initial stage, the analysis focuses on quantifying engine responses within the constraints of calibration settings while considering mechanical limitations as the primary restricting factors. This phase identifies clusters of data points representing potential optimized LCF operating conditions. Moving to the second stage, the study narrows down the scope by fixing the combustion phasing (expressed by the CA50) to ensure consistent combustion timing across the different LCFs, facilitating a controlled comparison of engine responses under similar combustion conditions. The third stage further refines the analysis by maintaining the same calibration settings, shedding light on how various LCFs impact engine performance while holding other variables constant. This stage is pivotal for isolating the specific effects of different LCFs within the engine. The fourth and final stage aims to pinpoint the optimal operating conditions for each LCF across different settings and compare them to conventional diesel B7 operation, providing valuable insights into the potential advantages and trade-offs associated with using LCFs compared to traditional diesel fuels.

Key findings include LCD100's higher fuel consumption due to its lower LHV, with moderate correlations between BSFC, NOx, soot, and CA50, while LCD66 exhibits lower correlations between NOx and BSFC but has higher median NOx emissions. MaxOME66 demonstrates lower BSFC than MaxOME33, mainly due to differences in oxygen content, and CN. MaxOME fuels (the fuels with the higher OMEx proportion) yield low soot emissions across all conditions. Comparing R33 and RE100, R33 shows higher BSFC and NOx emissions, despite similar CA50 and soot emissions distributions, indicating that oxygen levels compensate for the CN difference, resulting in favourable soot and NOx emissions for RE100. Furthermore, the study emphasizes the importance of careful engine calibration for high-load conditions to ensure both safety and performance. It also confirms the well-known NOx-soot tradeoff in diesel engines but highlights that some LCFs, such as LCD66, exhibit more favourable emission outcomes at maximum load.

Fuels with higher LHVs require less mass to reach operating conditions, leading to improved air-to-fuel ratio (AFR) at lower loads, and oxygenated fuels demonstrate benefits in terms of charge renewal efficiency at lower loads. Despite variations in consumption and emissions, various LCFs can achieve BSFC values comparable to diesel, particularly those with higher LHVs like RE100 and R33.

The relationship between fuel properties and engine performance is examined, revealing that factors such as LHV, CN, density, viscosity, total aromatics, and O-C ratio significantly affect fuel mass levels required to reach specific loads and speeds. Density shows a correlation with BSFC, with denser fuels generally exhibiting higher BSFC, possibly due to reduced fuel penetration into the cylinder, especially at lower loads. NOx emissions display complex relationships with individual fuel properties, influenced by combustion stoichiometry and oxygen content. Soot emissions exhibit a clearer relationship with fuel properties, particularly at low to medium engine loads, with higher LHV associated with elevated soot emissions and oxygen content playing a crucial role in reducing soot emissions, especially at low loads.

The study also compares LCFs under both direct drop-in conditions and optimized calibrations tailored to specific fuel types, revealing that optimization, which targets lower NOx emissions, may slightly elevate BSFC under certain conditions. Nonetheless, the optimized calibration generally results in BSFC levels comparable to conventional diesel for most LCFs. Low LHV fuels like MaxOME66 and LCD100 may exhibit higher BSFC with optimized calibration at medium-to-high loads. At low engine loads and speeds, optimization leads to fuel consumption reductions

across all tested LCFs, which can be beneficial for fuel economy in low-load urban scenarios.

The optimization effectively reduces NOx emissions, with reductions of up to 3 g/kWh across various conditions and fuels. The trade-off between NOx and soot emissions varies, but fuels with high oxygen content can simultaneously reduce NOx emissions and maintain lower soot levels compared to diesel. Under low-load conditions, HC and CO emissions may be higher with the LCFs. At higher engine loads and speeds, HC emissions tend to improve, especially with the optimized calibration, while CO emissions exhibit no clear correlation with specific fuel properties. Nevertheless, CO emissions remain within the range of a diesel engine, ensuring compatibility with exhaust temperatures and potential oxidation by an ATS.

2.3 Life Cycle Analysis of Low Carbon Fuels for Light-Duty Combustion Engine Vehicles

LCAs are critical tools for assessing the environmental impacts of products and processes. However, their results can vary due to factors such as data sources, scenarios, and uncertainties. This study aimed to minimize these errors and focused on evaluating the seven tested LCFs across different vehicle segments, comparing them to diesel to gauge their impact on the environment and human health. The study found that smaller vehicles have lower environmental impacts, and the use of renewable fuels, particularly those with carbon-negative production processes, can substantially reduce Global Warming Potential (GWP). Vehicle manufacturing and maintenance stages significantly influence GWP. Renewable liquid fuels showed potential for environmental impact similar to electric vehicles. Beyond GWP, the study examined other impact categories (terrestrial acidification, human ozone formation and particulate matter formation), highlighting the importance of addressing NOx emissions to reduce the negative impacts of ICEVs. In addition, unsustainable biofuel production can contribute to high water consumption, making it necessary to consider water footprints alongside carbon footprints in environmental assessments of LCFs.

3 Suggestions for future work

In the course of the research detailed in this thesis, several studies were recognized as potential avenues for further exploration. These endeavours could not be undertaken within the scope of this thesis, primarily due to time constraints or the need for specialized equipment not at our disposal. As a result, these ideas are

presented here as recommendations for future work, aimed at advancing the concept and addressing limitations that could bolster its practical utility in real-world applications.

3.1 Aftertreatment system evaluation and vehicle tests

This study would assess the potential benefits and challenges associated with the use of LCF using existing ATS. To achieve this, the complete optimized engine map would be calibrated to reduce engine-out emissions following the criteria detailed in this thesis. With the new engine maps, the commercial ATS components used in the vehicle models for the tested engine would be installed in the test bench: selective catalytic reduction (SCR), diesel particulate filter (DPF), and diesel oxidation catalyst (DOC). Finally, both stationary and transient test would be performed analysing the effect of the different LCFs on the ATS, such as specific cycles for homologation and other cycles, warm-up conditions, and idle operation. By measuring HC species and secondary emissions before and after ATS installation, insights into the impact of LCF on exhaust emissions would be gained. In addition particle matter (PM) sizing distribution and mass can be measured (also before and after the aftertreatment system) to evaluate both the differences of the LCFs compared to diesel and how the ATS reduces this pollutant.

This study is important due to the diverse compositions of LCF compared to diesel, which can cause the composition and temperatures of the exhaust gases to differ significantly from the operational designed targets of current ATS. The study would help advance understanding of LCF's viability in internal combustion engines for reducing the environmental impact of transportation and promoting sustainable energy sources.

Once the test bench phase of the study is completed the selection of the most promising LCFs should be done. Then the calibration maps obtained should be loaded in a vehicle ECU, and using on-board emission measurement equipment the impact of the LCFs on real driving tailpipe emissions would be assessed and compared to conventional fossil diesel.

3.2 Powertrain hybridization

Despite the notable carbon dioxide (CO_2) reduction benefits achieved by using LCFs throughout the whole lifecycle of the vehicle, current regulations focus mainly on reducing tank-to-wheel (TTW) CO_2 emissions. It is suggested that hybridizing the powertrain offers an advantage in this regard due to the system's capability to recover energy during operation and the engine's ability to operate at its maximum efficiency

range. These improvements can enhance the overall carbon footprint from TTW, and depending on the operating range potentially meet future emission targets.

Various hybrid configurations, including series, parallel, and power split, should be evaluated to determine which offers the greatest advantages. Preliminary simulation work can be done based on the results from this thesis. For example, selecting a series hybrid powertrain where the engine uses LCFs and the operating conditions are limited to the tested stationary operating conditions.

The work would assess the performance of the vehicle under the Worldwide Harmonized Light Vehicles Test Cycle (WLTC) with a GT-Power 0-D model. The goal being to compare the fuel consumption and engine-out NOx emissions of different LCFs against diesel as the reference fuel. A parametric study should be conducted for the hybrid vehicles, focusing on battery size, final drive ratio, and state of charge (SOC) differences; considering that larger battery sizes lead to higher fuel consumption due to the added weight. Additionally, the starting SOC greatly influences the vehicle's performance, with higher starting SOC values resulting in lower fuel consumption and lower engine-out NOx emissions, this should be accounted for by evaluating different starting SOC during the cycles.

The study would suggest potential advantages of the hybrid configurations in different scenarios like urban and interurban driving patterns, as well as highway. Similarly different vehicle loads should be evaluated to both estimate the charge depletion of the battery and the energy necessary from the LCFs. Future research on the topic could focus experimental tests with the powertrain that produces the best theoretical results from the simulations.

Bibliography

Chapter 1 – Introduction

1 W. Steffen, J. Rockström, K. Richardson, T. M. Lenton, C. Folke, D. Liverman, C. P. Summerhayes, A. D. Barnosky, S. E. Cornell, M. Crucifix, J. F. Donges, I. Fetzer, S. J. Lade, M. Scheffer, R. Winkelmann y H. J. Schellnhuber, «Trajectories of the Earth System in the Anthropocene,» *Proceedings of the National Academy of Sciences*, vol. 115, nº 33, pp. 8252-8259, 2018.

2 N. Wunderling, R. Winkelmann, J. Rockström y e. al., «Global warming overshoots increase risks of climate tipping cascades in a network model,» *Nature Climate Change*, vol. 13, pp. 75-82, 2023.

3 V. Masson-Delmotte, P. Zhai, H.-O. Pörtner, D. Roberts, J. Skea, P. Shukla, A. Pirani, W. Moufouma-Okia, C. Péan, R. Pidcock, S. Connors, J. Matthews, Y. Chen, X. Zhou, M. Gomis, E. Lonnoy, T. Maycock, M. Tignor y T. Waterfield, «Global Warming of 1.5°C. An IPCC Special Report on the impacts,» IPCC, 2018.

4 UN General Assembly, *United Nations Framework Convention on Climate Change : resolution / adopted by the General Assembly*, UN General Assembly, 1994.

5 J. Lelieveld, J. Evans, D. Giannadaki y A. Pozzer, «The contribution of outdoor air pollution sources to premature mortality on a global scale,» *Nature*, vol. 525, pp. 367-371, 2015.

6 H. Ritchie, M. Roser y P. Rosado, «CO_2 and Greenhouse Gas Emissions,» OurWorldInData.org, 2020. [En línea]. Available: https://ourworldindata.org/co2-and-greenhouse-gas-emissions. [Último acceso: April 2023].

7 H. Ritchie, «Cars, planes, trains: where do CO2 emissions from transport come from?,» Our World in Data, 06 October 2020. [En línea]. Available: https://ourworldindata.org/co2-emissions-from-transport. [Último acceso: 11 April 2023].

8 H. Ishaq y C. Crawford, «CO2-based alternative fuel production to support development of CO2 capture, utilization and storage,» *Fuel*, vol. 331, nº Part 2, p. 125684, 2023.

9 G. Puig-Samper Naranjo, D. Bolonio, M. F. Ortega y M.-J. García-Martínez, «Comparative life cycle assessment of conventional, electric and hybrid passenger vehicles in Spain,» *Journal of Cleaner Production*, p. 125883, 2021.

10 B. Sen, N. C. Onat, M. Kucukvar y O. Tatari, «Material footprint of electric vehicles: A multiregional life cycle assessment,» *Journal of Cleaner Production*, vol. 209, pp. 1033-1043, 2019.

11 E. Karaaslan, Y. Zhao y O. Tatari, «Comparative life cycle assessment of sport utility vehicles with different fuel options,» *Int J Life Cycle Assess*, vol. 23, p. 333–347, 2018.

12 L. La Picirelli de Souza, E. E. Silva Lora, J. C. Escobar Palacio, M. H. Rocha, M. L. Grillo Renó y O. J. Venturini, «Comparative environmental life cycle assessment of conventional

vehicles with different fuel options, plug-in hybrid and electric vehicles for a sustainable transportation system in Brazil,» *Journal of Cleaner Production*, vol. 203, pp. 444-468, 2018.

13 T. Gersdorf, P. Schaufuss, S. Schenk y P. Hertzke, «McKinsey Electric Vehicle Index: Europe cushions a global plunge in EV sales,» July 2020. [En línea]. Available: https://www.mckinsey.com/~/media/McKinsey/Industries/Automotive%20and%20Assembly/Our%20Insights/McKinsey%20Electric%20Vehicle%20Index%20Europe%20cushions%20a%20global%20plunge%20in%20EV%20sales/McKinsey-Electric-Vehicle-Index-Europe-cushions-a-global-plun. [Último acceso: 10 April 2021].

14 Z. Liu, J. Song, J. Kubal, N. Susarla, K. W. Knehr, E. Islam, P. Nelson y S. Ahmed, «Comparing total cost of ownership of battery electric vehicles and internal combustion engine vehicles,» *Energy Policy*, vol. 158, p. 112564, 2021.

15 Y. Zhou, R. Wen, H. Wang y H. Cai, «Optimal battery electric vehicles range: A study considering heterogeneous travel patterns, charging behaviors, and access to charging infrastructure,» *Energy*, vol. 197, p. 116945, 2020.

16 Y. Zeng, D. Chalise, s. D. Lubner, S. Kaur y R. S. Prasher, «A review of thermal physics and management inside lithium-ion batteries for high energy density and fast charging,» *Energy Storage Materials*, vol. 41, pp. 264-288, 2021.

17 European Comission, *Proposal for a REGULATION OF THE EUROPEAN PARLIAMENT AND OF THE COUNCIL amending Regulation (EU) 2019/631 as regards strengthening the CO2 emission performance standards for new passenger cars and new light commercial vehicles in line with the Union's inc,* Brussels: European Comission, 2021.

18 C. Zhang, X. Zhao, R. Sacchi y F. You, «Trade-off between critical metal requirement and transportation decarbonization in automotive electrification,» *Nature Communications*, vol. 14, p. 1616, 2023.

19 R. B. Kaunda, «Potential environmental impacts of lithium mining,» *Journal of Energy & Natural Resources Law*, vol. 38, nº 3, pp. 237-244, 2020.

20 A. M. Haidar, K. Muttaqi y D. Sutanto, «Technical challenges for electric power industries due to grid-integrated electric vehicles in low voltage distributions: A review,» *Energy Conversion and Management*, vol. 86, pp. 689-700, 2014.

21 N. Ortar y M. Ryghaug, «Should All Cars Be Electric by 2025? The Electric Car Debate in Europe,» *Sustainability*, vol. 11, nº 7, p. 1868, 2019.

22 F. Alanazi, «Electric Vehicles: Benefits, Challenges, and Potential Solutions for Widespread Adaptation,» *Applied Sciences*, vol. 13, nº 10, p. 6016, 2023.

23 B. Mohamed, B. Ali, B. Ahmed, B. Ahmed, L. Salah y D. Rachid, «Study of hydrogen production by solar energy as tool of storing and utilization renewable energy for the desert areas,» *International Journal of Hydrogen Energy*, vol. 41, nº 45, pp. 20788-20806, 2016.

24 D. Candelaresi, A. Valente, D. Iribarren, J. Dufour y G. Spazzafumo, «Comparative life cycle assessment of hydrogen-fuelled passenger cars,» *International Journal of Hydrogen Energy*, vol. 46, pp. 35961-35973, 2021.

25 O. Winjobi, J. C. Kelly y Q. Dai, *Life-cycle analysis, by global region, of automotive lithium-ion nickel manganese cobalt batteries of varying nickel content*, 2022.

26 M. Q. Wang, *GREET 1.5 - transportation fuel-cycle model - Vol. 1 : methodology, development, use, and results. Office of Scientific and Technical Information (OSTI)*, 1999.

27 D. A. Notter, M. Gauch, R. Widmer, P. Wäger, A. Stamp, R. Zah y H.-J. Althaus, «Contribution of Li-Ion Batteries to the Environmental Impact of Electric Vehicles,» *Environmental Science & Technology*, vol. 44, nº 17, pp. 6550-6556, 2010.

Chapter 2 – A Comprehensive Review of Low Carbon Fuels for Diesel Engines

1 U. K. Roy, T. Radu and J. L. Wagner, "Carbon-negative biomethane fuel production: Integrating anaerobic digestion with algae-assisted biogas purification and hydrothermal carbonisation of digestate," *Biomass and Bioenergy*, vol. 148, no. May, p. 106029, 2021.

2 P. Wienchol, A. Szlęk and M. Ditaranto, "Waste-to-energy technology integrated with carbon capture – Challenges and opportunities," *Energy*, vol. 198, no. May, p. 117352, 2020.

3 Kalghatgi, "Is it really the end of internal combustion engines and petroleum in transport?," *Applied Energy*, vol. 225, no. September, pp. 965-974, 2018.

4 E. Bannon, "Road to Zero: the last EU emission standard," *Transport & Environment*, pp. 1-19, 2020.

5 International Council on Clean Transportation, " EU: Heavy-duty: Emissions," TransportPolicy.net, [Online]. Available: https://www.transportpolicy.net/standard/eu-heavy-duty-emissions/. [Accessed 20 July 2020].

6 N. Duarte Souza Alvarenga Santos, V. Rückert Roso, A. C. Teixeira Malaquias, C. Baêta and J. Guilherme, "Internal combustion engines and biofuels: Examining why this robust combination should not be ignored for future sustainable transportation," *Renewable and Sustainable Energy Reviews*, vol. 148, no. September, p. 111292, 2021.

7 A. EL-Seesy, M. Nour, H. Hassan, A. Elfasakhany, Z. He and M. Mujtaba, "Diesel-oxygenated fuels ternary blends with nano additives in compression ignition engine: A step towards cleaner combustion and green environment," *Case Studies in Thermal Engineering*, vol. 25, no. June, p. 100911, 2021.

8 A. Arora, N. Niese, E. Dreyer, A. Waas and A. Xie, "Why Electric Cars Can't Come Fast Enough," BCG, 20 April 2021. [Online]. Available: https://www.bcg.com/publications/2021/why-evs-need-to-accelerate-their-market-penetration.

9 IEA, "Global EV Outlook 2021," IEA, Paris, 2021.

10 A. García, J. Monsalve-Serrano, D. Villalta and M. Guzmán-Mendoza, "Impact of low carbon fuels (LCF) on the fuel efficiency and NOx emissions of a light-duty series hybrid commercial delivery vehicle," *Fuel*, vol. 321, no. August, p. 124035, 2022.

11 E. Commission, "A European Strategy for low-emission mobility," European Union, 2020. [Online]. Available: https://ec.europa.eu/clima/eu-action/transport-emissions_en. [Accessed 6 June 2020].

12 Z. Mushtaq, R. Maqbool and K. Ahmad Bhat, "Chapter 13 - Genetic engineering and fifth-generation biofuels," in *Environmental Sustainability of Biofuels*, Elsevier, 2023, pp. 237-251.

13 K. Dutta, A. Daverey and J.-G. Lin, "Evolution retrospective for alternative fuels: First to fourth generation," *Renewable Energy*, vol. 69, no. September, pp. 114-122, 2014.

14 R. E. Sims, W. Mabee, J. N. Saddler and M. Taylor, "An overview of second generation biofuel technologies," *Bioresource Technology*, vol. Volume 101, no. 6, pp. 1570-1580, 2010.

15 Y. Y. Tye, K. T. Lee, W. N. W. Abdullah and C. P. Leh, "Potential of Ceiba pentandra (L.) Gaertn. (kapok fiber) as a resource for second generation bioethanol: Effect of various simple pretreatment methods on sugar production," *Bioresource Technology*, vol. 116, no. July, pp. 536-539, 2012.

16 J. Singh and S. Gu, "Commercialization potential of microalgae for biofuels production," *Renwable and Sustainable Energy Reviews*, vol. 14, no. 9, pp. 2596-2610, 2010.

17 E. Suali and R. Sarbatly, "Conversion of microalgae to biofuel," *Renewable and Sustainable Energy Reviews*, vol. 16, no. 6, pp. 4316-4342, 2012.

18 S. G. Hays and D. Ducat, "Engineering cyanobacteria as photosynthetic feedstock factories," *Photosynthesis Research*, vol. 123, pp. 285-295, 2015.

19 European Commission, "Communication from the Commission on voluntary schemes and default values in the EU biofuels and bioliquids sustainability scheme (2010/C 160/01)," Official Journal of the European Union , 2010.

20 S. Soam and K. Hillman, "Factors influencing the environmental sustainability and growth of hydrotreated vegetable oil (HVO) in Sweden," *Bioresource Technology Reports*, vol. 7, no. September, p. 100244, 2019.

21 A. P. Vyas, J. L. Verma and N. Subrahmanyam, "A review on FAME production processes," *Fuel*, vol. 89, no. 1, pp. 1-9, 2010.

22 B. Freedman, E. Pryde and T. Mounts, "Variables affecting the yields of fatty esters from transesterified vegetable oils," *Journal of the American Oil Chemists Society*, vol. 61, no. 10, pp. 1638-1643, 1984.

23 K. R. Jegannathan, S. Abang, D. Poncelet, E. S. C. Chan and P. Ravindra, "Production of biodiesel using immobilized lipase – a critical review," *Critical Reviews in Biotechnology*, vol. 28, no. 4, pp. 253-264, 2008.

24 S. Nasar, M. A. Hanif, U. Rashid, A. Hanif, M. N. Akhtar and C. Ngamcharussrivichai, "The production of fatty acid methyl esters (FAME) through transesterification is a crucial process for biodiesel production. To make this process more efficient and environmentally friendly, researchers are exploring various catalysts. Currently, both hom," *Catalysts*, vol. 11, no. 9, p. 1085, 2021.

25 M. Prussi, M. Yugo, L. De Prada, M. Padella, R. Edwards and L. Lonza, "JEC Well-to-Tank report v5, EUR 30269 EN," Publications Office of the European Union, Luxembourg,, 2020.

26 H. Cai, M. Prussi, L. Ou, M. Wang, M. Yugo, L. Lonza and N. Scarlat, "Decarbonization potential of on-road fuels and powertrains in the European Union and the United States: a well-to-wheels assessment," *Sustainable Energy Fuels*, vol. 6, pp. 4398-4417, 2022.

27 K. Tucki, O. Orynycz, R. Mruk, A. Świć and K. Botwińska, "Modeling of Biofuel's Emissivity for Fuel Choice Management," *Sustainability*, vol. 11, no. 23, p. 6842, 2019.

28 Q. Cheng, H. Tuomo, O. Kaario and L. Martti, "HVO, RME, and Diesel Fuel Combustion in an Optically Accessible Compression Ignition Engine," *Energy Fuels*, vol. 33, no. 3, pp. 2489-2501, 2019.

29 G. Labeckas and S. Slavinskas, "The effect of rapeseed oil methyl ester on direct injection Diesel engine performance and exhaust emissions," *Energy Conversion and Management*, vol. 47, no. 13-14, pp. 1954-1967, 2006.

30 A. Tsolakis, A. Megaritis, M. Wyszynski and K. Theinnoi, "Engine performance and emissions of a diesel engine operating on diesel-RME (rapeseed methyl ester) blends with EGR (exhaust gas recirculation)," *Energy*, vol. 32, no. 11, pp. 2072-2080, 2007.

31 M. Novakovic, S. Shamun, V. B. Malmborg, K. I. Kling, J. Kling, U. B. Vogel, P. Tunestal, J. Pagels and M. Tuner, "Regulated Emissions and Detailed Particle Characterisation for Diesel and RME Biodiesel Fuel Combustion with Varying EGR in a Heavy-Duty Engine," *SAE Technical Paper*, pp. 2019-01-2291, 2019.

32 Y. Kroyan, M. Wojcieszyk, O. Kaario, M. Larmi and K. Zenger, "Modeling the end-use performance of alternative fuels in light-duty vehicles," *Energy*, vol. 205, no. August, p. 117854, 2020.

33 A. Al Ezzi, M. A. Fayad, A. M. Al Jubori, A. A. Jaber, L. A. Alsadawi, H. A. Dhahad, M. T. Chaichan and T. Yusaf, "Influence of fuel injection pressure and RME on combustion, NOx emissions and soot nanoparticles characteristics in common-rail HSDI diesel engine," *International Journal of Thermofluids*, vol. 15, no. August, p. 100173, 2022.

34 M. Tongroon, A. Suebwong, M. Kananont, J. Aunchaisri and N. Chollacoop, "High quality jatropha biodiesel (H-FAME) and its application in a common rail diesel engine," *Renewable Energy*, vol. 113, no. December, pp. 660-668, 2017.

35 M. Unglert, D. Bockey, C. Bofinger, B. Buchholz, G. Fisch, R. Luther, M. Müller, K. Schaper, J. Schmitt, O. Schröder, U. Schümann, H. Tschöke, E. Remmele, R. Wicht, M. Winkler and Krahl, "Action areas and the need for research in biofuels," *Fuel*, vol. 268, no. May, p. 117227, 2020.

36 B. Cieślikowski, Process of Gradual Dysfunction of a Diesel Engine Caused by Formation of PM Deposits of FAME Origin, Springer Proceedings in Energy.

37 H. Aatola, M. Larmi, T. Sarjovaara and S. Mikkonen, "Hydrotreated Vegetable Oil (HVO) as a Renewable Diesel Fuel," *SAE International Journal of Engines,* vol. 1, no. 1, pp. 1251-1262, 2009.

38 R. Suarez-Bertoa, M. Kousoulidou, M. Clairotte, B. Giechaskiel, J. Nuottimäki, T. Sarjovaara and L. Lonza, "Impact of HVO blends on modern diesel passenger cars emissions during real world operation," *Fuel,* vol. 235, no. January, pp. 1427-1435, 2019.

39 L. Rantanen, R. Linnaila, P. Aakko and T. Harju, "NExBTL - Biodiesel Fuel of the Second Generation," *SAE Technical Paper,* pp. 2005-01-3771, 2005.

40 C. J. Hor, Y. H. Tan, N. M. Mubarak, I. S. Tan, M. L. Ibrahim, P. Yek, R. R. Karri and M. Khalid, "Techno-economic assessment of hydrotreated vegetable oil as a renewable fuel from waste sludge palm oil," *Environmental Research,* vol. 220, no. March, p. 115169, 2023.

41 R. Arvidsson, S. Persson, M. Fröling and M. Svanström, "Life cycle assessment of hydrotreated vegetable oil from rape, oil palm and Jatropha," *Journal of Cleaner Production,* vol. 19, no. 2-3, pp. 129-137, 2011.

42 R. Edwards, J.-F. Larive and J.-C. Beziat, "Well-to-Wheels Analysis of Future Automotive Fuels and Power Trains in the European Context - Report, Version 3c. EUR 24952 EN.," Publications Office of the European Union, Luxembourg, 2011.

43 J. Rodríguez-Fenández, J. J. Hernández, A. Calle-Asensio, Á. Ramos and J. Barba, "Selection of Blends of Diesel Fuel and Advanced Biofuels Based on Their Physical and Thermochemical Properties," *Energies,* vol. 12, no. 11, p. 2034, 2019.

44 Y. Li, H. Xu, R. Cracknell, R. Head and S. Shuai, "An experimental investigation into combustion characteristics of HVO compared with TME and ULSD at varied blend ratios," *Fuel,* vol. 255, no. November, p. 115757, 2019.

45 I. Bortel, J. Vávra and M. Takáts, "Effect of HVO fuel mixtures on emissions and performance of a passenger car size diesel engin," *Renewable Energy,* vol. 140, no. September, pp. 680-691, 2019.

46 J. Preuß, K. Munch and I. Denbratt, "Performance and emissions of renewable blends with OME3-5 and HVO in heavy duty and light duty compression ignition engines," *Fuel,* vol. 303, no. November, p. 121275, 2021.

47 A. Mancarella and O. Marello, "Effect of Coolant Temperature on Performance and Emissions of a Compression Ignition Engine Running on Conventional Diesel and Hydrotreated Vegetable Oil (HVO)," *Energies,* vol. 16, no. 1, p. 144, 2023.

48 J. Rodríguez-Fernández, M. Lapuerta and J. Sánchez-Valdepeñas, "Regeneration of diesel particulate filters: Effect of renewable fuels," *Renewable Energy,* vol. 104, no. April, pp. 30-39, 2017.

49 S. Hänggi, P. Elbert, T. Bütler, U. Cabalzar, S. Teske, C. Bach and C. Onder, "A review of synthetic fuels for passenger vehicles," *Energy Reports*, vol. 5, no. November, pp. 555-569, 2019.

50 H. Mahmoudi, M. Mahmoudi, O. Doustdar, H. Jahangiri, A. Tsolakis, S. Gu and M. LechWyszynski, "A review of Fischer Tropsch synthesis process, mechanism, surface chemistry and catalyst formulation," *Biofuels Engineering*, vol. 2, no. 1, pp. 11-31, 2017.

51 A. Y. Krylova, "Products of the Fischer-Tropsch synthesis (A Review)," *Solid Fuel Chemistry*, vol. 48, pp. 22-35, 2014.

52 J. C. Ruth and G. Stephanopoulos, "Synthetic fuels: what are they and where do they come from?," *Current Opinion in Biotechnology*, vol. 81, no. June, p. 102919, 2023.

53 V. B. Borugadda, G. Kamath and A. K. Dalai, "Techno-economic and life-cycle assessment of integrated Fischer-Tropsch process in ethanol industry for bio-diesel and bio-gasoline production," *Energy*, vol. 195, no. March, p. 116985, 2020.

54 C. M. Liu, N. K. Sandhu, S. T. McCoy and J. A. Bergerson, "A life cycle assessment of greenhouse gas emissions from direct air capture and Fischer–Tropsch fuel production," *Sustainable Energy & Fuels*, vol. 4, pp. 3129-3142, 2020.

55 B. Hao, C. Song, G. Lv, B. Li, X. Liu, K. Wang and Y. Liu, "Evaluation of the reduction in carbonyl emissions from a diesel engine using Fischer–Tropsch fuel synthesized from coal," *Fuel*, vol. 133, no. October, pp. 115-122, 2014.

56 A. Y. Khodakov, W. Chu and P. Fongarland, "Advances in the Development of Novel Cobalt Fischer−Tropsch Catalysts for Synthesis of Long-Chain Hydrocarbons and Clean Fuels," *Chemical Reviews*, vol. 107, no. 5, pp. 1692-1744, 2007.

57 P. Cai, C. Zhang, Z. Jing, Y. Peng, J. Jing and H. Sun, "Effects of Fischer-Tropsch diesel blending in petrochemical diesel on combustion and emissions of a common-rail diesel engine," *Fuel*, vol. 305, no. December, p. 121587, 2021.

58 H. Yuan, T. Tsukuda, Y. Yang, G. Shibata, Y. Kobashi and H. Ogawa, "Effects of Chemical Compositions and Cetane Number of Fischer–Tropsch Fuels on Diesel Engine Performance," *Energies*, vol. 15, no. 11, p. 4047, 2022.

59 M. H. McMillian and M. Gautam, "Consideration for Fischer-Tropsch Derived Liquid Fuels as a Fuel Injection Emission Control Parameter," *SAE Technical Paper*, p. 982489, 1998.

60 C. Zhang, Z. Jing, P. Cai, Y. Li, H. Sun, W. Huang, J. Jing, H. Wang and X. Yu, "Experimental investigation on combustion and emission characteristics of Fischer-Tropsch diesel/gasoline in a multi-cylinder heavy-duty diesel engine under different loads," *Fuel*, vol. 324, no. Part A, p. 124504, 2022.

61 J. V. Pastor, A. García, C. Micó and F. Lewiski, "An optical investigation of Fischer-Tropsch diesel and Oxymethylene dimethyl ether impact on combustion process for CI engines," *Applied Energy*, vol. 260, no. February, p. 114238, 2020.

62 M. Bassiony, A. Ibrahim and M. El-Kassaby, "An experimental study on the effect of using gas-to-liquid (GTL) fuel on diesel engine performance and emissions," *Alexandria Engineering Journal*, vol. 55, no. 3, pp. 2115-2124, 2016.

63 L. Ye, Y. Shi, T. Liu, Q. Zheng, M. M. Ashfaq, C. Sun, A. Shi and M. Ajmal, "Study on emission and particulate matter characteristics from diesel engine fueled with n-pentanol/Fischer–Tropsch diesel," *Energy Sources, Part A: Recovery, Utilization, and Environmental Effects*, 2020.

64 P. Cai, C. Zhang, Z. Jing, Y. Peng, J. Jing and H. Sun, "Effects of Fischer-Tropsch diesel blending in petrochemical diesel on combustion and emissions of a common-rail diesel engine," *Fuel*, vol. 305, no. December, p. 121587, 2021.

65 W. Zhong, J. Yang, L. Ruina and L. Shuai, "Gas emissions and particulate matter of non-road diesel engine fueled with F-T diesel with EGR," *Energy Sources, Part A: Recovery, Utilization, and Environmental Effects*, vol. 41, no. 5, pp. 542-555, 2019.

66 K. Yehliu, A. Boehman and O. Armas, "Emissions from different alternative diesel fuels operating with single and split fuel injection," *Fuel*, vol. 89, no. 2, pp. 423-437, 2010.

67 O. Armas, K. Yehliu and A. L. Boehman, "Effect of alternative fuels on exhaust emissions during diesel engine operation with matched combustion phasing," *Fuel*, vol. 89, no. 2, pp. 438-456, 2010.

68 Z. Wang, H. L. Liu, X. Ma, J. Wang, S. Shuai and R. D. Reitz, "Homogeneous charge compression ignition (HCCI) combustion of polyoxymethylene dimethyl ethers (PODE)," *Fuel*, vol. 183, no. November, pp. 206-213, 2016.

69 J. Yanowitz, M. A. Ratcliff, R. L. McCormick, J. D. Taylor and M. J. Murphy, "Compendium of Experimental Cetane Numbers," 2014.

70 W. Sun, W. Guoquing, L. Shuang, Z. Ruzheng, Y. Bin, Y. Jiuzhong, L. Yuyang, C. K. Westbrook and C. K. Law, "Speciation and the laminar burning velocities of poly(oxymethylene) dimethyl ether 3 (POMDME3) flames: An experimental and modeling study," *Proceeding of the Combustion Institute*, vol. 36, no. 1, pp. 1269-1278, 2017.

71 Y. R. Tan, M. L. Botero, Y. Sheng, J. A. H. Dreyer, R. Xu, W. Yang and M. Kraft, "Sooting characteristics of polyoxymethylene dimethyl ether blends with diesel in a diffusion flame," *Fuel*, vol. 224, no. July, pp. 499-506, 2018.

72 D. F. Rodríguez-Vallejo, A. Valente, G. Guillén-Gosálbez and B. Chachuat, "Economic and life-cycle assessment of OME3–5 as transport fuel: a comparison of production pathways," *Sustainable Energy Fuels*, vol. 5, pp. 2504-2516, 2021.

73 S. Deutz, D. Bongartz, B. Heuser, A. Kätelhön, L. S. Langenhorst, A. Omari, M. Walters, J. Klankermayer, W. Leitner, A. Mitsos, S. Pischinger and A. Bardow, "Cleaner production of cleaner fuels: wind-to-wheel – environmental assessment of CO2-based oxymethylene ether as a drop-in fuel," *Energy & Environmental Science*, vol. 11, pp. 331-343, 2018.

74 C. Hank, L. Lazar, F. Mantei, M. Ouda, R. J. White, T. Smolinka, A. Schaadt, C. Hebling and H.-M. Henning, "Comparative well-to-wheel life cycle assessment of OME3–5 synfuel

production via the power-to-liquid pathway," *Sustainable Energy & Fuels,* vol. 3, pp. 3219-3233, 2019.

75 J. Liu, H. Wang, Y. Li, Z. Zheng, Z. Xue, H. Shang and M. Yao, "Effects of diesel/PODE (polyoxymethylene dimethyl ethers) blends on combustion and emission characteristics in a heavy duty diesel engine," *Fuel,* vol. 177, no. August, pp. 206-216, 2016.

76 A. García, J. Monsalve-Serrano, D. Villalta and Á. Fogué-Robles, "Evaluating OMEx combustion towards stoichiometric conditions in a compression ignition engine," *Fuel,* vol. 303, no. November, p. 121273, 2021.

77 A. Omari, B. Heuser and S. Pischinger, "Potential of oxymethylenether-diesel blends for ultra-low emission engines," *Fuel,* vol. 209, no. December, pp. 232-237, 2017.

78 F. Zacherl, C. Wopper, P. Schwanzer and H.-P. Rabl, "Potential of the Synthetic Fuel Oxymethylene Ether (OME) for the Usage in a Single-Cylinder Non-Road Diesel Engine: Thermodynamics and Emissions," *Energies,* vol. 15, no. 21, p. 7932, 2022.

79 Z. Xing, M. Yu, C. Chen and X. Jiang, "A molecular investigation on the effects of OMEX addition on soot inception of diesel pyrolysis," *Fuel,* vol. 346, no. August, p. 128357, 2023.

80 S. Schemme, R. C. Samsun, R. Peters and D. Stolten, "Power-to-fuel as a key to sustainable transport systems – An analysis of diesel fuels produced from CO2 and renewable electricity," *Fuel,* vol. 205, no. October, pp. 198-221, 2017.

81 M. Kass, M. Wissink, C. Janke, R. Connatser and S. Curran, "Compatibility of Elastomers with Polyoxymethylene Dimethyl Ethers and Blends with Diesel," *SAE International Journal Advances and Current Practices In Mobility,* vol. 2, no. 4, pp. 1693-1973, 2020.

82 J. Tian, Y. Cai, Y. Shi, Y. Cui and R. Fan, "Effect of Polyoxymethylene Dimethyl Ethers/Diesel Blends on Fuel Properties and Particulate Matter Oxidation Activity of A Light-Duty Diesel Engine," *International Journal of Automotive Technology,* vol. 20, pp. 277-288, 2019.

83 M. Härt, K. Gaukel, D. Pélerin and G. Wachtmeister, "Oxymethylene Ether as Potentially CO2-neutral Fuel for Clean Diesel Engines Part 1: Engine Testing," *MTZ worldwide,* vol. 78, pp. 52-59, 2017.

84 M. K. Yesilyurt, M. Aydin, Z. Yilbasi and M. Arslan, "Investigation on the structural effects of the addition of alcohols having various chain lengths into the vegetable oil-biodiesel-diesel fuel blends: An attempt for improving the performance, combustion, and exhaust emission characteristics of a compressi," *Fuel,* vol. 269, no. June, p. 117455, 2020.

85 T. Verger, U. Azimov and O. Adeniyi, "Biomass-based fuel blends as an alternative for the future heavy-duty transport: A review," *Renewable and Sustainable Energy Reviews,* vol. 161, no. June, p. 112391, 2022.

86 F. Millo, F. Mallamo, T. Vlachos, C. Ciaravino, L. Postrioti and G. Buitoni, "Experimental Investigation on the Effects on Performance and Emissions of an Automotive Euro 5 Diesel

Engine Fuelled with B30 from RME and HVO," *SAE Technical Paper*, pp. 2013-01-1679, 2013.

87 B. Singh Chauhan, R. Kripal Singh and H. M. Cho, "Practice of diesel fuel blends using alternative fuels: A review," *Renewable and Sustainable Energy Reviews*, vol. 59, no. June, pp. 1358-1368, 2016.

88 O. Emenike, S. Michailos, K. J. Hughes, D. Ingham and M. Pourkashanian, "Techno-economic and environmental assessment of BECCS in fuel generation for FT-fuel, bioSNG and OMEx," *Sustainable Energy Fuels*, vol. 5, pp. 3382-3402, 2021.

89 M. R. Seraç, S. Aydın, A. Yılmaz and S. Şevik, "Evaluation of comparative combustion, performance, and emission of soybean-based alternative biodiesel fuel blends in a CI engine," *Renewable Energy*, vol. 148, no. April, pp. 1065-1073, 2020.

90 C. Kaewbuddee, E. Sukjit, J. Srisertpol, S. Maithomklang, K. Wathakit, N. Klinkaew, P. Liplap and W. Arjharn, "Evaluation of Waste Plastic Oil-Biodiesel Blends as Alternative Fuels for Diesel Engines," *Energies*, vol. 13, no. 11, p. 2823, 2020.

91 A. Atmanli and N. Yilmaz, "Comparative assessment of different diesel engines fueled with 1-pentanol and diesel blends," *Sustainable Energy*, vol. 40, no. 5, p. e13663, 2021.

92 T. Sathish, V. Mohanavel, M. Arunkumar, K. Rajan, M. E. Soudagar, M. Mujtaba, S. H. Salmen, S. A. Obaid, H. Fayaz and S. Sivakumar, "Utilization of Azadirachta indica biodiesel, ethanol and diesel blends for diesel engine applications with engine emission profile," *Fuel*, vol. 319, no. July, p. 123798, 2022.

93 P. Napolitano, C. Beatrice, C. Guido, N. Del Giacomo, L. Pellegrini and P. Scorletti, "Hydrocracked Fossil Oil and Hydrotreated Vegetable Oil (HVO) Effects on Combustion and Emissions Performance of "Torque-Controlled" Diesel Engines," *SAE Technical Paper*, pp. 2015-24-2497, 2015.

94 A. Gómez, R. García-Contreras, J. Soriano and C. Mata, "Comparative study of the opacity tendency of alternative diesel fuels blended with gasoline," *Fuel*, vol. 264, no. March, p. 116860, 2020.

95 M. G. Kassem, A.-M. M. Ahmed, H. H. Abdel-Rahman and A. H. Moustafa, "Use of Span 80 and Tween 80 for blending gasoline and alcohol in spark ignition engines," *Energy Reports*, vol. 5, no. November, pp. 221-230, 2019.

96 M. G. Bidir, N. Millerjothi, M. S. Adaramola and F. Y. Hagos, "The role of nanoparticles on biofuel production and as an additive in ternary blend fuelled diesel engine: A review," *Energy reports*, vol. 7, no. November, pp. 3614-3627, 2021.

97 A. García, J. Monsalve-Serrano, C. Micó and M. Guzmán-Mendoza, "Parametric evaluation of neat methanol combustion in a light-duty compression ignition engine," *Fuel Processing Technology*, vol. 249, no. October, p. 107850, 2023.

98 S. Shamun, C. Haşimoğlu, A. Murcak, Ö. Andersson, M. Tunér and P. Tunestål, "Experimental investigation of methanol compression ignition in a high compression ratio HD engine using a Box-Behnken design," *Fuel*, vol. 209, pp. 624-633, 2017.

99 A. Aziz, L. Xu, A. Garcia and M. Tuner, "Influence of Injection Timing on Equivalence Ratio Stratification of Methanol and Isooctane in a Heavy-Duty Compression Ignition Engine," *SAE Technical Paper*, pp. 2020-01-2069, 2020.

100 M. Ul Haq, A. T. Jafry, S. Ahmad, T. Ahmad Cheema, M. Q. Ansari and N. Abbas, "Recent Advances in Fuel Additives and Their Spray Characteristics for Diesel-Based Blends," *Energies*, vol. 15, no. 19, p. 7281, 2022.

101 V. Karthickeyan, S. Thiyagarajan, V. Edwin Geo, B. Ashok, K. Nanthagopal, O. H. Chyuan and R. Vignesh, "Simultaneous reduction of NOx and smoke emissions with low viscous biofuel in low heat rejection engine using selective catalytic reduction technique," *Fuel*, vol. 255, no. November, p. 115854, 2019.

102 J. Demuynck, C. Favre, D. Bosteels, F. Bunar, J. Spitta and A. Kuhrt, "Diesel Vehicle with Ultra-Low NOx Emissions on the Road," *SAE Technical Paper*, pp. 2019-24-0145, 2019.

103 R. Vallinayagam, S. Vedharaj, W. Yang, C. Saravanan, P. Lee, K. Chua and S. Chou, "Emission reduction from a diesel engine fueled by pine oil biofuel using SCR and catalytic converter," *Atmospheric Environment*, vol. 80, no. December, pp. 190-197, 2013.

104 L. Gren, V. B. Malmborg, J. Falk, L. Markula, M. Novakovic, S. Shamun, A. C. Eriksson, T. B. Kristensen, B. Svenningsson, M. Tunér, P. Karjalainen and J. Pagels, "Effects of renewable fuel and exhaust aftertreatment on primary and secondary emissions from a modern heavy-duty diesel engine," *Journal of Aerosol Science*, vol. 156, no. August, p. 105781, 2021.

105 Y. Wu, H. Li and G. Andrews, "Particle Emissions and Size Distribution across the DPF from a Modern Diesel Engine Using Pure and Blended GTL Fuels," *SAE Technical Paper*, pp. 2020-01-2059, 2020.

106 Y. Zhang, D. Lou, P. Tan, Z. Hu and L. Fang, "Effects of waste-cooking-oil biodiesel blends on diesel vehicle emissions and their reducing characteristics with exhaust after-treatment system," *Journal of Cleaner Production*, vol. 381, no. Part 1, p. 135190, 2022.

107 J. Hernández, J. Rodríguez-Fernández and A. Calle-Asensio, "When diesel NOx aftertreatment systems meet advanced biofuels," *Results in Engineering*, vol. 2, no. June, p. 100009, 2019.

108 V. Karthickeyan, B. Ashok, K. Nanthagopal, S. Thiyagarajan and V. Edwin Geo, "Investigation of novel Pistacia khinjuk biodiesel in DI diesel engine with post combustion capture system," *Applied Thermal Engineering*, vol. 159, no. August, p. 113969, 2019.

109 R. Novella, G. Bracho, J. Gomez-Soriano, C. S. Fernandes and T. Lucchini, "Combustion system optimization for the integration of e-fuels (Oxymethylene Ether) in compression ignition engines," *Fuel*, vol. 305, no. December, p. 121580, 2021.

110 T. Zhang, J. Eismark, K. Munch and Denbratt, "Effects of a wave-shaped piston bowl geometry on the performance of heavy duty Diesel engines fueled with alcohols and biodiesel blends," *Renewable Energy,* vol. 148, no. April, pp. 512-522, 2020.

111 J. Eismark, M. Christensen, M. Andersson, A. Karlsson and I. Denbratt, "Role of fuel properties and piston shape in influencing soot oxidation in heavy-duty low swirl diesel engine combustion," *Fuel,* vol. 254, no. October, p. 115568, 2019.

112 J. V. Pastor, J. M. Garcia-Oliver, C. Micó and F. J. Tejada, "Comparison of the Diffusive Flame Structure for Dodecane and OMEX Fuels for Conditions of Spray A of the ECN," *SAE Int. J. Adv. & Curr. Prac. in Mobility,* vol. 3, no. 1, pp. 402-411, 2021.

113 C. Kroeger, "A Neat Methanol Direct Injection Combustion System for Heavy-Duty Applications," *SAE Technical Paper,* p. 861169, 1986.

114 K. Hikino and T. Suzuki, "Development of Methanol Engine with Autoignition for Low Nox Emission and Better Fuel Economy," *SAE Technical Paper,* no. 891842, 1989.

115 M. Svensson, M. Tuner and S. Verhelst, "Low Load Ignitability of Methanol in a Heavy-Duty Compression Ignition Engine," *SAE Technical Paper,* pp. 2022-01-1093, 2022.

116 S. Sgouridis, Carbajales-Dale, Michael, D. Csala, M. Chiesa and U. Bardi, "Comparative net energy analysis of renewable electricity and carbon capture and storage," *Nature Energy,* vol. 4, pp. 456-465, 2019.

117 J. Ximinis, A. Massaguer and E. Massaguer, "Towards compliance with the prospective EURO VII NOx emissions limit using a thermoelectric aftertreatment heater," *Case Studies in Thermal Engineering,* vol. 36, no. August, p. 102182, 2022.

Chapter 3 – Tools and Methodology

1 ETAS Driving Embedded Excelence, "INCA Software Products," ETAS Driving Embedded Excelence, [Online]. Available: https://www.etas.com/en/products/inca_software_products.php. [Accessed 30 September 2021].

2 HORIBA, "DYNAS3 LI Low Inertia Series - AC Dynamometer," HORIBA, [Online]. Available: https://www.horiba.com/usa/products/detail/action/show/Product/dynas3-li-134/. [Accessed 31 May 2023].

3 KISTLER, *Piezoresistive Absolute Pressure Sensors,* Winterthur: KISTLER, 2009.

4 AVL, *PRESSURE SENSOR FOR COMBUSTION ANALYSIS (Datasheet),* AVL, 2018.

5 ABB, "Thermal mass flowmeter," ABB, 2023. [Online]. Available: https://new.abb.com/products/measurement-products/flow/thermal-mass-flowmeters/sensyflow-fmt700-p. [Accessed 31 May 2023].

6 AVL, *AVL BLOW BY METER,* AVL, 2009.

7 AVL, *AVL Fuel Balance,* Graz: AVL, 2009.

8 T.-V. Dinh, I.-Y. Choi, Y.-S. Son and J.-C. Kim, "A review on non-dispersive infrared gas sensors: Improvement of sensor detection limit and interference correction," *Sensors and Actuators B: Chemical*, vol. 231, pp. 529-538, 2016.

9 T. Holm, "Aspects of the mechanism of the flame ionization detector," *Journal of Chromatography A*, vol. 842, no. 1-2, pp. 221-227, 1999.

10 C.-L. Tsai, C.-S. Fann, S.-H. Wang and R.-F. Fung, "Paramagnetic oxygen measurement using an optical-fiber microphone," *Sensors and Actuators B: Chemical*, vol. 73, no. 2-3, pp. 211-215, 2001.

11 T. Collier, D. Gregory, M. Rushton and T. Hands, "Investigation into the Performance of an Ultra-fast Response NO Analyser Equipped with a NO2 to NO Converter for Gasoline and Diesel Exhaust NOx Measurements," *SAE Technical Paper*, no. 2000-01-2954, 2000.

12 The European Commission, *Commission Regulation (EU) 2016/427 of 10 March 2016 amending Regulation (EC) No 692/2008 as regards emissions from light passenger and commercial vehicles (Euro 6) (Text with EEA relevance)*, Official Journal of the European Union, 2016.

13 AVL, *AVL Smoke Meter - Emission Measurement Instruments*, Graz: AVL, 2011.

14 R. Christian, F. Knopf, A. Jasmek and W. Schindler, "A new method for the filter smoke number measurement with improved sensitivity," *MTZ Motortechnische Zeitschift*, vol. 54, pp. 16-22, 1993.

15 M. Das, M. Sarkar, A. Datta and A. Kumar Santra, "Study on viscosity and surface tension properties of biodiesel-diesel blends and their effects on spray parameters for CI engines," *Fuel*, vol. 220, no. May, pp. 769-799, 2018.

16 B. J., B. D. and A. Mitsos, "Production of Oxymethylene Dimethyl Ethers from Hydrogen and Carbon Dioxide - Part II: Modeling and Analysis for OME3-5," *Industrial and Engineering Chemistry Research*, vol. 58, pp. 556-5578, 2019.

17 T. L. Ullman, K. B. Spreen and R. L. Mason, "Effects of Cetane Number, Cetane Improver, Aromatics, and Oxygenates on 1994 Heavy-Duty Diesel Engine Emissions," *SAE Technical Paper*, no. 941020, 1994.

18 A. Demirbaş, "A direct route to the calculation of heating values of liquid fuels by using their density and viscosity measurements," *Energy Conversion and Management*, vol. 41, no. 15, pp. 1609-1614, 2000.

19 F. Payri, P. Olmeda, J. Martín and A. García, "A complete 0D thermodynamic predictive model for direct injection diesel engines," *Applied Energy*, vol. 88, no. 12, pp. 4632-4641, 2011.

20 M. Lapuerta, O. Armas and J. Hernández, "Diagnosis of DI Diesel combustion from in-cylinder pressure signal by estimation of mean thermodynamic properties of the gas," *Applied Thermal Engineering*, vol. 19, no. 5, pp. 513-529, 1999.

21 J. Martin, "Aportación al diagnóstico de la combustión en motores Diesel de inyección directa," *Doctoral Thesis, Universitat Politécnica de València, Departamento de Máquinas y Motores Térmicos*, 2007.

22 G. Woschni, "A universally applicale equation for the instantaneous heat transfer coefficient in the internal combustion engines," *SAE Technical paper*, no. 670931, 1967.

23 F. Payri, X. Margot, A. Gil and J. Martin, "Computational study of heat transfer to the walls of a DI diesel engine," *SAE Technical Paper*, no. 2005-01-0210, 2005.

24 A. Torregosa, P. Olmeda, B. Degraeuwe and M. Reyes, "A concise wall temperature model for DI Diesel engines," *Applied Thermal Engineering*, vol. 26, no. 11-12, pp. 1320-1327, 2006.

25 Z. Zhang, H. Liu, Z. Yue, Y. Wu, X. Kong, Z. Zheng and M. Yao, "Effects of Multiple Injection Strategies on Heavy-Duty Diesel Energy Distributions and Emissions Under High Peak Combustion Pressures," *Frontiers in Energy Research*, vol. 10, p. 857077, 2022.

26 I. Taymaz, "An experimental study of energy balance in low heat rejection diesel engine," *Energy*, vol. 31, no. 2-3, pp. 364-371, 2006.

27 J. Heywood, Internal Combustion Engine Fundamentals, McGraw-Hill Education, 2018.

28 J. Benajes, J. Lopez, R. Novella and A. Garcia, "Advanced methodology for improving testing efficiency in a single-cylinder research diesel engine," *Exp Tech*, vol. 32, pp. 41-47, 2008.

29 R. Durrett and M. Potter, "Renewable Energy to Power through Net-Zero-Carbon Fuels," in *THIESEL 2020 Conference on Thermo- and Fluid Dynamic Processes in Direct Injection Engines 8th-11th September 2020*, Valencia, 2020.

30 S. Biswas, A. S. Segupta, D. Kakati, P. Chakraborti and R. Banerjee, "Parametric optimization of the CNG/ethanol-induced RCCI profiles in biodiesel combustion through a robust design space foray," *Fuel*, vol. 332, no. Part 2, p. 126203, 2023.

31 S. d'Ambrosio, D. Iemmolo, A. Mancarella and R. Vitolo, "Preliminary Optimization of the PCCI Combustion Mode in a Diesel Engine through a Design of Experiments," *Energy Procedia*, vol. 101, no. November, pp. 909-916, 2016.

32 J. Sjoblom, J. Andric and E. Faghani, "Intrinsic Design of Experiments for Modeling of Internal Combustion Engines," *SAE Technical Paper*, pp. 2018-01-1156, 2018.

33 S. Ramalingan, S. Gomathinayakam, V. Mani and S. Kachapalayam, "Analysis of optimising injection parameters and EGR for DICI engine performance powered by lemongrass oil using Box–Behnken (RSM) modelling," *International Journal of Ambient Enegry*, vol. 43, no. 1, pp. 6362-6379, 2022.

34 D. Montgomery, Design and Analysis of Experiments, New York: John Wiley, 2019.

35 Analytical Methods Committee, AMCTB No 55, "Experimental design and optimisation (4): Plackett–Burman designs," *Anal. Methods*, vol. 5, no. 8, pp. 1901-1903, 2013.

36 P. Bruce and A. Bruce, Practical Statistics for Data Scientists, O'Reilly Media, Inc., 2017.

37 . James, . Witten, . Hastie and . Tibshirani, An Introduction to Statistical Learning: With Applications in R, New York: Springer, 2013.

38 G. Sierksma and Y. Zwols, Linear and Integer Optimization - Theory and Practice, Third Edition, New York: Chapman and Hall/CRC, 2015.

39 A. Schrijver, Theory of Linear and Integer Programming, New York: John Wiley & Sons, 1998.

Chapter 4 – Drop-in use of low carbon fuel blends in compression ignition engines

1 *Directive 2009/30/EC of the European Parliament and of the Council of 23 April 2009 amending Directive 98/70/EC as regards the specification of petrol, diesel and gas-oil and introducing a mechanism to monitor and reduce greenhouse gas emissions and amend,* Official Journal of the European Union, 2009.

2 Directive 2009/28/EC (2009) of the European Parliament and of the Council of 23 April.

3 O. I. Awad, R. Mamat, O. M. Ali, N. Sidik, T. Yusaf, K. Kadirgama and M. Kettner, "Alcohol and ether as alternative fuels in spark ignition engine: A review," *Renewable and Sustainable Energy Reviews,* vol. 82, no. 3, pp. 2586-2605, 2018.

4 P. Lacey, S. Gail, J. Kientz, G. Benoist, P. Downes and Daveau, "Fuel Quality and Diesel Injector Deposits," *SAE Int. J. Fuels Lubr.,* vol. 5, no. 3, pp. 1187-1198, 2012.

5 B. Ritcher, S. Crusius, U. Schümann and H. Harndorf, "Characterisation of Internal Deposits in Common-Rail Injectors," *MTZ Worldwide,* vol. 74, pp. 50-57, 2013.

6 T. Pham Huu, K. Nguyen Duc, T. Nguyen The, T. Nguyen Duy and N. The Luong, "An experimental study on wear, deposits, performance, and emissions of bio-fueled motorcycle engines," *Energy Sources, Part A: Recovery, Utilization, and Environmental Effects,* vol. 45, no. 1, pp. 1309-132, 2023.

7 A. Smith and R. Williams, "Linking the Physical Manifestation and Performance Effects of Injector Nozzle Deposits in Modern Diesel Engines," *SAE Int. J. Fuels Lubr.,* vol. 8, no. 2, pp. 344-357, 2015.

8 A. Kumar Agarwal, "Biofuels (alcohols and biodiesel) applications as fuels for internal combustion engines," *Progress in Energy and Combustion Science,* vol. 33, no. 3, pp. 233-271, 2007.

9 C. Bae and J. Kim, "Alternative fuels for internal combustion engines," *Proceedings of the Combustion Institute,* vol. 36, no. 3, pp. 3389-3413, 2017.

10 C. Guido, C. Beatrice and P. Napolitano, "Application of bioethanol/RME/diesel blend in a Euro5 automotive diesel engine: Potentiality of closed loop combustion control technology," *Applied Energy,* vol. 102, pp. 13-23, 2013.

11 M. D. Cárdenas, O. Armas, C. Mata and F. Soto, "Performance and pollutant emissions from transient operation of a common rail diesel engine fueled with different biodiesel fuels," *Fuel*, vol. 185, pp. 743-762, 2016.

12 T. Kalnes, T. Marker and D. R. Shonnard, "Green Diesel: A Second Generation Biofuel," *International Journal of Chemical Reactor Engineering*, vol. 5, no. 1, 2007.

13 S. Bezergianni and A. Dimitriadis, "Comparison between different types of renewable diesel," *Renewable and Sustainable Energy Reviews*, vol. 21, pp. 110-116, 2013.

14 A. García, A. Gil, J. Monsalve-Serrano and R. Lago-Sari, "OMEx-diesel blends as high reactivity fuel for ultra-low NOx and soot emissions in the dual-mode dual-fuel combustion strategy," *Fuel*, vol. 275, p. 117898, 2020.

15 M. H. Hassan and M. A. Kalam, "An Overview of Biofuel as a Renewable Energy Source: Development and Challenges," *Procedia Engineering*, vol. 56, pp. 39-53, 2013.

16 K. Kim, W. Lee, P. Wiersema, E. Mayhew, J. Temme, C.-B. M. Kweon and T. Lee, "Effects of the cetane number on chemical ignition delay," *Energy*, vol. 264, p. 126263, 2023.

17 C. Chase, C. Peterson, G. Lowe and P. Mann, "A 322,000 kilometer (200,000 mile) Over the Road Test with HySEE Biodiesel in a Heavy Duty Truck," *SAE Technical Paper*, no. SAE Technical Paper 2000-01-2647, 2000.

Chapter 5 – Optimization of low carbon fuel blends calibration in compression ignition engines

1 A. García, J. Monsalve-Serrano, C. Micó and M. Guzmán-Mendoza, "Parametric evaluation of neat methanol combustion in a light-duty compression ignition engine," *Fuel Processing Technology*, vol. 249, no. October, p. 107850, 2023.

2 M. H. M. Yasin, R. Mamat, A. F. Yusop, P. Paruka, T. Yusaf and G. Najafi, "Effects of Exhaust Gas Recirculation (EGR) on a Diesel Engine fuelled with Palm-biodiesel," *Energy Procedia*, vol. 75, no. August, pp. 30-36, 2015.

3 B. Rajesh Kumar and S. Saravanan, "Effect of exhaust gas recirculation (EGR) on performance and emissions of a constant speed DI diesel engine fueled with pentanol/diesel blends," *Fuel*, vol. 160, no. November, pp. 217-226, 2015.

4 E. Öztürk and Ö. Can, "Effects of EGR, injection retardation and ethanol addition on combustion, performance and emissions of a DI diesel engine fueled with canola biodiesel/diesel fuel blend," *Energy*, vol. 244, no. Part B, p. 123129, 2022.

5 A. García, J. Monsalve-Serrano, D. Villalta and M. Guzmán-Mendoza, "Parametric assessment of the effect of oxygenated low carbon fuels in a light-duty compression ignition engine," *Fuel Processing Technology*, vol. 229, no. October, p. 107199, 2022.

6 G. Karavalakis, D. Short, D. Vu, R. Russell, M. Hajbabaei, A. Asa-Awuku and T. D. Durbin, "Evaluating the Effects of Aromatics Content in Gasoline on Gaseous and Particulate Matter Emissions from SI-PFI and SIDI Vehicles," *Environ Sci Technol*, vol. 49, no. 11, pp. 7021-7031, 2015.

7 Y. Qian, Y. Qiu, Y. Zhang and X. Lu, "Effects of different aromatics blended with diesel on combustion and emission characteristics with a common rail diesel engine," *Applied Thermal Engineering*, vol. 125, no. October, pp. 1530-1538, 2017.

8 M. Elkelawy, E. Shenawy, S. A. Mohamed, m. M. Elarabi and H. A.-E. Bastawissi, "Impacts of EGR on RCCI engines management: A comprehensive review," *Energy Conversion and Management: X*, vol. 14, no. May, p. 100216, 2022.

9 J. Han, H. Bao and L. Somers, "Experimental investigation of reactivity controlled compression ignition with n-butanol/n-heptane in a heavy-duty diesel engine," *Applied Energy*, vol. 282, no. January, p. 116164, 2021.

10 H. Guo, W. S. Neill and B. Liko, "An Experimental Investigation on the Combustion and Emissions Performance of a Natural Gas - Diesel Dual Fuel Engine at Low and Medium Loads," in *Proceedings of the ASME 2015 Internal Combustion Engine Division Fall Technical Conference*, Houston, TX, USA, 2015.

11 A. Garcia, J. Monsalve-Serrano, D. Villalta, M. G. Guzman-Mendoza, P. Gaillard, R. Durrett, A. Vassallo and F. C. Pesce, "Evaluation of the Effect of Low-Carbon Fuel Blends' Properties in a Light-Duty CI Engine," *SAE Int. J. Adv. & Curr. Prac. in Mobility*, vol. 5, no. 3, pp. 1094-1106, 2022.

12 P. Hellier, M. Talibi, A. Eveleigh and N. Ladommatos, "An overview of the effects of fuel molecular structure on the combustion and emissions characteristics of compression ignition engines," *Proceedings of the Institution of Mechanical Engineers, Part D: Journal of Automobile Engineering*, vol. 232, no. 1, pp. 90-105, 2018.

13 J. J. López, J. García-Oliver, A. García and V. Domenech, "asoline effects on spray characteristics, mixing and auto-ignition processes in a CI engine under Partially Premixed Combustion conditions," *Applied Thermal Engineering*, vol. 70, no. 1, pp. 996-1006, 2014.

14 S. M. Miraboutalebi, P. Kazemi and P. Bahrami, "Fatty Acid Methyl Ester (FAME) composition used for estimation of biodiesel cetane number employing random forest and artificial neural networks: A new approach," *Fuel*, vol. 166, no. February, pp. 143-151, 2016.

15 A. A. Al-Harbi, A. J. Alabduly, A. M. Alkhedhair, N. B. Alqahtani and M. S. Albishi, "Effect of operation under lean conditions on NOx emissions and fuel consumption fueling an SI engine with hydrous ethanol–gasoline blends enhanced with synthesis gas," *Energy*, vol. 238, no. Part A, p. 121694, 2022.

16 D. Agarwal, S. Sinha and A. K. Agarwal, "Experimental investigation of control of NOx emissions in biodiesel-fueled compression ignition engine," *Renewable Energy*, vol. 31, no. 14, pp. 2356-2369, 2006.

17 S.-w. Lee, D. Tanaka, J. Kusaka and Y. Daisho, "Effects of diesel fuel characteristics on spray and combustion in a diesel engine," *JSAE Review*, vol. 23, no. 4, pp. 407-414, 2002.

18 J. Reijinders, M. Boot and P. de Goey, "Impact of aromaticity and cetane number on the soot-NOx trade-off in conventional and low temperature combustion," *Fuel*, vol. 186, no. December, pp. 24-34, 2016.

19 S. Saxena and I. D. Bedoya, "Fundamental phenomena affecting low temperature combustion and HCCI engines, high load limits and strategies for extending these limits," *Progress in Energy and Combustion Science*, vol. 39, no. 5, pp. 457-488, 2013.

Chapter 6 – Life Cycle Analysis of Low Carbon Fuels for Light-Duty Combustion Engine Vehicles

1 W. Steffen, J. Rockström, K. Richardson, T. M. Lenton, C. Folke, D. Liverman, C. P. Summerhayes, A. D. Barnosky, S. E. Cornell, M. Crucifix, J. F. Donges, I. Fetzer, S. J. Lade, M. Scheffer, R. Winkelmann and H. J. Schellnhuber, "Trajectories of the Earth System in the Anthropocene," *Proceedings of the National Academy of Sciences*, vol. 115, no. 33, pp. 8252-8259, 2018.

2 N. Wunderling, R. Winkelmann, J. Rockström and e. al., "Global warming overshoots increase risks of climate tipping cascades in a network model," *Nature Climate Change*, vol. 13, pp. 75-82, 2023.

3 V. Masson-Delmotte, P. Zhai, H.-O. Pörtner, D. Roberts, J. Skea, P. Shukla, A. Pirani, W. Moufouma-Okia, C. Péan, R. Pidcock, S. Connors, J. Matthews, Y. Chen, X. Zhou, M. Gomis, E. Lonnoy, T. Maycock, M. Tignor and T. Waterfield, "Global Warming of 1.5°C. An IPCC Special Report on the impacts," IPCC, 2018.

4 UN General Assembly, *United Nations Framework Convention on Climate Change : resolution / adopted by the General Assembly*, UN General Assembly, 1994.

5 G. Puig-Samper Naranjo, D. Bolonio, M. F. Ortega and M.-J. García-Martínez, "Comparative life cycle assessment of conventional, electric and hybrid passenger vehicles in Spain," *Journal of Cleaner Production*, p. 125883, 2021.

6 B. Sen, N. C. Onat, M. Kucukvar and O. Tatari, "Material footprint of electric vehicles: A multiregional life cycle assessment," *Journal of Cleaner Production*, vol. 209, pp. 1033-1043, 2019.

7 E. Karaaslan, Y. Zhao and O. Tatari, "Comparative life cycle assessment of sport utility vehicles with different fuel options," *Int J Life Cycle Assess*, vol. 23, p. 333–347, 2018.

8 L. La Picirelli de Souza, E. E. Silva Lora, J. C. Escobar Palacio, M. H. Rocha, M. L. Grillo Renó and O. J. Venturini, "Comparative environmental life cycle assessment of conventional vehicles with different fuel options, plug-in hybrid and electric vehicles for a sustainable transportation system in Brazil," *Journal of Cleaner Production*, vol. 203, pp. 444-468, 2018.

9 C. Zhang, X. Zhao, R. Sacchi and F. You, "Trade-off between critical metal requirement and transportation decarbonization in automotive electrification," *Nature Communications*, vol. 14, p. 1616, 2023.

10 K. Petrauskienė, M. Skvarnavičiūtė and J. Dvarionienė, "Comparative environmental life cycle assessment of electric and conventional vehicles in Lithuania," *Journal of Cleaner Production*, vol. 246, p. 119042, 2020.

11 H. Ritchie, M. Roser and P. Rosado, "CO_2 and Greenhouse Gas Emissions," OurWorldInData.org, 2020. [Online]. Available: https://ourworldindata.org/co2-and-greenhouse-gas-emissions. [Accessed April 2023].

12 European Commission, "Shedding light on energy in the EU," Eurostat, Publications Office, 2023.

13 IEA, "CO2 Emissions in 2022," IEA, Paris, 2023.

14 H. Ritchie, "Cars, planes, trains: where do CO2 emissions from transport come from?," Our World in Data, 06 October 2020. [Online]. Available: https://ourworldindata.org/co2-emissions-from-transport. [Accessed 11 April 2023].

15 M. Bui, C. S. Adjiman, A. Bardow, E. J. Anthony, A. Boston, S. Brown, P. S. Fennell, S. Fuss, A. Galindo, L. A. Hackett, J. P. Hallett, H. J. Herzog, G. Jackson, J. Kemper, S. Krevor, G. C. Maitland, M. Matuszewski, I. S. Metcalfe, C. Petit, G. Puxty, J. Reimer, D. Reiner, E. Rubin, S. Scott, N. Shah, B. Smit, J. Trusler, P. Webley, J. Wilcox and N. Mac Dowell, "Carbon capture and storage (CCS): the way forward," *Energy & Environmental Science*, vol. 11, no. 5, pp. 1062-1176, 2018.

16 D. L. Sanchez, J. H. Nelson, J. Johnston, A. Mileva and D. M. Kammen, "Biomass enables the transition to a carbon-negative power system across western North America," *Nature Climate Change*, vol. 5, pp. 230-234, 2015.

17 M. Pérez-Fortes, J. C. Schöneberger, A. Boulamanti and E. Tzimas, "Methanol synthesis using captured CO2 as raw material: Techno-economic and environmental assessment," *Applied Energy*, vol. 161, pp. 718-732, 2016.

18 E. Commission, J. R. Centre, M. Prussi, M. Yugo and L. De Prada, "JEC well-to-tank report V5 : JEC well-to-wheels analysis : well-to-wheels analysis of future automotive fuels and powertrains in the European context," Publications Office, 2020.

19 S. Schemme, R. Can Samsun, R. Peters and D. Stolten, "Power-to-fuel as a key to sustainable transport systems – An analysis of diesel fuels produced from CO2 and renewable electricity," *Fuel*, vol. 205, pp. 198-221, 2017.

20 Eurostat, "Gross and net production of electricity and derived heat by type of plant and operator," 04 04 2023. [Online]. Available: https://ec.europa.eu/eurostat/databrowser/view/nrg_ind_peh/default/table?lang=en. [Accessed 11 04 2023].

21 R. B. Kaunda, "Potential environmental impacts of lithium mining," *Journal of Energy & Natural Resources Law*, vol. 38, no. 3, pp. 237-244, 2020.

22 B. E. Murdock, K. E. Toghill and N. Tapia-Ruiz, "A Perspective on the Sustainability of Cathode Materials used in Lithium-Ion Batteries," *Advance Energy Materials*, vol. 11, no. 39, p. 2102028, 2021.

23 International Organization for Standardization, *ISO 14040:2006 environmental management - life cycle assessment - principles and framework*, Geneva: ISO, 2006.

24 I. O. f. Standardization, *ISO 14044:2006 environmental management - life cycle assessment - requirements and guidelines*, Geneva: ISO, 2006.

25 M. Finkbeiner, A. Inaba, R. Tan, K. Christiansen and H.-J. Klüppel, "The New International Standards for Life Cycle Assessment: ISO 14040 and ISO 14044," *The International Journal of Lifecycle Assessment*, vol. 11, pp. 80-85, 2006.

26 H. H. Khoo and R. B. H. Tan, Life cycle assessment: New developments and multi-disciplinary applications, New Jersey: World Scientific, 2022.

27 D. Candelaresi, A. Valente, D. Iribarren, J. Dufour and G. Spazzafumo, "Comparative life cycle assessment of hydrogen-fuelled passenger cars," *International Journal of Hydrogen Energy*, vol. 46, pp. 35961-35973, 2021.

28 O. Winjobi, J. C. Kelly and Q. Dai, *Life-cycle analysis, by global region, of automotive lithium-ion nickel manganese cobalt batteries of varying nickel content*, 2022.

29 M. Q. Wang, *GREET 1.5 - transportation fuel-cycle model - Vol. 1 : methodology, development, use, and results. Office of Scientific and Technical Information (OSTI)*, 1999.

30 D. A. Notter, M. Gauch, R. Widmer, P. Wäger, A. Stamp, R. Zah and H.-J. Althaus, "Contribution of Li-Ion Batteries to the Environmental Impact of Electric Vehicles," *Environmental Science & Technology*, vol. 44, no. 17, pp. 6550-6556, 2010.

31 M. F. Torchio and M. G. Santarelli, "Energy, environmental and economic comparison of different powertrain/fuel options using well-to-wheels assessment, energy and external costs – European market analysis," *Energy*, vol. 35, no. 10, pp. 4156-4171, 2010.

32 J. Desantes, R. Novella, B. Pla and M. Lopez-Juarez, "Impact of fuel cell range extender powertrain design on greenhouse gases and NOX emissions in automotive applications," *Applied Energy*, vol. 302, p. 117526, 2021.

33 A. García, J. Monsalve-Serrano, S. Martinez-Boggio and R. Soria Alcaide, "Carbon footprint of battery electric vehicles considering average and," *Energy*, vol. 268, p. 126691, 2023.

34 J. Desantes, R. Novella, B. Pla and M. Lopez-Juarez, "Impact of the Powertrain Sizing on Cradle-to-Grave Emissions and Fuel Cell Degradation in a FCV with a Range-Extender Architecture," *SAE Technical Paper*, no. 2022-01-0681, 2022.

35 Ö. Andersson and P. Börjesson, "The greenhouse gas emissions of an electrified vehicle combined with renewable fuels: Life cycle assessment and policy implications," *Applied Energy*, vol. 289, p. 116621, 2021.

36 U. Tietge, P. Mock, V. Franco and N. Zacharof, "From laboratory to road: Modeling the divergence between official and real-world fuel consumption and CO2 emission values in the German passenger car market for the years 2001–2014," *Energy Policy*, vol. 103, pp. 212-222, 2017.

37 M. A. Huijbregts, Z. J. Steinmann, P. M. F. Elshout, G. Stam, F. Verones, M. Vieira, M. Zijp, A. Hollander and R. van Zelm, "ReCiPe2016: a harmonised life cycle impact

assessment method at midpoint and endpoint level," *The International Journal of Life Cycle Assessment,* vol. 22, pp. 138-147, 2017.

38 G. Wernet, C. Bauer, B. Steubing, J. Reinhard, E. Moreno-Ruiz and B. Weidema, "The ecoinvent database version 3 (part I): overview and methodology. The International Journal of Life Cycle Assessment," *The International Journal of Life Cycle Assessment,* vol. 21, p. 1218–1230, 2016.

39 J. N. A. H.-J. D. G. D. R. Frischknecht R., H. T., H. S., H. R., N. T., R. G. and S. M., "The ecoinvent database: Overview and methodological framework," *International Journal of Life Cycle Assessment,* vol. 10, pp. 3-9, 2005.

40 Pré, "PRé: enabling fact-based sustainability," 2023 PRé Sustainability B.V. , [Online]. Available: https://pre-sustainability.com/about/about-pre/. [Accessed 12 April 2023].

41 Sphera, "LCA for Experts (GaBi)," Sphera, [Online]. Available: https://sphera.com/life-cycle-assessment-lca-software/. [Accessed 12 April 2023].

42 I. T. Herrmann and A. Moltesen, "Does it matter which Life Cycle Assessment (LCA) tool you choose? – a comparative assessment of SimaPro and GaBi," *Journal of Cleaner Production,* vol. 86, pp. 163-169, 2015.

43 A. Burnham, M. Q. Wang and Y. Wu, "Development and applications of GREET 2.7 -- The Transportation Vehicle-CycleModel," 2006.

44 J. Kelly, J. Han, Q. Dai and A. Elgowainy, "Update of Vehicle Weights in the GREET ® Model," 2017.

45 T. Li, H. Zhang, Z. Liu, Q. Ke and L. Alting, "A system boundary identification method for life cycle assessment," *The International Journal of Life Cycle Assessment,* vol. 19, pp. 646-660, 2013.

46 J. Guinée, M. Gorrée, R. Heijungs, G. Huppes, R. Kleijn, A. d. Koning, L. v. Oers, A. Wegener Sleeswijk, S. Suh, H. Udo de Haes, H. d. Bruijn, R. Duin and M. Huijbregts, Handbook on Life Cycle Assessment: Operational Guide to the ISO Standards, Boston: Kluwer Academic Publishers, 2002.

47 *Commission Recommendation (EU) 2021/2279 of 15 December 2021 on the use of the Environmental Footprint methods to measure and communicate the life cycle environmental performance of products and organisations,* Official Journal of the European Union, 2021.

48 M. Goedkoop, R. Heijungs, M. Huijbregts, A. De Schryver, J. Struijs and R. van Zelm, *ReCiPe 2008: A life cycle impact assessment method which comprises harmonised category indicators at the midpoint and endpoint levels. First edition. Report i: Characterization,* the Netherlands: Ruimte en Milieu, Ministerie van Volkshuisvesting, Ruimtelijke Ordening en Milieubeheer, 2009.

49 M. Z. Hauschild and M. A. J. Huijbregts, "Chapter 1. In Life cycle impact assessment," in *Introducing life cycle impact assessment,* Springer, 2015.

50 Odyssee-Mure, "Sectoral Profile - Overview," Enerdata, [Online]. Available: https://www.odyssee-mure.eu/publications/efficiency-by-sector/overview/. [Accessed 20 April 2023].

51 A. Funazaki, K. Taneda, K. Tahara and A. Inaba, "Automobile life cycle assessment issues at end-of-life and recycling," *JSAE Review*, vol. 24, no. 4, pp. 381-386, 2003.

52 S. Karagoz, N. Aydin and V. Simic, "End-of-life vehicle management: a comprehensive review," *Journal of Material Cycles and Waste Management*, vol. 22, pp. 416-442, 2020.

53 GreenDelta, "OpenLCA," [Online]. Available: https://www.openlca.org/.

54 ChrisFix, "How Much Weight can you REMOVE from your Car? (Weight Reduction)," Youtube, 5 June 2021. [Online]. Available: https://www.youtube.com/watch?v=MCiNGmwopx4. [Accessed 29 March 2023].

55 S. Dudes, "How Much Weight Can You REMOVE From Your Car?," Youtube, 12 March 2022. [Online]. Available: https://www.youtube.com/watch?v=RSJuXoQwPsg. [Accessed 29 March 2023].

56 R. a. Race, "Clio RS 182 - Weight Reduction For Extra Speed - Budget Track Car Build Project pt.6," Youtube, 9 November 2017. [Online]. Available: https://www.youtube.com/watch?v=bG09BbxNpxA. [Accessed 29 March 2023].

57 M. Pilotto Cenci, T. Scarazzato, D. Dotto Munchen, P. C. Dartora, H. M. Veit, A. Moura Bernardes, P. R. Dias and ç, "Eco-Friendly Electronics—A Comprehensive Review," *Advanced Materials Technologies*, vol. 7, no. 2, p. 2001263, 2021.

58 G. W. Schweimer and M. Levin, "Life Cycle Inventory for the Golf A4," Volkswagen AG, Wolfsburg, 2000.

59 A. García, J. Monsalve-Serrano, S. Martinez-Boggio and S. Tripathi, "Techno-economic assessment of vehicle electrification in the six largest global automotive markets," *Energy Conversion and Management*, vol. 270, p. 116273, 2022.

60 A. Temporelli, M. L. Carvalho and P. Girardi, "Life Cycle Assessment of Electric Vehicle Batteries: An Overview of Recent Literature," *Energies*, vol. 13, no. 11, p. 2864, 2020.

61 M. Shafique, A. Azam, M. Rafiq and X. Luo, "Life cycle assessment of electric vehicles and internal combustion engine vehicles: A case study of Hong Kong," *Research in Transportation Economics*, vol. 91, p. 101112, 2022.

62 T. R. Hawkins, B. Singh, G. Majeau-Bettez and A. Hammer Strømman, "Comparative Environmental Life Cycle Assessment of Conventional and Electric Vehicles," *Journal of Industrial Ecology*, vol. 17, no. 1, pp. 53-64, 2012.

63 M. Collins, K. Schiebel and P. Dyke, "Life Cycle Assessment of Used Oil Management (ERM)," Environmental Resources Management, 2017.

64 A. Soler, V. Gordillo, W. Lilley, P. Schmidt, W. Werner, T. Houghton and S. Dell'Orco, "E-Fuels: A techno-economic assessment of European domestic production and imports towards 2050," Concawe, Brussels, 2022.

65 M. Prussi, M. Yugo, L. De Prada, M. Padella, R. Edwards and L. Lonza, "JEC Well-to-Tank report v5, EUR 30269 EN," Publications Office of the European Union, Luxembourg,, 2020.

66 J. Benajes, A. Garcia, J. Monsalve-Serrano and R. Sari, "Evaluating the Efficiency of a Conventional Diesel Oxidation Catalyst for Dual-Fuel RCCI Diesel-Gasoline Combustion," *SAE Technical Paper,* no. 2018-01-1729, 2018.

67 A. Srinivasacharya Ayodhya and K. Gottekere Narayanappa, "An overview of after-treatment systems for diesel engines," *Environmental Science and Pollution Research,* vol. 25, pp. 35034-35047, 2018.

68 A. Simons, "Road transport: new life cycle inventories for fossil-fuelled passenger cars and non-exhaust emissions in ecoinvent v3," *The International Journal of Life Cycle Assessment,* vol. 21, pp. 1299-1313, 2016.

69 R. Suarez-Bertoa, P. Mendoza-Villafuerte, F. Riccobono, M. Vojtisek, M. Pechout, A. Perujo and C. Astorga, "On-road measurement of NH3 emissions from gasoline and diesel passenger cars during real world driving conditions," *Atmospheric Environment,* vol. 166, pp. 488-497, 2017.

70 P. Mock, "World-Harrmonized Light-Duty Vehicles Test Procedure," The International Council on Clean Transportation, 2013.

71 European Commission, Directorate-General for Internal Market, Industry, Entrepreneurship and SMEs , *Proposal for a REGULATION OF THE EUROPEAN PARLIAMENT AND OF THE COUNCIL on type-approval of motor vehicles and engines and of systems, components and separate technical units intended for such vehicles, with respect to their emissions and battery durabili,* 2022.

72 A. García, J. Monsalve-Serrano, D. Villalta and M. Guzmán-Mendoza, "Optimization of low carbon fuels operation on a CI engine under a simplified driving cycle for transportation de-fossilization," *Fuel,* vol. 310, no. Part A, p. 122338, 2022.

73 A. García, J. Monsalve-Serrano, D. Villalta and M. Guzmán-Mendoza, "Impact of low carbon fuels (LCF) on the fuel efficiency and NOx emissions of a light-duty series hybrid commercial delivery vehicle," *Fuel,* vol. 321, p. 124035, 2022.

74 C.-F. Tsai, W.-C. Lin, Y.-H. Hu and G.-T. Yao, "Under-sampling class imbalanced datasets by combining clustering analysis and instance selection," *Information Sciences,* vol. 477, pp. 47-54, 2019.

75 T. Mühlenstädt and S. Kuhnt, "Kernel interpolation," *Computational Statistics & Data Analysis,* vol. 55, no. 11, pp. 2962-2974, 2011.

76 Gamma Technologies, LLC, "GT-POWER," Gamma Technologies, LLC, 2020.

77 M. Okubo and T. Kuwahara, "Chapter 4 - Operation examples of emission control systems," in *New Technologies for Emission Control in Marine Diesel Engines*, Butterworth-Heinemann, 2020, pp. 145-210.

78 B. Rossomando, E. Meloni, G. De Falco, M. Sirignano, I. Arsie and V. Palma, "Experimental characterization of ultrafine particle emissions from a light-duty diesel engine equipped with a standard DPF," *Proceedings of the Combustion Institute,* vol. 38, no. 4, pp. 5695-5702, 2021.

79 Tesla, "Impact Report," Tesla, 2021.

80 P. Zapp, A. Schreiber, J. Marx, M. Haines, J.-F. Hake and J. Gale, "Overall environmental impacts of CCS technologies—A life cycle approach," *International Journal of Greenhouse Gas Control,* vol. 8, pp. 12-21, 2012.

81 A. Dutta, "Life Cycle Assessment Strategies for Carbon Capture and Utilization Processes," in *Life Cycle Assessment*, WORLD SCIENTIFIC, 2022, pp. 55-75.

82 K. Hayashi, M. Okazaki, N. Itsubo and A. Inaba, "Development of damage function of acidification for terrestrial ecosystems based on the effect of aluminum toxicity on net primary production," *The International Journal of Life Cycle Assessment,* vol. 9, pp. 13-22, 2004.

83 J. Lelieveld, J. Evans, D. Giannadaki and A. Pozzer, "The contribution of outdoor air pollution sources to premature mortality on a global scale," *Nature,* vol. 525, pp. 367-371, 2015.

84 N. Cihat Onat, G. M. Abdella, M. Kucukvar, A. A. Kutty, M. Al-Nuaimi, G. Kumbaroğlu and M. Bulu, "How eco-efficient are electric vehicles across Europe? A regionalized life cycle assessment-based eco-efficiency analysis," *Sustainable Development,* vol. 29, no. 5, pp. 941-956, 2021.

85 E. Karaaslan, Y. Zhao and O. Tatari, "Comparative life cycle assessment of sport utility vehicles with different fuel options," *The International Journal of Life Cycle Assessment,* vol. 23, pp. 333-347, 2018.

86 European Commission, "European Platform on LCA | EPLCA," European Commission, 29 June 2018. [Online]. Available: https://eplca.jrc.ec.europa.eu/ELCD3/datasetDownload.xhtml. [Accessed 2023 March 29].

87 "Amazon," Amazon, [Online]. Available: https://www.amazon.com/. [Accessed 29 April 2023].